Bioorganic Chemistry 93 (2019) 103299

Contents lists available at ScienceDirect

Bioorganic Chemistry

journal homepage: www.elsevier.com/locate/bioorg

Critical evaluation of current Alzheimer's drug discovery (2018–19) & futuristic Alzheimer drug model approach

Atukuri Dorababu

Department of Studies in Chemistry, SRMPP Govt. First Grade College, Huvinahadagali 583219, Karnataka, India

ARTICLE INFO

Keywords:
Alzheimer disease
AChE inhibitor
BuChE inhibitor
BACE1
MAO

ABSTRACT

Alzheimer's disease (AD), a neurodegenerative disease responsible for death of millions of people worldwide is a progressive clinical disorder which causes neurons to degenerate and ultimately die. It is one of the common causes of dementia wherein a person's incapability to independently think, behave and decline in social skills can be quoted as major symptoms. However the early signs include the simple non-clinical symptoms such as forgetting recent events and conversations. Onset of these symptoms leads to worsened conditions wherein the AD patient suffers severe memory impairment and eventually becomes unable to work out everyday tasks. Even though there is no complete cure for AD, rigorous research has been going on to reduce the progress of AD. Currently, a very few clinical drugs are prevailing for AD treatment. So this is the need of hour to design, develop and discovery of novel anti-AD drugs. The main factors for the cause of AD according to scientific research reveals structural changes in brain proteins such as beta amyloid, tau proteins into plaques and tangles respectively. The abnormal proteins distort the neurons. Despite the high potencies of the synthesized molecules; they could not get on the clinical tests up to human usage. In this review article, the recent research carried out with respect to inhibition of AChE, BuChE, NO, BACE1, MAOs, Aβ, H3R, DAPK, CSF1R, 5-HT4R, PDE, σ_1R and GSK-3β is compiled and organized. The summary is focused mainly on cholinesterases, Aβ, BACE1 and MAOs classes of potential inhibitors. The review also covers structure activity relationship of most potent compounds of each class of inhibitors alongside redesign and remodeling of the most significant inhibitors in order to expect cutting edge inhibitory properties towards AD. Alongside the molecular docking studies of the some final compounds are discussed.

1. Introduction

Alzheimer disease (AD) is chronic neurodegenerative disease which has slow impact at initial stages and gradually takes control over person's mental power [1]. The most general symptom is unable to recall the recent events in early stages of AD [1]. Seventy percent of AD patients get the disease through genetic inheritance [2]. Roughly, AD affects approximately 6% of the people aging 65 years and above [3]. Statistics revealed that approximately 29.8 million people were living with AD in 2015 [4]. The mutations in three genes are responsible for AD in most of the autosomal family types; those are amyloid precursor protein (AAP) and Presenilins 1 and 2 genes [5]. Mutations in AAP and presenilin genes elevate the small protein, Aβ_{42} product that becomes most important component of senile plaques [6]. ABCA7 and SORL1 are remaining two genes attributed to autosomal dominant AD [7]. Different drug therapies were hypothesized; those are cholinergic hypothesis (based on reduced neurotransmitter acetylcholine synthesis and medications are designed to treat acetylcholine deficiency) [8,9], amyloid hypothesis (hypothesizes that extracellular beta (Aβ) deposit/amyloid plaques are responsible for AD) [10,11], Tau hypothesis (proposes that the AD is caused by tau protein abnormality) [11]. A large number of factors are responsible for the cause of AD which may be mentioned as factors such as genetic, lifestyle and environmental factors. Most of the drugs discovered could not reach clinical stage as they have not possessed the properties with respect to drug likeliness. Currently, the most important medications for the treatment of AD are

Abbreviations: Aβ, Amyloid beta; AD, Alzheimer's disease; BACE1, beta-site amyloid precursor protein cleaving enzyme 1; CAS, catalytic active site; CSF1R, colony-stimulating factor 1 receptor; DAPK, death-associated protein kinase; *ee*AChE, electrophorus electricus acetylcholinesterase; GSK-3β, glycogen synthase kinase 3 beta; H3R, histamine 3 receptor; 5-HT, 5-hydroxytryptamine; 5-HT4R, 5-hydroxytryptamine receptor 4; LOX-5, lipoxygenase-5 enzyme; **MAO**s, monoamine oxidases; NO, neuroinflammation; NSAIDs, non-steroidal anti-inflammatory drugs; PAS, peripheral anionic site; PDE, phosphodiesterase; *Rat*BuChE, rat butylcholinesterase; σ_1R, sigma-1 receptor

E-mail address: dora1687@gmail.com.

https://doi.org/10.1016/j.bioorg.2019.103299
Received 19 July 2019; Received in revised form 14 September 2019; Accepted 16 September 2019
Available online 19 September 2019

acetylcholine esterase inhibitors. The various compounds synthesized possessing anti-AD properties are classified into different groups based upon the type of the enzyme being inhibited by the drug molecule. Classification may also depend the type of receptors such as CSF1R, H3R, 5-HT4R, σ_1R being inhibited by the designed drug molecules. Each class/group of inhibitors is sub classified based on the main chemical entity/chemical frame work utilized for the drug molecule design. Here in, the recent research contributed towards the anti-AD drug design and discovery by various researchers is collated and organized in systematic manner. The review is limited to cholinesterase inhibitors, monoamine oxidase inhibitors, BACE1 and beta-amyloid inhibitors in addition to little coverage on other inhibitors such as NO, H3R, DAPK, CSF1R, 5-HT4R, PDE, σ_1R, LOX-5 and GSK-3β. The remarkable inhibitor in each sub-class of inhibitors is identified and these have been utilized for reconstruct of potent drug molecules which are hypothesized to be prominent inhibitors with respect to AD. All the potent molecules in each class of inhibitors have been docked with corresponding enzyme crystal structure; where in the significant inhibitors have formed favorable interactions with various amino acid residues.

2. Multifunctional/multitarget inhibitors

2.1. 1-Benzylamino-2-hydroxyalkyl derivatives

Multi-target approach for drug discovery is gaining importance and AD is a complex disease which has multiple enzymes for its cause; to mention, β-secretase, γ-secretase, acetylcholinesterase, butyrylcholinesterase etc. Alongside, multifunctional drugs of AD are engineered in a way to efficiently inhibit BACE1, amyloid β aggregation, Tau aggregation and monoamineoxidases. So, multiple therapeutic targets would be essential for effective treatment for AD. Hence, design and development of multi-target directed ligands (MTDLs) that could inhibit more than one enzyme responsible for AD. The current research based on MTDLs has become potential approach to counter AD [12,13]. In this conjuncture, P. Dawid and his coworkers [14] have designed 1-benzylamino-2-hydroxyalkyl derivatives as multifunctional anti-alzheimer agents which could inhibit AChE, BuChE, BACE-1, amyloid β aggregation, and tau aggregation. Molecular modeling studies were also performed to explain enzyme-ligand interactions which would be helpful in structure-activity relationship study. The design was based on the structure of the standard compounds Donepezil **1** and BACE1 inhibitor, NVP-BXD-552 **2** (Fig. 1).

Using Tacrine and Donepezil as reference compounds, the synthesized compounds were evaluated for inhibition of *ee*AChE, *eq*BuChE, and *h*BuChE enzymes. In that, only compound **3** (Fig. 2) shown moderate inhibitory activity towards *ee*AChE and *eq*BuChE with IC_{50} values 3.62 and 9.36 μM respectively.

In case of inhibitory activity towards *eq*BuChE, compounds **4** (IC_{50} = 1.49 ± 0.03 μM), **5** (IC_{50} = 1.59 ± 0.05 μM), **6** (IC_{50} = 1.55 ± 0.05 μM), and **7** (IC_{50} = 2.92 ± 0.1 μM) (Fig. 3) were potent compounds. SAR studies revealed that the potential inhibitors possess 2,2-diphenylethylamine or 3,3-dipheylpropylamine structural unit.

In the BACE1 inhibition activity, derivatives **4**, **9** (IC_{50} = 63.76 ± 3.27 μM) (Figs. 3 and 4) having 2,2-diphenylamine and **8** (IC_{50} = 79.68 ± 2.72 μM), **10** (IC_{50} = 101.90 ± 2.76 μM) (Fig. 4) possessing structural moiety, 4-(bis(4-fluorophenyl)methyl) piperazine have yielded good results.

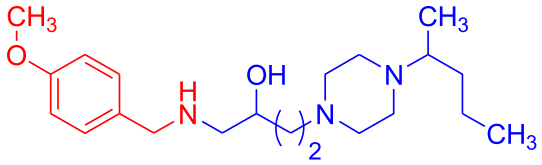

3

Fig. 2. Structure of *ee*AChE/BuChE dual inhibitor.

The best inhibitors among the Aβ aggregation inhibitors were compounds **7** (72.2% ± 2.1) and **11** (84.9% ± 0.8, IC_{50} = 1.22 μM). Again these derivatives contain diphenylamine as the common structural entity. Whereas, compounds **6** (55.1% ± 3.6), **7** (44.4% ± 4.5) (Fig. 3), **11** (62.7% ± 1.2) and **12** (68.4% ± 3.4) (Fig. 5) stood as the potent inhibitors among the Tau aggregation inhibitors.

2.2. 2,5-Dihydroxyterephthalamide derivatives

The studies revealed that non-steroidal anti-inflammatory drugs could abate occurrence of AD through control of inflammatory factors and oxygen free radical release which are caused by Aβ deposition [15,16]. It is evident that salicylic acid possesses NSAIDs property and AChE inhibition property [17] and hence it was utilized in the design of multi-target drugs for AD. Also, alkybenzylamine modified genistein derivatives were reported as multifunctional drugs for AD [18]; likewise memoquin **14** (Fig. 7) was found to exhibit multifunctional drug properties [19]. These inspired Q. Song et al [20] to design a set of 2,5-dihydroxyterephthalamide (DHTA) derivatives wherein 2,5-dihydroxyterephthalic acid **13** (Fig. 6) and appropriate secondary amine flanked the alkyl chain as appendants. The lead compounds were tested for Aβ aggregation and AChE inhibition activity. Using donepezil and rivastigmine as reference compounds, AChE and BuChE inhibitory activities were performed. The activity suggested that some compounds were better than the reference compound rivastigmine.

The inhibitory activity of DHTA derivatives (0.56–30.80 μM) was far better than that of DHTA (> 100 μM) which inferred that the introduction of alkybenzylamine has significantly increased the AChE inhibitory activity. In the tested compounds, the derivatives with alkyl chain length 3, 4, 6 have exhibited good activity. Also, in the compounds of particular chain length; the presence of secondary amine, (2-methoxy benzyl) ethylamine has resulted in highest activity (**15–17**, Fig. 7). Therefore, alkyl chain length and type of secondary amine has prominent effect on the AChE inhibitory activity. The most potent AChE inhibitor was found to be derivative **16**, inferring that four carbon chain length suits best for inhibition. Annoyingly, most of the DHTA derivatives were weak inhibitors of BuChE. A few of the synthesized compounds namely; compound **18** (17.30 ± 0.33 μM), **19** (19.20 ± 0.65 μM) and **20** (40.30 ± 0.56 μM) (Fig. 8) have exhibited relatively good activity. The results have revealed that in the potent BuChE inhibitory activity, (2-methoxy benzyl) methylamine moiety has greater impact along with alkyl chain length.

In the inhibitory activity of A$\beta_{1\text{-}42}$ aggregation, almost all DHTA derivatives have shown excellent activity (self-induced: 71.6–99.9% and Cu^{2+}-induced: 57.6–89.9%) at 25 μM concentration compared to

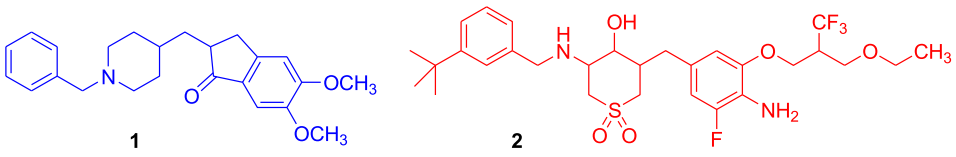

1 **2**

Fig. 1. Structures of Donepezil and BACE1 inhibitors.

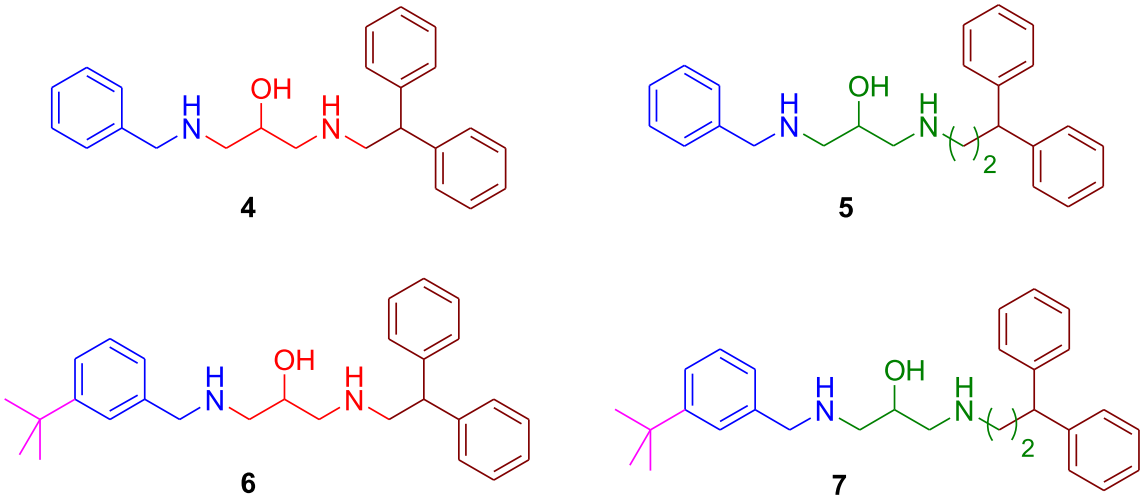

Fig. 3. Structures of *eq*BuChE inhibitors (**4**–**7**), BACE1 inhibitors (**4**), A*β* aggregation inhibitors (**7**) and Tau aggregation inhibitors (**6** &**7**).

reference compound curcumin (40.2 ± 0.9% and 66.0 ± 1.3%). Here also, the alkylbenzylamine moiety has induced significant effect on the activity.

Molecular docking studies of compound **16** (Fig. 9) in active pocket of *Tc*AChE exhibited hydrogen bonding interaction of phenolic hydroxy and carbonyl groups with amino acid residues Asp72 and Try121 respectively. The parallel π-π interactions were observed for *N*-(methoxybenzyl) ethylamine moiety with Trp84 and compound **16** shown hydrophobic interactions with Gly117, Gly118, Gly123, Try130 and Glu199. Furthermore, the amide portion and the benzene moieties have good interactions with Phe331 and Tyr334.

2.3. 3-Phenylcoumarin–lipoic acid conjugates

Lipocrine **21** (Fig. 10), a conjugate of tacrine and lipoic acid was reported as AChE, BuChE, AChE-induced A*β* aggregation inhibitor [21] where in lipoic acid was reported as an oxidant. Benzopyranone derivatized coumarins possess properties to relieve the neurological diseases like AD [22,23]. Similarly, 3-arylcoumarins such as AP2469, **22** (Fig. 10) was reported as AChE and A*β* aggregation inhibitor [24,25].

All these structural motifs were introduced in order to enhance the anti-AD properties and synthesized 3-arylcoumarin derivatives [26]. The title compounds were screened for inhibitory activities of AChE, BuChE and A*β* aggregation. Out of the tested compounds, few compounds **23**–**26** (Fig. 11) have yielded good results towards AChE and BuChE. The common factor responsible for good activity is alky chain/carbon spacer of four carbons. In particular benzocoumarin analog, **26** stood top of potent AChE/BuChE inhibitors. It was also supported by kinetic study (K_i = 10.98 μM) which inferred a mixed type inhibitory activity for derivative **26** with interactions at both CAS and PAS of AChE. Hence, both appropriate carbon spacer (butyl) and benzocoumarin moiety have produced synergetic effect on AChE inhibition.

The selected compounds **25** and **26** were evaluated for A*β*-aggregation inhibition with respect to self and AChE-induced A*β*-aggregation using donepezil and rifampicin as reference compounds

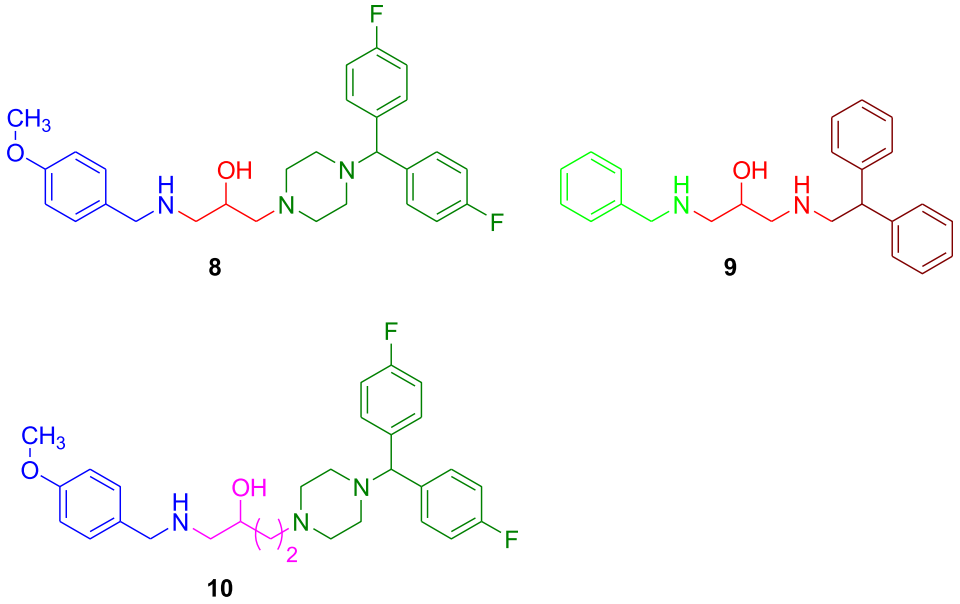

Fig. 4. Structures of potent BACE1 inhibitors.

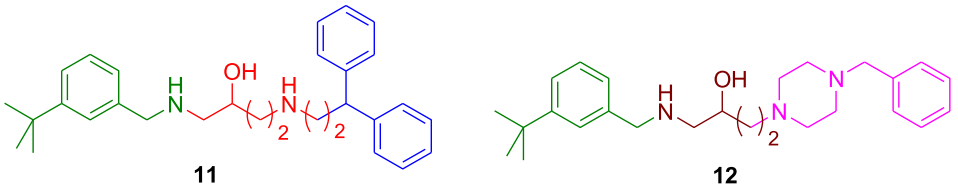

Fig. 5. Structures of Aβ inhibitor **11** and Tau inhibitor **12.**

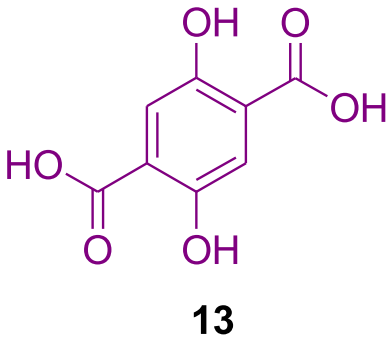

Fig. 6. Structure of 2,5-dihydroxyterphthalic acid.

(Table 1). In this activity, 8-methoxycoumarin derivative **25** was very potent and also better than the reference compounds used. But compound **26** exhibited weak activity.

2.4. 5,6-Dimethoxybenzo[d]isothiazol-3(2H)-one-N-alkylbenzylamine derivatives

Prominent antimicrobial agents, sulfonamide derivatives have been described to exhibit monoamine oxidase inhibitory activity [27]. Saccharin-*N*-alkylamine analogs (**27**, Fig. 12) were reported as neuroprotection agents; more importantly they have shown moderate potencies towards Aβ-aggregation and also efficient selective inhibitory activity towards AChE [28]. To elevate the Aβ-aggregation inhibitory activity, the π-π stacking between the compound and the PAS of AChE was improved. Also considering the structural similarities between donepezil and saccharin in addition to binding of donepezil benzyl moiety to the CAS through a π-π interaction, Xu et al. [29] have modified 5,6-dimethoxybenzo[*d*]isothiazole-3(2*H*)-one with apt benzylamine and using different lengths of carbon linkers to afford 5,6-dimethoxybenzo[*d*]isothiazol-3(2*H*)-one-*N*-alkylbenzylamine derivatives. Furthermore, 5,6-dimethoxybenzo[*d*]isothiazol-3(2*H*)-one 1-oxide and 1,1-dioxide alkylbenzylamine derivatives were synthesized selectively and tested for AChE, MAO, Aβ-aggregation inhibition.

Some of the compounds have exhibited good activity relative to reference compound donepezil towards *ee*AChE and *Rat*BuChE. The derivatives which shown *ee*AChE inhibitory activity less than 1 μM are represented in Table 2 along with corresponding percentage inhibition values of *Rat*BuChE.

When the structures of potent molecules are observed, the important things revealed are; carbon spacer present in those was either butyl or hexyl and *N*-alkylbenzylamine was essential moiety. Compounds containing carbon spacer with less than 4 carbons were not good at inhibition; hence the hypothesized reason quoted, carbon spacer would be too short to make interaction with PAS and CAS of AChE. Amongst the screened compounds, *N*-ethyl-benzylamine analog, **30** (Table 2 and Fig. 13) was the best derivative. Whereas the most of the synthesized compounds had a very good inhibitory activity towards *Rat*BuChE compared to donepezil. To mention, compound **30** was best *ee*AChE/*Rat*BuChE dual inhibitor.

Using recombinant human MAO-A & MAO-B, and clorgyline, rasagiline and iproniazid as reference compounds, title compounds were

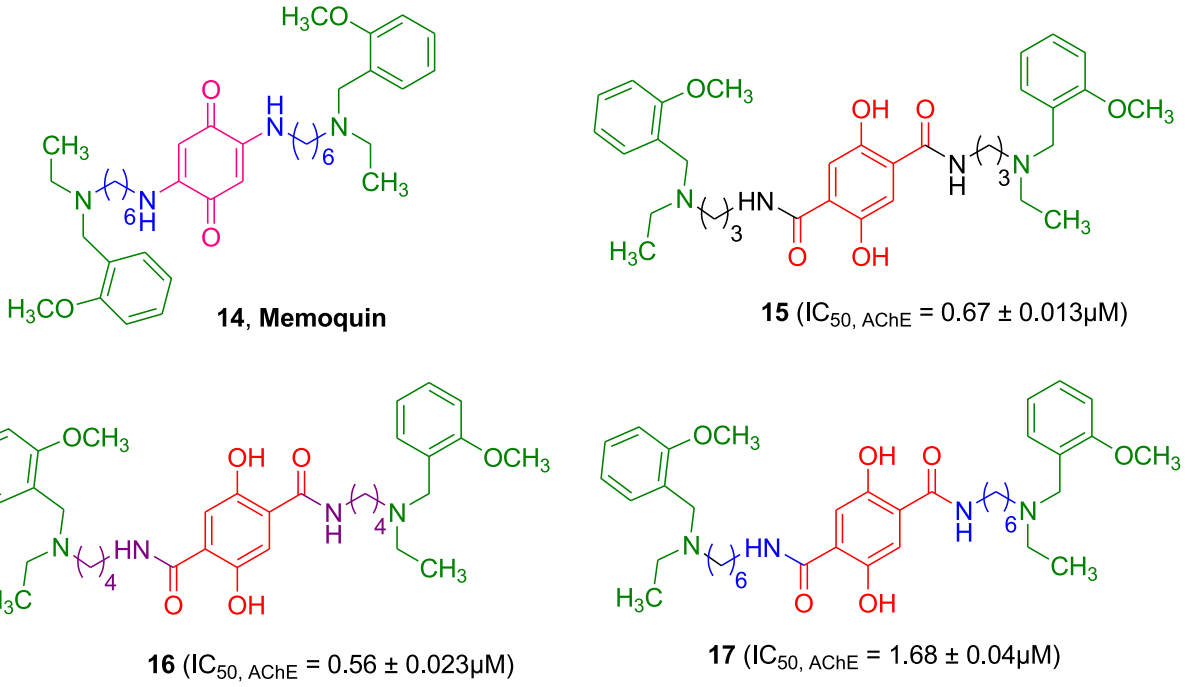

Fig. 7. Structures of memoquin and potent AChE inhibitors.

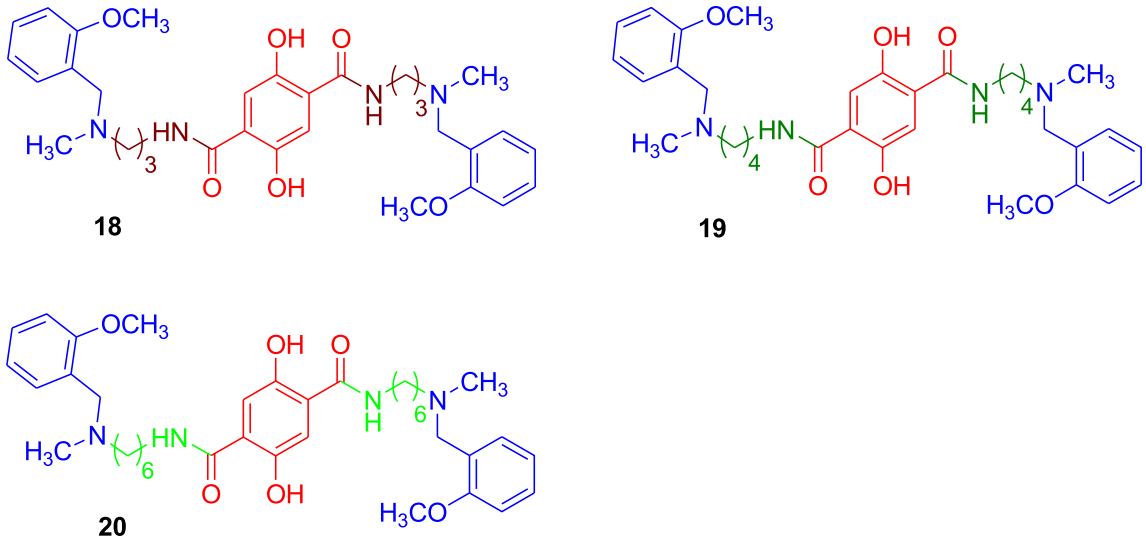

Fig. 8. Illustration of structures of potent BuChE inhibitors.

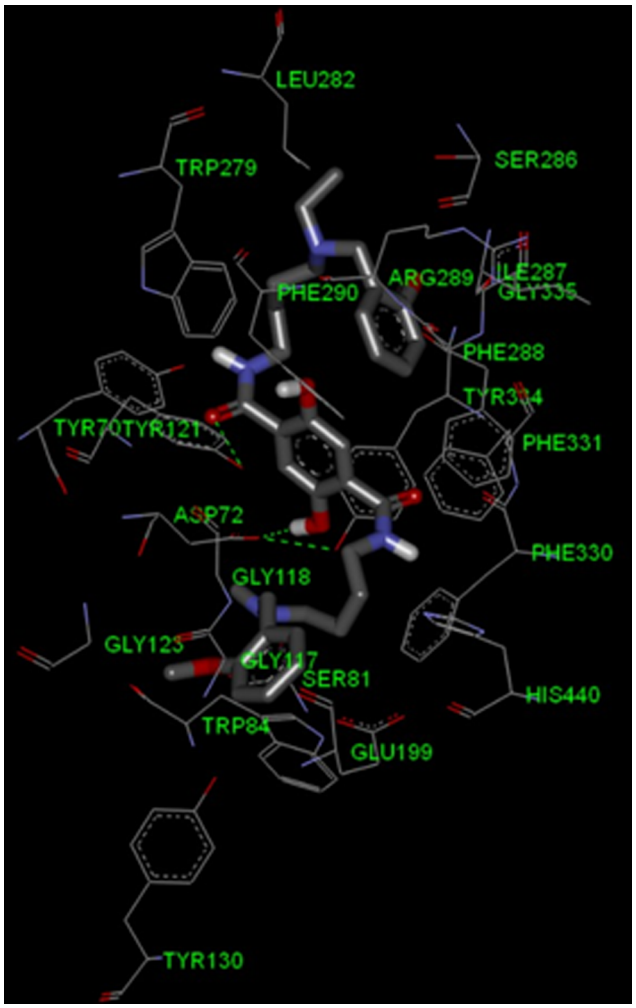

Fig. 9. Molecular docking analysis of compound **16** with *Tc*AChE [20].

evaluated for monoamine oxidase inhibition activity. Most of the compounds were active against MAO-A and a few against MAO-B where in compound **33** (IC_{50} = 3.4 ± 0.03 μM) and **36** (IC_{50} = 12.4 ± 0.13 μM) (Fig. 14) were most potent derivatives towards MAO-A and MAO-B respectively. Here also hexyl carbon spacer had shown its impact on inhibitory activity. In the self-induced A$\beta_{1\text{-}42}$ aggregation inhibition activity performed in presence of curcumin as reference compound, most of the compounds had a descent activity. Few derivatives with competitive inhibitions were **30**, **32**, **36** and **37** (Fig. 14). Compound **32** (48.0 ± 1.53%) stood a top among the self-induced A$\beta_{1\text{-}42}$ aggregation inhibitors.

The compound **30** was subjected to docking analysis (Fig. 15) with *Tc*AChE active binding site in which benzylamine moiety interacted with Tyr130 through π-π stacking and hydrophobic affinities were also noticed with amino acid residues Gly441, Trp84, Leu127, Ser124, Glu199, Gly123 and Gly117. Alongside, 5,6-dimethoxybenzo[*d*]isothiazol-3-one moiety has also formed hydrophobic interactions with Tyr334, Gly335, Ile287, Ser286, Arg289 and Phe290. The intramolecular H-bond is existed between sulfur atom and Tyr121 and folded conformation of long methylene chain has hydrophobic affinity with His440, Tyr121, Ser122, Gly118 and Ser200 residues.

2.5. 2,4-Dioxochroman benzyl modified pyridinium derivatives

Acetylcholine should be maintained up to sufficient level but increase in AChE enzyme in AD patients would result in enzymatic degradation of actylcholine [30]. Therefore, inhibition of AChE might be an efficient approach for AD treatment [31]. M. Mostofi et al [32] have designed benzofuran-based chalconoids, **38** (Fig. 16) possessing benzylpyridinium moieties as AChE inhibitors. Similarly *N*-benzyl pyridinium modified coumarin derivatives, **39** (Fig. 16) were reported to exhibit anti-AChE properties [33]. Therefore, benzyl and pyridinium groups might have special ability in AChE inhibition which inspired to design 1-benzyl-3-((((2,4-dioxochroman-3-ylidene)methyl)amino)methyl)pyridinium bromides and evaluate for anti-AD properties [34].

Using donepezil as reference compound, title compounds were screened for anti-AChE and anti-BuChE activities. Part of the synthesized compounds has yielded descent activity towards AChE, among them the derivatives **40–42** (Fig. 17) with electron withdrawing groups (chloro, bromo and nitro) at 2-position of benzyl ring given the best results. In these compounds alteration with respect to either position of substitution on benzyl ring or nature of the substituent led to reduced activity. The synthesized derivatives exhibited moderate anti-BuChE activity and the 2,3-dichloro derivative, **43** (Fig. 17) was reported as most potent molecule among them and its activity was as good as the donepezil. Most potent activity of compound **40** was also proved by docking studies where in **40** has occupied CAS and PAS sites of AChE in addition to establishment of π-π interactions with the aid of 2,4-dioxochroman ring and also non-classical hydrogen bond with the residues

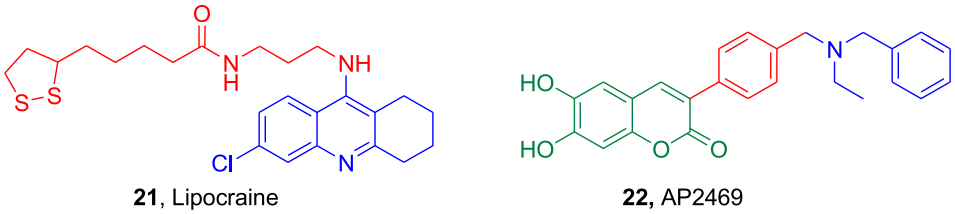

Fig. 10. Structures of Lipocrine and anti-AD agent AP2469.

Phe33 and Tyr121 (Fig. 18**a**). Alongside, compound **43** has shown interactions with some of amino acid residues, 2,4-dioxochroman moiety formed hydrogen bonds with Gly117 & His438 and π-π interactions were resulted with the residues Phe329 and Trp231 (Fig. 18**b**).

Compound **40** exhibited remarkable self-induced A*β*-aggregation inhibitory activity (20.38 ± 1.51%) at 10 μM concentration. The activity was better than the reference compound donepezil (14.70 ± 2.35%). Again compound **40** has its effect on *β*-secretase inhibitory activity (BACE-1) at 50 μM concentration. Even though its activity was comparatively lower (IC_{50} = 41.4 ± 22.4 μM) than that of reference compound OM99-2 (IC_{50} = 0.014 μM), it stood as the most potent among the tested compounds.

2.6. Phenylpyridazine bearing carboxamide & propanamide derivatives

Minaprine **44** (Fig. 19), a pyridazine analog was employed as an antidepressant drug; like some of the CNS agents, minaprine interacts with neuro-receptors and reported as weak AChE inhibitor (IC_{50} = 85 μM) [35]. Hence, pyridazine derivatives would be descent candidates for AD treatment.

In continuation of the research on cholinesterase inhibitors [36,37], 6-(substituted phenyl)pyridazine-3-carboxamide, and 6-(substituted phenyl)pyridazine-3-yl propanamide derivatives along with the [1,1′-biphenyl]-4-carboxamide & ([1,1′-biphenyl]-4-yl)propanamide derivatives were designed and subsequently evaluated for cholinesterase and A*β*-aggregation inhibitory activities [38]. Cholinesterase inhibitory

Table 1
A*β*-Aggregation inhibitory values of selected compounds.

Compound	Inhibition of A*β*-aggregation (%)	
	Self-induced	*h*AChE-induced
25	62.4 ± 4.2	58.6 ± 2.7
26	na	5.8 ± 1.9
Rifampicin	27.5 ± 4.3	12.2 ± 3.0
Donepezil	22 ± 5.4	26.1 ± 2.5

na - not active.

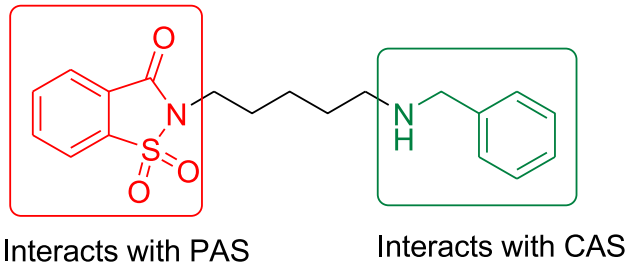

Fig. 12. Depiction of interaction of Saccharin-*N*-alkylamine analog structural units with PAS and CAS [29].

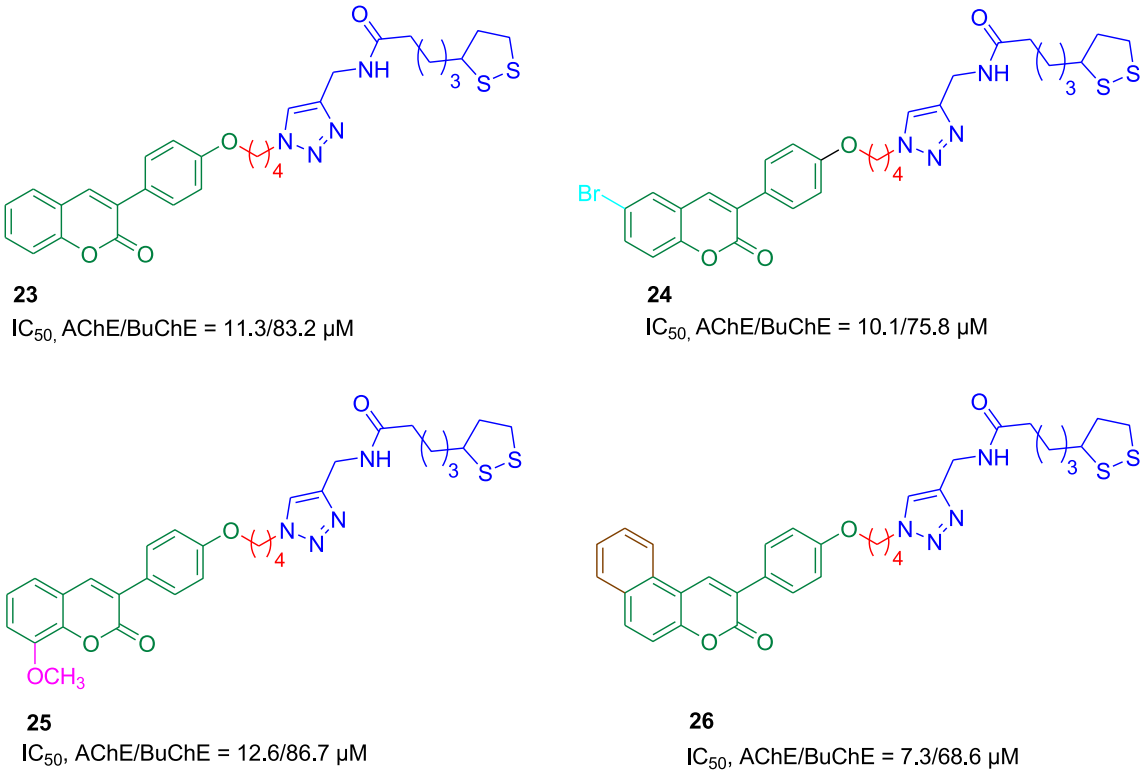

Fig. 11. Representation of potent AChE/BuChE inhibitors.

Table 2
Depiction of AChE and BuChE inhibitory values of the potent compounds.

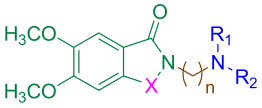

Compd	X	n	NR_1R_2	*ee*AChE	*Rat*BuChE
				IC_{50} (μM)	% inhibition
28	S	4	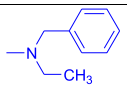	0.80 ± 0.02	21.8 ± 0.40
29	S	6	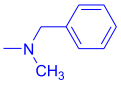	0.35 ± 0.01	23.1 ± 0.43
30	S	6	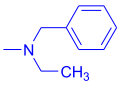	0.29 ± 0.01	48.2 ± 0.83
31	S	6	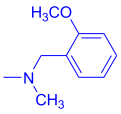	0.61 ± 0.02	28.8 ± 0.51
32	S	6	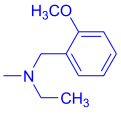	0.46 ± 0.02	46.9 ± 0.81
33	S	6	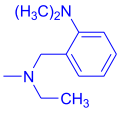	0.56 ± 0.01	46.8 ± 0.80
34	SO	6	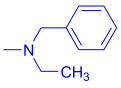	0.38 ± 0.01	8.1 ± 0.24
35	SO	6	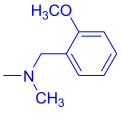	0.80 ± 0.01	28.7 ± 0.52
Donepezil	-	-	-	0.023 ± 0.003	IC_{50} = 21.4 ± 0.097 μM

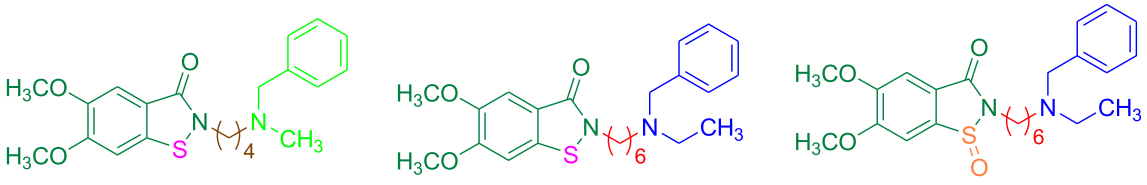

29 **30** **34**

Fig. 13. Structures of *ee*AChE/*Rat*BuChE dual inhibitors.

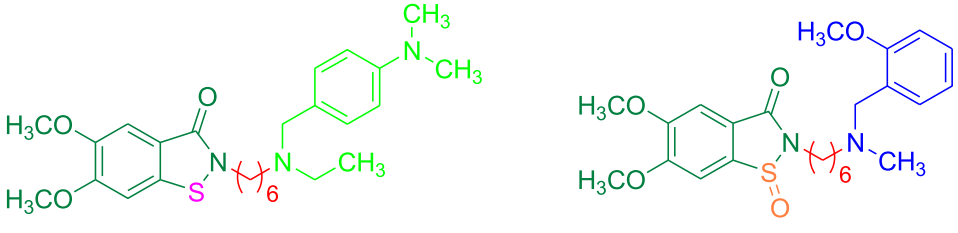

36 **37**

Fig. 14. Depiction of structure of potent MAO-B inhibitor (**36**) and A$\beta_{1\text{-}42}$ aggregation inhibitor (**37**).

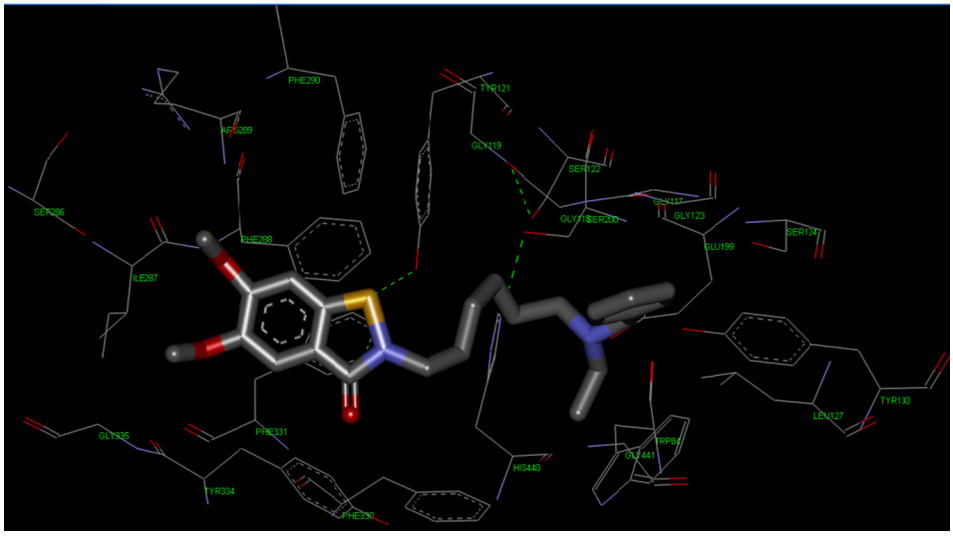

Fig. 15. Molecular binding studies of compound **30** with *Tc*AChE binding site [29].

activities were performed using donepezil and galantamine as reference compounds. Most of the carboxamide derivatives were active towards AChE but propanamide analogs have not shown significant activity. Among the AChE inhibitory compounds, derivatives **45–48** (Fig. 20) have been reported as the most potent compounds compared to donepezil (IC_{50} = 0.058 ± 0.001 μM) where in all these compounds entail common side chain, 1-benzylpiperidine.

The synthesized compounds have not exhibited good impact on BuChE; however, compounds **45** (IC_{50} = 9.80 μM) and **48** (IC_{50} = 1.48 μM) have shown good results. Compound **48** given better results than that of donepezil (IC_{50} = 3.7 μM). The result suggested that both biphenyl and 1-benzylpiperidine motifs were necessary for anti-BuChE activity.

Some six derivatives were selectively evaluated for self-induced Aβ-aggregation and AChE-induced Aβ-aggregation inhibitory activities using phenol red and donepezil HBr as reference compounds at 100 μM concentration. The results indicated that the AChE-induced activity was better than self-induced and compounds **49** and **50** (Fig. 21) exhibited comparable inhibitory activity.

2.7. Clioquinol-rolipram/roflumilast hybrids

The redundancy of some metal ions such as Cu^{2+}, Zn^{2+} and Fe^{2+} in addition to β-amyloid peptides in the brains of AD patients would be main ingredients for plaques [39,40]. Aβ-Aggregation results from complexation of β-amyloid peptides and metal ions like Cu^{2+}, leading to subsequent synaptic damage [41]. Studies have revealed that clioquinol (CQ) **51** (Fig. 22) and its derivatives could inhibit Aβ-aggregation and degrade extracellular Aβ peptides [42].

Recent approach for AD treatment is to inhibit phosphodiesterase enzymes (PDEs) [43] where in PDEs were responsible for hydrolysis of the intracellular second messenger cyclic adenosine monophosphate (cAMP). PDE4D is one of sub type of PDEs. Rolipram **52** and roflumilast **53** (Fig. 22) were reported as PDE4 inhibitors [44]. Considering all these developments, structural frame work units were compiled to synthesize clioquinol-rolipram/roflumilast derivatives and hence evaluating their PDE4D and Aβ-aggregation inhibitory activities [45].

The synthesized compounds had nice inhibitory activity towards PDE4D compared to reference compounds rolipram and roflumilast. Overwhelmingly, four compounds **54–57** (Fig. 23) among the tested compounds exhibited the inhibitory activity as good as reference compounds and even better than the reference compounds (IC_{50}, PDE4D2 values are 0.621 ± 0.028 μM and 0.480 ± 0.035 μM for rolipram and roflumilast respectively). The potent inhibitors were possessed either unsubstituted 8-hydrozyquinoline moiety (**54** & **56**) or iodine at 7-position on 8-hydroxyquinoline (**55** & **57**). Other substitutions or change in position of substituents have not yielded fruitful results.

In the metal-induced Aβ-aggregation inhibition performed using clioquinol as reference compound, compounds **54** (Aβ + Cu^{2+} + **54**, 46%) and **56** (Aβ + Cu^{2+} + **56**, 51%) were reported as most potent among the screened compounds; and shown better results than clioquinol itself (Aβ + Cu (II) + CQ, 66%).

The compound **56** was investigated for its docking studies with PDE4D. The hydrophobic amino acid residues, Phe372 and Ile336 form sandwich outer cover around compound **56**. The molecular docking studies inferred that the compound **56** has favorable hydrogen-bond interaction with amide nitrogen of the Gln369 through cycloproylmethyl and difluoromethyl oxygen of derivative **56** (Fig. 24). Also, it was reported that a similar binding mode was observed for compound **56** and roflumilast.

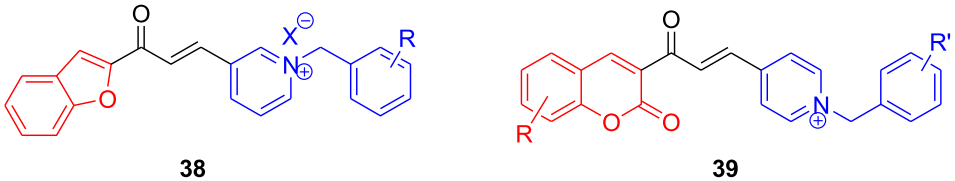

Fig. 16. General structure of benzofuran-based chalconoids (**38**) and *N*-benzyl pyridinium modified coumarin derivatives (**39**).

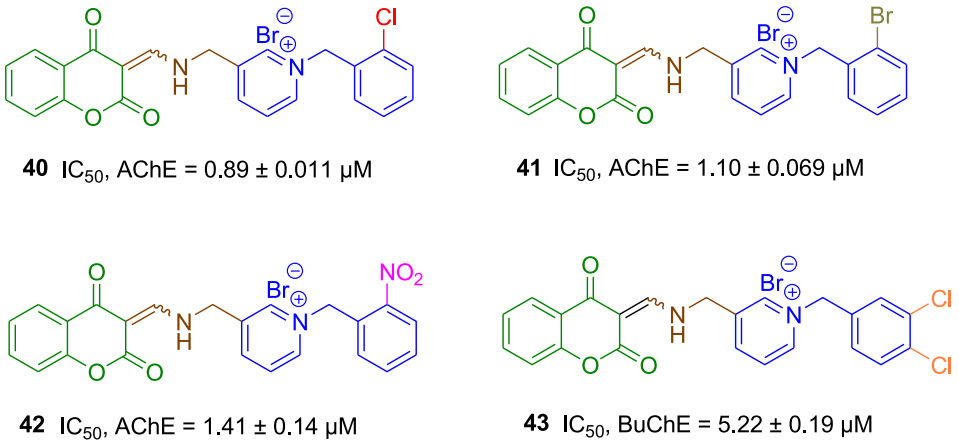

Fig. 17. Structures with their IC_{50} values of AChE inhibitors (**40–42**) and BuChE inhibitor (**43**).

2.8. Coumarin-dithiocarbamate hybrids

Pharmacologically active coumarin analogs play significant role even in the biological activities related to neurological disorders [46,47]. Coumarin was able to form π-π interactions by binding to PAS of AChE [48]. Also, dithiocarbamate was used as significant pharmacore for drug design [49]. A series of coumarin-dithicarbamate derivatives were engineered in order to enhance the anti-AD properties (Fig. 25); and then evaluated for their anti-cholinesterase and Aβ-aggregation activities [50].

Using donepezil and tacrine as reference compounds, inhibitory values against cholinesterases were determined for synthesized compounds and the inhibitory values of the potent derivatives were provided in Table 3. In general, cyclic amines as side chain have exhibited higher activity than that of acyclic amines. Piperidine side chain derivatized compound **63** has given the best result.

Hence, keeping the basic structure of the molecule same; the length of carbon linker was extended gradually from two carbons to eight carbons to afford the potent derivatives **66–69**. Among them, the derivative **67** (Fig. 26) with four carbon linker yielded highest result; it was 1.5 fold higher potent than donepezil. The derivative with eight carbon linker which is not tabulated has not shown good activity. In the molecular docking studies of compound **67** (Fig. 27), coumarin moiety was reported to bind to the PAS of AChE, thereby establishing π-π stacking interaction with Trp286 and hydrogen bond with Ser293 in PAS. In addition to this, the piperidinyl dithiocarbamate moiety has hydrophobic interactions with Gly448, Trp86, Try336 and Gly121 of AChE.

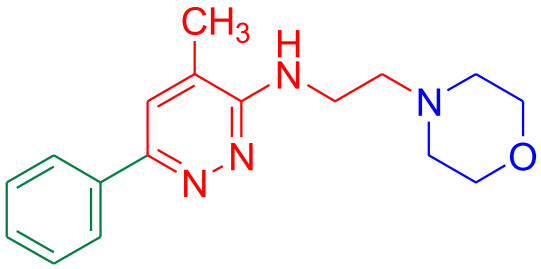

Fig. 19. Structure of antidepressant drug minaprine.

The final compounds were found to be only moderate or weak

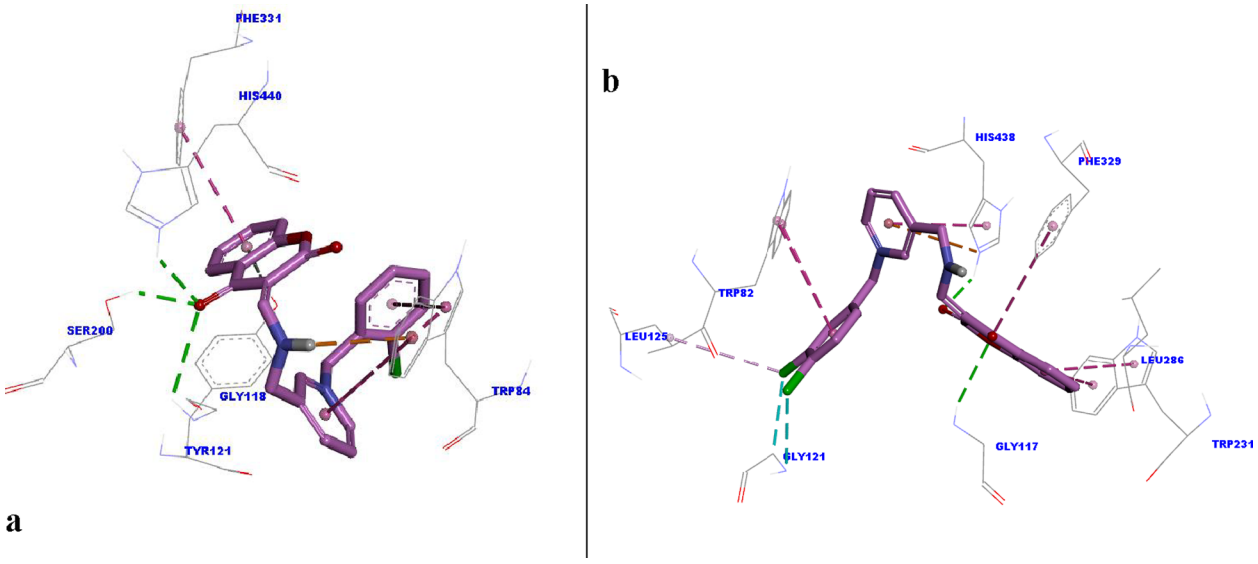

Fig. 18. Interaction of compound **40** in the active site of AChE (**a**), compound **43** in the active site of BuChE (**b**) [34].

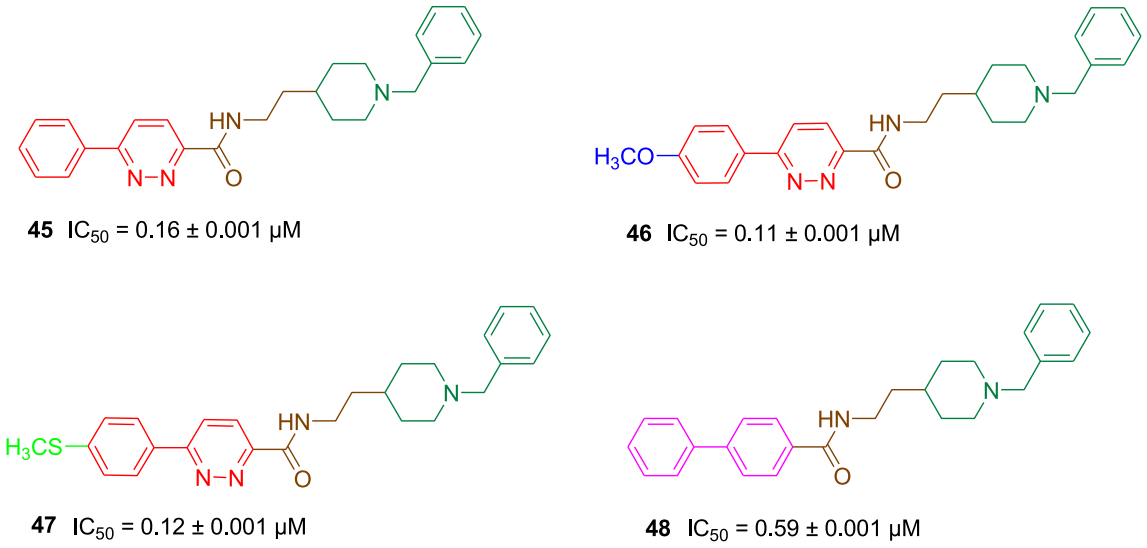

Fig. 20. Demonstration of structures of most potent AChE inhibitors.

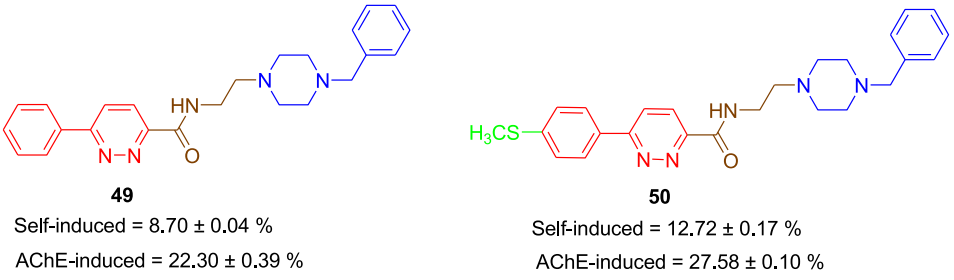

Fig. 21. Structures of potent Aβ-aggregation inhibitors with percentage inhibitions.

inhibitors of BuChE and they were considered to be selective AChE inhibitors.

The synthesized compounds have exhibited moderate to good activity in the self-induced $A\beta_{1\text{-}42}$ aggregation inhibitory activity using curcumin as reference compound at 25 μM concentration. Most of them were potent inhibitors; however exclusively compounds **65** (43.53%), **67** (40.19%) and **68** (40.03%) stood as the best $A\beta_{1\text{-}42}$ aggregation inhibitors. Percentage inhibition of these compounds was better than that of curcumin (39.62 ± 3.35%).

2.9. Coumarin-dithiocarbamate derivatives

Coumarin derivatives have been described as AChE inhibitors by binding to PAS of AChE [51]. Coumarin could occupy the substrate cavity of MAO-B; hence it possesses MAO-B inhibitory activity [52]. An increasing number of MTDLs possessing both AChE and MAO-B inhibitory activity was prepared using coumarin structural unit [53]. Recently a research team has reported that dithiocarbamate moiety has the ability to bind to CAS of AChE [50]. Special properties of coumarin and dithiocarbamate moieties have been considered and design of coumarin-dithicarbamate hybrid compounds **70** (Fig. 28) was undertaken [54]. The title compounds were evaluated for cholinesterase and MAOs inhibitory activities.

With the general structure **70**, the designed derivatives were evaluated for *ee*AChE, *eq*BuChE, *h*MAO-A and *h*MAO-B inhibitory activities. In those compounds **71** (IC_{50} = 0.082 ± 0.003 μM), **72** (IC_{50} = 0.088 ± 0.007 μM), **73** (IC_{50} = 0.061 ± 0.002 μM) (Fig. 28) were reported as descent AChE inhibitors. In particular, compound **73**

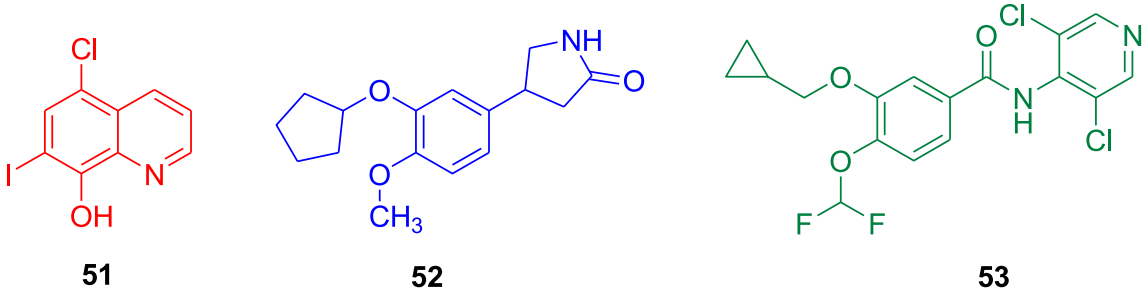

Fig. 22. Structures of Aβ-aggregation inhibitor (**51**) and PDE4D inhibitors (**52** and **54**).

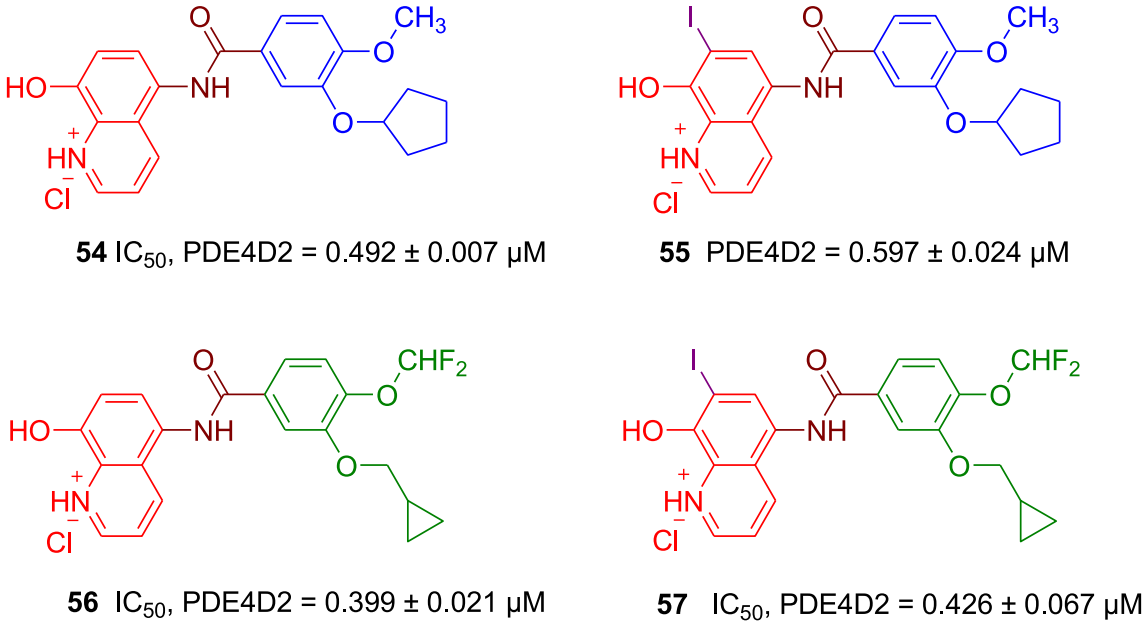

54 IC_{50}, PDE4D2 = 0.492 ± 0.007 μM

55 PDE4D2 = 0.597 ± 0.024 μM

56 IC_{50}, PDE4D2 = 0.399 ± 0.021 μM

57 IC_{50}, PDE4D2 = 0.426 ± 0.067 μM

Fig. 23. Structures of potent PDE4D2 inhibitors with their inhibitory values.

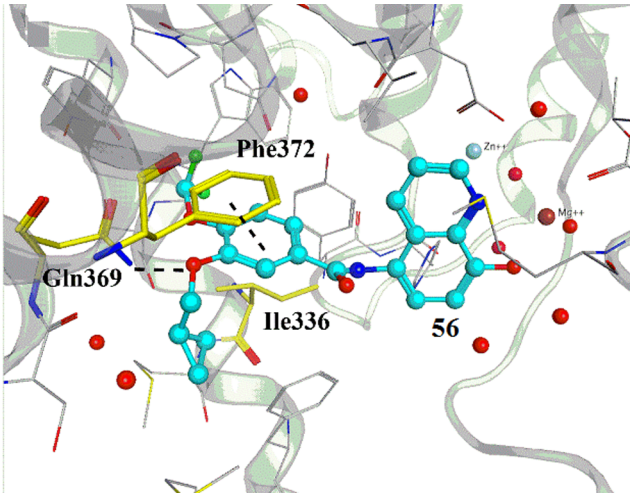

Fig. 24. Binding mode of the compound **56** with PDA4D [45].

with chloro group at 3-position and methyl at 4-position has yielded lowest IC_{50} value.

Most of the synthesized compounds shown moderate inhibitory values towards BuChE compared to reference compound donepezil. However, only a few compounds were active with respect to *h*MAO-A and *h*MAO-B inhibitory activity. Compound **71** possessing methyl motifs at 3- & 4- positions found to be most potent *h*MAO-A inhibitor (IC_{50} = 0.654 ± 0.021 μM). While compounds **71** (IC_{50} = 0.662 ± 0.023 μM), **72** (IC_{50} = 0.251 ± 0.007 μM), **73** (IC_{50} = 0.363 ± 0.009 μM), and **74** (IC_{50} = 0.336 ± 0.012 μM) (structure similar to **71** but three carbon linker) were found to be potent MAO-B inhibitors.

Because of best activity of **73**, it was considered for redesign and evaluated for their anti-AD properties. While retaining the coumarin moiety, modification of carbon spacer was made in the carbamate moiety; where in piperidine was also substituted by different secondary amines to afford potent compounds **74–78** (Table 4). The derivative with 2-methylpiperidine secondary amine, **74** was the best AChE inhibitor.

There was no much improvement in the BuChE inhibitory activities. However, a little enhancement was seen in case of *h*MAO-A inhibitory values; wherein compounds **79** (IC_{50} = 5.85 ± 0.18 μM) and **80** (IC_{50} = 2.09 ± 0.08 μM) (Fig. 29) were notable. While great improvement was observed in anti-MAO-B inhibitory values in which compound **79** (IC_{50} = 0.101 ± 0.024 μM) with 4-isopropyl-*N*-piperazine was better inhibitor compared to reference compound rasagiline (IC_{50} = 0.138 ± 0.004 μM). Few selected compounds were allowed to inhibit *h*AChE enzyme and the results revealed that 2-methyl-*N*-

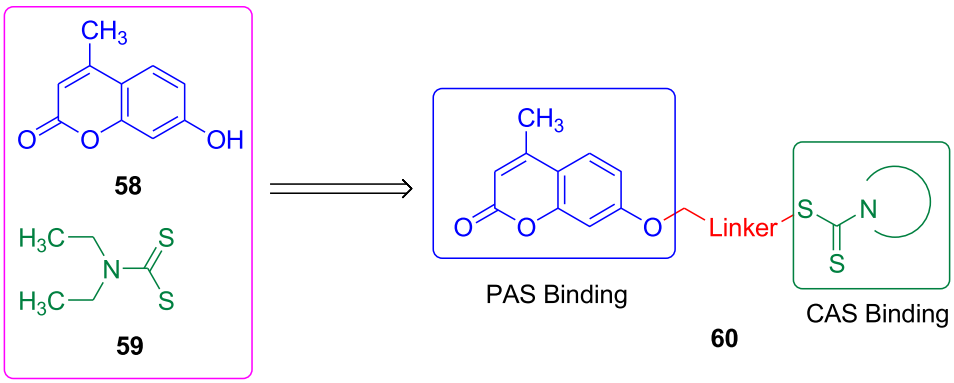

Fig. 25. Illustration of design strategy of coumarin-dithiocarbamate derivatives [50].

Table 3
AChE and BuChE inhibitory values of cumarin-dithiocarbamate derivatives.

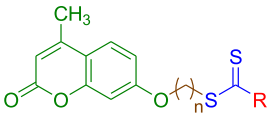

Compd	n	R	AChE IC_{50} (μM)	BuChE (%)
61	2		1.94 ± 0.56	10.89 ± 1.58
62	2		0.89 ± 0.11	Not active
63	2		0.47 ± 0.23	37.24 ± 5.13
64	2		1.99 ± 0.06	28.10 ± 2.82
65	2	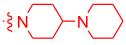	1.16 ± 0.12	24.27 ± 2.06
66	3		0.29 ± 0.07	31.24 ± 3.12
67	4		0.027 ± 0.002	15.29 ± 1.95
68	5		0.21 ± 0.03	10.10 ± 1.02
69	6		0.61 ± 0.08	6.21 ± 0.99
Donepezil		-	0.041 ± 0.001	IC_{50} = 4.22 ± 0.20 μM
Tacrine		-	0.43 ± 0.02	IC_{50} = 0.021 ± 0.001 μM

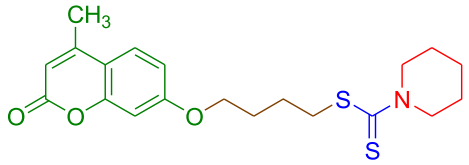

67

Fig. 26. Structure of most potent coumarin-dithiocarbamate derivative.

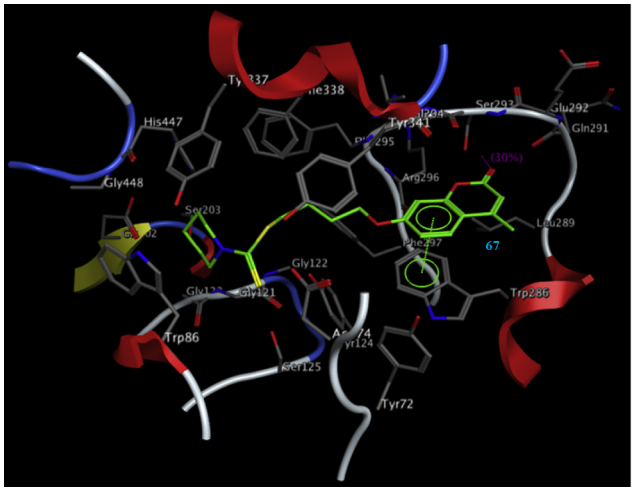

Fig. 27. Docking model of compound **67** with *h*AChE [50].

piperazine analog **74** (IC_{50} = 0.0089 ± 0.0004 μM) stood top in inhibition activity.

2.10. Miconazole analogues

BuChE has been reported to play significant role in A*β*-aggregation during initial stages of plaque formation [55]. Selective BuChE inhibition has described to abate *β*-amyloid precursor secretion and *β*-amyloid and subsequently useful for AD treatment [56]. Indoleamine 2,3-dioxygenase 1 (IDO1) induction was reported as a pathogenic factor of A*β* related inflammation in AD [57]. Anti-fungal agent, miconazole **81** (Fig. 30) was reported as AChE and BuChE inhibitor [58]. It was also possessed the properties to inhibit IOD1 efficiently [59]. Hence, in order to develop efficient drugs for AD treatment miconazole derivatives were prepared as BuChE/IOD1 dual inhibitors [60].

The title compounds were tested for Anti-AChE and BuChE inhibitory activities using miconazole as reference compound. Most of the compounds were comparatively AChE active but the compounds **82–85** were most notable AChE inhibitors; where in compounds **82** & **84** were as potent as miconazole (IC_{50} = 21.4 ± 3.5 μM) and compounds **83** & **85** (Fig. 31) exhibited better activity than that of reference compound miconazole. Compared to miconazole anti-BuChE activity (IC_{50} = 6.8 ± 1.4 μM), the synthesized molecules have shown moderate inhibitory values. However, compound **86** (Fig. 32) has exhibited comparable inhibitory activity (IC_{50} = 8.3 ± 1.6 μM).

Most of the synthesized compounds have resulted comparable inhibitory activities with respect to IOD1 activity. The compounds **82** (IC_{50} = 1.1 ± 0.2 μM), **87–89** (Fig. 32) have exhibited descent activity. In that, compound **82**, **87** and **88** were better than even miconazole. The results revealed that para-position has much beneficial

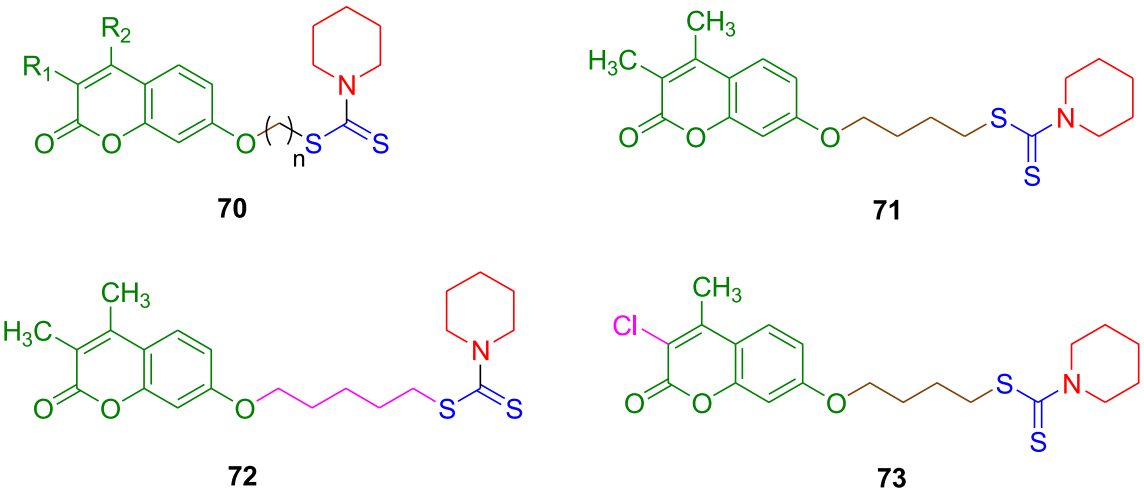

Fig. 28. General structure of coumarin-dithiocarbamate derivatives (**70**) and structures of potent coumarin-dithiocarbamate derivatives (**71–73**).

Table 4
*Ee*AChE and *eq*BuChE inhibitory values of coumarin-dithiocarbamate derivatives.

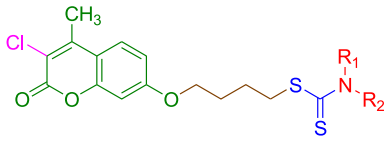

Compd	NR_1R_2	*ee*AChE	*eq*BuChE
		IC_{50}(μM)	% inhibition
74		0.0068 ± 0.0002	21.94 ± 1.01
75		0.044 ± 0.002	23.28 ± 0.87
76		0.217 ± 0.006	8.93 ± 0.41
77		0.167 ± 0.008	39.11 ± 1.80
78		0.386 ± 0.014	16.08 ± 0.64
Donepezil	-	0.041 ± 0.001	4.22 ± 0.20

effect. Molecular docking studies of the most potent compounds have shown favorable interactions with the enzymes and thereby supporting the biological activity results.

2.11. Isoflavone derivatives

Histamine and acetylcholine are prominent neuroconducters in CNS associated with memory and cognitive function *via* histamine 3 receptor

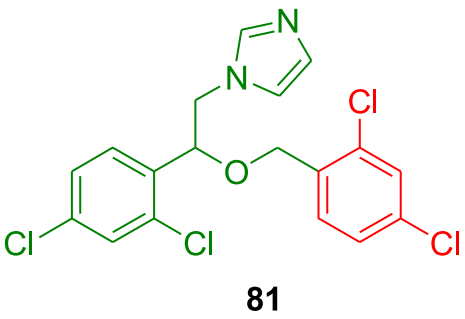

Fig. 30. Structure of anti-fungal agent micanozole.

(H3R) and AChE respectively [61,62]. Constitutive H3R activation was reported to inhibit neurotransmitter release and subsequently leading to brain disorders such as AD. ABT238, **90** and GSK-239512, **91** (Fig. 33) were reported as selective antagonists of H3R. Some studies have reported that isoflavone derivatives as cholinesterase inhibitors [63,64]. The H3R antagonists and isoflavone derivatives have given inspiration for synthesis of a series of isoflavone derivatives as AChE/H3R dual inhibitors [65].

Using cholinesterase inhibitors donepezil and rivastigmine as reference compounds; the synthesized compounds were evaluated for AChE and BuChE inhibitory activities. Compounds **92–95** (Fig. 34) were found to be most potent AChE inhibitors. In particular compound **94** with *N*-ethyl-*N*-methylamine moiety at 7-position was found to exhibit better activity compared to reference compound donepezil (IC_{50} = 0.084 ± 0.0003 μM). From the above activity the optimal carbon linker found to be four carbon alkyl chain between isoflavone and secondary amine. Compound **92** possessing tacrine as substituent exhibited potent BuChE inhibitory activity comparable to reference compound rivastigmine (IC_{50} = 0.058 ± 0.001 μM) and a few compounds have inhibited moderate activity.

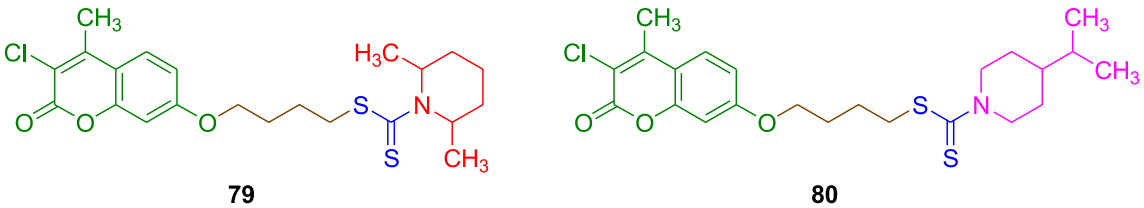

Fig. 29. Structures of most potent MAO inhibitors.

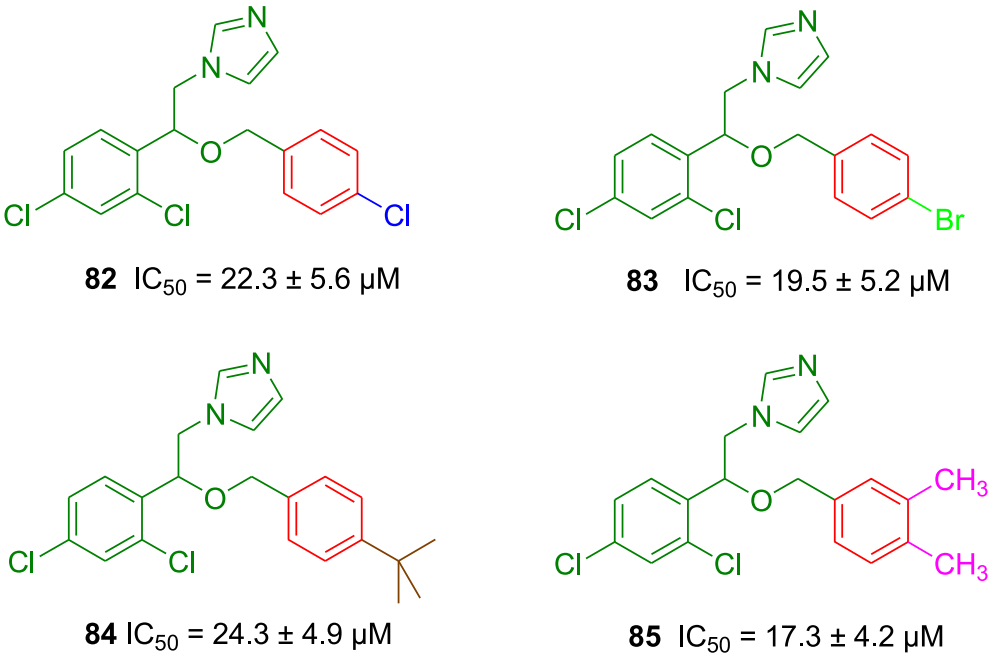

Fig. 31. Structures of potent miconozole derivatives with anti-AChE inhibitory values.

AChE inhibitors have continued to show inhibitory activity even towards H3R. Surprisingly, two compounds **93** (IC_{50} = 0.41 ± 0.01 μM) and **94** (IC_{50} = 0.27 ± 0.004 μM) were found to exhibit higher activity compared with reference compound thioperamide (IC_{50} = 1.03 ± 0.01 μM). Compound **93** was approximately 2.5 fold potent and **94** with fourfold activity compared to reference compound. While, compound **95** has bestowed descent activity (IC_{50} = 1.94 ± 0.01 μM). It was observed that the results were obtained by substitution of piperidine on both sides of isoflavone and optimizing the carbon to four atoms.

In the molecular modeling, the isoflavone of **94** (Fig. 35) was found to possess π-π interactions with Trp371, Tyr115 and Tyr374 in addition to a salt bridge with Glu206 that has contributed for overall stabilization. It has formed hydrogen bond interactions with amino acid residues Tyr70 and Gly117. The aromatic ring of **94** could form π-π interactions with Tyr34 and Phe331 in the catalytic cleft.

2.12. Piperidinehydrazide-hydrazones

N-Benzylpiperidine moiety, a fragment of donepezil possesses favorable interactions with AChE active site and its protonable nitrogen plays significant role in enzyme-ligand interactions [66,67]. The

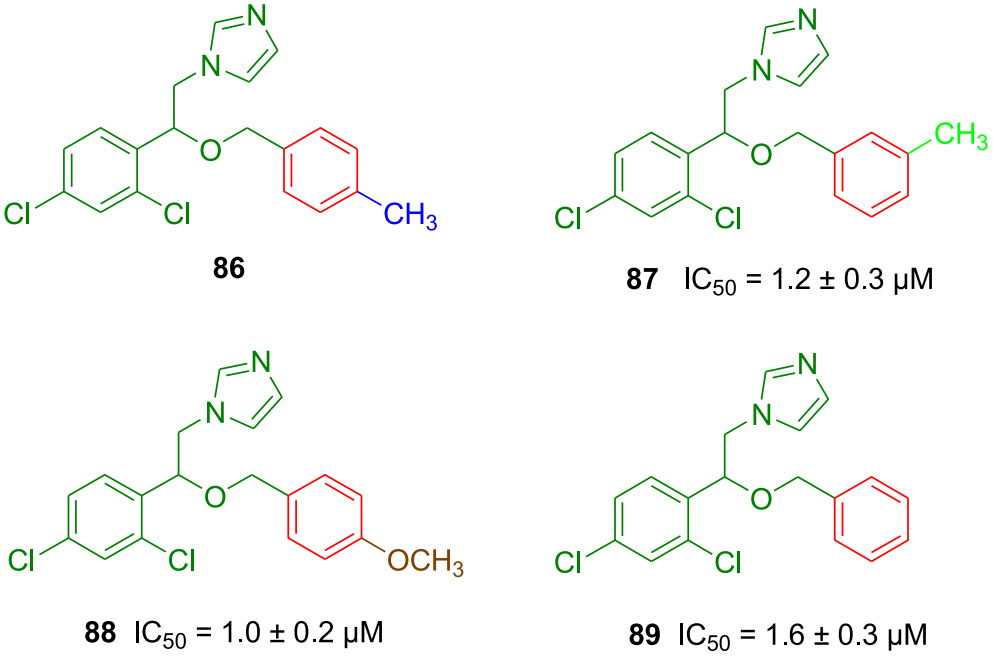

Fig. 32. Structures of potent BuChE inhibitor (**86**) and potent IOD1 inhibitors (**87**–**89**).

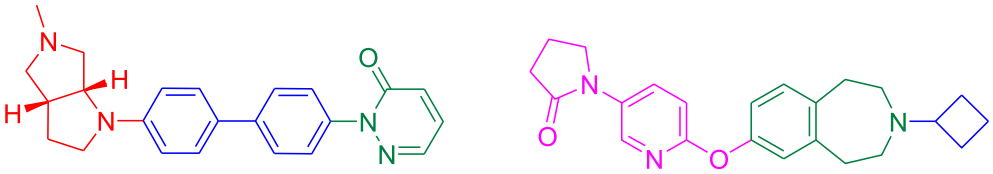

90 91

Fig. 33. Structures of H3R antagonists.

compounds comprising hydrazide-hydrazone functionalities were reported to exhibit anti-AD properties such as antioxidant properties [68]. A series of novel piperidine hydrazine-hydrazone derivatives were designed, synthesized and their AChE, BuChE, Aβ_{42} inhibitory properties were evaluated [69].

Using the reference compounds tacrine HCl, galantamine and rivastigmine, inhibitory activities were determined for synthesized compounds on *ee*AChE and *eq*BuChE enzymes. Annoyingly, Most of the derivatives were AChE inactive compared to tacrine and galantamine and inhibitory values were out of the boundary. However, a few compounds exhibited good activity comparable with that of rivastigmine (IC_{50} = 10.87 ± 0.24 μM). Among them compound **96** was twofold higher potent (IC_{50} = 5.68 ± 0.48 μM) than rivastigmine. In case of *eq*BuChE inhibition, some compounds shown closer inhibitory values to that of galantamine and rivastigmine but no single derivative could reach tacrine. However, the most potent *eq*BuChE inhibitor **97** (IC_{50} = 0.81 ± 0.03 μM) was approximately 200 times less potent than tacrine (IC_{50} = 0.0098 ± 0.0002 μM) (Fig. 36).

Aβ_{42}-Aggregation inhibition activity was performed using curcumin as reference compound at 100 μM concentration. Moderate inhibition was observed in which two derivatives **96** (79.34 ± 1.04%) and **98** (69.99 ± 0.86%) were notable inhibitors at 100 μM compared to curcumin (98.38 ± 0.03%). While at 25 μM concentration, compounds **96** (53.18 ± 0.85%) and **97** (46.03 ± 0.99%) were potent inhibitors compared to curcumin (92.79 ± 0.10%).

The synthesized compounds were also tested for *h*AChE and *h*BuChE inhibitory activity; where in only compounds **99** (IC_{50} = 9.56 ± 0.33 μM) and **100** (IC_{50} = 3.23 ± 0.13 μM) (Fig. 37) had comparable activity towards *h*AChE and *h*BuChE enzymes respectively.

2.13. Pterostilbene β-amino alcohol derivatives

A natural compound pterostilbene (trans-3,5-dimethoxy-4′-hydroxystilbene) **101** (Fig. 38), obtained from blue berries possesses some important biological properties such as self-induced Aβ-aggregation and

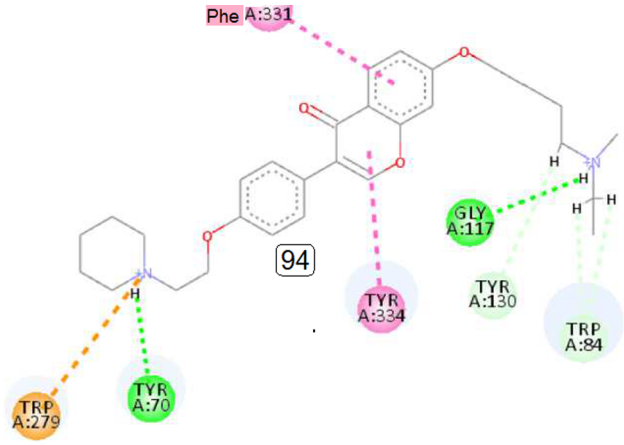

Fig. 35. Representation of compound **94** with AChE [65].

neuroprotection [70,71]. Tertiary amine moiety was reported as cholinesterase inhibitor *via* H-bond formation between compound **102** and CAS of AChE; thereby inhibiting AChE [72,73]. Hence pterostilbene β-amino alcohol derivatives **102** (Fig. 38) were designed by appending pterostilbene and tertiary amine structural units on carbon chain bearing chiral hydroxyl group [74].

There was no remarkable AChE and BuChE inhibitory activity found when compared to reference compounds donepezil and rivastigmine. Only one compound **103** (Fig. 39) exhibited potent anti-AChE activity among the evaluated compounds which was twofold less potent (IC_{50} = 24.04 ± 1.48 μM) compared to rivastigmine (IC_{50} = 12.50 ± 1.60 μM). In case of BuChE inhibitory activity, three compounds were active and remainder was completely inactive at that concentration. Among them compound **104** (IC_{50} = 8.3 ± 1.67 μM) stood as the best compared to donepezil (IC_{50} = 20.7 ± 1.36 μM).

In the self-induced Aβ-aggregation inhibition activity, moderate to most remarkable activities were observed. Compared to reference

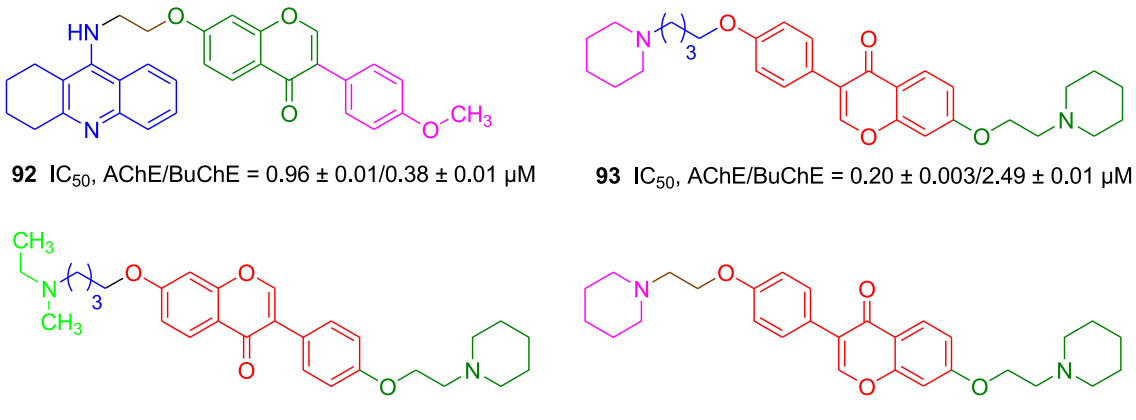

92 IC_{50}, AChE/BuChE = 0.96 ± 0.01/0.38 ± 0.01 μM

93 IC_{50}, AChE/BuChE = 0.20 ± 0.003/2.49 ± 0.01 μM

94 IC_{50}, AChE/BuChE = 0.081± 0.0002/2.89 ± 0.02 μM

95 IC_{50}, AChE/BuChE = 0.35 ± 0.01/2.92 ± 0.01 μM

Fig. 34. Structures of potent AChE/BuChE inhibitors.

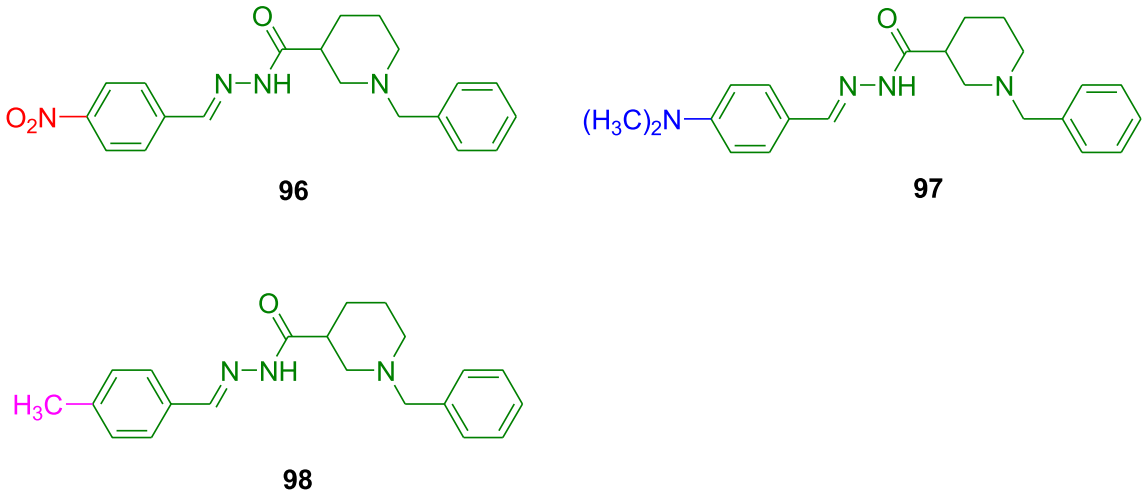

Fig. 36. Structures of piperidine hydrazide-hydrazones derivatives as potent *ee*AChE/*eq*BuChE inhibitors.

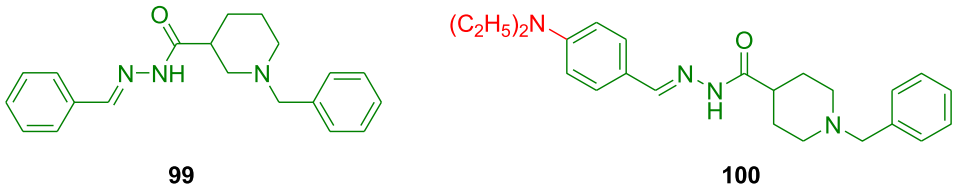

Fig. 37. Structures of potent *h*AChE inhibitor (**99**) and potent *h*BuChE inhibitor (**100**).

compounds pterostilbene (36.21 ± 1.9%), resveratrol (42.86 ± 1.7%) and curcumin (44.25 ± 1.5%), derivatives **104**, **105** and **106** (Fig. 40) have exhibited better inhibition percentages (59.72 ± 1.9%), (58.43 ± 1.5%) and (55.87 ± 0.9%) respectively. The results revealed that benzylamine substituted derivatives exhibited higher activities compared to aliphatic amine substituted compounds.

2.14. Flavonoid–*N*,*N*-dibenzyl(*N*-methyl)amine hybrids

Several studies have demonstrated that there is correlation between inhibition of BACE1 and low levels of pathogenic Aβ peptides [75,76]. Overexpression of Lipoxygenase-5 (LOX-5) enzyme present in CNS leads to both tau and amyloid deposits [77]. Reduction of amyloid and tau deposits was possible by the use of LOX-5 inhibitor zileuton **107** (Fig. 41) [78]. A flavonoid structural unit derived from 4-chromenone or 4-quinolone possesses prominent pharmacological properties such as BACE1 inhibitory activity [79], LOX-5 inhibitory activity [80] and MAO inhibitory activities [81]. *N*,*N*-Dibenzyl(*N*-methyl)amine moiety present in AP2238 **108** has proved to have interactions with CAS of AChE [82]. Taken together, a series of flavonoid–*N*,*N*-dibenzyl(*N*-methyl)amine analogs were designed and synthesized [83].

The synthesized compounds were screened for human cholinesterase inhibition activities using donepezil as reference compound; where in, the derivatives were found to be selective *h*AChE inhibitors. A very weak *h*BuChE inhibition was observed. However potent inhibitory activity was reported for the compounds **109–112** (Fig. 42) and in those, 6,7-dimethoxy analog **112** was most potent compound but 100 times less potent than donepezil (IC_{50} = 0.01 ± 0.002 μM). All the potent compounds possessed chromone moiety in which compound with 6,7-dimethoxy moiety and chromone unit attached to benzene at 4′-position has shown greatest impact on AChE inhibitory activity.

In the *h*MAO-A and *h*MAO-B activities, compound **109** (IC_{50} = 1.6 ± 0.4 μM) was found to be approximately fourfold higher potent compared to reference compound iproniazid (IC_{50} = 6.7 ± 0.8 μM) and others were weak *h*MAO-B inhibitors. Whereas, derivative **112** (IC_{50} = 8.1 ± 0.4 μM) had possessed almost comparable MAO-B inhibitory activity with that of iproniazid (IC_{50} = 7.5 ± 0.4 μM). Structure activity relationship of MAO inhibitors and AChE inhibitors could be compared as both inhibitory activities were exhibited by similar derivatives.

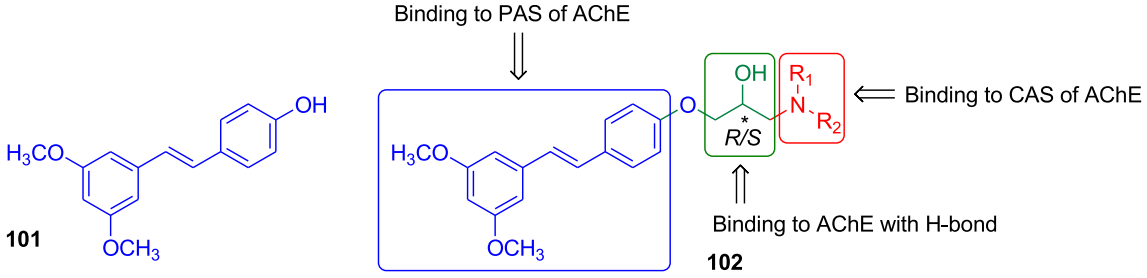

Fig. 38. Structural design of pterostilbene β-amino alcohol derivatives [74].

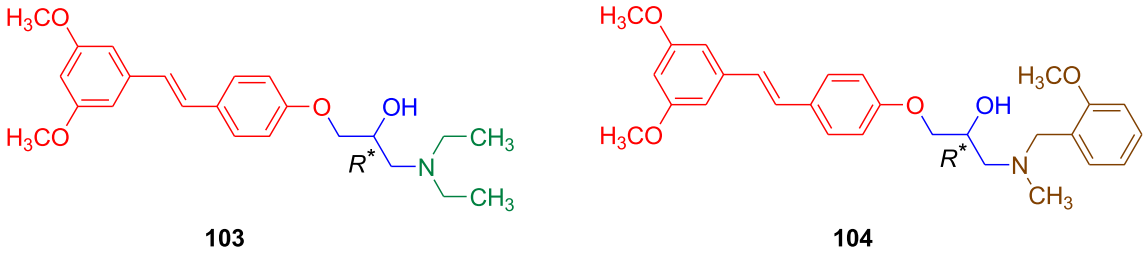

Fig. 39. Structures of potent AChE inhibitor (**103**) and potent BuChE inhibitor (**104**).

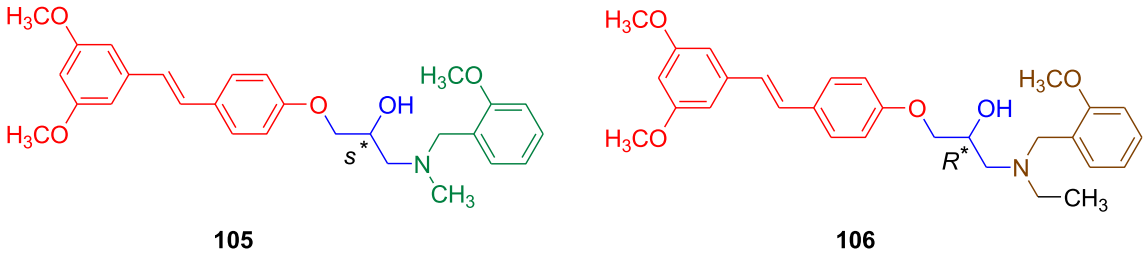

Fig. 40. Depiction of structures of most potent Aβ-inhibitors.

Newly synthesized compounds were evaluated for BACE1 inhibitory activity in which almost all compounds exhibited inhibition percentages below 35%; however a single derivative where in 6,7-dimethoxy-4-chromenone having meta-substitution on benzene ring **113** (Fig. 43) shown around 80% inhibitory activity.

None of the synthesized compounds inhibited *h*LOX-5 effectively compared to reference compounds zileuton and NDGA. The derivative **109** (IC_{50} = 12.4 ± 0.5 μM) was most potent among the tested compounds but its inhibition activity was approximately **100** times less potent compared to zileoton (IC_{50} = 0.15 ± 0.03 μM).

2.15. 1,2,3-Triazolechromenone carboxamide derivatives

Coumarin and 1,2,3 triazole structural moieties were endorsed to have anti-AD properties [84,85]. Coumarin-3-carboxamide derivatives have been reported to show anti-AChE activity [86]. It was demonstrated that 1,2,3-triazole incorporated phenthridinium derivatives **114** and **115** (Fig. 44) possessed remarkable AChE inhibitory activity [87]. Iminochromene-2*H*-carboxamide derivatives having 1,2,3-triazole unit were reported to have BACE1 inhibitory activity [88]. Considering these developments, a series of 1,2,3-triazolechromenone carboxamide derivatives were synthesized and tested for their cholinesterase and BACE1 inhibitory studies [89].

In the AChE inhibitory activity of designed compounds, only a few derivatives have exhibited comparable activity; particularly compound **116** (IC_{50} = 1.80 ± 0.09 μM) possessing benzyl piperidine moiety appended to amide functionality and 3,4-dimethylbenzyl group attached to 1,2,3-triazole was most potent molecule compared to reference compound donepezil (IC_{50} = 0.027 ± 0.002 μM). Alongside, compound **117** was second most potent compound (IC_{50} = 2.04 ± 0.16 μM) with 3,4-dimethylbenzyl moiety connected to 1,2,3-triazole ring (Fig. 45). Whereas, among the tested compounds with respect to BuChE inhibition, derivatives **118** and **119** yielded remarkable results with IC_{50} values 1.71 ± 0.21 μM and 1.85 ± 0.32 μM respectively. The activity of the compounds **118** and **119** was approximately 2.5-fold higher than donepezil (IC_{50} = 4.32 ± 0.65 μM). Both potent molecules were having chlorobenzyl group substituted on 1,2,3-triazole and *N*-propylmorpholine connected to amide functional group. Accordingly, it was hypothesized that 3-chloro or 3,4-dichlorobezyl moiety was very crucial for anti-BuChE activity. Also the presence of *N*-propylmorpholine unit bestowed best BuChE results selectively.

BACE1 inhibitory activity was determined using the reference compound OM99-2; wherein compound **116** (IC_{50} = 0.014 μM) exhibited relatively strongest activity compared to OM99-2 (IC_{50} = 21.13 μM).

Compound **116** was docked with AChE (Fig. 46) in which **116** was exactly positioned in the enzyme active site and allows its interaction with amino acid residues. Planar coumarin fragment has π-π stacking interactions with aromatic amino acids Tyr69 and Trp278; likewise similar interactions were observed for 1,2,3-triazole linker with amino acid residue Trp278. The NH of amide functionality formed hydrogen bond with Tyr120. The hydrophobic cavity of Ile286 and Phe289 allows substituted benzyl group connected to 1,2,3-triazole to accomodate in it. Alongside, formation of π-π interaction of benzyl moiety with Trp83 was possible.

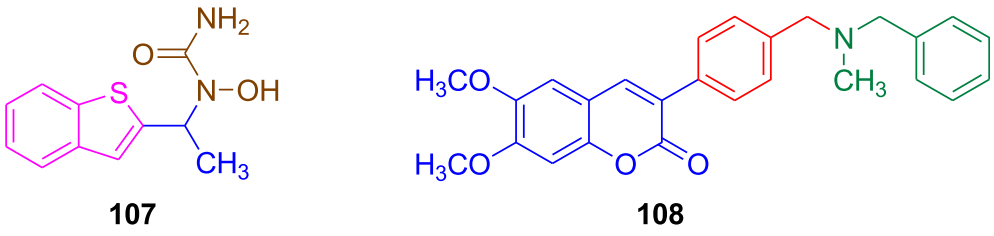

Fig. 41. Structure of LOX-5 inhibitor (**107**) and AChE inhibitor (**108**).

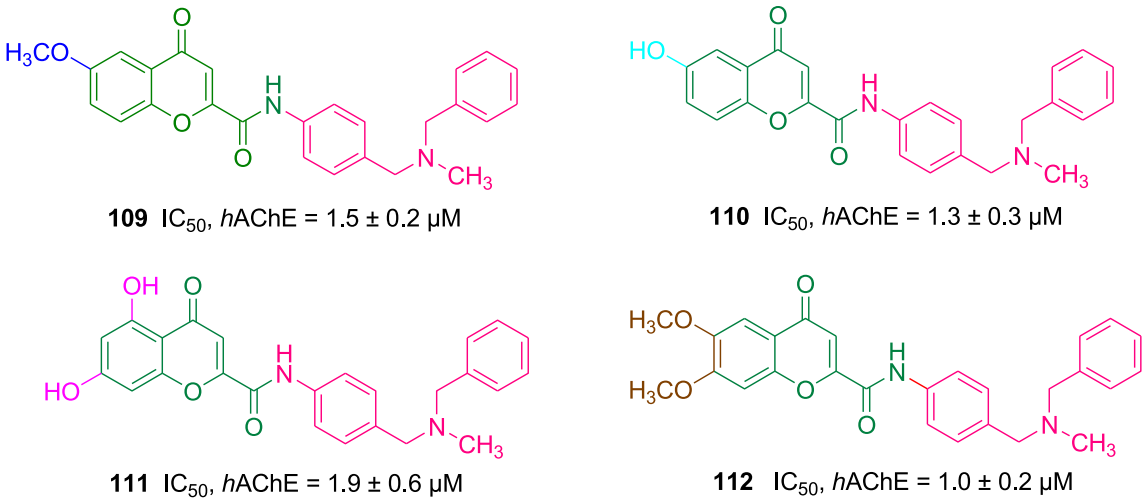

Fig. 42. Structures of significant *h*AChE inhibitors with their IC_{50} values.

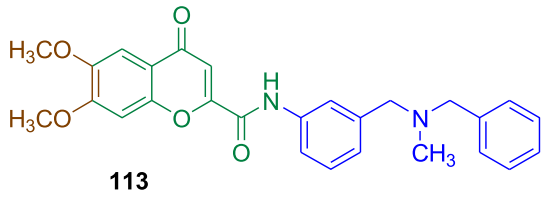

Fig. 43. Structure of potent *h*LOX-5 inhibitor.

2.16. 3-Arylcoumarin derivatives

3-Arylcoumarin derivatives have found to possess MAO inhibitory activity [90,91] and cholinesterase inhibition activity [92] in addition to other prominent pharmacological activities. Likewise, 3-arylcoumarin analogs were engineered and followed by performing cholinesterase and MAO inhibitory activities [93].

Compound **120** (IC_{50} = 3.04 ± 0.32 μM) (Fig. 47) entailing hydroxy groups at meta- & para-positions of (3-aryl) moiety and alongside another two hydroxyl moieties at 7- & 8-positions of coumarin was reported as most potent AChE inhibitory compound compared to donepezil (IC_{50} = 0.021 ± 0.0001 μM). Few compounds were moderate inhibitors and most of them were weak inhibitors. While a few derivatives have shown comparable inhibitory activity with that of reference compound donepezil (IC_{50} = 4.10 ± 0.18 μM); among them coumarin analog **121** (IC_{50} = 2.76 ± 0.18 μM) (Fig. 47) was most potent derivative possessing twice inhibitory potential than that of donepezil. It comprises *p*-hydroxy group on (3-aryl) moiety and hydroxy groups at 5- & 7-positions. The compounds **121** and **122** have selective AChE and BuChE inhibitory properties respectively.

Most of the synthesized compounds were far from reachable, compared to MAO inhibitory activity of the reference compound rasagiline (IC_{50} = 0.125 ± 0.0005 μM). However, AChE inhibitor **120** was also successful in becoming most potent MAO inhibitor (IC_{50} = 27.03 ± 0.50 μM).

2.17. 3-Hydrazinyl 1,2,4-triazine analogs

Acylguanidine **122** was designed as BACE1 inhibitor which could form key H-bond interactions with catalytic dyad and it also reveals that polar group requirement is essential for enzyme's active site inhibition [94]. Recently, 2-thiophene-2-yl-1,2,4-triazine derivatives **123** were demonstrated to exhibit potent BACE1 inhibitory activity, along with antioxidant and metal chelating properties [95]. Amino methylene derivatized with triazole **124** (Fig. 48) was reported with BACE1 inhibition and neuroprotection properties [88]. Collective information about BACE1 inhibitors has inspired for the development of 3-hydrazinyl 1,2,4-triazine analogs [96] and then the synthesized derivatives were allowed to inhibit BACE1 and Aβ-aggregation.

The synthesized compounds have been tested for BACE1 inhibitory activity using OM99-2 as reference compound. The reference compound was active even at nanomolar concentration (IC_{50} = 14. ± 2.8 nM) but the designed molecules exhibited only up to micromolar level; where in compound **125** (IC_{50} = 8.55 ± 3.37 μM)

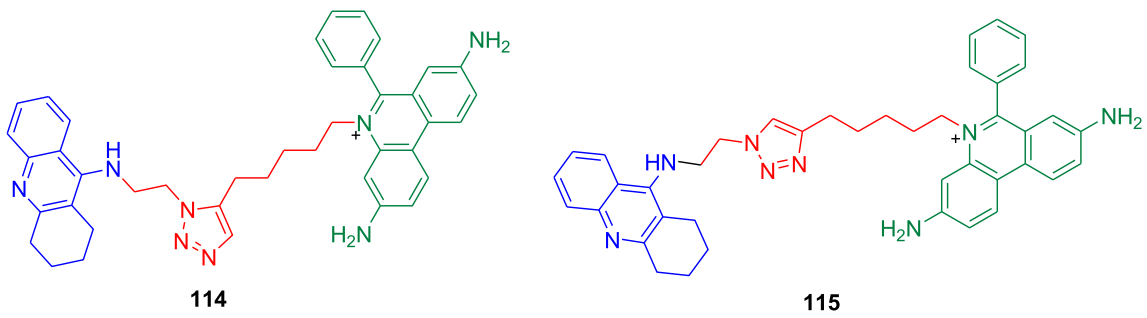

Fig. 44. Structures of 1,2,3-triazole incorporated phenthridinium derivatives.

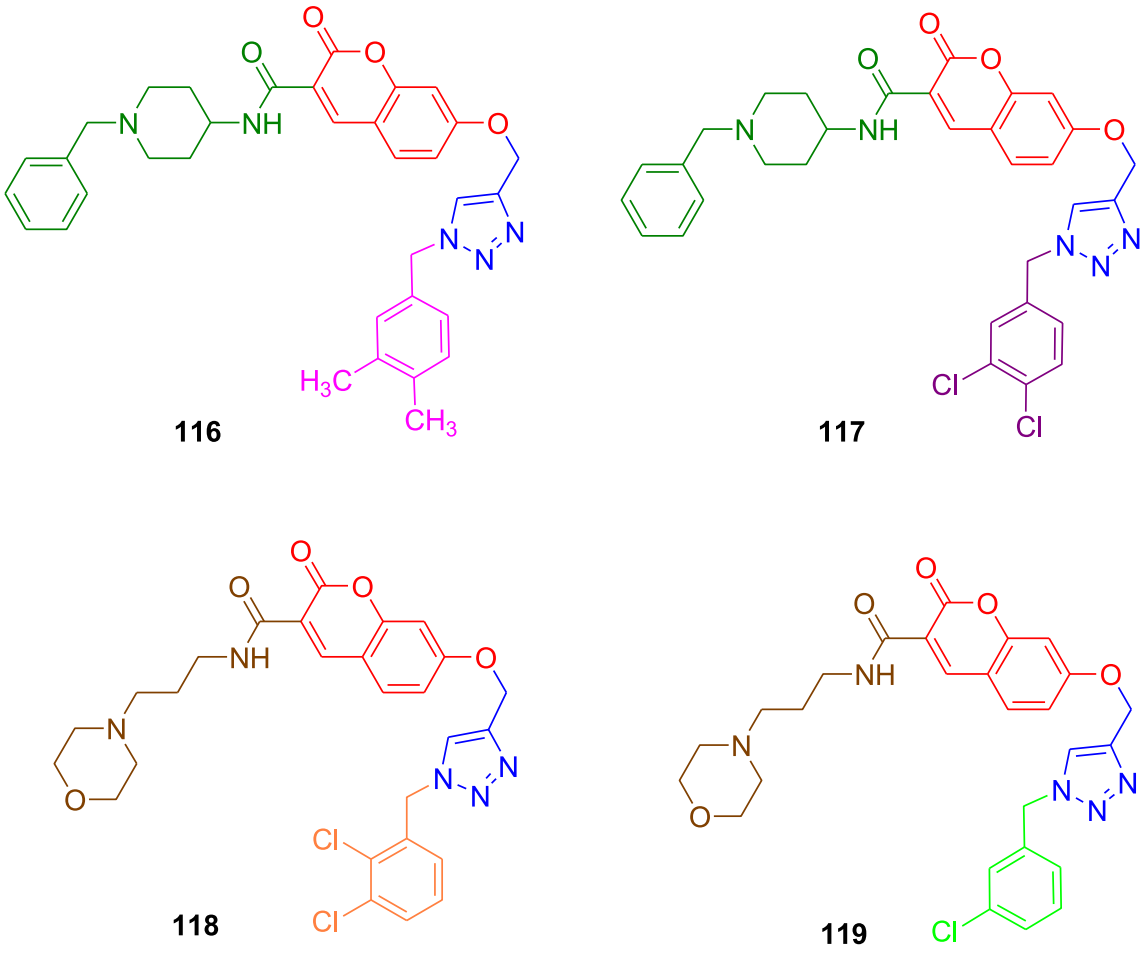

Fig. 45. Illustration of structures of most potent AChE inhibitors (**116** & **117**) and BuChE inhibitors (**118** & **119**).

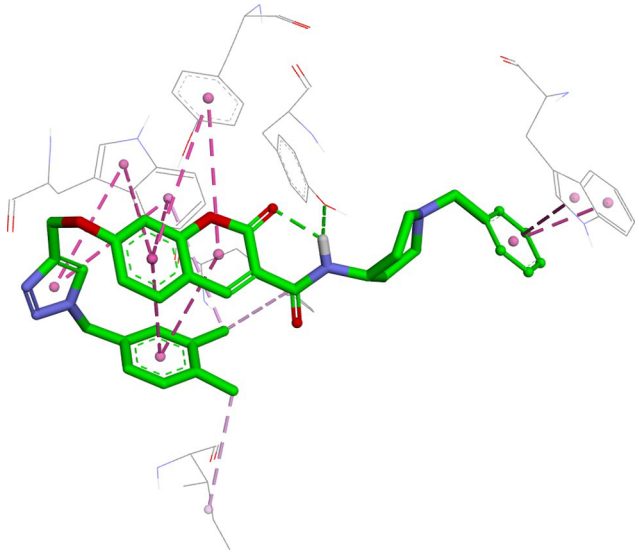

Fig. 46. Demonstration of binding mode of compound **116** with active site of AChE [89].

and **126** (IC_{50} = 11.42 ± 2.01 μM) (Fig. 49) have shown some comparable activity. The compound **125** was the most potent one possessing 4-nitrobenzyl moiety appended to 1,2,3-triazole. Docking studies of compound **125** (Fig. 50) with BACE1 revealed that it has involved in H-bond interaction between hydrazine linker and amino acid residues Asp228 and Asp32. In addition, the triazine ring of compound **125** was accommodated in S1 pocker and formed π-π interactions with Try71.

Regarding $A\beta_{25\text{-}35}$-induced cell death test among the screened compounds, compounds **125** and **126** have shown moderate neuroprotective activity with 10% and 14% respectively at 5 μM.

2.18. Natural products from various origins

Natural products (NPs) have been identified and developed as CNS therapeutic agents [97]. The FDA approved drug galantamine for AD treatment is derived from natural products. Nitrogen containing alkaloids were reported to possess anti-AD properties [98,99]. A large number of natural products were listed as BACE1 inhibitors [100]. Several flavonoids and phenolic acids were described as potential cholinesterase inhibitors [101]. In this regard, few unreported natural products were identified and evaluated for anti-AD characteristics [102].

One hundred and two natural products were analyzed for AChE, BuChE, and BACE1 inhibitory activities. Based on percentage inhibition of the derivatives in which few natural products shown descent activities were tested for their IC_{50} values with respect to AChE, BuChE and BACE1 inhibitions (Table 5).

Among the screened natural products, embelin **127**, L-tetrahydropalmatine **128** and papaverine **129** (Table 5 & Fig. 51) have shown remarkable inhibitory activities. Compound **127** 3-undecyl-1,4-benzoquinone, was most potent natural compound among three *ee*AChE inhibitory compounds. Compound **128** has exhibited descent *rHu*AChE

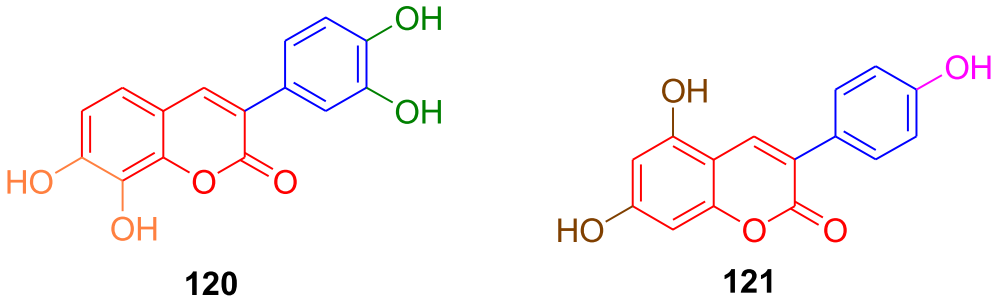

Fig. 47. Structures of most potent AChE/MAO inhibitor (**120**) and BuChE inhibitor (**121**).

inhibitory activity. Surprisingly compound **127** has *eq*BuChE inhibitory as good as the reference compound donepezil. In case of BACE1 inhibition activity again compound **127** stood top and almost sevenfold higher potent compared to reference compound bisdesmethoxy curcumin. However it was approximately 100 times weaker than that of BAE1 inhibitor IV.

2.19. 4′-Hydroxy-flurbiprofen mannich base derivatives

NSAIDs are able to control the release of inflammatory factors and oxygen free radicals formed by Aβ-deposition [15]. For instance flurbiprofen **130** was largely utilized as NSAID and it was also reported to exhibit $A\beta_{1\text{-}42}$-deposition and τ-protien inhibitory properties [103]. 4′-Hydroxy-flurbiprofen-chalcone derivatives have shown good Aβ-aggregation inhibitory and antioxidant activities [104]. Phenolic mannich base analogs **131** (Fig. 52) were reported to possess remarkable metal chelating, antioxidant and AChE inhibitory activities [105,106]. In view to develop descent multifunctional drugs for AD treatment, 4′-hydroxy-flurbiprofen mannich base derivatives were synthesized; subsequently their anticholinesterase, Aβ-aggregation inhibitory activities have been determined [107].

Using flurbiprofen, curcumin and donepezil as reference compounds self-induced and Cu^{2+}-induced Aβ-aggregation inhibitory activities were performed. Most of the derivatives were as potent as the reference compound curcumin (41.30 ± 0.90%) in case of self-induced Aβ-aggregation activity. In that, compound **132** has exhibited significant activity (65.03 ± 4.58%) which has 1.5-fold better activity compared to curcumin. Among the Cu^{2+}-induced inhibitors, moderate activity was shown by majority of compounds; however only one derivative **133** (42.52 ± 2.35%) (Fig. 53) was most potent compared to flurbiprofen (7.56 ± 0.21%) and curcumin (67.20 ± 1.30%). From the results, it was evident that potent molecules possess flurbiprofen moiety derivatized with *N*-ethyl benzylamine. Whereas aliphatic amine derivatized molecules exhibited relatively weaker activity.

Regarding *ee*AChE and *Rat*BuChE inhibitory activities performed using donepezil as reference compound, few derivatives have shown comparable AChE activity; while compound **134** was remarkable inhibitor possessing threefold higher activity (45.50 ± 0.58%) compared to lead compound flurbiprofen (15.60 ± 1.02%). Likewise, compound **134** (16.30 ± 1.65%) was also a descent inhibitor of BuChE among other derivatives. Its activity was almost comparable to donepezil (20.70 ± 1.36 μM) and others were weak inhibitors. Further, *N*-alkyl-benzylamine moiety has shown its impact towards the cholinesterase inhibitory activities also.

Molecular docking studies of remarkable Aβ-aggregation inhibitor **132** (Fig. 54) in active site of Aβ has shown anchoring of dimethylamino group and ester groups of compound **132** with Leu17, Leu34, Ile31 *via* hydrophobic interactions. The *p*-dimethylamino-benzyl amine motif and biphenyl moiety have binding affinities with His13 and Phe20 through perpendicular π-π interactions.

2.20. Chalcone mannich base derivatives

Selegiline **135** associated with AD treatment has been reported as selective MAO-B inhibitor [108]. Chalcones, *trans* 1,3-diphenyl-2-propen-1-ones **136** were utilized as precursors of flavonoids and isoflavonoids [109]; and chalcones have shown neuroprotective properties [110]. Some of the synthetic and natural chalcone analogs have been identified as cholinesterase and MAO inhibitors [111,112]. Accordingly, chalcone mannich base derivatives **137**, (Fig. 55) have been designed and screened for anti-AD properties [113].

The synthesized compounds were tested for AChE and BuChE inhibitory activities using donepezil as reference compound. Large number of derivatives shown descent activity; where in the inhibitory activity of potent compounds was depicted in Table 6 & Fig. 56. The most potent inhibitory activity was exhibited by compound **146** which

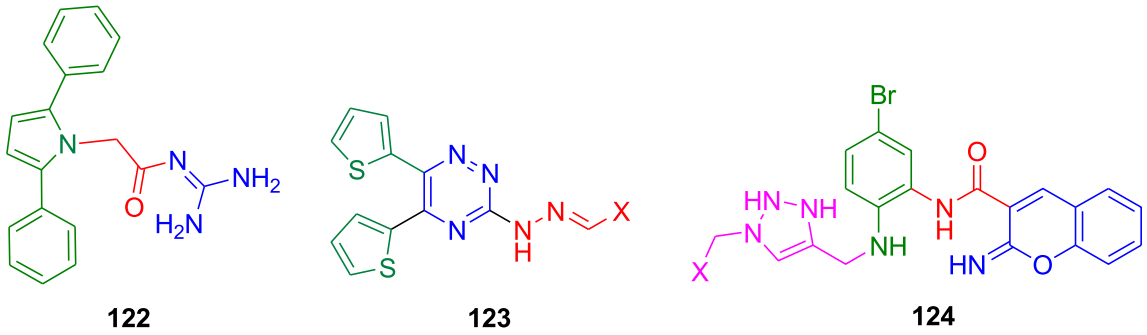

Fig. 48. Structures of potent BACE1 inhibitors for design of new BACE1 inhibitors.

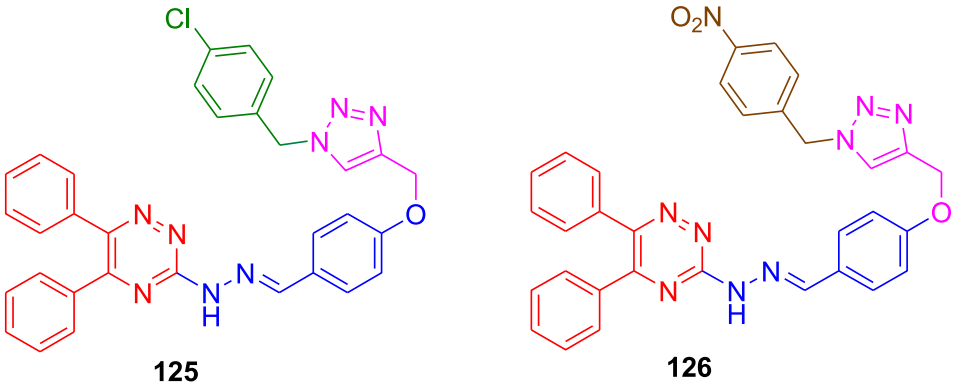

Fig. 49. Structures of the most potent BACE1 inhibitors.

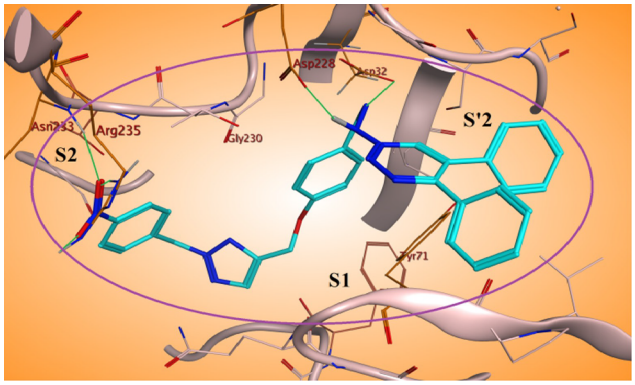

Fig. 50. Illustration of binding of compound **125** with BACE1 [96].

was twice as potent as donepezil (IC_{50} = 0.12 ± 0.01 μM). The potent activity could be related to the amine moiety and its position. All the potent compounds possessed aliphatic amines rather than benzylamine. The compounds **146** and **147** entailing bis-substitution have shown good activity. All the potent compounds have chalcone structural unit except compound **145** which contains propionyl moiety flanked by substituted aryl groups.

The synthesized compounds have scarcely exhibited BuChE inhibitory activity. Most of them were weak inhibitors in which compound **145** (29.2 ± 1.20%) has shown relatively better activity.

In the self-induced Aβ-aggregation inhibitory activity, some of the compounds have shown good percentage inhibitions. Among them derivative **148** (Fig. 57) has exhibited significant inhibitory percentage (68.3 ± 1.3%) better than the reference compound curcumin (51.5 ± 0.9%). Whereas the AChE inhibitor **147** (61.5 ± 1.1%) was also a potent Cu^{2+}-induced Aβ-aggregation inhibitor which was just comparable to curcumin (67.2 ± 1.3%).

MAO-A & MAO-B Inhibitory activities were determined for the designed derivatives using the reference compounds clorgyline, rasagiline and iproniazid. The synthesized compounds were selective MAO-B inhibitors which was evident from poor MAO-A percentage inhibition values. Derivative **142** (63.4 ± 1.3%) was only compound with descent MAO-A inhibitory percentage. However, most of the compounds have shown excellent MAO-B inhibitory activity. Compound **148** bestowed with significant activity (IC_{50} = 0.14 ± 0.61 μM); most potent among the good inhibitors was compound **149** (Fig. 57) with IC_{50} value 0.14 ± 0.14 μM.

2.21. Tetrahydroacridine derivatives

Tacrine (9-amino-1,2,3,4-tetrahydroacridine, THA) was FDA approved drug for its anti-AChE and anti-BuChE properties in AD treatment [114]. However due to its menacing side effects such as hepatoxicity, it has been withdrawn from usage. The tacrine hybrids with flavonoids such as curcumin were shown to exhibit cholinesterase and Aβ-aggregation inhibitory properties [115]. Research has been undergoing based on tacrine to reduce hapatoxicity [116]. A new series of derivatives based on tetrahydroacridine appending to nicotinamide moiety were designed and evaluated for cholinesterase, Aβ-aggregation inhibitory activities [117].

Almost half of the synthesized compounds were very potent (Table 7) and they have shown activity in the nanomolar concentration with IC_{50} values 1.02–4.20 μM which were of higher potencies compared to reference compound tacrine. The most potent compound was tacrine derivative **150** (Fig. 58) possessing three carbon linker flanked by cyclohexaquinoline and dichloronicotinamide moieties. Rough decrease in AChE inhibitory activity was observed with increase in alkyl chain length. However descent activity was seen for the compound **154**

Table 5
Anti-AD properties of potent natural compounds.

Compd no.	Compd	IC_{50} (μM) ± SEM			
		*ee*AChE	*rHu*AChE	*eq*BuChE	BACE1
127	Embelin	2.50 ± 0.082	7.91 ± 0.14	5.45 ± 0.16	2.11 ± 0.33
128	L-Tetrahydropalmatine	2.92 ± 0.56	5.39 ± 0.31	160.43 ± 15.78	nd
129	Papaverine	6.98 ± 0.44	> 100	39.57 ± 0.85	nd
	Donepezil	0.049 ± 0.001	0.032 ± 0.002	5.52 ± 1.05	nd
	Bisdesmethoxy-curcumin	nd	nd	nd	15.23 ± 1.43
	BACE-1 inhibitor IV	nd	nd	nd	0.018 ± 0.001

nd – not determined.

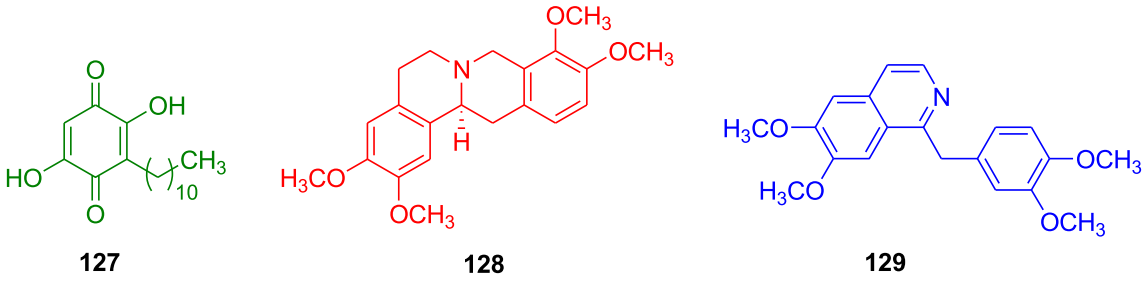

127 128 129

Fig. 51. Structures of potent anti-AD natural molecules.

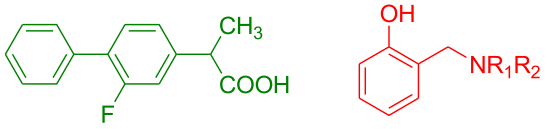

130 131

Fig. 52. Structure of flurbiprofen (**130**), general structure of phenolic mannich bases (**131**).

with longest carbon linker. In case of BuChE inhibitory activity, gradual reduction in the activity has been observed with the highest activity for compound **154** (Fig. 58 & Table 7).

Since compound **150** was most potent AChE inhibitor; it was selected for A*β*-aggregation inhibitory activity at various concentrations. Highest inhibitory activity (46%) was recorded at 50 μM concentration.

Molecular docking studies of AChE inhibitor **150** (Fig. 59) revealed binding of phenyl moiety with gorge wall on the border of PAS and anionic site. H-bond in between amide group and Tyr121, interaction between chlorine atom and Phe288 main chain were possible due to three carbon linker. Longer alkyl chains resulted in decreased binding interactions. While potent BuChE inhibitor **154** (Fig. 60) could form H-bond interaction between amide group and Tyr332, halogen bond between dichloropyridine and Tyr282 in addition to π-π stacking in between tacrine moiety and Trp82.

2.22. Cyclopentaquinoline hybrids

Memantine **155** (Fig. 61) targets *N*-methyl-*D*-asperate receptors and thereby demonstrated for safe use in AD treatment [118]. Tetrahydroacridine derivatives possessing dichloronicotinamide unit have

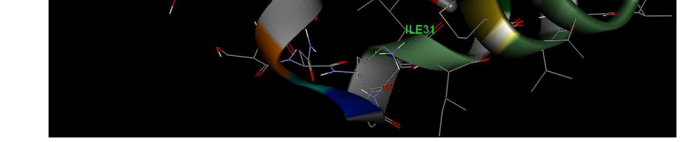

Fig. 54. Demonstration of binding interactions of potent A*β* inhibitor **132** in A*β* active site [107].

been reported as multifunctional targets for treatment of AD [117]. The multifunctional ligands capable of double binding with CAS and PAS in addition to A*β*-aggregation inhibition were designed [119,120]. Such vivid drug designs paved to development of cyclopentaquinoline hybrids and further their anti-AD properties were characterized [121].

Considering donepezil and tacrine as reference compounds AChE and BuChE inhibitory activities were determined. Almost all compounds exhibited a remarkable AChE inhibitory activity (Table 8). Compounds **156–160** have shown higher potency compared to both

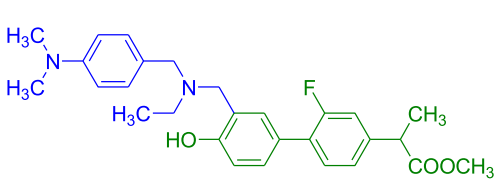

132

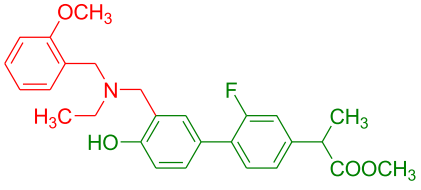

133

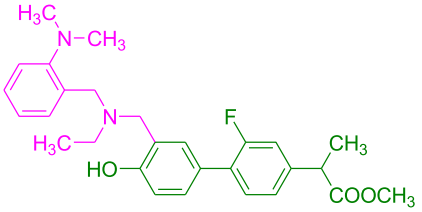

134

Fig. 53. Structures of most A*β*-aggregation inhibitors (**132** & **133**) and cholinesterase inhibitors (**134**).

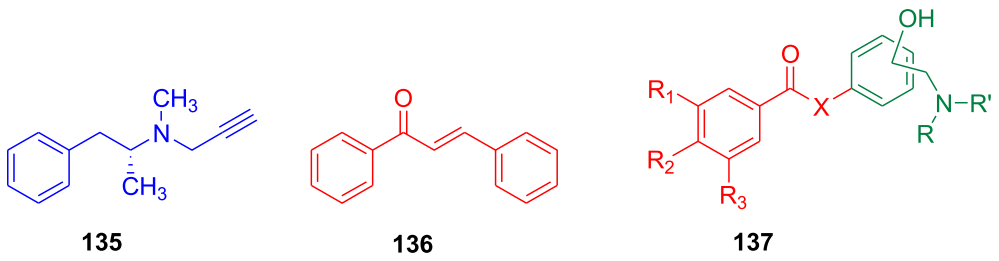

Fig. 55. Structure of selegiline (**135**) and design strategy of chalcone mannich bases (**136**).

Table 6
*ee*AChE and BuChE inhibitory values of chalcone mannich bases.

Compd	IC_{50}(μM) ± SD *ee*AChE	Compd	IC_{50}(μM) ± SD *ee*AChE
138	0.89 ± 0.03	**143**	0.56 ± 0.04
139	0.44 ± 0.04	**144**	0.92 ± 0.0
140	0.49 ± 0.02	**145**	0.30 ± 0.01
141	0.88 ± 0.03	**146**	0.07 ± 0.01
142	0.37 ± 0.02	**147**	0.18 ± 0.03

reference compounds. Whereas all the synthesized compounds possessed higher potency compared to tacrine. The most potent inhibitor among the tested compounds was compound **157** with three carbon linker flanked by cyclopentaquinoline and dichloronicotinamide units. All the title compounds have been reported as better BuChE inhibitors compared to donepezil; however compared to tacrine only compound **161** possessing seven-carbon linker yielded most potent activity. The exact structure activity relationship and precise correlation could not be established.

Most potent AChE inhibitor **157** was chosen for A*β*-aggregation inhibition at various concentrations. It has exhibited remarkable potencies at 50 μM and 100 μM concentrations with inhibition percentages 54.30% and 92.78% respectively.

2.23. Hybrids of donepezil, chromone and melatonin

Melatonin **164** (Fig. 62), an oxidant [122] has been reported as descent neuroprotective agent [123] alongside possessing A*β*-aggregation inhibition activity [124]. MAO inhibitory activity of chromone **165** [125] and anti-AD properties of donepezil were compiled with melatonin to synthesize new hybrid compounds in order to enhance the anti-AD properties. [126].

AChE and BuChE inhibitory activities of synthesized compounds **166–171** (Fig. 63) were performed using tacrine and donepezil as reference compounds. Regarding human cholinesterase inhibitory activity compound **166** possessing two carbon linker in between melatonin-chromone conjugate and donepezil moieties in addition to methoxy group at 5-position of indole (IC_{50} = 0.36 ± 0.16 μM) has exhibited some activity compared to tacrine (IC_{50} = 0.424 ± 21 μM). But, few derivatives have shown descent *h*BuChE inhibitory activity. In comparison to tacrine (IC_{50} = 45.8 ± 3.0 nM), derivative **167** having propoxy group on indole was most potent one (IC_{50} = 11.90 ± 0.05 nM). In the *ee*AChE activity, most of the compounds shown good inhibitory activities and remarkable activity was

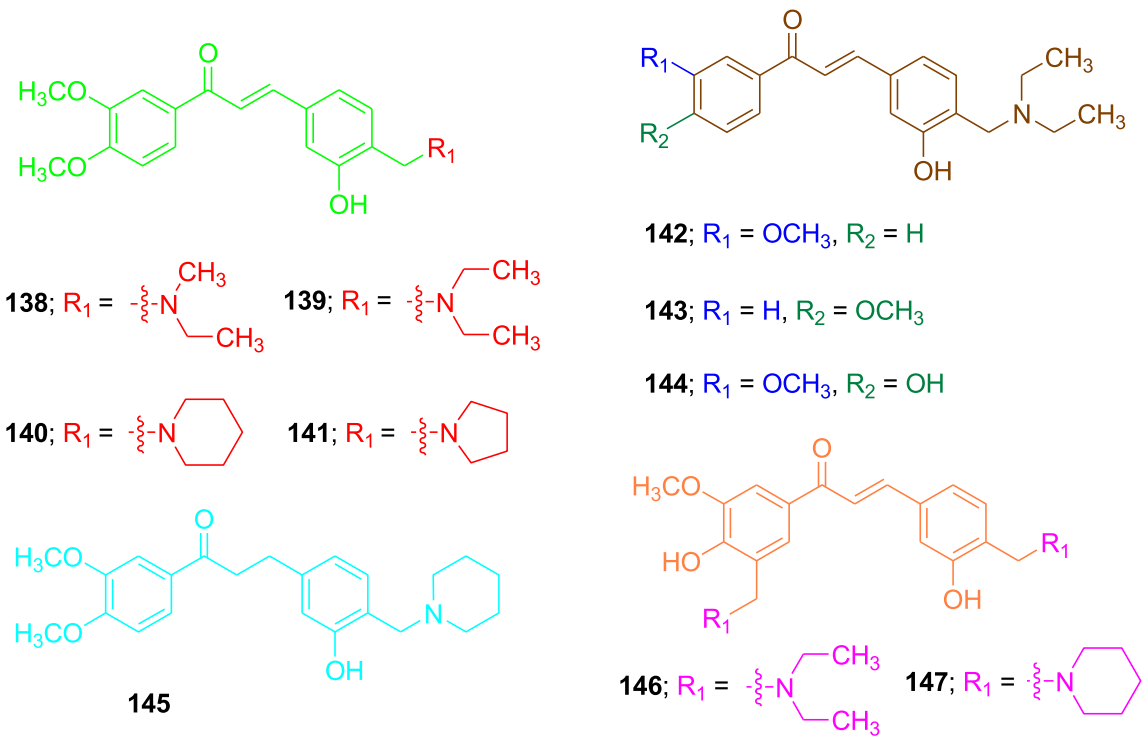

Fig. 56. Structures of the chalcone-mannich base derivatives as potent AChE inhibitors.

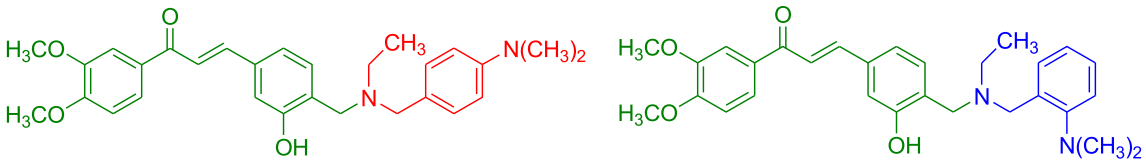

Fig. 57. Structures of potent MAO-A (**148**) and potent MAO-B inhibitor (**149**).

Table 7
Potent AChE and BuChE inhibitory values of tacrine derivatives.

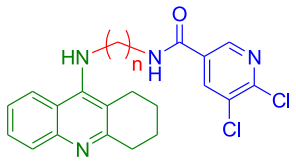

Compd	n	AChE	BuChE
		IC_{50} ± SEM (nM)	IC_{50} ± SEM (nM)
150	3	1.02 ± 0.10	159.74 ± 1.72
151	4	1.65 ± 0.26	41.45 ± 3.84
152	5	2.90 ± 0.30	13.48 ± 0.63
153	6	4.20 ± 0.43	12.86 ± 0.35
154	9	3.12 ± 0.41	3.33 ± 0.64
Tacrine	-	89.91 ± 9.14	14.98 ± 0.007

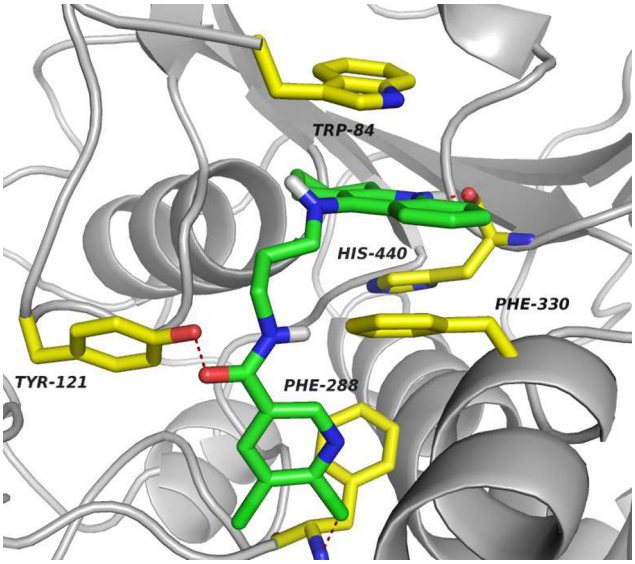

Fig. 59. Molecular docking of compound **150** with AChE active site [117].

observed for the derivative **169** (IC_{50} = 0.06 μM), and **171** having propoxy moiety (0.08 μM) compared to tacrine (IC_{50} = 0.03 ± 0.01 μM). All the potent *ee*AChE inhibitors entail four-carbon linker. While compound **168** with isopropoxy moiety (IC_{50} = 0.00629 μM) yielded comparable result with that of tacrine (IC_{50} = 0.0051 μM). The compound **170** bearing –OCH_3 at indole 5-position elicited excellent *h*BuChE inhibitory (IC_{50} = 0.011 μM); its activity is approximately fourfold stronger potency compared to tacrine (IC_{50} = 0.045 μM); while *h*AChE inhibitory potency was found to be descent activity (IC_{50} = 1.73 ± 0.34 μM).

Most of the compounds were MAO-B inactive and the derivative which exhibited good activity was compound **171** (IC_{50} = 1.39 ± 0.11 μM); however the synthesized derivatives were not good MAO-B inhibitors and hardly shown any activity.

AChE modeling analysis of compound **170** (Fig. 64) with *h*AChE shown that indole moiety was aligned towards catalytic triad residues His447, Ser203, and Glu334. Indole moiety was reported to form π-π interaction and amide-π affinity with Trp86 and Gly120 respectively. Alongside, the –NH and methoxy moieties have H-bonded with Glu202 and Ser125 respectively. The chromone part has exhibited π- π stacking interaction with Tyr124 and Trp286; while *N*-benzylpiperidinium motif shown affinity with Leu289 and Ser293 away from PAS.

In case of BuChE modeling (Fig. 65), the docking results indicated that chromone moiety has π-π type interactions with Phe329 and Trp231. The indole ring resulted π-π stacking interaction with Trp82 and His438 of the catalytic triad. Apart from this, the –NH involved in the formation of His438. The hydrogen bond interaction between the carbonyl group of the di-substituted amide with Thr120 and NH group of the mono-substituted amide with Asp70 was observed.

2.24. Kojotacrine derivatives

Multi-target small molecules (MTSMs) have emerged as most promising therapeutic strategy for design and discovery of novel drugs in AD treatment [127]. Despite the hepatotoxicity of tacrine, a large number of tacrine based drugs were being designed [128]. Kojic acid **172** (Fig. 66), a metabolite derived from fungus was reported as antioxidant [129]. Hence antioxidant kojic acid was modified with AChE

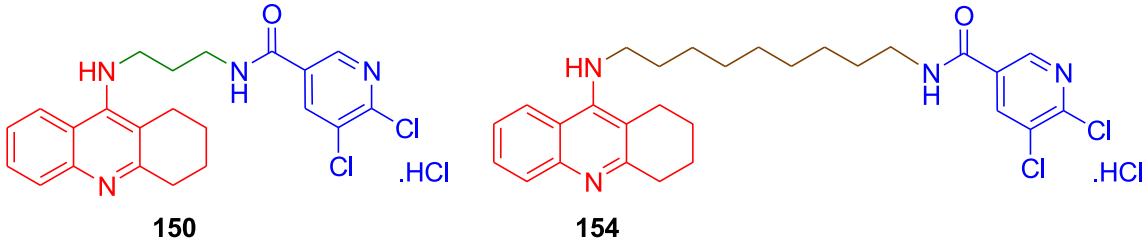

Fig. 58. Illustration of structures of most potent AChE inhibitor (**150**) and BuChE inhibitor (**154**).

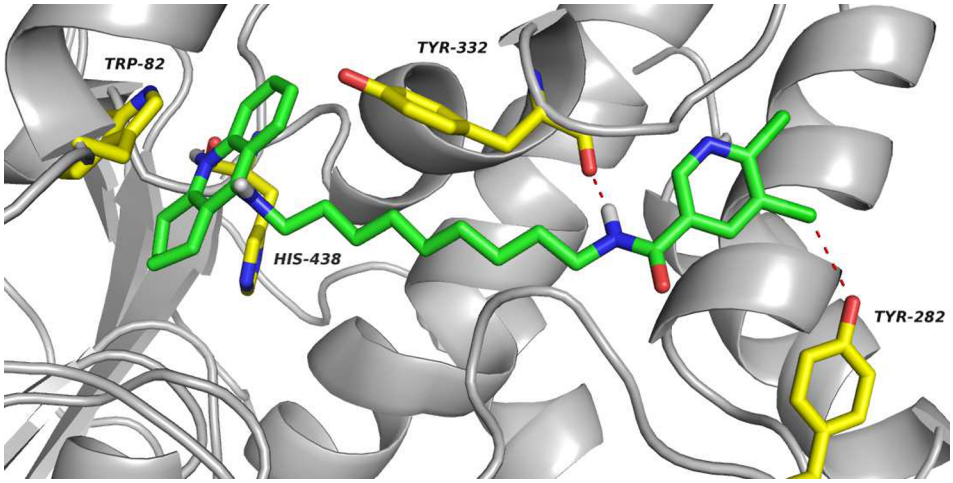

Fig. 60. Molecular docking of compound **154** in active site of BuChE active [117].

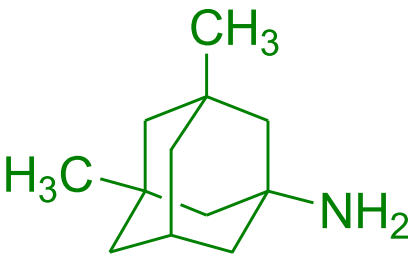

155

Fig. 61. Structure of memantine (**155**).

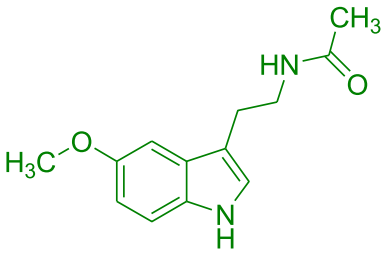

164 **165**

Fig. 62. Structure of melatonin (**164**) and chromone (**165**).

Table 8
AChE and BuChE inhibitory activities of cyclopentaquinoline hybrids.

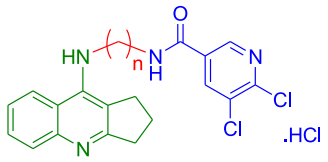

Compd	n	AChE	BuChE
		IC_{50} ± SEM (μM)	IC_{50} ± SEM (μM)
156	2	0.065 ± 0.007	1.863 ± 0.083
157	3	0.052 ± 0.002	0.158 ± 0.029
158	4	0.744 ± 0.046	0.797 ± 0.086
159	5	0.285 ± 0.038	0.460 ± 0.038
160	6	0.053 ± 0.005	0.127 ± 0.014
161	7	0.125 ± 0.021	0.071 ± 0.012
162	8	0.152 ± 0.045	0.108 ± 0.006
163	9	0.155 ± 0.045	0.082 ± 0.030
Donepezil	-	0.103 ± 0.016	11.826 ± 2.060
Tacrine	-	0.163 ± 0.041	0.020 ± 0.003

inhibitor tacrine to afford a series of kojic acid modified tacrine derivatives **173** and thereby evaluating their anti-AD properties [130].

Tacrine and kojic acid as reference compounds acetylcholinesterase inhibitory activities of title compounds were performed. The tested compounds have shown moderate anti-*ee*AChE activity. Among them the tacrine derivative **174** (IC_{50} = 0.64 ± 0.06 μM) (Fig. 67) with 3-methoxyphenyl moiety exhibited highest activity which was approximately twentyfold less potent compared to that of tacrine (IC_{50} = 0.031 ± 0.006 μM). Although *eq*BuChE inhibitory activities were weak compared to tacrine (IC_{50} = 0.005 ± 0.001 μM); most potent (IC_{50} = 4.54 ± 0.20 μM) compound reported was **175** possessing 3-flurophenyl structural unit. Similarly weak inhibitory activities were observed in case of *h*AChE inhibition compared to kojic acid (IC_{50} = 2.51 ± 0.17 μM).

Few compounds were selected for $A\beta_{1\text{-}40}$-aggregation inhibitory activity using melatonin and kojic acid as reference compounds. In those, derivative **174** has shown descent activity (42.92 ± 0.20%) at 3 μM concentration but comparatively less potent than that of melatonin (60.02 ± 3.57%) and kojic acid (65.11 ± 0.20%).

2.25. Bis-aryltriazole derivatives

Radiolabelled diphenyltriazole derivatives **176** (Fig. 68) were reported as imaging agents that could target Aβ-plaques [131]. The triazole acetamide scaffolds have been described to possess Aβ-aggregation inhibitory properties [132]. 1,2,3-Triazole derivatives were highlighted to exhibit anti Aβ-aggregation properties [133]. Jiaranaikulwanitch et al. have described tryptoline and tryptamine triazole

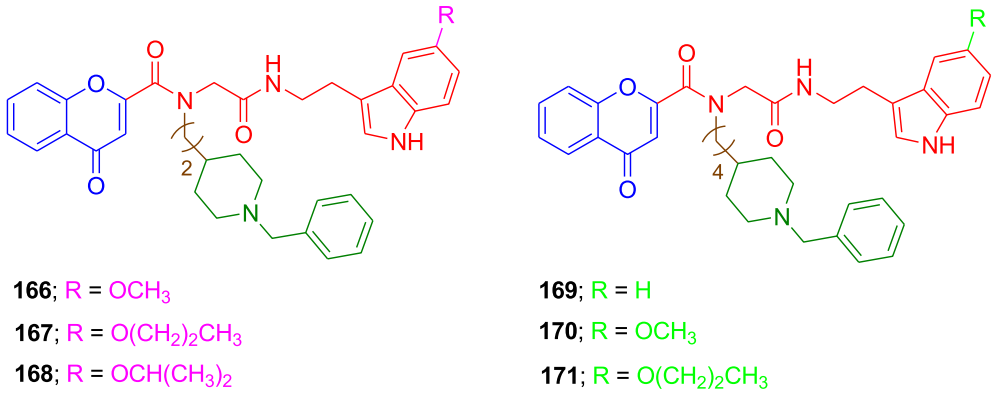

Fig. 63. Structures of potent cholinesterase inhibitors and MAO inhibitors.

derivatives **177** as multifunctional ligands in AD treatment [134]. In this regard, a set of bis-aryltriazole derivatives were designed and screened for their anti-AD properties [135].

Most of the synthesized compounds have shown moderate to good self-induced Aβ_{42}-aggregation inhibitory activities. Among them, compounds **178** and **179** (Fig. 69) exhibited descent activity and in particular derivative **179** (96.89%) comprising *o*-CH_3 on phenyl ring was most potent molecule compared to reference compound curcumin (95.14%). Based on the percentage inhibitions, the IC_{50} value of the compound **179** was found to be 8.605 ± 0.129 μM and that of curcumin was 6.385 ± 0.009 μM. Also, the formation of amyloid fibrils was significantly reduced by the compound **179** which was attributed to the presence of strong negative inductive effect of $-CF_3$ moiety. Inhibitory activity was also performed on Cu^{2+}-induced aggregation with compound **179** where in the formation of Aβ fibrils was 42% higher compared to self-induced Aβ activity. When compound **179** and clioquinol were incubated separately for Aβ_{42} fibril disaggregation at 40 μM and the results were found to be 61.42% and 65.34% disaggregation for compound **179** and clioquinol respectively.

The potent Aβ_{42} aggregation inhibitor **179** (Fig. 70) was subjected to molecular docking studies with Aβ_{42} monomer and Aβ_{42} photofibril. In case of docking with Aβ_{42} monomer, triazole nitrogen atom was hydrogen bonded with Ala42 in addition to hydrophobic interaction of compound **179** with the amino acid residues Ala30, Ile31, Leu34, Met35, Gly38, Val39, Val40, Ile41 and Ala42 of Aβ_{42} monomer. Meanwhile, in the docking with Aβ_{42} photofibril, a H-bond was observed between triazole nitrogen and Ile41 and second hydrogen bonding was formed by amide NH with Val39. Alongside, hydrophobic interactions were noticed with the amino acids Leu17(D), Phe19(D), Leu17(E), Phe19(E), Gly37(E), Gly38(E), Val39(E), Val40(E), and Ile41(E).

2.26. *N*-Benzylpiperidine scaffolds

The compounds possessing BACE1 inhibitory activity also reported to exhibit prominent antioxidant activity [136]. *N*-Benzylpiperidine bearing donepezil was described to bind to the CAS of AChE [137]. Alongside, the indanone unit of donepezil was modified to improve BACE1 inhibitory potential [138]. Accordingly, the new series of *N*-benzylpiperidine scaffolds have been synthesized and their cholinesterase and Aβ-aggregation activities were evaluated [139].

Most of the designed scaffolds have shown good *h*AChE inhibitory

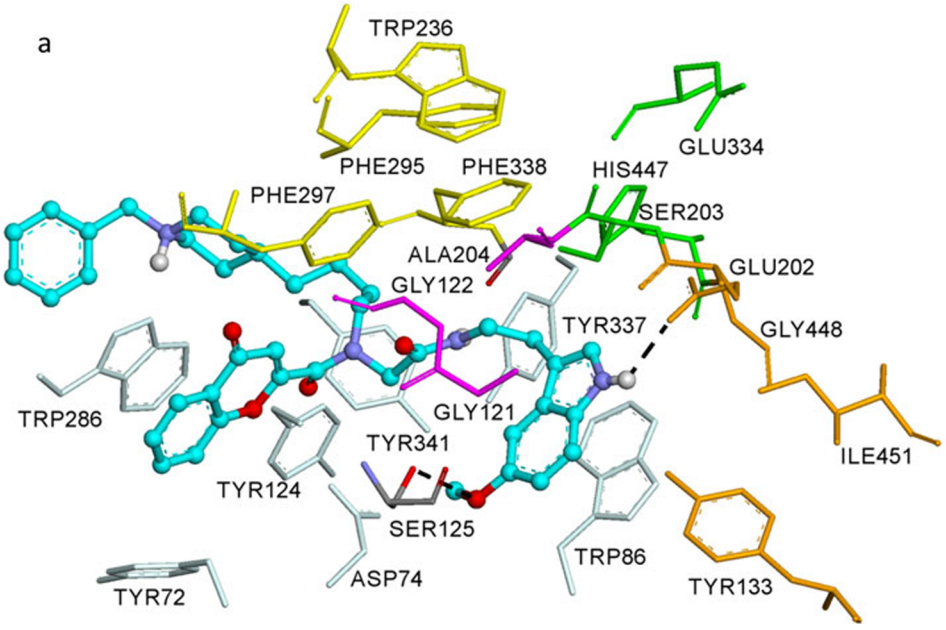

Fig. 64. Illustration of binding mode of compound **170** with *h*AChE active site [126].

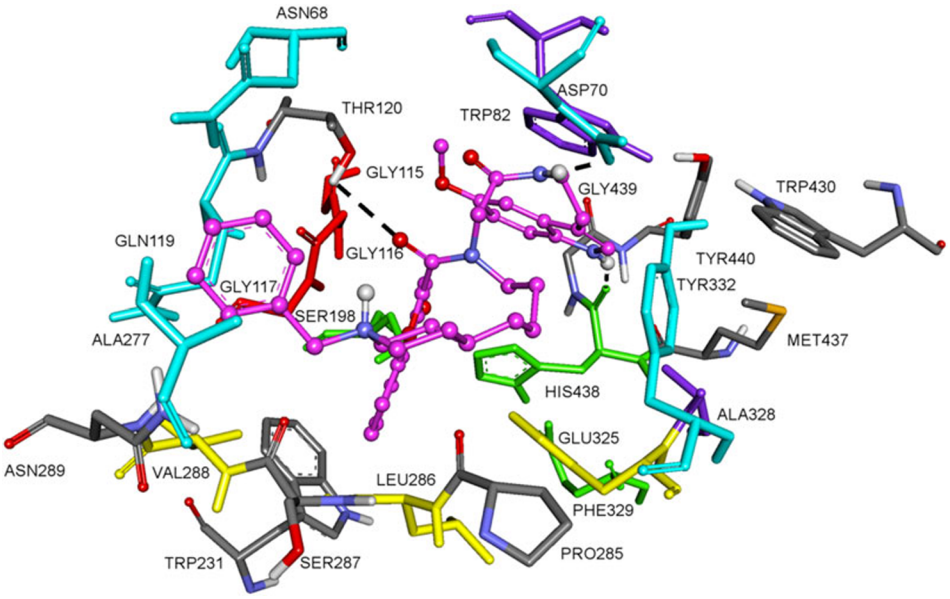

Fig. 65. Docking analysis of compound **170** on *h*BuChE [126].

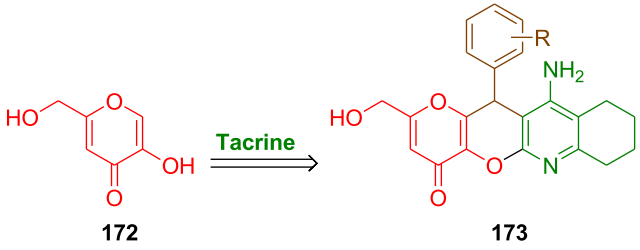

Fig. 66. Illustration of strategic design of kojic acid modified tacrine derivatives.

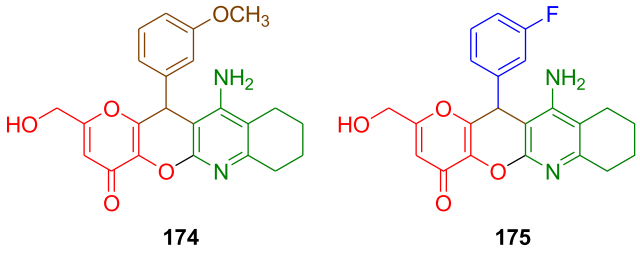

Fig. 67. Structure of *ee*AChE/A*β*-inhibitor (**174**) and *eq*BuChE inhibitor.

activity compared to reference compound rivastigmine and even higher potencies than rivastigmine. However, a few compounds (Table 9 and Fig. 71) have exhibited activity close to donepezil. Amongst them, benzylamine modified *N*-benzylpiperidine **180** possessing electron withdrawing group $-CF_3$ exhibited significant activity. In case of BuChE inhibition half of the title compounds had moderate activity compared to reference compounds. The derivatives which have shown comparable BuChE inhibitory values were provided in Table 9. The prominent *h*BuChE inhibitor **183** was threefold less potent compared to rivastigmine.

Descent BACE1 inhibitory activities were observed in case of most of the tested compounds compared to donepezil and few compounds had very good activity (Table 9). Again compound **181** exhibited excellent *h*BACE1 inhibitor activity which was more potent compared to donepezil. Besides significant activity of compound **181**, almost similar *h*BuChE inhibitory activity (IC_{50} = 0.28 ± 0.03 μM) was observed for the schiff base analog with $-CF_3$ group **180**. Keen observation of the results revealed mostly the electron withdrawing groups at the 4-position have yielded highest inhibitory values.

The synthesized compounds were also allowed to inhibit A*β* at various concentrations. Significant figures have been observed for the compounds **181** and **185**. These derivatives (**181**; self-induced: 50.1% & AChE-induced: 89.0%, **185**; self-induced: 44.1% & AChE-induced: 69.3%) have exhibited higher aggregation inhibitory properties compared to donepezil (Self-induced: 41.6%; AChE-induced; 62.8%).

Compound **181** was investigated for docking analysis with AChE and BACE1 active sites (Fig. 72). In AChE docking analysis, benzylpiperidine has formed polar interactions with Ser203 and His447. Where as, the benzyl moiety has interacted with Trp86 *via* π-π stacking and with Glu202. When it comes to the docking studies with BACE1, compound **181** has established significant interactions with the

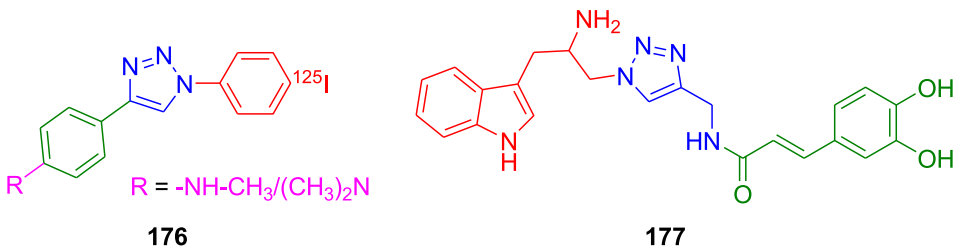

Fig. 68. Structures of radiolabelled diphenyltriazole derivatives (**176**) and tryptamine triazole derivatives (**177**).

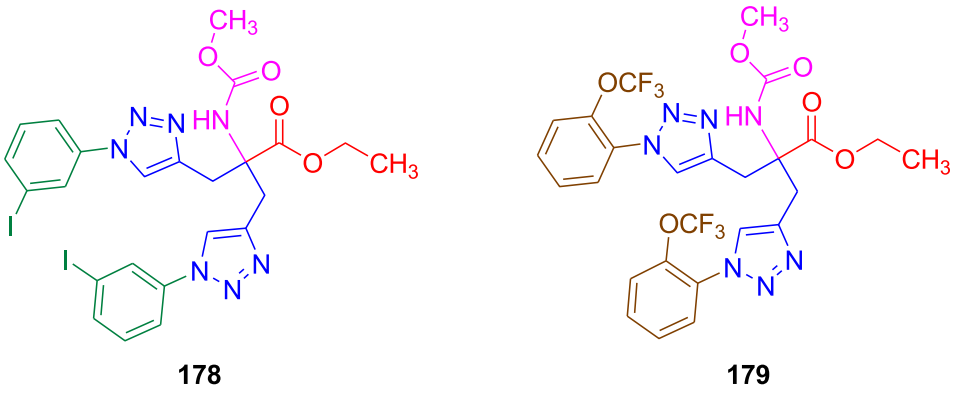

Fig. 69. Structures of potent Aβ_{42}-aggregation inhibitors.

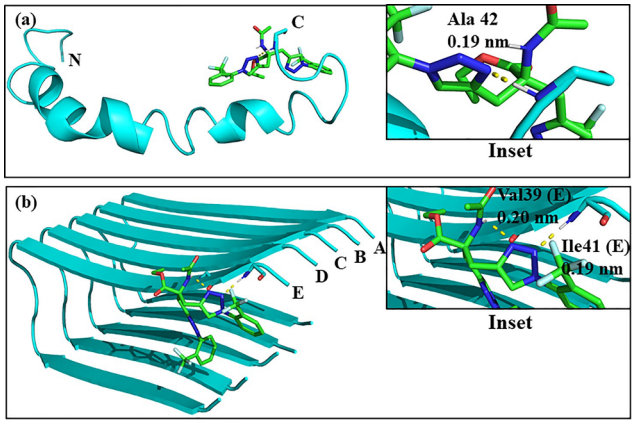

Fig. 70. Molecular binding analysis of compound **179** with Aβ_{42} monomer (**a**) and Aβ_{42} photofibril (**b**) [135].

catalytic aspartate residues Asp32 and Asp228 through ionic salt bridge/H-bonding. The methanamide fragment has hydrogen bonded with Tyr124.

2.27. *N*-Benzylpyridinium-based analogs

Replacement of indanone moiety of donepezil with different aromatic and heteroaromatic rings led to potent AChE inhibitors [140]. Benzylpyridinium derivatized compounds were demonstrated that they have the capability to interact with catalytic site of the AChE [141]. A series of heteroaromatic scaffolds **188** (Fig. 73) possessing *N*-benzylpyridinium motif as essential part was designed [142]. Benzothiazole compounds were described to have interaction with Aβ-peptides and could reduce the soluble amyloid oligomers [143]. Hybrid compounds of tacrine and phenylbenzothiazole moieties **189** (IC_{50}, AChE = 0.017 μM) were reported as multifunctional anti-AD agents [144]. Considering all these, anti-AD agents have been designed by appending *N*-benzylpyridinium motif on benzoheterocycles [145].

Using donepezil as reference compound the lead compounds were assessed for AChE inhibitory activity. Moderate to most potent activities for compounds **190–194** were observed; notable activities are depicted in Table 10. Approximately twofold higher AChE inhibitory activity was found for plane benzypyridinium appended benzothiazole **190** (Table 10 & Fig. 74) compared to donepezil. All the potent AChE inhibitors possessed with benzothiazole moiety. Unmentioned benzoxazole and benzimidazole derivatized benzylpyridinum derivatives were not as potent as benzothiazole analogs in case of AChE inhibition.

Except two compounds **190** and **191** which were dual inhibitors, other derivatives **195–197** (Table 11) were selective BuChE inhibitors. Compared to donepezil every derivative was reported to possess higher activity. Even in case of BuChE inhibitory activity benzothiazole derivatives have shown their impact except compound **195** which is a benzoxazole derivative.

Alongside, AChE and BuChE inhibitory activities, some selected compounds **190** and **198** (Fig. 74) were allowed inhibit A$\beta_{1\text{-}42}$-

Table 9
Cholinesterase inhibitory values and BACE1 inhibitory values of *N*-benzylpiperidine derivatives.

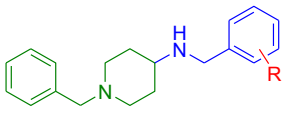

Compd	R	IC_{50} (μM) ± SEM		Compd	R	IC_{50} (μM) ± SEM
		*h*AChE	*h*BuChE			*h*BACE1
181	4-CF_3	0.11 ± 0.02	3.0 ± 0.06	**181**	4-CF_3	0.22 ± 0.02
182	4-OCF_3	0.59 ± 0.05	3.5 ± 0.06	**185**	4-NO_2	0.43 ± 0.04
183	2,4-diCl	0.62 ± 0.05	3.5 ± 0.09	**186**	4-Cl	0.66 ± 0.06
184	2,4-diF	0.71 ± 0.06	3.1 ± 0.10	**187**	4-F	0.55 ± 0.03
Donepezil		0.033 ± 0.01	1.4 ± 0.06	**Donepezil**		0.24 ± 0.03
Rivstigmine		1.9 ± 0.06	1.1 ± 0.04			

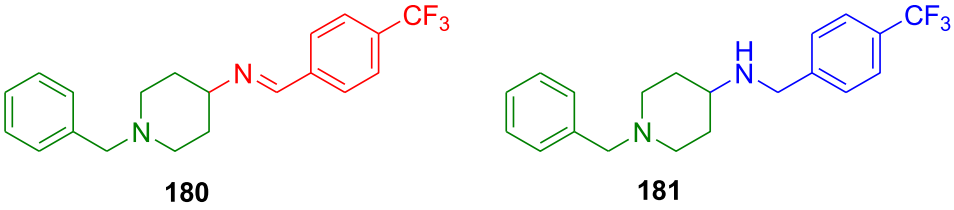

Fig. 71. Structures of most potent *h*AChE and *h*BuChE inhibitors.

aggregation using donepezil and rifampicin as reference compounds at 100 μM concentration. Derivative **190** (44.9 ± 3.6%) had twice as potentiality as donepezil (22.0 ± 5.4%) and rifampicin (27.5 ± 4.3%) with respect to self-induced Aβ-aggregation inhibition. Compound **198** (28.9 ± 1.5%) was also as potent as rifampicin. Regarding AChE-induced Aβ-aggregation inhibition, both the compounds **190** (18.3 ± 8.5%) and **198** (12.1 ± 3.6%) exhibited similar potencies compared to rifampicin (12.2 ± 3.0%) and higher potencies compared to donepezil (26.1 ± 2.5%).

The docking of compound **190** (Fig. 75) with AChE active site reveals formation of π-π stacking of benzyl moiety with His439 and Trp83. Where as, the pyridinium ring has descent interaction with Phe329 through π-cation affinity and π-stacking. Further, positively charged nitrogen has aligned towards Asp71 residue.

2.28. Pyrano[4,3-b][1]benzopyranone derivatives

Many bioactive molecules were described as interested candidates for cholinesterase inhibition, BACE1 inhibition, MAO inhibition and Aβ-aggregation inhibition [146]. Chromone derivatized pyrano[4,3-*b*][1]benzopyranones have possessed significant biological activities [147,148]. These paved to synthesis of a series of pyrano[4,3-*b*][1]benzopyranones **199** (Fig. 76**)** and their MAO and cholinesterase inhibitory activities were determined [149].

Literally the synthesized derivatives have not shown any AChE inhibitory activity. Similarly a very weak BuChE inhibitory activity was observed for most of the derivatives. Among them, compounds **200** (IC_{50} = 20 μM) and **201** (IC_{50} = 21 μM) (Fig. 77) seems to show some comparable activity with that of reference compound (IC_{50} = 7.1 μM). Both compounds **200** and **201** have almost similar BuChE inhibitory activity and only structural difference lies with the presence of −Cl group at 8-position of benzopyranone derivative **201**.

Surprisingly almost half of the synthesized compounds were moderate to potent MAO-A inhibitors. Compounds **202** (IC_{50} = 7.7 μM) and **203** (IC_{50} = 4.3 μM) (Fig. 78) were descent MAO-A inhibitors where in compound **203** with methoxy moiety at 8-position alongside butoxy group in the exo configuration at 3-position has exhibited higher potential than the reference compound (IC_{50} = 4.6 μM). Regarding MAO-B inhibitory activity, few derivatives resulted comparable activity with that of reference compound. Benzopyranone derivative **201** (IC_{50} = 0.20 μM) and **204** (IC_{50} = 0.39 μM) (Fig. 78), endo-isomer of compound **203** were significant inhibitors. The exo-isomer **201** was as potent as the reference compound (IC_{50} = 0.22 μM).

2.29. Pyrazolone schiff bases

Moclobemide **205** is a second generation MAO inhibitor devoid of problems such as drug-drug interactions, fatal hypersensitive crisis [150]. A cyclic hydrazine constituting pyrazoline **206** (Fig. 79) and pyrazolidine structural units form a prominent pharmacore and reported to be present in several MAO inhibitors and cholinesterase inhibitors [151]. Pyrazole scaffolds were utilized in the AChE and MAO inhibitor design strategy [152]. Encouragement of these drug discovery developments led to design of new pyrazolone schiff base derivatives [153].

Majority of the synthesized compounds could reach 30–40% AChE inhibitory activity at 100 μM concentration; the reference used was donepezil with inhibitory percentage 98.56 ± 1.76%. Reduced BuChE inhibitory activity was observed compared to AChE activity. In both the inhibition activities, compounds **207** and **208** (Fig. 80) yielded excellent results compared to reference compounds. In comparison with donepezil, compounds **207** (78.20 ± 1.20%) possessing 4-piperidinophenyl moiety and **208** (88.12 ± 1.07%) comprising 4-[3-(dimethylamino)propoxy]phenyl motif have shown close AChE inhibitory percentages with that of donepezil (98.56 ± 1.76%). Similarly compound **207** (78.20 ± 1.20%) had almost close BuChE potential with that of tacrine (82.14 ± 2.69%) and derivative **208** (88.12 ± 1.07%) has exhibited most potent activity. In spite of prominent cholinesterase activity of **207** and **208**; these were tested for AChE inhibitory activities at various concentrations and their IC_{50} values were determined to be 0.285 ± 0.009 μM and 0.057 ± 0.002 μM respectively. In these two selective inhibitors, compound **208** revealed its potent activity but twice less potent compared to donepezil (0.029 ± 0.001 μM).

The title compounds scarcely exhibited any MAO-A inhibitory

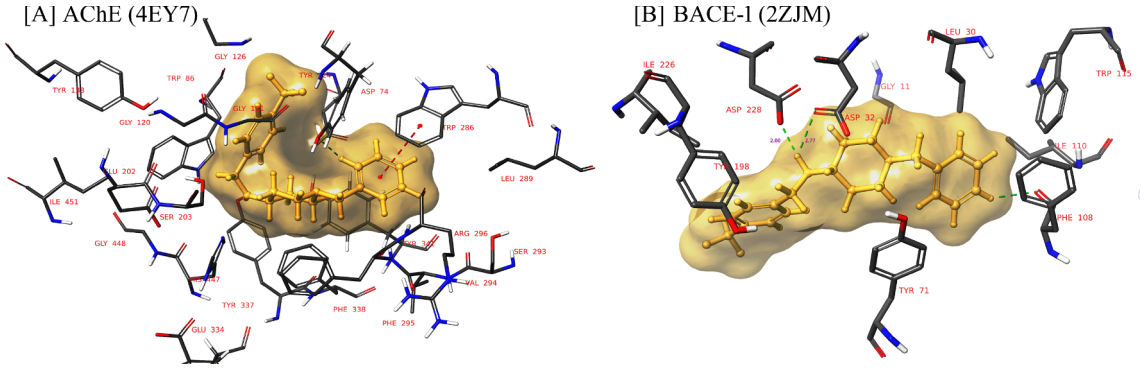

Fig. 72. Demonstration of binding interactions of compound **181** with AChE (**A**) and BACE1 (**B**) [139].

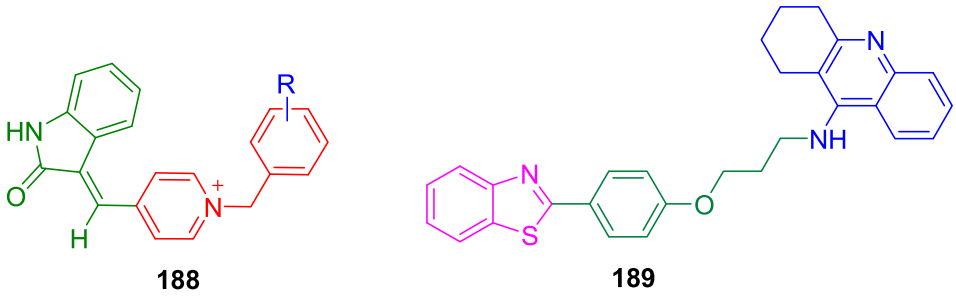

Fig. 73. Structures of indolinone derivative (**188**) and benzothiazole-tacrine hybrid (**190**).

Table 10
AChE inhibitory values of *N*-benzylpyridinium modified benzothiazole derivatives.

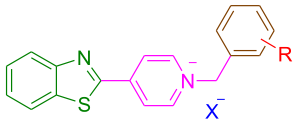

Compd	R	X	AChE IC_{50} (nM)
190	H	Br	14 ± 0.7
191	2-Cl	Cl	22 ± 1.5
192	3-CH_3	Cl	21 ± 1.8
193	3-F	Cl	23 ± 0.6
194	2-Cl, 6-F	Cl	27 ± 1.4
Donepezil	-	-	23 ± 1.3

Table 11
BuChE inhibitory values of *N*-benzylpyridinium modified benzoheterocycles.

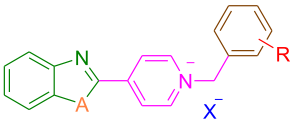

Compd	A	R	X	BuChE IC_{50} (nM)
190	S	H	Br	182 ± 5.6
191	S	2-Cl	Cl	348 ± 6.3
195	O	H	Br	280 ± 9.8
196	S	2-NO_2	Cl	331 ± 11.2
197	S	2,6-diCl	Cl	379 ± 8.9
Donepezil		-	-	3400 ± 23

activity. Astonishingly, greatest inhibitory percentages were observed in case of MAO-B inhibition. Almost all tested compounds shown at least 40% inhibitory activity. In those compounds *p*-hydroxyphenyl analog **209** (85.13 ± 1.08%), **210** (89.10 ± 1.24%) and **211** (87.22 ± 1.18%) (Fig. 81) have exhibited significant inhibitory percentages compared to selegiline (96.88 ± 1.31%). The results revealed that these were selective MAO-B inhibitors. Here structure and corresponding activity could not be correlated precisely as the inhibitors possessed electron donating and electron withdrawing moieties at different positions of phenyl ring.

Molecular docking analysis of compound **210** (Fig. 82) with MAO-B active site exhibited following results. Carbonyl group of pyrazole established H-bond with Cys172 residue; the pyrazole ring has interacted with Tyr32 *via* π-π stacking. Moreover, the nitrogen atom of $–NO_2$ group has led to the cation-π interaction with Tyr435.

2.30. Indole-piperidine analogs

Alongside classical targets such as ChEs, secretases, MAOs, etc., modulation of 5-HT receptors [154] (5-HT_4R &5-HT_6R) of seretonergic system were also considered for progress in AD treatment. 5-HT_4R Activation could lead to amyloid protein precursor cleavage which

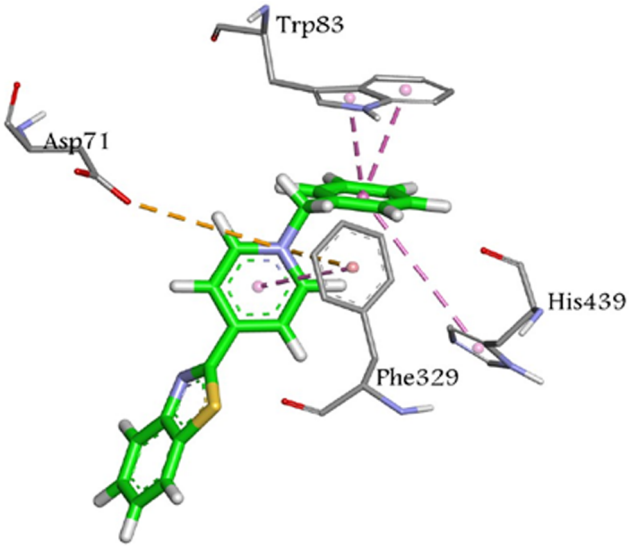

Fig. 75. Illustration of binding affinities of compound **190** with AChE active site [145].

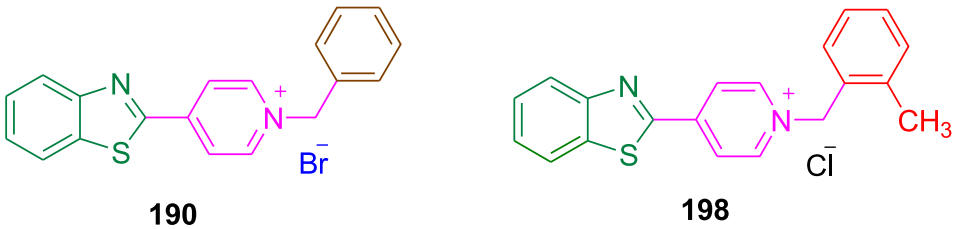

Fig. 74. Structures of AChE/BuChE/Aβ-aggregation inhibitor (**190**) and Aβ-aggregation inhibitor (**198**).

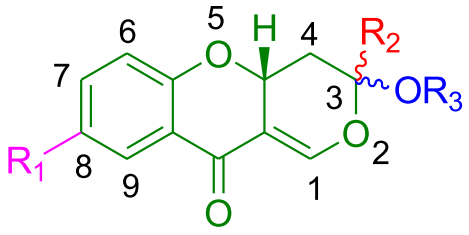

199

Fig. 76. Illustration of design strategy of cholinesterase/MAO inhibitors.

subsequently resulting into formation of a neurotrophic protein, sAPPα [155]. RS67333 **212** (Fig. 83), 5-HT_4R antagonist when administered in a transgenic mouse model, significant reduction of amyloidogenesis was observed [156]. σ_1R Off-target approach has been a promising route for AD treatment; [157] compound **213** has shown affinity towards σ_1R. Taken together all these facts in addition to potent σ_1R antagonist property of indole modified haloperidol-inspired molecules [158], a series of novel indole-piperidine analogs were designed by introducing pharmacologically significant structural parts of **212** and donepezil [159].

Using the reference compound donepezil and donecopride, *h*AChE inhibitory activity of synthesized compounds was determined. All most all derivatives exhibited 70–98% inhibition. Despite the descent percentage inhibitions, only two compounds **214** (97%) and **215** (98%) (Fig. 84) have shown significant inhibitory activities with IC_{50} values 20.4 ± 0.8 nM and 13.3 ± 0.4 nM compared to donepezil (IC_{50} = 6.0 ± 0.6 nM) and donecopride (IC_{50} = 16 ± 5 nM).

Although many derivatives were assessed to possess 100% 5-HT4R inhibitions, only compound **216** (K_i = 25 ± 1.6 nM) could show significant kinetic inhibitory activity compared to RS67333 (K_i = 9.33 ± 5 nM). Other derivatives were weak inhibitors. The inhibitory percentages and kinetic inhibitory values could not be rationally correlated. However in case of σ_1R inhibition, few compounds were active in which compounds **215** (K_i = 3.3 ± 0.7 nM) and **217** (K_i = 5.1 ± 1.7 nM) (Fig. 85) could be mentioned as prominent inhibitors. Out of these, compound **215** was the most potent and half as potent as haloperidol (K_i = 1.6 ± 0.7 nM). Compound **215** possessing propionyl moiety flanked by indole and benzylpiperidine units was AChEI/σ_1R dual inhibitor. Indole *N*-substitution of the derivatives has resulted in reduced inhibitory activity.

2.31. Salicylamide derivatives

In spite of descent AChE inhibitory activity of salicylic acid **218** and its derivatives [17], new salicylamide derivatives **220** were designed by appending pharmacore of chromone-2-carboxamido-alkylbenzylamines **219** (Fig. 86) and synthesized [160].

The designed salicylamide derivatives have been screened for inhibition of cholinesterase inhibition (*Rat*AChE, *Rat*BuChE and *ee*AChE) using reference compounds rivastigmine and donepezil. The inhibitory activities revealed that the tested derivatives were selective AChE inhibitors as BuChE activity could hardly be observed. Although the tested compounds were only weak *Rat*AChE inhibitors compared to donepezil (IC_{50} = 0.015 ± 0.002 μM), compounds **221** (IC_{50} = 31.4 ± 0.73 μM), **222** (IC_{50} = 21.2 ± 1.10 μM) and **223** (IC_{50} = 10.4 ± 0.478 μM) (Fig. 87) had significant activities compared to rivastigmine (IC_{50} = 37.1 ± 1.22 μM). Regarding *ee*AChE inhibitory activity, again compounds **222** (IC_{50} = 17.7 ± 0.20 μM) and **223** (IC_{50} = 15.2 ± 0.33 μM) have shown impact in comparison with rivastigine (IC_{50} = 23.2 ± 0.44 μM) but tenfold lower activity compared to donepezil (IC_{50} = 0.021 ± 0.003 μM).

The synthesized compounds were evaluated for Aβ-aggregation inhibition activity with curcumin as reference compound. Most of the derivatives have given descent self-induced Aβ-aggregation inhibition percentages. Amongst them AChE inhibitors **221** (45.1 ± 2.0%) and **223** (42.5 ± 0.9%) exhibited prominent inhibitory percentages and higher activity compared to curcumin (40.2 ± 0.9%). However, majority of the derivatives exhibited poor Cu^{2+}-induced activity. Most potent derivative **223** (31.4 ± 1.0%) was approximately half as potent as curcumin (66.0 ± 1.3%).

In the structures of the cholinesterase/Aβ-aggregation inhibitors, the four/six carbon linker in between salicylamide and *N*-alkylbenzylamine motifs was most beneficial. Also, *N*-methy/ethyl benzylamine or *N*-methy/ethyl *o*-methoxybenzylamine moieties with appropriate combination of carbon spacers (four/six) have yielded the best results.

The molecular modeling studies of compound **223** (Fig. 88) revealed hydrogen bonding interaction of amide NH with Phe331 residue. Side chain *N*-(2-methoxybenzyl) ethylamine portion has formed parallel π-π stacking affinity with Trp84 and hydrophobic interaction with residues Asp72, Phe330, His440 and Gly441. Special conformation of methylene side chain and salicylamide ring in the gorge has formed Gly118, Tyr121, Trp279, Ser286, Ile287, Phe288, Phe290, Phe331, Tyr334 and Gly335 through hydrophobic interaction.

2.32. Tetrahydroisoquinoline-benzimidazole hybrids

Benzimidazole based compounds were reported to exhibit BACE1 inhibitory activity [161] in addition to anti-inflammatory activities. The significant biological activities such as anti-oxidation, neuroprotection and anti-AD properties [162] were exhibited by tetrahydroisoquinoline analogs. Based on the anti-AD properties of benzimidazole and tetrahydroisoquinoline derivatives, a set of hybrid tetrahydroisoquinoline-benzimidazoles **224** (Fig. 89) were engineered [163].

Resveratrol was used as positive control for determination of neuroinflammation inhibitory activity. Except two derivatives, all the compounds have exhibited excellent NO inhibitory activity which have twice the activity shown by resveratrol (IC_{50} = 11.1 ± 1.3 μM). Among those 6-hydroxybenzimidazole analog **225** (IC_{50} = 3.80 ± 0.42 μM), 6-methoxybenzimidazole derivative **226** (IC_{50} = 5.07 ± 0.54 μM) and 6-fluorobenzimidazol derivative attached to benzene **227** (IC_{50} = 5.42 ± 1.21 μM) (Fig. 90). Compound **225** was threefold higher potent compared to reference compound. Electron withdrawing effects have found to be more beneficial for NO

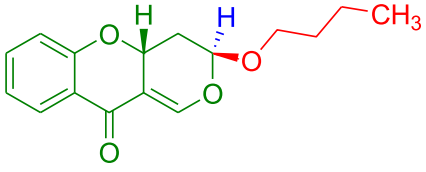

200

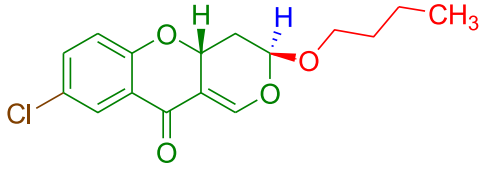

201

Fig. 77. Structures of potent BuChE inhibitors.

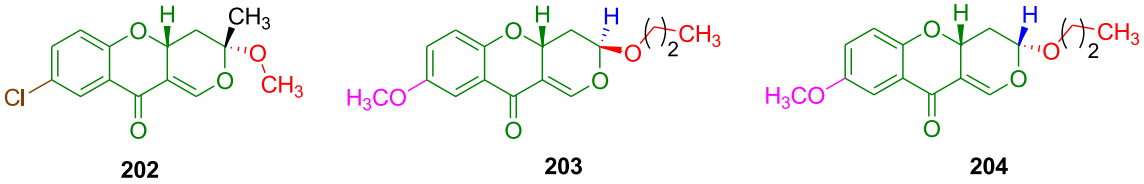

Fig. 78. Structures of potent MAO inhibitors.

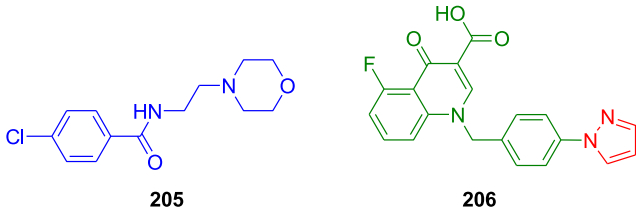

Fig. 79. Structure of moclobemide (**205**) and pyrazole derivative (**206**).

inhibitory activity. Although compounds **225** and **226** do not have electron withdrawing groups attached to benzimidazole moieties but they have electron withdrawing pyridine structural units. Whereas derivative **227** has electron withdrawing 6-fluorobenzimidazole attached to simple phenyl ring.

Most of the synthesized compounds were BACE1 inhibitors determined using MK-8931 as positive control. However, three derivatives namely 6-trifluoromethoxybenzimidazole analog **228** (98.7 ± 1.0%), 6-chlorobenzimidazole attached to pyridine and phenyl ring for **229** (95.3 ± 2.3%) and **230** (92.7 ± 4.3%) respectively (Fig. 91). The IC_{50} values of derivatives **228**, **229** and **230** were 1.1 ± 0.02 μM, 1.8 ± 0.3 μM and 1.3 ± 0.03 μM respectively. In comparison with MK-8931 (IC_{50} = 0.0207 ± 0.0012 μM), the potent inhibitors exhibited were fiftyfold less potential. All the inhibitors (NO/BACE1) have possessed 6-substituted benzimidazole structural units which might be beneficial for exact fit into the active site of enzyme.

2.33. Donepezil-butylated hydroxytoluene hybrids

8-Hydroxyquinoline derivatives have been reported to possess anti-AD characteristics [164]. An FDA approved drug donepezil was patented for its reversible acetylcholinesterase inhibitory activity [165]. Another patented molecule was phenolic antioxidant butylated hydroxytoluene **231** (Fig. 92) [166]. These facts of pharmacological significance have led to design of donepezil-butylated hydroxytoluene analogs **232** [167].

Cholinesterase inhibitory activities were performed using donepezil as reference compound. Compared to donepezil, most of the synthesized compounds have exhibited moderate *ee*AChE and *eq*BuChE inhibitory activities. In that, compound **233** (IC_{50} = 0.53 ± 0.11 μM) (Fig. 93) was most potent *ee*AChE inhibitory compound but tenfold less potent than that of donepezil (IC_{50} = 0.05 ± 0.01 μM). Whereas, compound **234** (IC_{50} = 5.38 ± 0.4 μM) exhibited only half of the *eq*BuChE inhibitory activity shown by donepezil (IC_{50} = 2.48 ± 0.11 μM). Likewise, inhibitory activity was also performed towards *h*AChE. In comparison with donepezil (IC_{50} = 0.048 ± 0.003 μM), low profile of inhibitory activity towards was observed towards *h*AChE; amongst them derivative **235** (IC_{50} = 1.38 ± 0.11 μM) stood atop. While compound **235** (IC_{50} = 9.61 ± 0.51 μM) was most potent among the *h*BuChE inhibitors and exhibited one-third activity compared to donepezil (IC_{50} = 3.17 ± 0.10 μM).

A very weak MAO-A inhibitory activity was shown by title compounds in which derivative **236** (Fig. 94) the most potent molecule exhibited only 49.2% inhibitory activity. In case of MAO-B inhibitory activity, a few compounds yielded significant activity particularly compound **233** (IC_{50} = 8.5 ± 0.3 μM) (Fig. 93) was as potent as donepezil (IC_{50} = 8.5 ± 0.6 μM). Accordingly derivative **237** (IC_{50} = 11.7 ± 0.2 μM) has shown comparable activity with that of reference compound.

Another series of derivatives with substitutions on phenyl ring of benzylpiperidine moiety were designed. These derivatives were also allowed for inhibition of cholinesterases and MAOs. Among the cholinesterase inhibitors only the derivative **238** (IC_{50} = 0.075 ± 0.6 μM) (Fig. 95) was an excellent *ee*AChE inhibitor which can be comparable with that of donepezil (IC_{50} = 0.05 ± 0.01 μM). The derivative **239** (IC_{50} = 0.75 ± 0.11 μM) was also able to exhibit significant *h*AChE inhibitory activity. Weak and moderate inhibitory activities were exhibited towards *h*BuChE and *eq*BuChE respectively.

This series of derivatives have been screened for *h*MAO inhibitory activity using iproniazid. No single synthesized compound has exhibited significant *h*MAO-A inhibitory activity. However, all the tested compounds have exhibited descent MAO-B inhibitory activity and half of which were as potent as iproniazid (IC_{50} = 8.75 ± 0.6 μM). Compounds **239** (IC_{50} = 6.7 ± 1.2 μM) and **240** (IC_{50} = 6.5 ± 0.5 μM) have exhibited highest activity even greater than iproniazid. All the MAO inhibitors (except **236**) had possessed α, β-unsaturated amide linker flanked by butlylated hydroxyphenyl and benzylpiperidine moieties.

The potent AChE/MAO inhibitor **233** and AChE inhibitor **238** were selected for $A\beta_{42}$ aggregation inhibitory activity using curcumin as reference compound. Noteworthy results were obtained in range of 43.5–56.7% activity compared to curcumin (52.6%) towards self-induced activity. Particularly, derivative **238** had higher potency. However diminished AChE-induced activity was observed for compound **233** and **238** with percentage inhibitions 38.4% and 40.1% respectively.

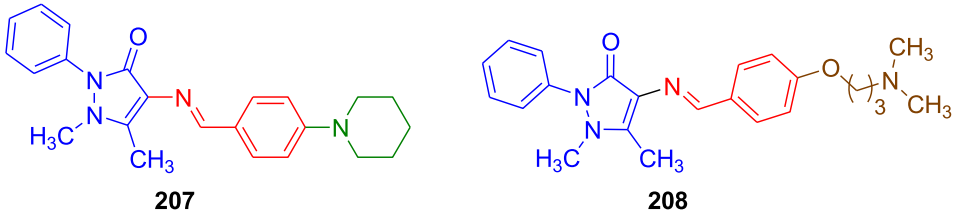

Fig. 80. Structures of AChE/BuChE inhibitors.

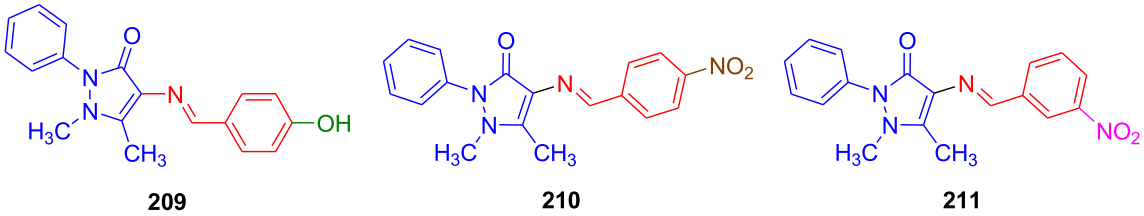

Fig. 81. Structures of prominent MAO inhibitors.

2.34. 1,2,3-Triazole appended tacrine-coumarin hybrids

Tacrine as specific catalytic anionic site inhibitor and coumarin scaffold that has affinity towards the PAS of ChEs have been reported by many researchers [168]. Coumarin and tacrine scaffolds **241** and **242** (Fig. 96) were developed and demonstrated for inhibition of cholinesterases [110,115,168]. Based on anti-AD properties of coumarin-tacrine derivatives [169], 1,2,3-triazole appended tacrine-coumarin hybrids were engineered and synthesized [170].

All the synthesized compounds were evaluated for cholinesterase inhibitory activities using tacrine and donepezil as references. All most all the derivatives exhibited good inhibitory activity; where in large fraction of synthesized compounds showing descent AChE inhibitory activity were provided in Table 12. In those, derivative **245** possessing −Cl at 6-position of tacrine and $-CH_3$ at 4-position of coumarin flanking alkyltriazole moiety (Fig. 97) had highest AChE inhibitory activity; its activity was twice the activity of both donepezil and tacrine.

Similarly a very nice activity was observed towards BuChE inhibitory activity and all the evaluated derivatives exhibited higher potency compared to donepezil. However comparable BuChE inhibitory activity was shown by half of the compounds where in most potent compound **250** entailed methylene triazole conjugated plane tacrine and plane coumarin flanking pentyl chain (Table 12 & Fig. 97) was far most potent compared to tacrine.

The moderate BACE1 inhibitory activity was observed for synthesized compounds where in OM99-2 used as reference compound. In comparison with OM99-2 (IC_{50} = 14.7 ± 2.83 nM) potent AChE inhibitor **245** shown 28.69 ± 4.79% and 13.97 ± 12.99% inhibition at 50 μM and 10 μM respectively.

2.35. 2-Benzofuran carboxamide-benzylpyridinum salts

The novel derivatives have been designed possessing dual inhibitory activity which might be promising approach for AD treatment [171]. Benzofuran-2-carboxamide derivatives are well known for their AChE inhibitory activity [172]. Similarly benzofuran based scaffolds were demonstrated to exhibit cholinesterase inhibitory activity [173]. With these evidences of cholinesterase inhibitory activities, a set of *N*-benzylpyridinium halides have been synthesized and their cholinesterase inhibitory activities were screened [174].

The lead compounds have shown excellent inhibitory activity towards BuChE. Some of the BuChE inhibitory activities were provided in Table 13. Among them, benzofuran derivative **256** (Table 13 & Fig. 98) in which benzene ring of benzylpyridinium attached with –F and NO_2 moieties at 2- & 6-postions respectively was most potent molecule. It has possessed hundred-fold higher potency compared to donepezil. Both electron donating and electron withdrawing groups have shown their impact on BuChE inhibitory activity.

However, a very poor AChE inhibitory activity was observed for designed compounds. The moderate inhibitory activity was shown by the compounds **258** and **259** (Fig. 98) with IC_{50} values 2.0 ± 0.8 μM and 2.1 ± 0.1 μM respectively which were approximately seventyfold less potent compared to donepezil (IC_{50} = 0.031 ± 0.005 μM). Hence, the results revealed that the synthesized compounds were selective AChE inhibitors.

The amyloid-*β*-self-aggregation inhibitory activity was determined at 10 μM concentration using donepezil and rifampicin as reference compounds. The activity results indicated the inhibitory percentages of the derivatives were potent BuChE inhibitors where in **256** (33.1 ± 11.2%) and AChE inhibitor **259** (46.4 ± 2.2%) were better

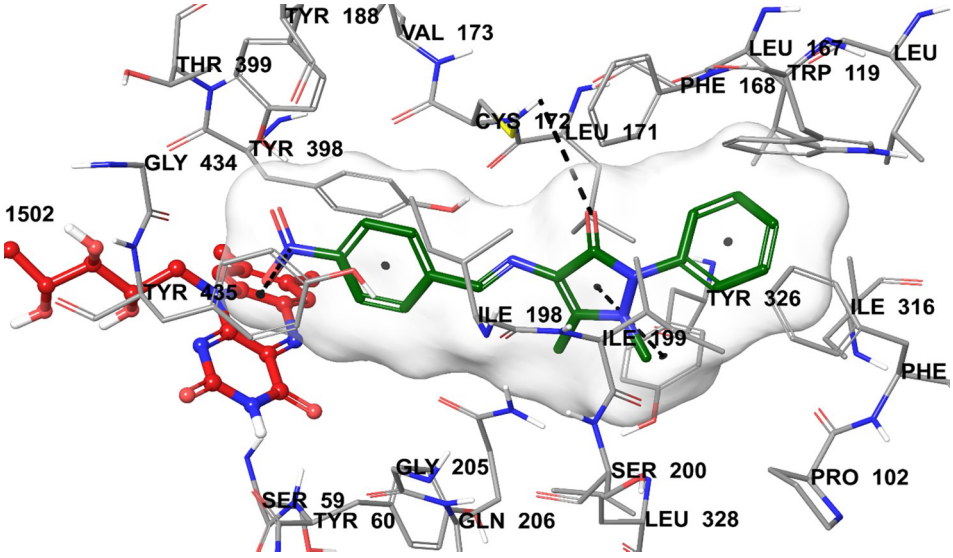

Fig. 82. Binding interactions of potent MAO-B inhibitor **210** with MAO-B active site [153].

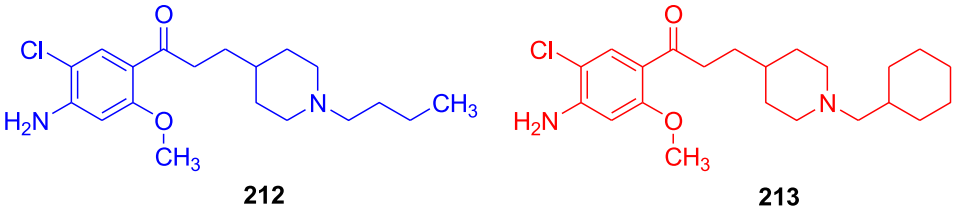

Fig. 83. Structure of RS67333 (**212**) and σ_1R antagonist (**213**).

than the donepezil (22.0 ± 5.4%) and rifamficin (27.5 ± 4.3%). The methoxy group on phenyl ring of benzylpyridinium moiety might be reason for twofold activity compared to reference compounds.

Docking interaction of compound **256** with BuChE (Fig. 99) revealed a H-bond between oxygen of benzofuran and Ser198 amino acid. Pyridinium nitrogen makes π-cation interaction with aromatic residues Phe329 and Trp82 by virtue of its positive charge. Furthermore, benzyl pyridinium moiety has π-π affinity with Tyr332 residue.

2.36. Coumarin-pyridinium hybrids

Coumarin motifs found in natural products were reported to have many biological properties in addition to anti-AD properties [175]. Many coumarin based scaffolds are under clinical trials for anti-cholinesterase properties [47]. Based on the previous research on coumarin and pyridinium moieties [176,177] coumarin-pyridinium hybrid derivatives were designed [178].

In the cholinesterase inhibitory activity determined using rivastigmine and donepezil as reference compounds. Compared to both reference compounds (**rivastigmine**: IC_{50} = 7.72 ± 0.02 μM, **donepezil**: IC_{50} = 8.06 ± 0.38 μM), the tested compounds exhibited descent anti-BuChE activity; particularly 3-chloro benzylpyridinium analog **260** (IC_{50} = 0.32 ± 0.06 μM) and 2,3-dichloro benzylpyridinium derivative **261** (IC_{50} = 0.43 ± 0.03 μM) (Fig. 100) have exhibited excellent activity. Whereas no single derivative was a potent AChE inhibitor compared to donepezil (IC_{50} = 0.028 ± 0.002 μM). However, in comparison with rivastigmine (IC_{50} = 11.07 ± 0.01 μM), few compounds have resulted good activity; among them 3-fluoro benzylpyridinium derivative **262** (IC_{50} = 10.14 ± 0.14 μM) was a potent inhibitor.

The significant cholinesterase inhibitors **260** (BuChE) and **262** (AChE) were chosen for inhibition of *β*-secretase (BACE1) using OM99-2 as a positive control. BACE1 inhibitory percentages obtained were in accordance to cholinesterase inhibitory values observed previously; moderate and weak activities were shown by derivatives **260** (6.7%) and **262** (22%) respectively compared to **OM99-2** (IC_{50} = 0.014 μM).

The most potent BuChE inhibitor **260** (Fig. 101**)** was subjected to docking in the active site of BuChE wherein alignment of coumarin ring towards Trp231 and Phe329 residues *via* π-π stacking was observed. In addition, π-π stacking was also formed between benzyl moiety and Trp82. The phenyl ring of coumarin has affinities with Leu286 and Val288 through π-alkyl and pyridinium moiety has affinity with Trp residue *via* π-alkyl interactions.

3. Cholinesterase inhibitors

Acetylcholine enzyme acts as a neurotransmitter of the peripheral and central nervous system (CNS). It establishes neural conduction at the neuromuscular junctions in the peripheral nervous system and in particular controls the memory and learning process in the CNS. Two enzymes that hydrolyze the acetylcholine are the AChE and BChE enzymes leading to disruption of neurotransmission. Hence, inhibition of cholinesterases would be a novel approach for AD treatment.

3.1. Aryl-1,2,3-triazolyl benzylpiperidine

Based on donepezil structure, two series of derivatives were engineered wherein the first series constitute replacement of 5,6-dimethoxy-1-indanone moiety by 1,2,3-triazole conjugated with substituted/un-substituted aromatic scaffolds and in the second series, replacement was made with azido amino acids to yield aryl-1,2,3-triazolyl benzylpiperidine analogs [179].

Using donepezil as reference compound, the cholinesterase inhibitory activities were determined. Compared to donepezil (IC_{50} = 0.0057 ± 0.0005 μM), the synthesized derivatives have not shown any significant *h*AChE inhibitory activity. Lower moderate activity (IC_{50} = 3.94 ± 0.26 μM) was observed in case of compound **263**. Surprisingly, towards *h*BuChE inhibition spectacular activity has been exhibited by the evaluated compounds except three compounds. Among those, benzimidazole thiol derivatized triazole analog **264** (IC_{50} = 0.065 ± 0.002 μM), amino acid azide derivative **265** and its acetyl analog **266** yielded the best results with IC_{50} values 0.0099 ± 0.0043 μM and 0.00017 ± 0.000021 μM respectively. Compared to donepezil (IC_{50} = 9.14 ± 0.56 μM), the derivative **266** (Fig. 102) with BuChE inhibitory value (IC_{50} = 1.7 dM) at decimolar concentration level was 54000-fold higher potent. So it can be concluded that all the tested compounds were selective BuChE inhibitors.

The most significant BuChE inhibitory activity of **266** was supported by the molecular docking studies (Fig. 103). In this, π-π aromatic interactions were observed for benzyl group with Trp430 and Trp82 side chains in addition to H-bond interaction carbonyl of acetyl group and Thr284 side chain. The impressive activity of **266** was related to its flipped conformation within the active site which is attributed to the acetyl group that hides corresponding primary amine.

3.2. Imidazole analogs

Heteroaromatic rings such as benzimidazole and other heterocycles have been reported to possess promising acetylcholinesterase inhibitory

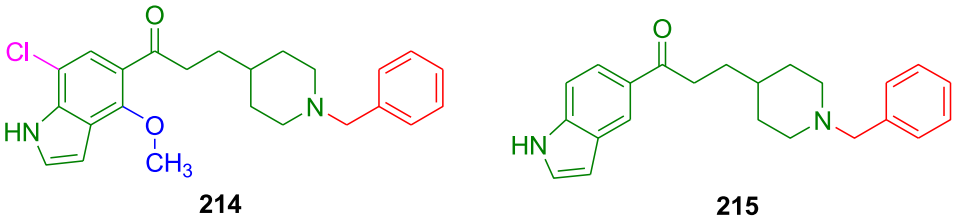

Fig. 84. Structure of significant *h*AChE inhibitors.

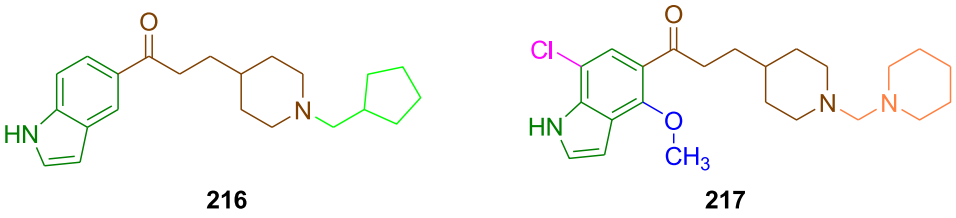

Fig. 85. Structures of prominent HT4R inhibitor (**216**) and σ_1R antagonist (**217**).

activity [180,181]. Inspired by the potent AChE and BuChE inhibitory activity of thiazole derivatives, [182] new series of derivatives was designed by substitution of sulfur of thiazole with nitrogen to afford 2-substituted-4,5-diphenyl-1*H*-imidazole analogues [183]. The *in vitro* cholinesterase inhibitory activities were determined for synthesized molecules.

Donepezil and galantamine were used as reference compounds for determination of percentage inhibitions of AChE and BuChE at 10 μM. Few derivatives have shown moderate to descent AChE activity; 3-hydroxyphenyl derivative **267** (65.08 ± 4.34%) and 3,4-dimethoxy analog **268** (67.33%) (Fig. 104) were the compounds which exhibited good inhibitory activity compared to donepezil (91.07 ± 8.23%). In spite of potent activity of compound **268**, it was excluded from potent molecules as the solubility issues arisen. In case of BuChE activity, most of the compounds exhibited inactive or weak activity. However compounds **269** (79.45 ± 6.60) and **270** (81.28 ± 6.85) were as potent as galantamine (80.77 ± 8.01). IC_{50} values of significant AChE inhibitor **267** and **270** have been determined and compared to donepezil (AChE: IC_{50} = 0.1 μM,) and galantamine (AChE: IC_{50} = 1.6 μM, BuChE: IC_{50} = 3.31 μM). The inhibitory results indicated that compound **267** was inactive towards BuChE and moderate inhibitor (IC_{50} = 5.33 μM) of AChE. The derivative **270** has not shown inhibition towards AChE but exhibited significant inhibitory activity (IC_{50} = 4.99 μM) on BuChE.

3.3. p-Aminobenzoic acid derivatives

4-Aminopyridine scaffolds were designed and demonstrated as potential cholinesterase inhibitors [184,185]. Lot of research has been carried out on *m*- & *p*-aminobenzoic acid derivatives towards cholinesterase inhibition and results inferred that *p*-substituted analogs had higher inhibitory activity than that of *m*- or *o*-substituted derivatives [186,187]. In this regard, carbazides of *p*-aminobenzoic acid were prepared and screened for cholinesterase inhibitory activity [188].

Large portion of the synthesized compounds were weak inhibitors of AChE and BuChE. Few derivatives have shown moderate activity towards AChE. In comparison with donepezil, simple benzophenone analog **271** (IC_{50} = 0.056 ± 0.016 μM), 4-hydroxy benzophenone derivative **272** (IC_{50} = 0.050 ± 0.01 μM) and 4,4′-dihydroxybenzophenone derivative **273** (IC_{50} = 0.046 ± 0.01 μM) (Fig. 105) were most significant AChE inhibitors and these were almost as potent as donepezil (IC_{50} = 0.040 ± 0.012 μM). Keen observation of the AChE inhibitory activity revealed that benzophenone carbazides of *p*-aminobenzoic acid were selective AChE inhibitors. While the synthesized compounds displayed weak to good BuChE inhibitory activity compared to donepezil (IC_{50} = 15.240 ± 0.42 μM). However, only a few compounds have exhibited moderate inhibitory values compared to rivastigmine (IC_{50} = 1.660 ± 0.44 μM); amongst them simple acetophenone derivative **274** (IC_{50} = 1.112 ± 0.76 μM) has shown greater potency than that of rivstigmine and 3-methoxy-4-hydroxy acetophenone analog **275** (IC_{50} = 5.840 ± 1.75 μM) (Fig. 105) was a moderate BuChE inhibitor.

Docking simulation of compound **273** (Fig. 106) in AChE active site exhibited π-π stacking between biphenyl portion with *p*-hydroxy substituent and Trp279. The compound **273** has also formed interaction with the PAS residues such as Tyr70, Try121, and Tyr334 by hydrophobic pocket and Asp72 through charged interaction. Besides these interactions, compound **273** has descent affinity with acyl binding pocket with residues Phe288, Phe290, and Phe331.

3.4. Phenyl benzoxazole derivatives

Various hybrid compounds of phenyl benzoxazole tethered to berberine and tacrine have been designed and synthesized as acetylcholinesterase inhibitors [144]. Likewise, coumarin, piperazine, and piperidine derivatized benzoxazole molecules were reported to exhibit AChE inhibition at nanomolar to micromolar concentration [189,190]. Based on Gaussian quantitative structure-activity relationship (QSAR) drug design [191], novel series of phenyl benzoxazole derivatives was synthesized as potent cholinesterase inhibitors [192].

In the inhibitory activity towards AChE, poor to moderate potencies were seen. A few compounds **276–279** with good yet lower activity compared to donepezil are provided in Table 14. The derivative **277** with 4-chloro phenyl linked to diaminoalkanol chain was most potent inhibitor among the synthesized compounds. Accordingly poor BuChE inhibitory activity has been exhibited by most of the tested compounds. However few compounds provided in Table 14 were potent inhibitors and all of them exhibited 3–7 fold higher potency compared to donepezil. The derivatives provided in Table 14 were dual inhibitors having the capability of inhibiting both AChE and BuChE.

3.5. Tetrasubstituted thiazoles

Aryl urea/thiourea containing coumarinyl thiazoles have been reported to play significant role in inhibition of cholinesterases [193]. An

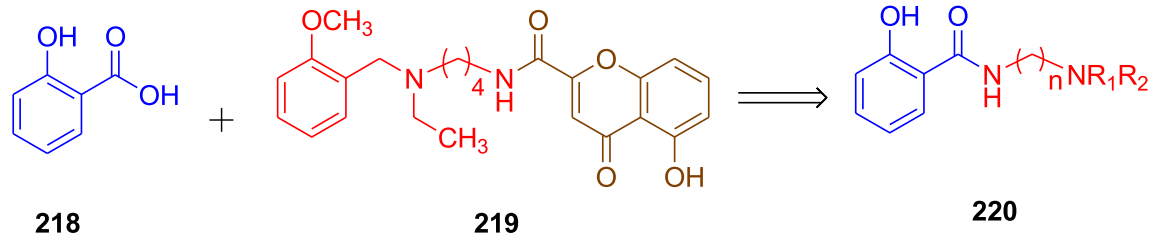

Fig. 86. Illustration of strategic design of salicylamide derivatives.

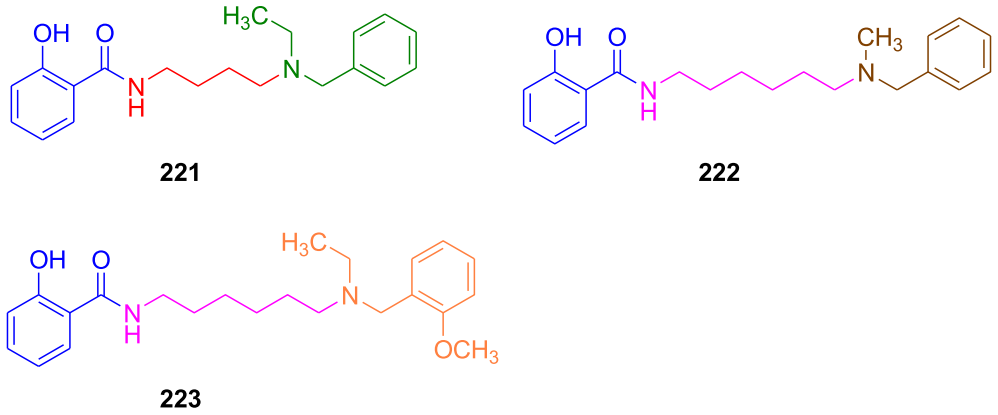

Fig. 87. Structures of potent cholinesterase/Aβ-aggregation dual inhibitors.

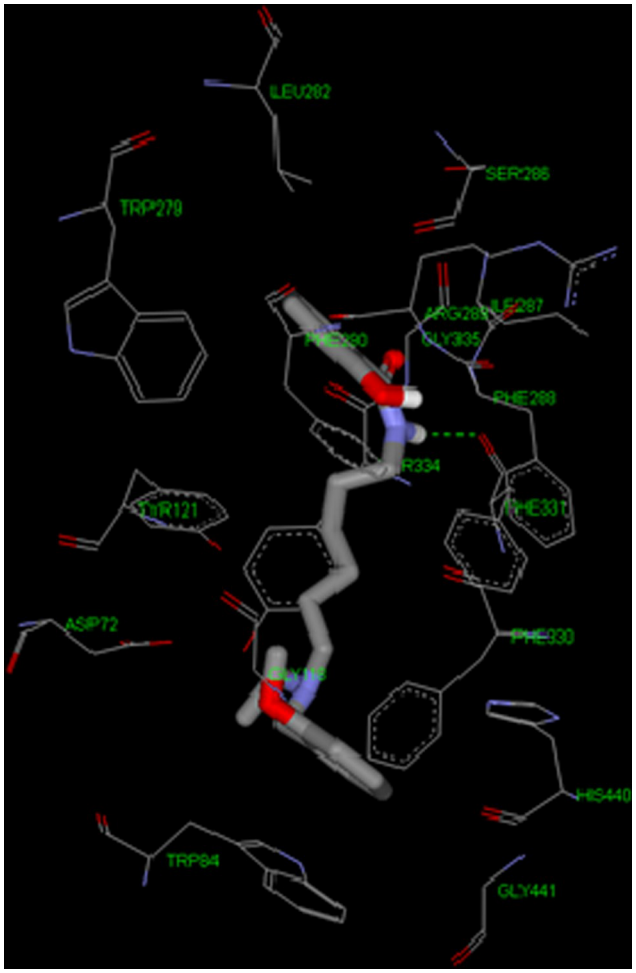

Fig. 88. Representation of compound **223** having interaction with AChE [160].

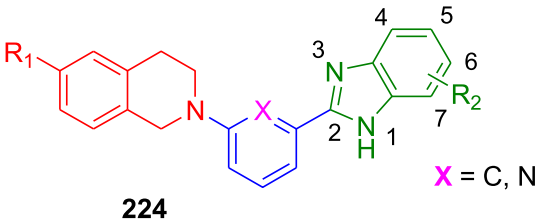

Fig. 89. Depiction of design of tetrahydroisoquinoline-benzimidazole hybrids.

excellent inhibitory activity towards AChE and BuChE was exhibited by fluorobenzo[*d*]thiazol-2-yl)ethanamine [194]. In this context, multi-substituted thiazoles from 1,3-disubstituted thiourea analogs were engineered and subsequently *in silico* cholinesterase inhibitory activity was determined [195].

Moderate AChE inhibitory values were observed for synthesized compounds compared to reference compounds donepezil and galantamine. Among the evaluated derivatives **280** (IC_{50} = 1.03 ± 0.06 μM) and **281** (IC_{50} = 1.69 ± 0.08 μM) (Fig. 107) have exhibited comparable activity. Although these two compounds exhibited lower activity compared to donepezil (IC_{50} = 0.032 ± 0.003 μM); they have comparable activity with that of ralantamine (IC_{50} = 0.62 ± 0.01 μM). More than half of the synthesized compounds were as potent as donepezil (IC_{50} = 6.41 ± 0.34 μM); two compounds **281** (IC_{50} = 0.75 ± 0.08 μM) and **282** (IC_{50} = 0.49 ± 0.04 μM) (Fig. 107) have yielded higher potencies than that of galatamine (IC_{50} = 0.87 ± 0.03 μM). Compound **280** with electron donating methyl groups on phenyl rings was a selective AChE inhibitor and derivative **282** with electron withdrawing –Cl atoms on phenyl ring shown selective BuChE inhibitory activity. Whereas the compound **281** with electron donating $–CH_3$ moiety and electron withdrawing OCH_3 (negative inductive effect) acted as AChE/BuChE dual inhibitor.

Binding interactions of compound **280** (Fig. 108) in active site of the AChE revealed sandwich type binding of 2-oxo-2-phenylacetyl group by aromatic residues Tyr72, Tyr337 and Trp86 through π-π stackings. In continuation, π-π interactions were also formed by the 2-methyl benzamide moiety with amino acid Trp86. The *p*-tolyl-thiazol-2(3*H*)-imine portion was found to be stacked active pocket center and attribute to the potential activity of the compound **280**.

3.6. Tricyclic fused ring system

A novel homodimer of tacrine with heptylene spacer, *bis*-tacrine (**283**, Fig. 109) was reported as dual binding site inhibitor. *Bi*- and tricyclic fused ring systems entailing quinolizidinyl moiety have been designed as acetylcholinesterase inhibitors [196]. Similarly phenothiazine and phenoselenazine derivatives **284** and **285** were potent towards cholinesterases [197]. Taking consideration of all these cholinesterase inhibitors, novel tricyclic fused ring derivatives were designed as ChE inhibitors [198].

The tricyclic fused ring derivatives have been allowed to inhibit cholinesterases using donepezil and tacrine as reference compounds. Tricyclic analog **286** (Fig. 110) in which desloratadine tethered to carbazole moiety by hexylene chain has shown potent AChE and BuChE inhibitory activities with IC_{50} values 0.10 ± 0.009 μM and 4.3 ± 0.08 μM. Both AChE and BuChE inhibitory activities were enhanced by substitution of carbazole with indanone moiety for the compound **287** has resulted into most potent cholinesterase activity.

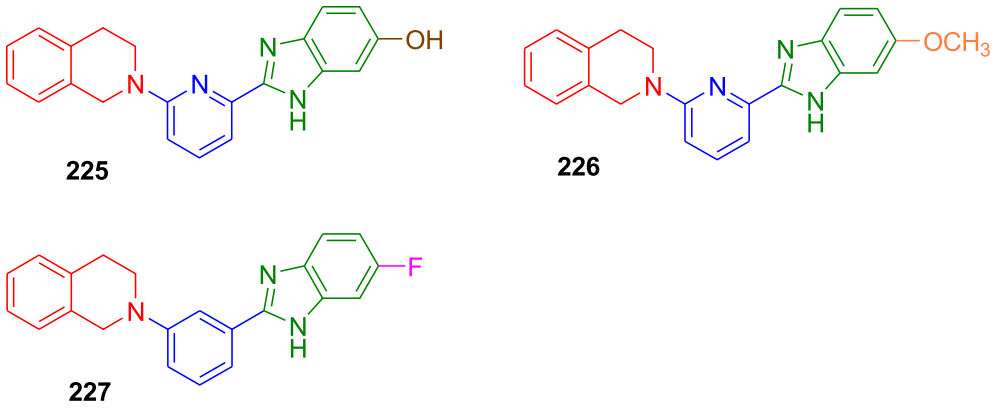

Fig. 90. Structures of potent neuroinflammatory inhibitors (NO).

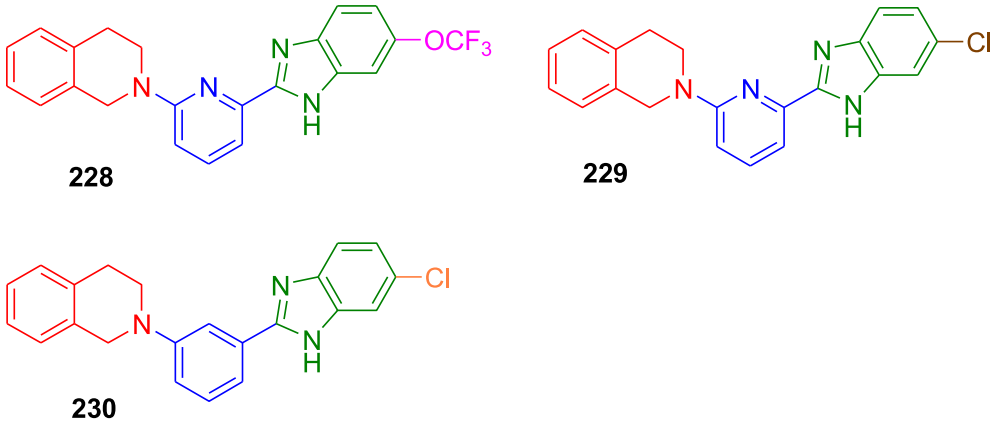

Fig. 91. Structures of prominent BACE1 inhibitors.

The inhibitory activities of derivative **287** with IC_{50} values 0.09 ± 0.003 μM and 1.04 ± 0.08 μM towards AChE and BuChE respectively were comparable with that of donepezil (AChE: IC_{50} = 0.05 ± 0.01 μM, BuChE: IC_{50} = 5.4 ± 0.27 μM) and tacrine (AChE: IC_{50} = 0.4 ± 0.019 μM, BuChE: IC_{50} = 0.06 ± 0.009 μM). Remaining compounds have exhibited weak to moderate inhibitory activity.

The most potent *ee*AChE inhibitor **287** (Fig. 111) established H-bond and π-π interactions with key amino acid residues in molecular docking studies. Where as, the carbonyl group of tricyclic indanone ring formed H-bond interactions with catalytic triad residue Ser200. Further, phenyl ring at 4-position has interacted with Trp84 *via* π-π stacking.

3.7. 3-(4-Aminophenyl)-coumarin derivatives

The schiff base scaffolds comprising triazole ring, uracil moiety and aryl methanesulfonate derivatives have been reported as prominent AChE and BuChE inhibitors [199,200]. Coumarin and benzylpiperidine were set into single molecular frame to afford benzylpiperidine derivatives as inhibitors of cholinesterases [171]. Hence, focus was put into design and preparation of 3-(4-aminophenyl)-coumarin derivatives [201].

Although, most of the evaluated molecules have not shown significant AChE inhibitory activity; some derivatives had moderate activity and in particular naphthalene analog **289** (IC_{50} = 0.128 ± 0.011 μM) (Fig. 112) has relatively good activity yet tenfold less potent compared to donepezil (IC_{50} = 0.012 ± 0.001 μM). 4-Chloromethylene phenyl analog **288** was found to be strongest AChE inhibitor (IC_{50} = 0.091 ± 0.011 μM). Approximately half of the synthesized derivatives were descent BuChE inhibitors. 3-Fluoro phenyl derivative **290** (IC_{50} = 0.905 ± 0.081 μM) and 4-fluoro phenyl analog **291** (IC_{50} = 0.559 ± 0.017 μM) (Fig. 112) were potent BuChE inhibitors; where in compounds **290** and **291** have shown twofold and

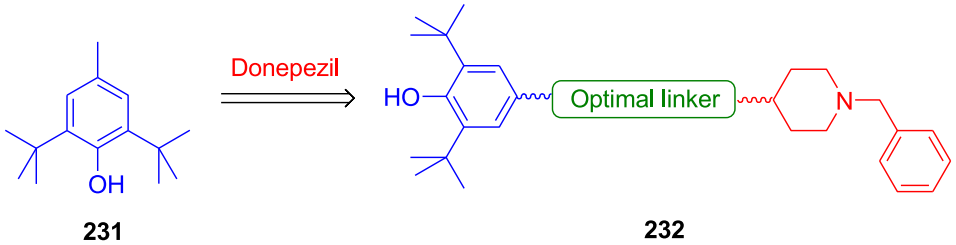

Fig. 92. Demonstration of design of donepezil-butylated hydroxytoluene analogs.

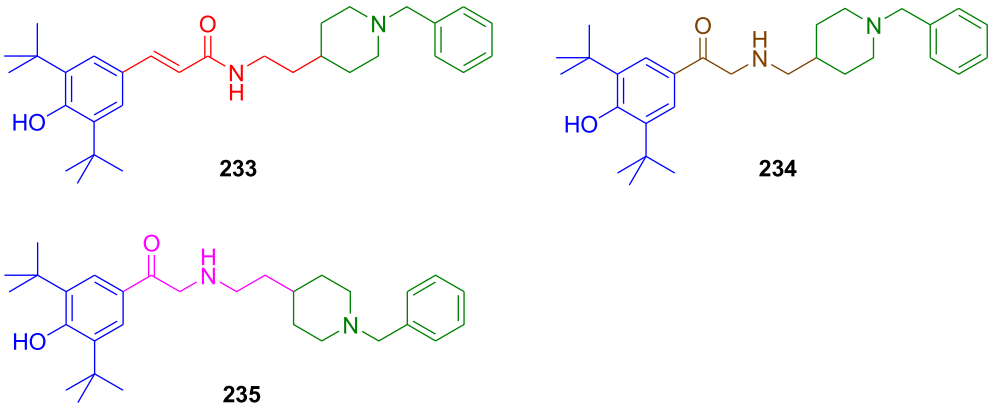

Fig. 93. Structures of donepezil-butylated hydroxytoluene hybrids possessing significant cholinesterase inhibitors.

fourfold higher potencies than that of donepezil (IC_{50} = 2.665 ± 0.015 μM).

3.8. Biphenyl-3-oxo-1,2,4-triazine conjugated piperazine derivatives

1,2,4-Triazine was reported as attractive moiety towards potential AChE inhibitory activities [202,203]. The literature so far indicated that vicinal biaryl-1,2,4-triazine derivatives **292** could modulate cholinesterase activity through intrinsic antioxidant property [204]. 3-Thioalky-5,6-biaryl-1,2,4-triazine scaffolds **293** (Fig. 113) possess the capability to suppress ROS generation and induce oxidative stress-induced cell death [205]. Despite the lower AChE inhibitory activity of piperazine motif; its derivatives have been reported to have substantial neuroprotective activity [206]. All these consequently led to design of 1,2,4 triazine derivatized piperazine derivatives [207].

Triazine derivatives were analyzed for anti-ChE activity using donepezil as reference compound. Except few derivatives, most of the synthesized molecules were descent AChE inhibitors. Significant activity exhibited by the triazine derivatives was provided in Table 15. Almost comparable potencies were shown by the 4-methoxy benzyl analog **298** and simple benzyl derivative **299** (Fig. 114) with that of donepezil. Three carbon spacer tethered by biaryl triazine and piperazine moiety on either sides was more beneficial in both AChE and BuChE inhibitors which was inferred by the potent cholinesterase inhibitory values.

In spite of the best AChE inhibitory activity of the synthesized derivatives; most of them were inactive towards BuChE. Only a few derivatives have exhibited comparable activity. Particularly compound benzylpiperidine derivative **299** (IC_{50} = 4.6 ± 0.19 μM) and 4-fluorobenzyl piperidine scaffold **301** (IC_{50} = 5.2 ± 0.19 μM) were almost as potent as donepezil (IC_{50} = 4.1 ± 0.28 μM).

The molecular docking studies of significant AChE inhibitor **299** (Fig. 115) on AChE has shown following results. The polar interactions were observed for compound **299** between benzylpeperidine and aminoacid residues His440 and Ser200. The derivative also forms π-π stacking interactions and cation-π interaction with the Trp84. While the cation quarternery nitrogen exhibited cation-π interaction with Phe330, Phe331 and Phe334. Apart from this, π-π stacking interactions were also observed in between Trp279 and biaryl nucleus.

3.9. Indol-3-acetic acid-tacrine hybrids

Indol-3-acetic acid scaffolds **302** (Fig. 116) have been developed as anti-AD compounds possessing weak to moderate cholinesterase inhibitory activity [208,209]. Potent anti-AD properties of indol-3-acetic acid (IAA) analogs have paved to structural modification of tacrine with IAA and design of new IAA-tacrine derivatives **303** [210].

All the synthesized derivatives have been allowed for AChE and BuChE inhibitory evaluation where in tacrine was used as a positive control. The synthesized compounds include two series of molecules; indol-3-acetic acid linked to secondary amines/amides/alkoxide/esters/sulfonates through alkyl chain form first series of derivatives and the second set entails indol-3-acetic acid tethered to tacrine bridged with alkyl chain. The first series of derivatives have shown inhibitory activity neither towards AChE nor towards BuChE.

While most of the IAA-tacrine derivatives of second series have managed to produce good AChE and BuChE inhibitory values compared to that of tacrine. Compounds **304–308** (Table 16) have descent AChE inhibitory activity among the competing inhibitors. The AChE inhibitory value of most potent inhibitor **306** possessing pentylene chain (Fig. 117) was comparable to that of tacrine. Regarding inhibitory activity towards BuChE, strongest inhibitory activity was observed for compounds **304–306**. Compared to tacrine, these compounds have very high inhibitory values; particularly compound **305** with butylene chain had approximately fivefold higher potency than that of reference compound.

3.10. Uracil derivatives

5-Fluorouracil **307** (Fig. 118), a well-known antineoplastic drug has been used for inhibition of thymidine phosphorylase. Likewise, fluoroxyuridine **308**, a uracil analog was reported to treat malignant neoplasms of the liver and gastrointestinal tract and hepatic metastases. Similarly, lymphatic malignancies which causes gastrointestinal and

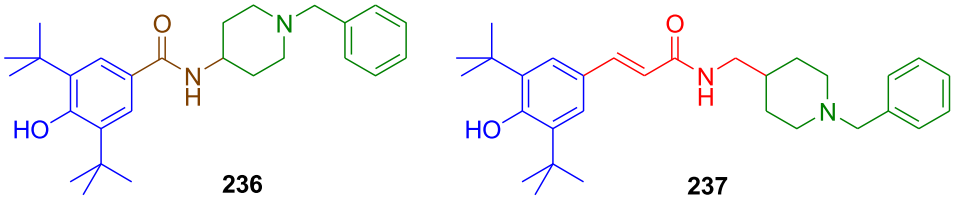

Fig. 94. Structures of compounds showing significant MAO inhibitory activity.

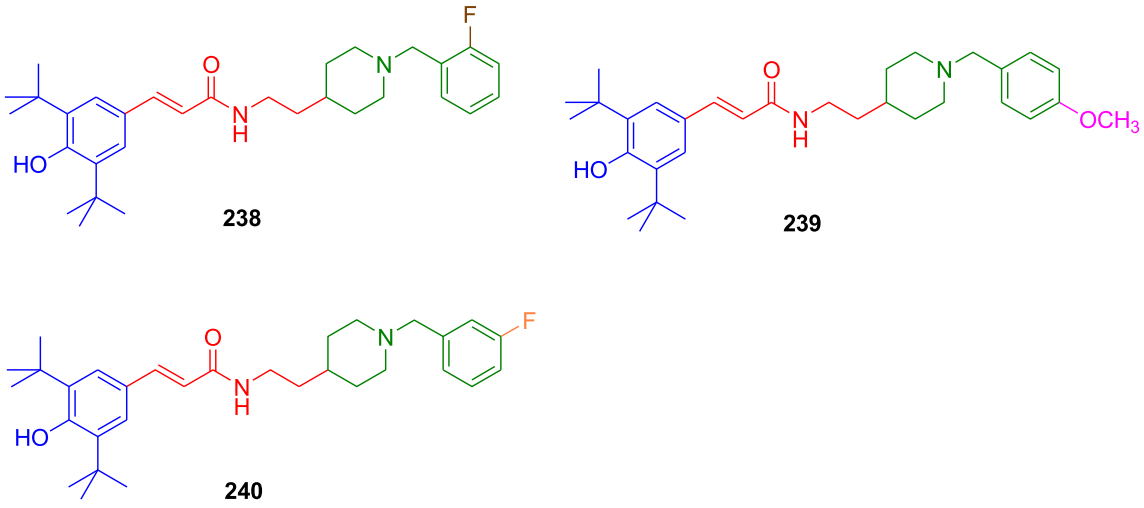

Fig. 95. Structures of AChE (**238**) and MAO inhibitors (**239** & **240**).

bone marrow damage were treated by uramustine **309** [211,212]. Till now uracil derivatives have utilized mostly for cancer treatment. Researchers have investigated some reported uracil drugs for their cholinesterase inhibitory activity [213].

The uracil was derivatized at N_1, C_5 and C_6 positions to afford the various uracil analogs. These derivatives were tested for cholinesterase inhibitory activities using neostigmine as reference compound. Few compounds have exhibited comparable AChE inhibitory activity with that of neostigmine; significant AChE inhibitory values for compounds **310–314** are given in Table 17. Compound **312** (Fig. 119) with *p*-toluene sulfonyl moiety at N_1 and bromo group at C_5-position has exhibited strong inhibitory activity; approximately 1.5 higher potency than that of neostigmine. In case of inhibitory activity towards BuChE, weak activity was seen for all most all derivatives. However the potent AChE inhibitor **312** (IC_{50} = 0.137 μM) was also a significant BuChE inhibitor but 1.6-fold lower potent than that of neostigmine.

In the molecular docking studies of AChE/BuChE dual inhibitor **312** (Fig. 120), locates itself between aminoacid residues Ser125 and Glu202 and forms descent H-bond interaction with Glu202 and π-π stacking affinity with Trp86. Regarding BuChE, the aromatic rings have formed π-π stacking interaction with Trp82 and Tyr332; while uracil ring has H-bonded with residues Glu197 and His438.

4. Monoamine oxidases

Monoamine oxidase (MAO) enzymes comprise of flavin adenine dinucleotide (FAD) which exist as two different isoforms (MAO-A and MAO-B) [214]. MAOs were reported to have prominent role in treatment of AD and regulate xenobiotic amine and monoamine neurotransmitters. Usually the AD patients express symptoms related to depression [215]. MAO-A inhibitors were reported as significant antidepressants and therefore used to treat parkinson disease and AD [216]. Since MAO-Bs were the culprits responsible for the increased

Table 12
Cholinesterase inhibitory values of tacrine-coumarin hybrids.

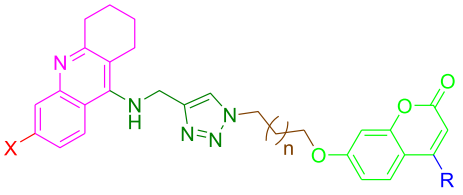

Compd	n	R	X	AChE (IC_{50}, μM)	BuChE (IC_{50}, μM)
243	1	H	H	ns	0.032 ± 0.011
244	1	H	Cl	0.056 ± 0.011	ns
245	1	Me	Cl	0.027 ± 0.009	ns
246	2	H	H	0.046 ± 0.021	ns
247	2	H	Cl	0.044 ± 0.014	0.060 ± 0.004
248	2	Me	H	0.066 ± 0.005	0.078 ± 0.010
249	2	Me	Cl	0.068 ± 0.009	ns
250	3	H	H	0.095 ± 0.014	0.006 ± 0.002
251	3	H	Cl	0.052 ± 0.026	0.070 ± 0.016
252	3	Me	H	0.050 ± 0.033	0.038 ± 0.004
253	3	Me	Cl	0.039 • ± 0.021	ns
Tacrine				0.048 • ± 0.011	0.010 ± 0.004
Donepezil				0.039 • ± 0.097	8.416 • ± 0.628

ns - not significant.

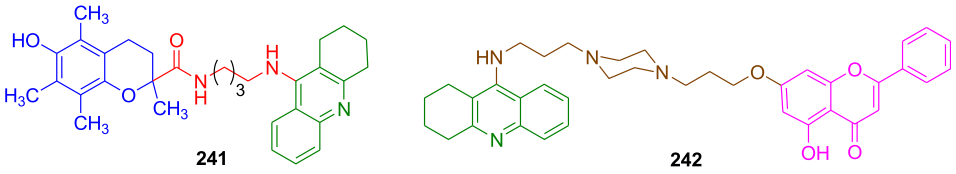

Fig. 96. Structures of significant AChE inhibitors.

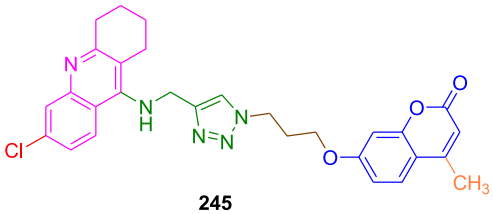

245

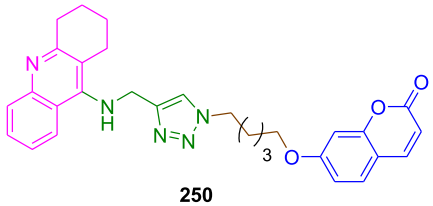

250

Fig. 97. Structures of excellent inhibitors of cholinesterase.

Table 13
BuChE inhibitory values of benzofuran carboxamide-benzyl-pyridinum salts.

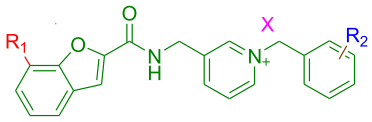

Compd	R_1	R_2	X	IC_{50} (μM) BuChE
254	H	3-CH_3	Br	0.11 ± 0.01
255	H	2-NO_2	Br	0.15 ± 0.01
256	H	2-F, 6-NO_2	Br	0.054 ± 0.002
257	OCH_3	2,4-diCl	Cl	0.18 ± 0.01
Donepezil	-	-	-	5.4 ± 0.1

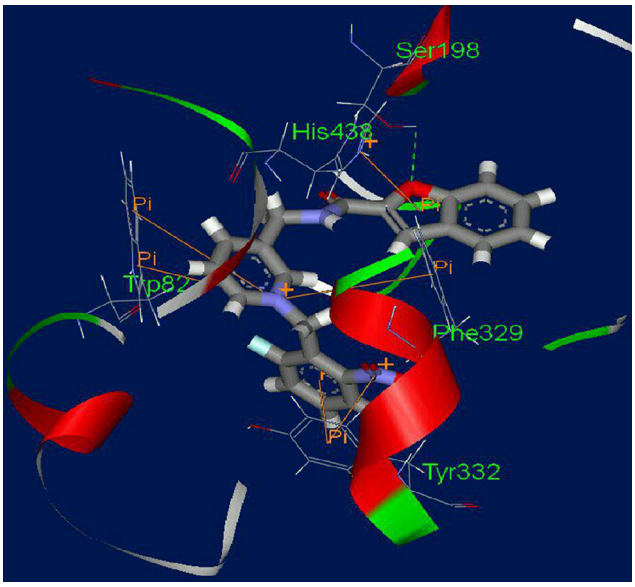

Fig. 99. Interaction of most potent BuChE inhibitor **256** in BuChE active site [174].

expression of γ-secretase and *β*-secretase and improvement of A*β*-plaques [217], inhibition of MAO-Bs would aid in AD treatment.

4.1. 3-(E)-Styryl-2H-chromene derivatives

Pharmacological significant structural moiety chromone, a structural analog of chromene was reported for its potent MAO inhibitory property [218,219]. (*E*)-Styrylisatin [220] and (*E*)-8-styrylcaffeine [221], structurally related derivatives of resveratrol were report to possess inhibitory effects on MAOs. Thus having confirmed the anti-AD properties of chromene and styryl derivatives, both moieties were fit into single molecular frame to afford a series of 3-(*E*)-styryl-2*H*-chromene derivatives [222].

Pargyline is used as a positive control for MAO inhibitory activity of styryl-chromene scaffolds at 10 μM. No single compound of the evaluated derivatives has shown good MAO-A inhibitory properties. Except few derivatives, all the synthesized molecules were successful in inhibiting MAO-B (Table 18); these derivatives have far higher potency compared to pargyline.

Among the significant MAO-B inhibitors with IC_{50} values 0.010–0.048 μM, compound **316** (Fig. 121) possessing simple chromene linked to *p*-fluoro styryl moiety was the strongest MAO-B inhibitor with 22 times higher potency compared to pargyline. Similarly, compound **319** having 7-methoxy chromene tethered to 4-fluoro styryl structural

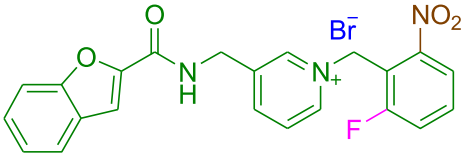

256

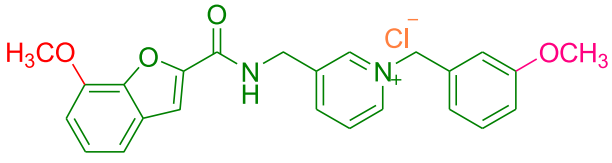

258

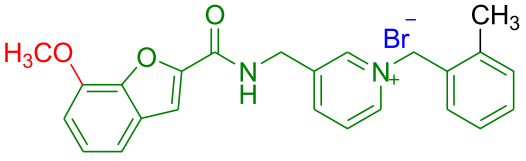

259

Fig. 98. Structures of potent cholinesterase inhibitors.

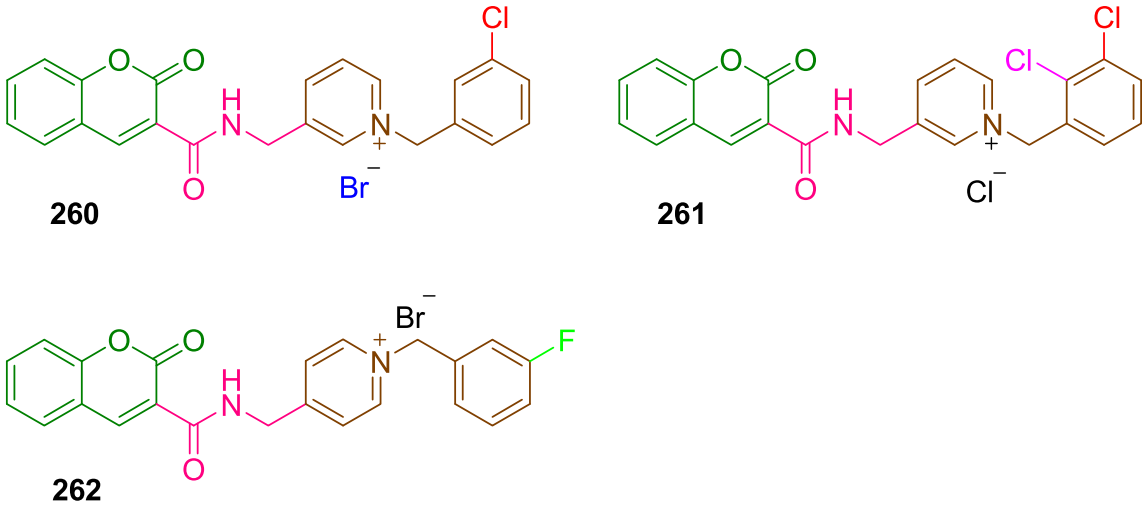

Fig. 100. Structures of significant inhibitors of ChEs.

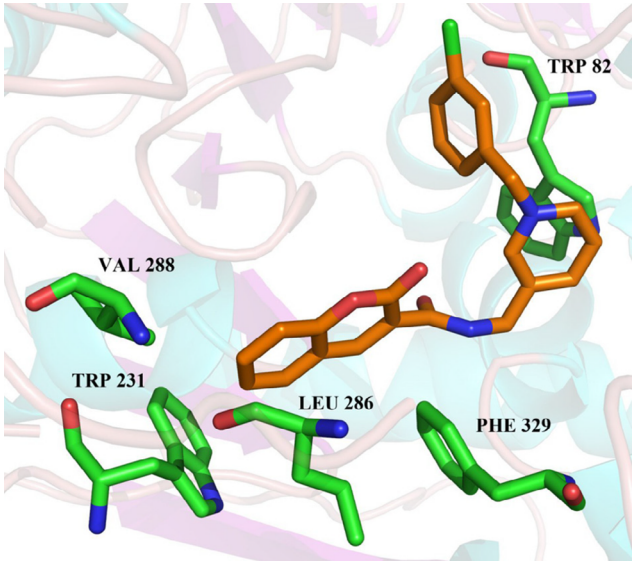

Fig. 101. Depiction of binding mode of compound **260** in BuChE active site [178].

unit was also having significant inhibitory activity; where in its activity was fifteen-fold higher potency than that of pargyline. Small and highly electronegative fluoro group at 4-position of styryl moiety in compound **316** has rendered the strongest activity. However introduction of methoxy group at 7-postion of chromene in case of compound **319** has resulted in abated inhibitory activity. All the synthesized 3-(*E*)-styryl-2*H*-chromene derivatives were exclusively selective MAO-B inhibitors.

4.2. Isoprenyl-resveratrol dimer derivatives

Resveratrol, a polyphenol analog has been used in the treatment of AD [223] and it could interfere with the formation of Aβ and improve antioxidant activity [224]. Resveratrol was found in oligomeric forms in which trans-veniferin **325** (Fig. 122) has higher potency than that of resveratrol. It has been reported that natural products possessing isoprene moiety have good pharmacological properties in addition to antioxidant properties [225]. In this regard isopentadienyl derivatives exhibited higher potencies towards anti-inflammation and antioxidant activity compared to resveratrol [226,227]. These findings led to the design of resveratrol appending to the isoprene structural unit [228].

The synthesized molecules were screened for *h*MAO-A and *h*MAO-B inhibitory properties using iproniazid as a reference compound. In the *h*MAO-A activity weak, moderate and potent activities were observed for various tested molecules; approximately half of them have comparable inhibitory activity. Particularly the best inhibitory activity towards MAO-A was displayed by compound **326** (Fig. 123) with IC_{50} value 2.60 ± 0.04 μM which is threefold higher potent than that of iproniazid (IC_{50} = 6.85 ± 0.33 μM) and derivative **327** (IC_{50} = 8.12 ± 0.05 μM) was one of the significant MAO-A inhibitors. In case of MAO-B inhibitory activity, every tested derivative was a significant inhibitor. Except one compound, all other compounds have elicited greater potency than that of iproniazid (IC_{50} = 8.35 ± 0.46 μM); particularly compounds **326** (IC_{50} = 0.92 ± 0.11 μM) and **328** ((IC_{50} = 1.90 ± 0.65 μM) were most active molecules with ninefold and fourfold higher inhibitory activities respectively in comparison with iproniazid.

4.3. Lazabemide derivatives

Most of the MAO inhibitors have been successful only up to the stage of *in vitro* activity screening [229]; few drugs namely moclobemide, isoniazid **329**, isocarboxazid **330**, lazabemide **331**, and safinamide (Fig. 124) were successful up to usage level. MAO inhibitory activity in all these molecules was attributed to the amide functionality present in them [230]. This very statement triggered to design the novel lazabemide derivatives with amide groups [231].

Rasagiline and moclobemide were used as reference compounds for determination of MAO inhibitory properties of the synthesized lazabemide derivatives. The reference compound rasagiline itself was having larger IC_{50} value (401.32 ± 3.11 μM) and compared to it, most of the tested derivatives were MAO-A active. However in comparison with moclobemide (IC_{50} = 6.30 ± 0.12 μM), most of the evaluated derivatives were weak inhibitors; a few derivatives namely hydroxyethylene moiety tethered to *p*-chloro benzamide **333** (IC_{50} = 7.49 ± 0.10 μM), hydroxylbutylene analog **334** (IC_{50} = 3.12 ± 0.05 μM) and aminobutylene derivative of *p*-chloro benzamide **335** (IC_{50} = 5.04 ± 0.13 μM) (Fig. 125) have potencies that could reach inhibitory activity of moclobemide. Increase of two methylene units in compound **233** affording **234** which resulted in doubling of activity. However, replacement of hydroxy group by amine for derivative **335** led to slightly reduced

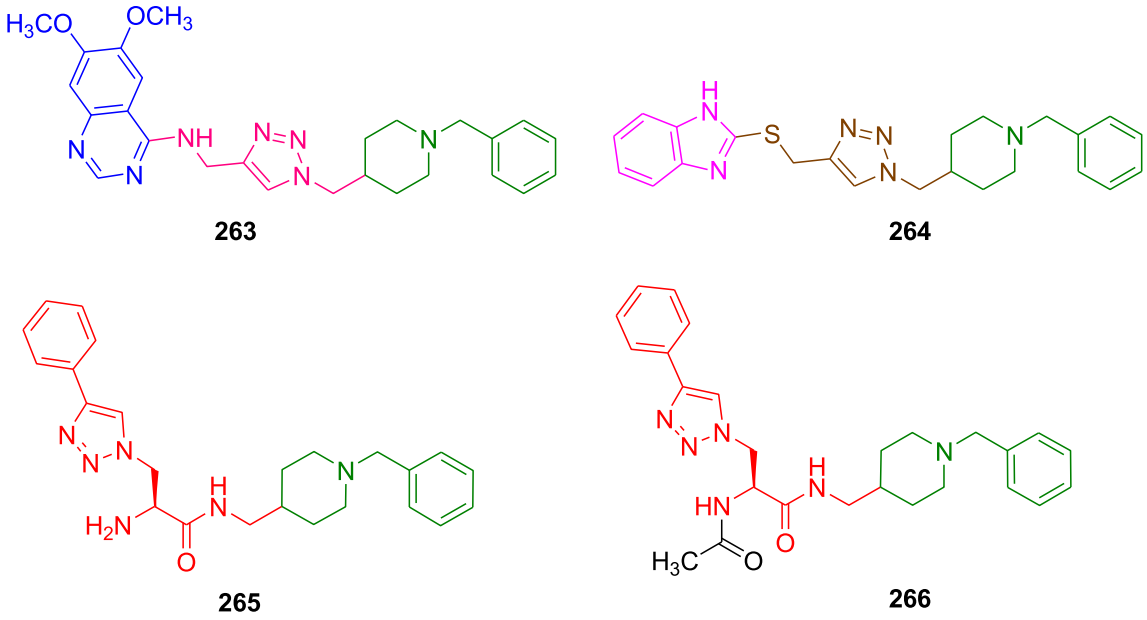

Fig. 102. Structures of prominent cholinesterase inhibitors.

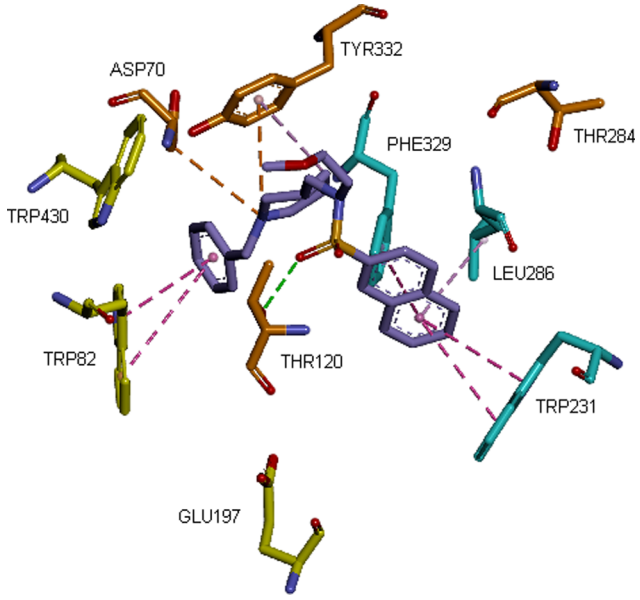

Fig. 103. Demonstration of binding interaction of compound **266** in *h*BuChE active site [179].

activity. The significant MAO-A inhibitors were *p*-chlorobenzamide derivatives; the significant activity was decreased upon substitution of *p*-chlorobenzamide with *m*-chloropyridine motif. The resulted derivatives were MAO-B inhibitors where in the inhibitory selectivity has shifted from MAO-A to MAO-B. Approximately half of the evaluated derivatives have shown descent MAO-B inhibitory activity compared to moclobemide (IC_{50} = 783.31 ± 3.28 μM). While moderate to poor activity was observed when compared to rasagiline (IC_{50} = 10.36 ± 0.21 μM). Among the good inhibitors, compound **336** (IC_{50} = 12.78 ± 0.34 μM) and **337** (IC_{50} = 5.04 ± 0.06 μM) exhibited higher potencies. Similar to the MAO inhibitors, even in MAO-B inhibitors (**336** and **337**) increased alkyl chain length has doubled the inhibitory activity.

4.4. 4(3H)-Quinazolinone derivatives

Quinazolinone scaffolds have been investigated to possess wide range of biological activities and substituted quinazolinone derivatives have MAO and AChE inhibitory properties [232]. Hydrazine and pyrazoline containing quinazolinone analogs **338**, **339** (Fig. 126) have been possessed good MAO inhibitory potencies [233]. Accordingly, descent MAO inhibitory properties were possessed by 4(3*H*)-quinazolinone moieties [234–238]. Some representative MAO inhibitors include quinazolinone derivatives **340–342** (Fig. 126). In order to investigate the better MAO inhibitory properties of quinazolinone moiety, 6-mono- and N_3/C_6-disubstituted derivatives of 4(3*H*)-quinazolinone were engineered [239].

The synthesized quinazolinone scaffolds were allowed to inhibit MAO-A and MAO-B using toloxatone and lazabemide as reference compounds. The designed molecules include two series of derivatives namely; N_3-substituted quinazolinone analogs and N_3- & C_6-di-substituted derivatives. Both the series of quinazolinone scaffolds have not exhibited any inhibitory activity towards MAO-A. Even in case of MAO-B inhibitory activity, most of the derivatives were inactive. However, only a few derivatives have shown weak to moderate activity. To mention, *p*-fluoro benzyl motif of compound **343** (IC_{50} = 0.685 ± 0.013 μM) and *p*-cyano benzyl derivative **344** (IC_{50} = 0.847 ± 0.078 μM) (Fig. 127) of N_3- & C_6-substituted quinazolinone series were most potent MAO-B inhibitors among the competing inhibitors; yet the activity displayed by these compounds was approximately one-tenth of the inhibitory activity of lazabemide (IC_{50} = 0.091 μM). Hence, the synthesized molecules possess MAO-B selectivity. The inhibitory results inferred that di-substitution was crucial for MAO-B inhibitory activity. Highly negative inductive effects of fluoro and cyano groups at 4-position have contributed to the good inhibitory values.

The interaction of potent MAO-B inhibitor **373** was checked with molecular docking studies (Fig. 128). H-Bond has occurred with Thr201 in the entrance cavity of substrate. A large number of pi-interactions are noticed with amino acid residues Tyr398, Tyr326, Ile199, Cys172, Leu171 and Leu88. Potential steric repulsion is observed between Tyr326 and quinazolinone carbonyl functionality.

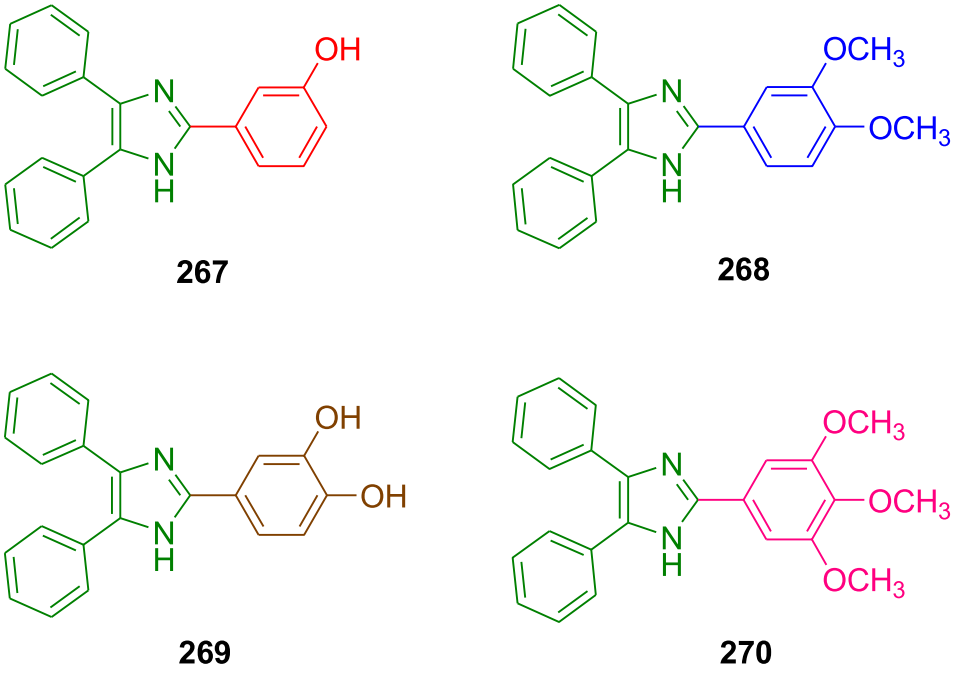

Fig. 104. Structures of potent AChE inhibitors (**267** & **268**) and BuChE inhibitors (**269** & **270**).

4.5. Chalcone analogs

Some chalcone derivatives were developed and reported to possess reversible selective MAO-B inhibitory properties. The effect of introduction of benzodioxol ring into the chalcone molecule appended with various substituents has been demonstrated [240]. In this regard, a series of chalcone scaffolds have been engineered and prepared [241] in order to get better reversible inhibitory properties.

*h*MAO Inhibitory activity of the designed chalcone derivatives was determined using pargyline and (*R*)-deprenyl as positive controls. Observation of inhibitory activity results revealed that most of the tested compounds have good MAO-B inhibitory properties. Out of these descent inhibitors, seven derivatives **345–351** (Table 19) have exhibited potent activity at nanomolar concentration. All the potent derivatives (except compound **345**) depicted in Table 19 have higher potencies compared to (*R*)-deprenyl; especially the derivative **348** (Fig. 129) with 4-chloro moiety on benzoyl benzene benzene ring and 4-NO_2 attached to benzene of *β*-carbon was bestowed most significant

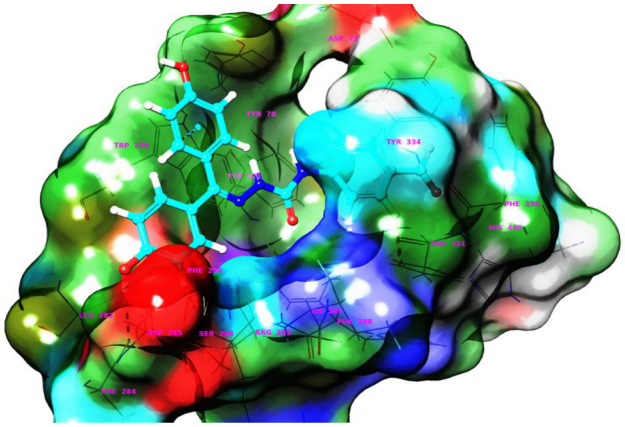

Fig. 106. Docking analysis of compound **273** on AChE [188].

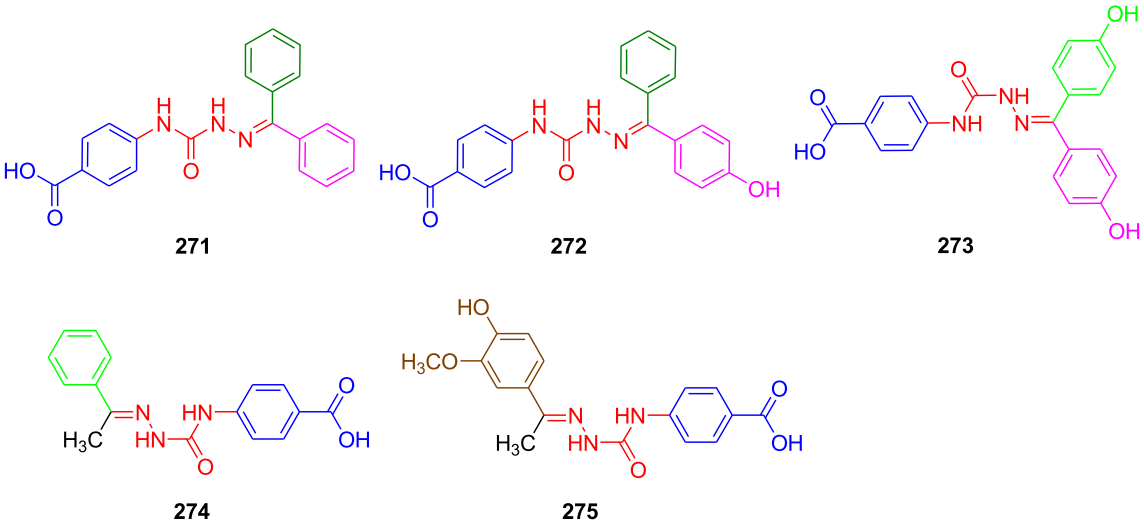

Fig. 105. Illustration of structures of *p*-aminobenzoic acid derivatives as potent cholinesterase inhibitors.

Table 14
Structures and their inhibitory values of benzoxazole derivatives.

Compd	Structure	IC_{50} (μM) ± SEM	
		AChE	BuChE
276	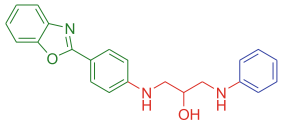	0.842 ± 0.042	3.54 ± 0.10
277	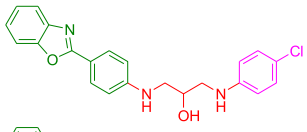	0.363 ± 0.017	2.29 ± 0.09
278	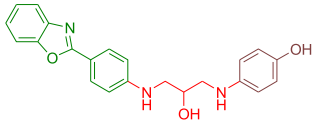	0.807 ± 0.04	2.74 ± 0.10
279	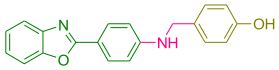	0.723 ± 0.03	4.71 ± 0.13
Donepezil		0.04 ± 0.01	15.24 ± 0.88

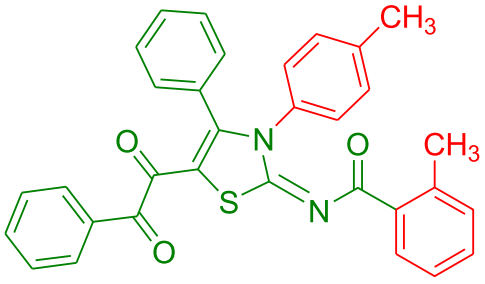

280

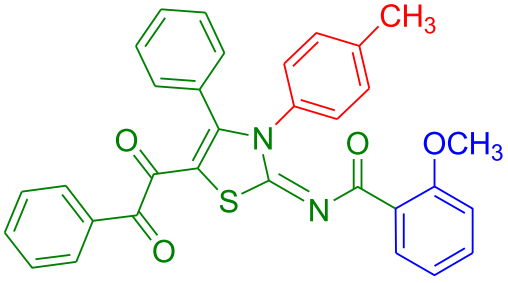

281

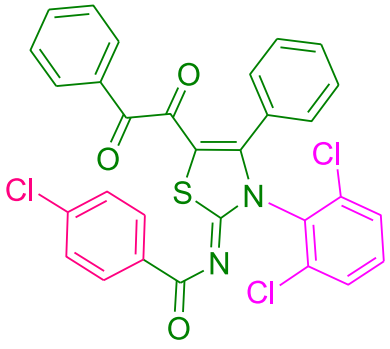

282

Fig. 107. Demonstration of structures of prominent cholinesterase inhibitors.

result with twofold greater MAO-B inhibitory value than that of (*R*)-deprenyl. Replacement of either 4-Cl or 4-NO_2 has led to reduced activity indicating that best binding of chalcone to MAO-B occurs when the two benzene rings attached with −Cl and −NO_2 at para-positions.

Whereas, inhibitory activity towards MAO-A was not shown by some derivatives. However, descent inhibitory activity was also observed for few derivatives; amongst them compound **348** (IC_{50} = 0.149 ± 0.011 μM) and derivative **352** (IC_{50} = 0.173 ± 0.003 μM) (Fig. 129) were most prominent MAO-A inhibitors. Unlike the MAO-B inhibitors, chalcone scaffolds with 1,3-dioxolane fused at 3,4-positions of benzoyl benzene ring and electronegative elements (−Cl/Br) at 4-position of benzene appended to *β*-carbon have results with the best inhibitory values. MAO-A Selectivity was observed in these derivatives. However compound **353** is found to be MAO-A/

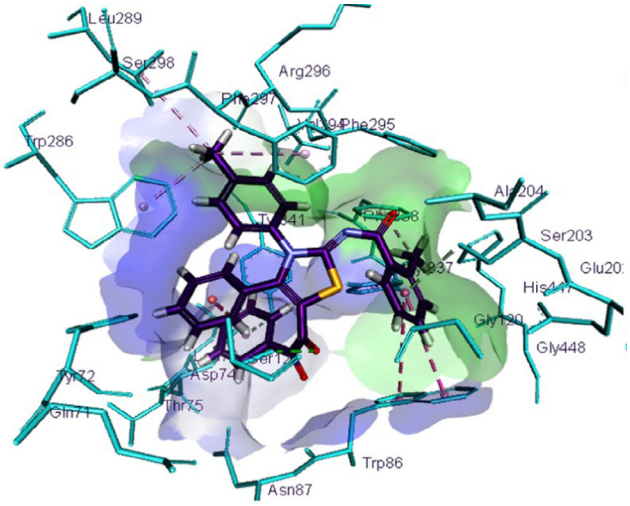

Fig. 108. Representation of binding mode of compound **280** with AChE [195].

MAO-B dual inhibitor with IC_{50} value 0.050 ± 0.002 μM towards MAO-B.

The potent MAO-B inhibitors **348** and **352** investigated for their molecular binding studies in MAO-B active site (Fig. 130). In this study, Tyr398 and Tyr435 along with FAD, formed an aromatic cage. Amino acid Ile199 functions as gateway between entrance and substrate-binding pockets *via* open or closed conformation poses. Tyr398 and Tyr435 amino acid residues formed binding interactions with electron-deficient aromatic rigs of chalcone. Carbonyl oxygen exhibited H-bond with Cys172 of MAO-B active site.

4.6. Thiazole analogs

A large number of thiazole compounds have been designed for their potent MAO inhibitory properties. Some researchers demonstrated arylidene-hydrazinyl-thiazole containing thiazoles **353** (Fig. 131) as significant MAO inhibitors [242,243]. Hydrazinyl-thiazole scaffolds were suggested to be enzyme inhibitors [244–246]. Recently, benzylidene-hydrazinyl-thiazoles have been designed and determined their MAO inhibitory activity [247]. These findings have inspired to design new series of benzylidene-hydrazinyl-thiazole analogs [248].

Benzylidene-hydrazinyl-thiazole derivatives were allowed to inhibit the MAOs using moclobemide and selegiline as reference compounds. All the synthesized molecules were active towards both MAO-A and MAO-B enzymes. The derivatives have exhibited strong MAO-A inhibitory activity in the range IC_{50} = 0.123–0.849 μM. The most potent inhibitors include compound **354** (IC_{50} = 0.134 ± 0.004 μM) where in 3,4-dihydroxy benzene appended to thiazole, 4-methyl piperidine attached at 4-position of benzylidene-hydrazinyl motif and **355** (IC_{50} = 0.123 ± 0.005 μM), 3-methyl analog of **354** (Fig. 132). The significant inhibitors **354** and **355** have shown 49-fold higher potency than that of moclobemide (IC_{50} = 6.054 ± 0.174 μM). All the evaluated compounds have exhibited moderate activity towards MAO-B. The very same potent MAO-A inhibitors **354** (IC_{50} = 0.027 ± 0.001 μM) and **355** (IC_{50} = 0.025 ± 0.001 μM) continued their legacy even towards strong inhibition of MAO-B also. These inhibitors were 1.5 times higher potent compared to selegiline (IC_{50} = 0.039 ± 0.001 μM). The efficiency of MAO inhibitory activity was at its peaks with the presence of strong electron donating hydroxy groups at 3,4-postions of benzene attached to thiazole.

The molecular binding studies were conducted for MAO-A/MAO-B inhibitor **355** (Fig. 133) in MAO-A enzyme active site. Compound **355** has resulted π-π interaction with Tyr444; while hydrazine N1 has formed a H-bond with Tyr444. The −OH group of compound **355** has interacted with amino acid residue Lys305. Van der waals interactions are observed with residues such as Tyr60, Phe99, Phe103, Pro104, Trp119, Leu164, Leu167, Phe168, Leu171, Cys172, Ile198, Ser200, Gln206, Leu328, Tyr398 and Tyr435. Also, electrostatic interactions are noticed with amino acids Phe103, Leu167, Leu171, Ile198, Tyr326 and Leu328.

Where as, in the molecular binding properties with MAO-B active site, phenyl ring next to the piperidine has an interaction with Tyr326 *via* π- π stacking. Thiazole ring and Tyr398 are in good interaction through π-π stacking. 3-OH Group has formed two H-bonds with Ser59 and Tyr60; while 4-OH group has interacted with Gly434 *via* H-bond. Besides, compound **355** has Van der waals affinities with Gly58, Ser59, Tyr60, Phe103, Trp119, Leu164, Leu167, Phe168, Leu171, Cys172, Ile198, Ile199, Gln206, Ile316, Tyr326, Phe343, Tyr398 and Tyr435 residues.

5. Amyloid beta-aggregation inhibitors

According to amyloid hypothesis, main cause of AD was formation and aggregation of the *β*-amyloid peptide [249,250]. As a consequence of enzymatic cleavage of the amyloid precursor protein (APP) by BACE1 and γ-secretase, a neurotoxic peptide, A*β* comprising 37–42 amino acids is formed; particularly A*β* possessing 42 amino acids is culprit for the cause of conditions such as neuron loss, neuroinflammation, oxidative stress, cognitive and psychological ailments. Hence, reduction of A*β* in CNS could be a novel approach for AD treatment [251,252]. Close relationship prevail in between PAS (peripheral anionic site) of AChE and aggregation of Amyloid fibrils [253].

5.1. 2,3-Diaminopyridine analogs

Glycogen synthase kinase-3 (GSK-3) was one of hypothesis postulated for cause of AD [254,255]. The activated GSK-3*β* impairs the interaction between tau proteins and microtubules by

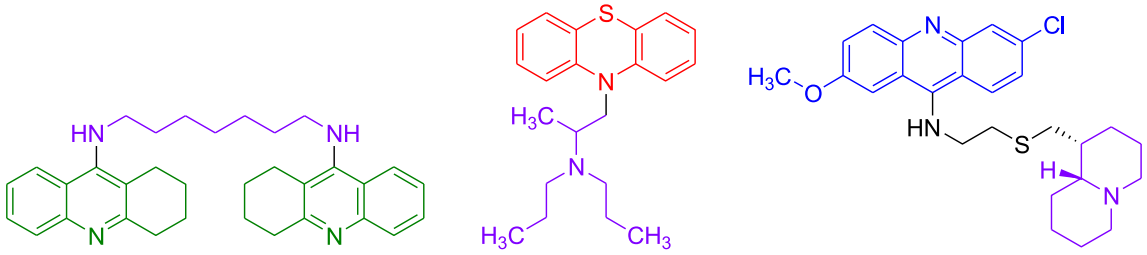

283 284 285

Fig. 109. Structures of tricyclic analogs possessing cholinesterase inhibitory activity.

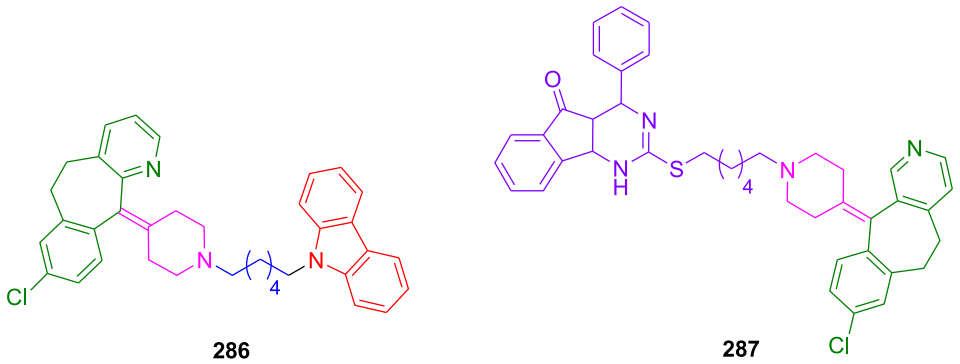

Fig. 110. Structures of significant tricyclic cholinesterase inhibitors.

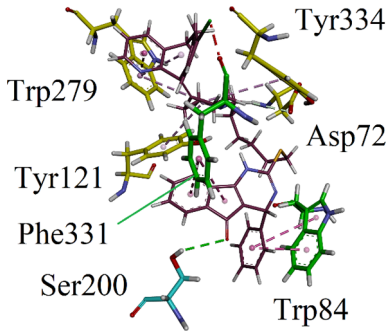

Fig. 111. Depiction of binding interactions of compound **287** with *ee*AChE active site [198].

hyperphosphorylating the tau protein and subsequently resulting into neurofibrillary tangles and it ultimately leads to neuronal cell death [256]. GSK-3β is also responsible for increased activity of BACE1 which is one of the culprits for Aβ formation [257,258]. Hence, inhibition of GSK-3β would pave to an effective way for AD treatment. Also, inhibition of metal-induced Aβ accumulation is one of the approaches for clinical treatment of AD.

The compound **356** (Fig. 134), possessing pyrrolopyridinone moiety has been reported to have potent GSK-3β inhibitory properties [259]. In this regard, novel GSK-3β inhibitors were designed by incorporating *N*-(pyridine-2-yl)cyclopropanecarboxamide structural unit [260]. Totally three series of 2,3-diaminopyridine scaffolds were designed in which 2-aminopyridine was linked to *N*-(pyridine-2-yl)cyclopropanecarboxamide by amide moiety **357**/imine **358**/methylene amine **359** (Fig. 135).

The designed derivatives were screened for GSK-3β inhibitory activity wherein staurosporine was used as a positive control. Although three series of *N*-(pyridine-2-yl)cyclopropanecarboxamides have been tested for the inhibitory activity; only the derivatives where in 2-aminopyridine moiety linked *N*-(pyridine-2-yl)cyclopropanecarboxamides have shown significant GSK-3β inhibitory effects. Amongst them the compound **360** (IC_{50} = 71 ± 4.6 μM) possessing simple 2-aminopyridine, 5-phenyl-2-aminopyridine analog **361** (IC_{50} = 49 ± 3.2 μM) and, 5-pyridine-2-aminopyridine analog **362** (IC_{50} = 38 ± 2.8 μM) (Fig. 136) were noteworthy molecules. The imine linker has provided beneficial factors for inhibition of GSK-3β. Imine linker and pyridine ring at 5-position of 2-aminopyridine of compound **362** have synergistic effect in GSK-3β inhibitory activity and its activity was comparable with that of reference staurosporine (IC_{50} = 24 ± 3.0 μM).

The potent GSK-3β inhibitors **360**, **361** and **362** have been hypothesized to have good Aβ aggregation inhibitory activity and chosen for that particular inhibitory activity. There was no effect of the tested compounds on Aβ aggregation and disaggregation in control test. Whereas in Cu^{2+}-induced A$\beta_{1\text{-}42}$ aggregation, descent inhibitory effects were observed. In comparison with reference clioquinol (38.8%), the compounds **360**, **361** and **362** have inhibitory percentages 24.3%,

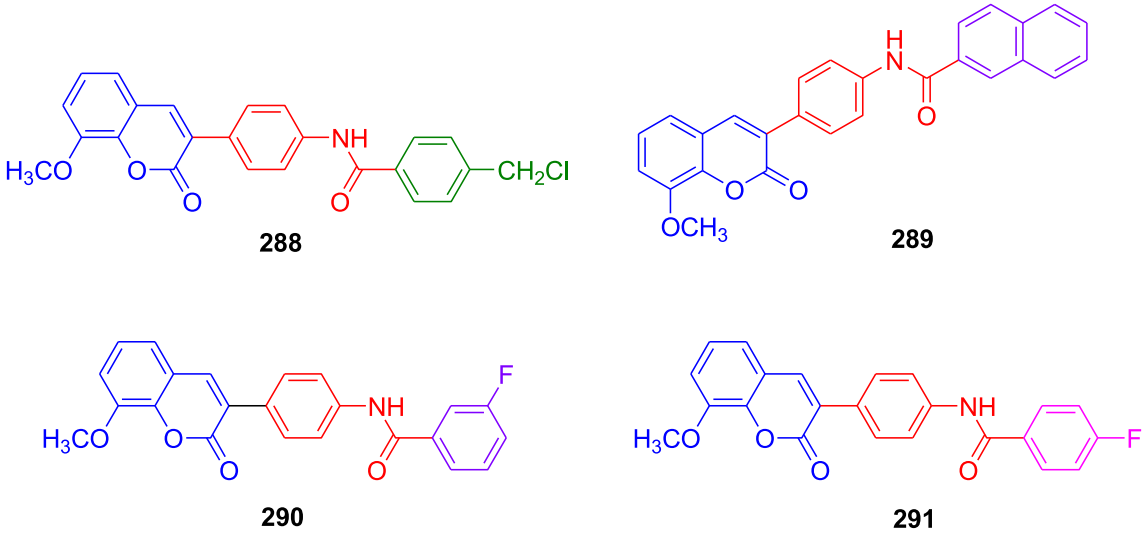

Fig. 112. Illustration of structures of significant AChE and BuChE inhibitors.

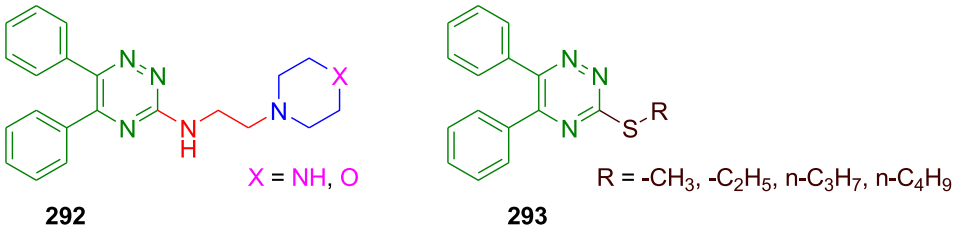

292 293

Fig. 113. Structures of 5,6-biaryl-1,2,4-triazine scaffolds with anti-AD properties.

Table 15
AChE inhibitory values of 5,6-biaryl-1,2,4-triazine derivatives.

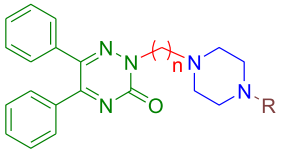

Compd	n	R	AChE IC_{50} (μM)
294	2	$-CH(C_6H_5)_2$	0.5 ± 0.04
295	2	$-CH_2C_6H_5$	0.5 ± 0.04
296	3	$4\text{-}NO_2C_6H_5$	0.5 ± 0.02
297	3	$4\text{-}F\text{-}C_6H_5$	0.4 ± 0.03
298	3	$4\text{-}OCH_3C_6H_5$	0.3 ± 0.03
299	3	$-CH_2C_6H_5$	0.2 ± 0.01
300	4	$4\text{-}OCH_3C_6H_5$	0.5 ± 0.03
Donepezil			0.1 ± 0.01

63.0% and 33.8% respectively. The compound **361** was found to be relatively strong A$\beta_{1\text{-}42}$ aggregation inhibitor than that of clioquinol. Likewise the same compounds were allowed to disaggregate Cu^{2+}-induced A$\beta_{1\text{-}42}$ aggregation; where in the evaluated derivatives **360**, **361** and **362** have shown 42.5%, 66.1% and 50.9% disaggregation rates, respectively compared to clioquinol (34.9%). Even in this activity the compound **361** managed to be most potent inhibitor.

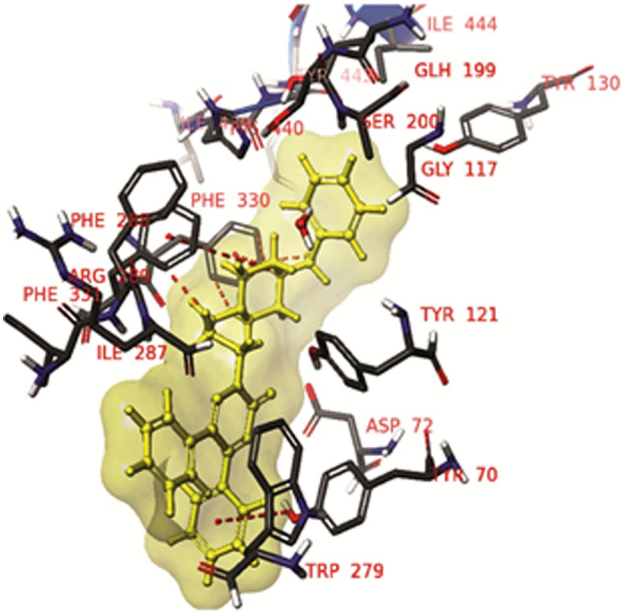

Fig. 115. Docking of compound **299** with active site of AChE [207].

In the molecular docking studies of compound **362** (Fig. 137) with GSK-3*β*, the pyridine nitrogen and amide hydrogen of *N*-(pyridin-2- yl) cyclopropanecarboxamide moiety have good interactions with Val135 *via* hydrogen bonds. The pyridine nitrogen of 2,3-diaminopyridine motif has exhibited another hydrogen bond with Lys85. Besides this, 5-(4-pyridyl) moiety has shown good interaction with Phe67 through hydrophobic and π-π stacking. These prominent interactions have contributed to potent GSK-3*β* activity.

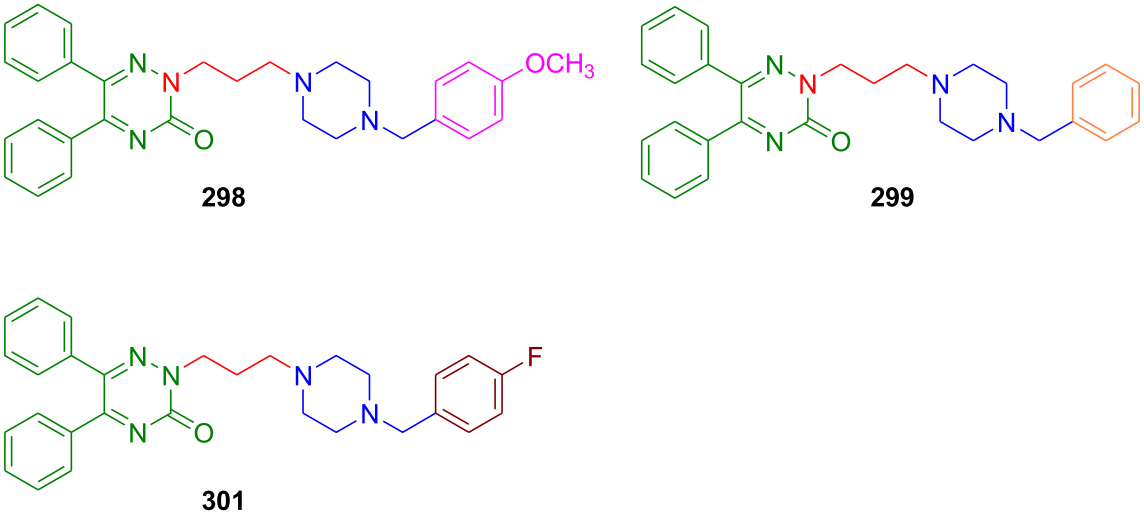

298 299 301

Fig. 114. Demonstration of potent triazine-piperazine scaffolds towards ChEs.

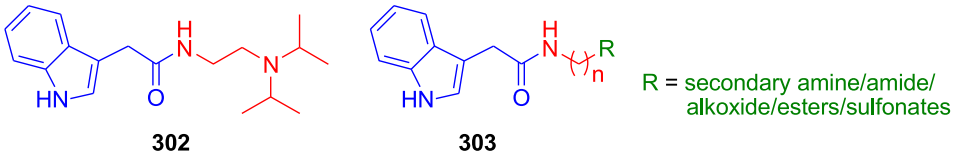

302 303

Fig. 116. Structure of potent AChE inhibitor (**302**) and illustration of design strategy (**303**).

Table 16
Cholinesterase inhibitory activity of IAA-tacrine derivatives.

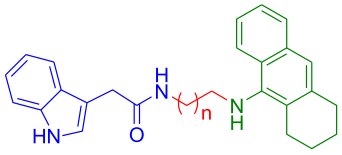

Compd	n	IC_{50} (μM)	
		AChE	BuChE
304	3	0.395 ± 0.010	0.076 ± 0.004
305	4	0.264 ± 0.008	0.057 ± 0.008
306	5	0.173 ± 0.012	0.066 ± 0.003
307	6	0.376 ± 0.022	0.246 ± 0.028
308	7	0.353 ± 0.003	0.150 ± 0.021
Tacrine		0.158 ± 0.021	0.268 ± 0.037

5.2. 2-Substituted-8-aminoquinoline derivatives

Since excess copper ion concentration in the brain is responsible for the formation of Cu-amyloids; there is urgent need for scavenge of Cu^{2+} trapped in amyloids by organic ligand chelation and thus the process would be an effective approach for AD treatment. Recently research has been going towards the discovery of organic ligands to chelate metal ions from Cu-amyloids [261,262] and thus restoring metal homeostasis in AD-brain. Bidentate ligands clioquinol and PBT2 could not be used for copper chelation as they form ternary complexes with Cu-amyloids [263,264]. However tetradentate ligands of the PA1637 series were described as copper homeostasis regulators and inhibitors of ROS production inhibitors induced by Cu-amyloids. All these have inspired the researchers to design new series of 2-substitiuted-8-aminoquinoline scaffolds [265].

Among the various 8-aminoquinoline derivatives, the compounds **363–366** (Fig. 138) have shown prominent chelation activity (Table 20). The activity of the compounds particularly 6,8-dichloro aminoquinolines **363** and **366** have exhibited best activities towards both Cu^{2+} and Zn^{2+} ions.

5.3. Sarsasapogenin-triazolyl hybrids

Few natural products were reported to play significant role in drug discovery and development. For instance, heparzine A **367**, a lycopodium alkaloid was recognized as reversible acetylcholinesterase inhibitor [266]; curcumin and resveratrol could be included in the category of Aβ-aggregation inhibitors [267,268]. Catechins, namely epigallocatechin-3-gallate **368** present in green tea in the phase III clinical trial of AD treatment [269]. Sarsasapogenin **369** (Fig. 139), an active ingredient of Rhizoma Anamarrhenae has been reported to possess Aβ inhibitory properties [270]. In addition to this, significant neuroprotective activities were exhibited by sarsasapogenin analogs with substituted 3-carbamate and 26-amino acid methyl ester groups [271]. Also, a series of 3-benzyloxy scaffolds of 26-amino acid methyl ester substituted sarsasapogenin derivatives reported to have prominent neuroprotective effects than that of sarsasapogenin [272]. Studies have reported that triazole derivatives can bind to enzymes and exhibit anti-AD properties, particularly inhibition towards Aβ-aggregation [273]. Thus, the promising sarsasapogenin was derivatized with pharmacological important triazole to afford hybrid molecules [274].

The derivatives were engineered such that the pyran motif of sarsasapogenin was substituted by arylalkyl triazole through alkylamide spacer on one end and benzylation of hydroxy group on the other end of sarsasapogenin.

Aβ-Aggregation inhibitory activity of sarsasapogenin-triazole derivatives was determined using curcumin and sarsasapogenin as reference compounds. Most of the designed derivatives have shown higher potencies compared to curcumin (55.87 ± 3.57%). Particularly, *p*-methoxybenzyl derivative **370** (84.74 ± 1.25%) and 2-methylene thiazole analog **371** (75.06 ± 2.42%) (Fig. 140) were most potent compounds; their inhibitory percentages were far higher than that of curcumin. The 4-methoxybenzyl and 2-methylene thiazole structural units attribute to the beneficial effects on Aβ-aggregation inhibitory activity.

6. BACE1 inhibitors

Sequential proteolytic cleavage of APP at the β-site a transmembrane aspartyl protease, BACE1 and γ-secretase leads to the generation and release of amyloid beta protein, Aβ peptide in the brain [275]. Amyloid-beta comprising 40 or 42 amino acid residues needs two sequential cleavages of the APP. Initially, soluble extracellular fragment and a cell membrane-bound fragment, C99 were produced on APP cleavage by BACE1. Further, C99 cleavage by γ-secretase within its transmembrane domain generates the intracellular domain of APP and finally produces Aβ. Therefore, inhibition of amyloidogenic secretases particularly BACE1 would be an attractive target for AD treatment. Studies report that BACE1 inhibitors exhibit great potentiality in reducing concentration of Aβ in brain [276].

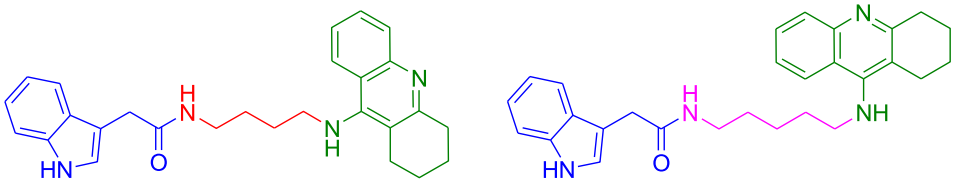

305 306

Fig. 117. Structure of most potent BuChE inhibitor (**305**) and AChE inhibitor (**306**).

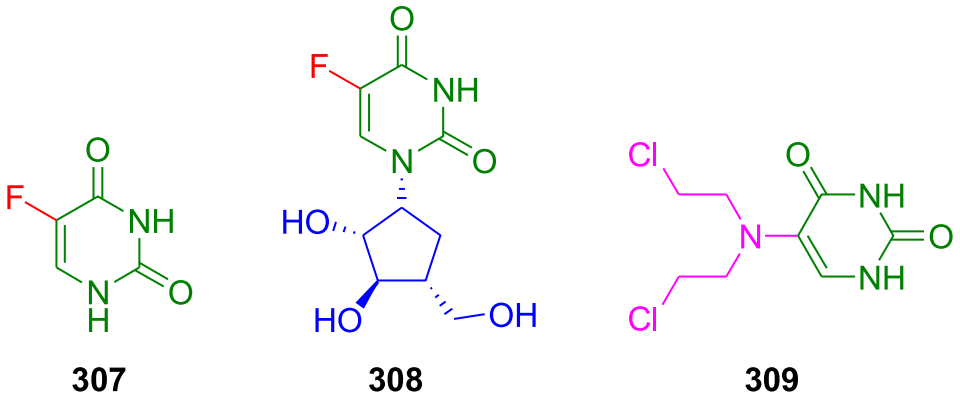

Fig. 118. Structures of uracil derivatives.

Table 17
AChE inhibitory values of significant uracil derivatives.

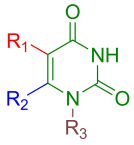

Compd	R_1	R_2	R_3	IC_{50} (μM) AChE
310	H	H	$COCH_3$	0.136
311	Br	H	H	0.151
312	Br	H	SO_2PhCH_3	0.088
313	Br	H	SO_2CH_3	0.111
314	H	CH_3	H	0.191
	Neostigmine			0.136

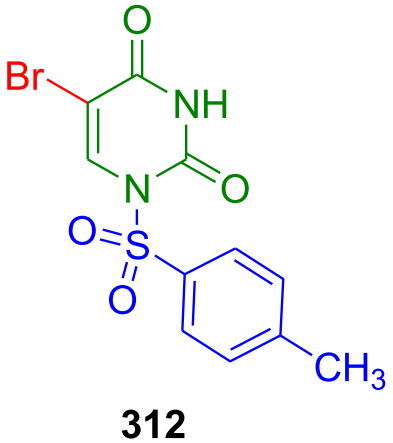

Fig. 119. Structure of uracil analog possessing potent AChE and BuChE inhibitory activities.

6.1. Thiophenyl-triazine derivatives

The small molecules such as acyl guanidine, aminoimidazole, amino/iminohydantoin, aminothiazoline, aminooxazoline and 2-aminopyridine have been developed as potential BACE1 inhibitors to combat AD [277,278]. In spite of the demand of potential drugs for AD treatment, dithiophene and 1,2,4-triazine derivatives **372** (Fig. 141) were designed and tested for BACE1 inhibitory potential [279]. The 1,2,4-triazine was appended to substituted aryl group *via* hydrazine linker at 3-position and thiophene rings at 5- & 6- positions.

BACE1 inhibitory activity was performed using reference compounds OM99-2 and quercetin. Most of the evaluated derivatives were inactive towards BACE1. However, few derivatives shown weak activity; particularly 2,4-dihydroxyphenyl derivative **373** (IC_{50} = 0.91 ± 0.25 μM) and indole analog **374** (IC_{50} = 0.69 ± 0.20 μM) (Fig. 142) have some significant activity yet 65-fold and 50-fold lower activity respectively compared to OM99-2 (IC_{50} = 0.014 ± 0.003 μM). The BACE1 inhibitory activity indicated that 2,4-dihydroxyphenyl and indole motifs in combination with dithiophene moiety could form the best interaction with BACE1. Especially the triazines with aryl group possessing electron withdrawing substituents have hardly exhibited any inhibitory activity. But compound **373** with lower IC_{50} value elicited 100% inhibitory percentages both at 50 μM and 10 μM concentrations; while the compound **374** has revealed 100% inhibition at 10 μM.

Molecular binding studies of compound **373** with BACE1 (Fig. 143) revealed best results; wherein, the two hydroxy moieties of dihydroxyphenylhydrazone of compound **373** has formed two H-bond interactions with Phe108 and Gln73. In addition to these, H-bond affinities were observed for 1,2,4-triazole and hydrazinyl linker with amino acid residues such as Asp32 and Asp228.

6.2. Fluoro-benzimidazole derivatives

Benzimidazole scaffolds have been demonstrated to have anti-AD properties. Accordingly, fluoro-benzimidazole derivatives were synthesized and their BACE1 inhibitory activity was determined [280]. The evaluated molecules have shown weak to moderate activity. Out of the tested triazine scaffolds, compound **375** (IC_{50} = 0.51 μM) (Fig. 144) was found to be most potent BACE1 inhibitor. In spite of the best activity of **375**; it was further modified by substitution of 4-fluorobenzyl motif at N_1-position of benzimidazole to afford **376** with IC_{50} value 5.6 μM. Even though, the inhibitory activity of derivative **376** was not greater than the parent compound **375** but relatively stronger than those of remaining derivatives. In addition to this, the benzimidazole analog **377** (IC_{50} = 1.3 μM) with $-CF_3$ at C_2-position of benzimidazole was found to be descent BACE1 inhibitor.

7. Tau inhibitors

The tau protein composed of 441 amino acid residues found in large

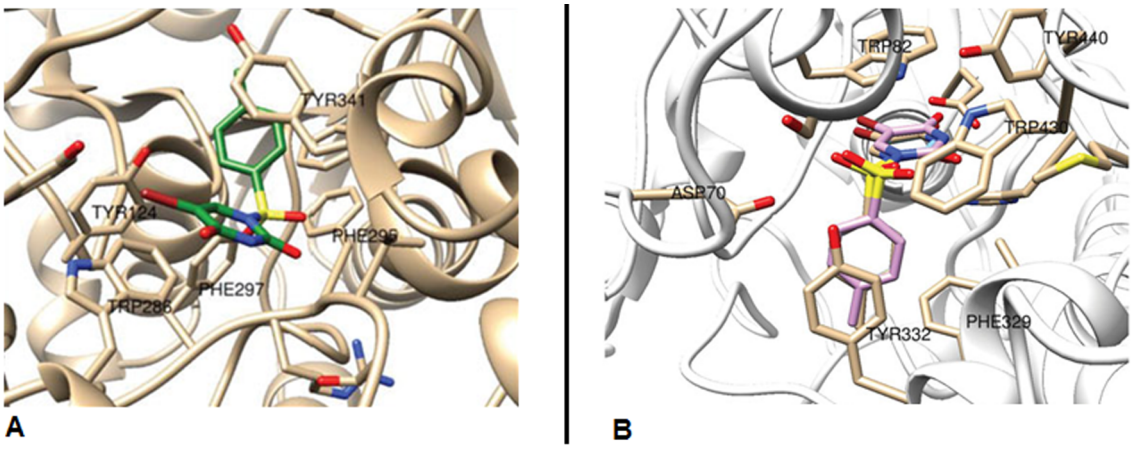

Fig. 120. Representation of binding affinities of compound **312** in the binding pocket of AChE (A) and BuChE (B) [213].

Table 18
MAO-B inhibitory values of chromene-styryl derivatives.

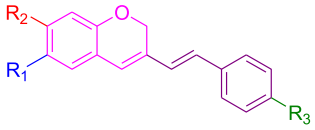

Compd	R_1	R_2	R_3	IC_{50} (μM) MAO-B
315	H	H	H	0.041
316	H	H	F	0.010
317	H	H	Cl	0.021
318	OCH_3	H	H	0.020
319	OCH_3	H	F	0.015
320	H	OCH_3	H	0.042
321	H	OCH_3	F	0.016
322	H	OCH_3	Cl	0.026
323	Cl	H	H	0.048
324	Cl	H	F	0.019
Pargyline				0.22

quantities in neurons; generally bound to microtubules. Unlike to its natural state, tau protein is mostly unfolded in solution [281,282]. Whereas in the diseases pertaining to neurological disorders, tau protein is aggregated leading to formation of amyloid fibrils [283]; that subsequently results in AD. In other words the microtubules are stabilized by tau protein in healthy brain. However, hyperphosphorylated tau protein forms paired helical filaments which aggregate into neurofibrillary tangles. Alzheimer was the first to report aggregation of tau protein to form intracellular tangles.

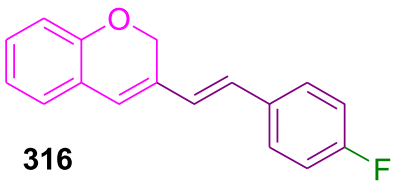

316

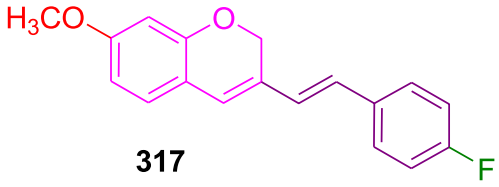

317

Fig. 121. Structures of significant MAO-B inhibitors.

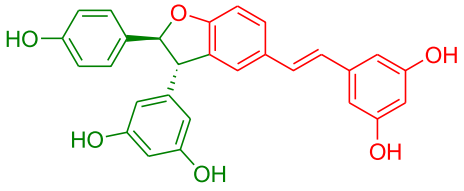

325

Fig. 122. Structure of trans-veniferin.

7.1. Pyridine-pyrimidine-benzamide analogs

Death-associated protein kinase (DAPK1) was described as promising target for neurodegenerative diseases [284,285]. DAPK1 was believed to be involved in phosphorylation of tau protein. Hence, design and discovery of DAPK1 would be viable drug target [286]. Colony-stimulating factor 1 receptor (CSF1R) inhibition was shown to reduce microglia-dependent neuroinflammation and neurodegenerative diseases [287,288]. Alongside, CSF1R inhibitors have been reported to inhibit tau protein transmission from neuron to neuron and thereby reducing microglial-assisted neurotoxicity [289]. In order to inhibit tau and subsequently combat AD, a set of pyridine-pyrimidine-benzamide analogs **378** (Fig. 145) were designed and evaluated for their DAPK1 and CSF1R inhibitory activities [290].

The synthesized pyrimidine-benzamide derivatives displayed moderate to descent CSF1R inhibitory activity to some extent. Few derivatives namely; compound **379** (IC_{50} = 0.12 ± 0.003 μM) possessing 3,5-dimethoxybenzamide moiety at C_5-position, 4-methoxyphenoxy motif at C4-postion and 4-morpholinophenyl on NH of 2-aminopyrimidine ring, 3-methoxybenzamide analog **380** (IC_{50} = 0.78 ± 0.04 μM) and compound **381** (IC_{50} = 0.15 ± 0.006 μM) (Fig. 146), 2-fluoropyridine analog of derivative **379** were notable CSF1R inhibitors. Combination of 3,5-dimethoxybenzamide, 4-methoxyphenoxy motif and 4-morpholinophenyl groups have bestowed the compound **379** with most potent activity. The inhibitory percentages of compounds **379**, **380** and **381** were

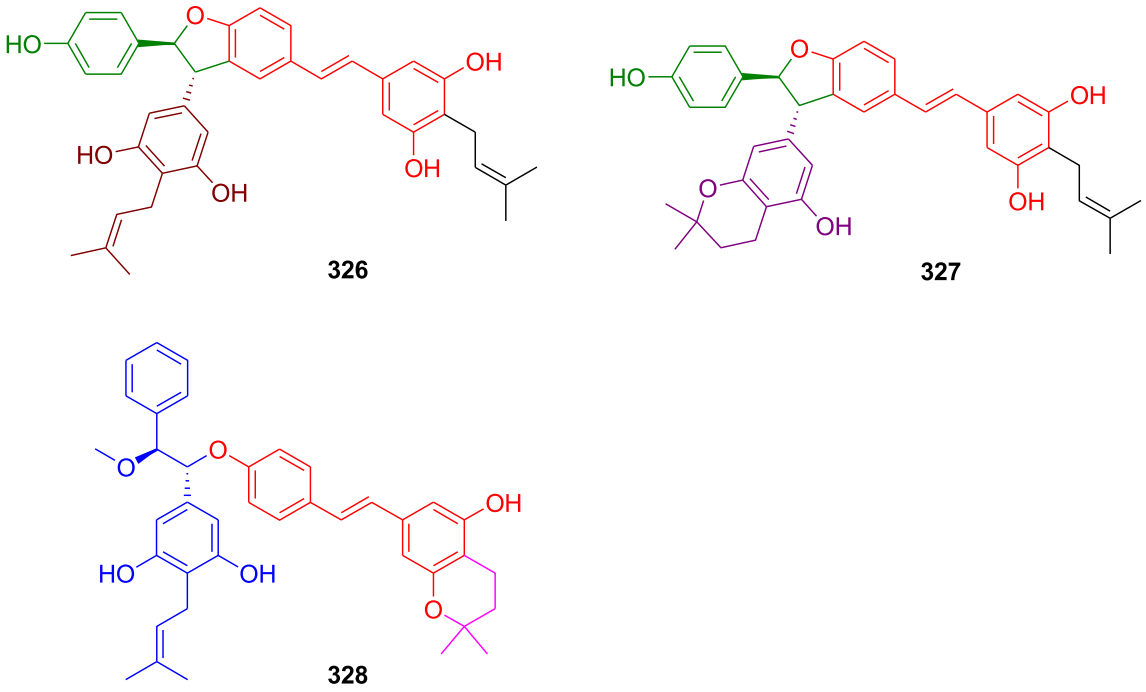

Fig. 123. Structures of molecules with most potent MAO inhibitory activity.

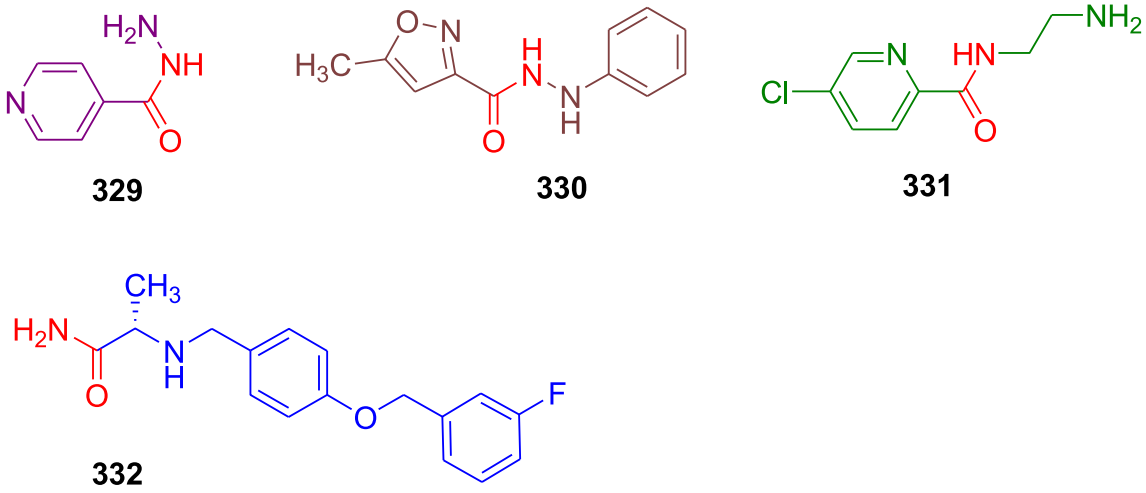

Fig. 124. Structures of standard MAO-inhibitors.

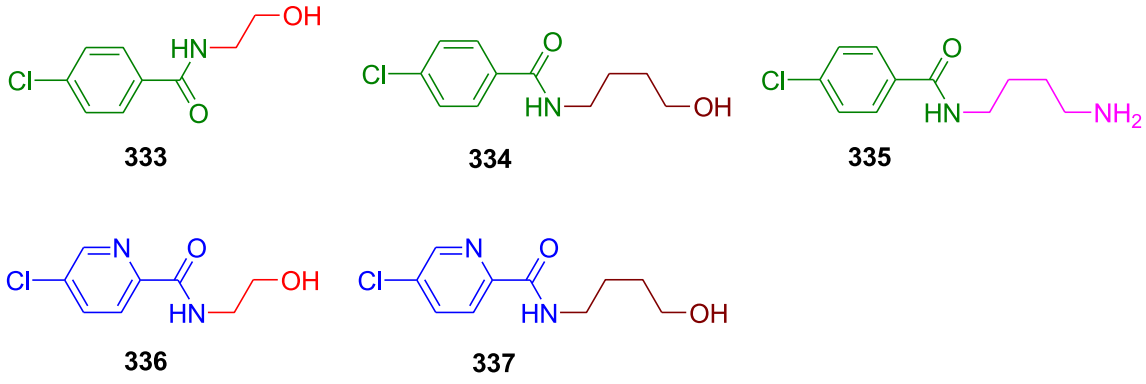

Fig. 125. Demonstration of lazabemide derivatives as MAO inhibitors.

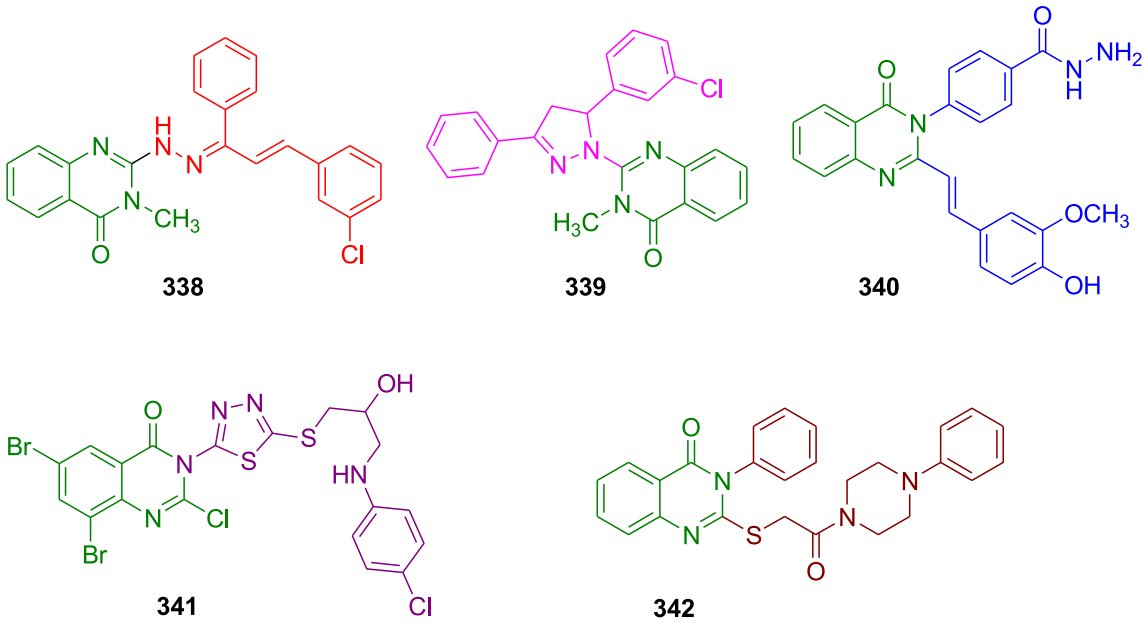

Fig. 126. Structures of potent MAO inhibitors.

95.34 ± 1.28%, 91.85 ± 1.31% and 77.94 ± 0.52% respectively.

In case of DAPK inhibitory activity, most of the derivatives were inactive. However few derivatives yielded significant results which include derivative **382** (IC_{50} = 2.61 ± 0.31 μM) (Fig. 147) bearing 3-trifluoromethylbenzamide moiety at C_5-position, 4-methoxyphenoxy motif at C_4-postion and 4-morpholinophenyl on NH of 2-aminopyrimidine ring. While, the compound **383** (IC_{50} = 2.69 ± 0.21 μM), 4-morpholinopyridine analog of **379** has shown similar potency as that of compound **382**. However the most potent DAPK inhibitory activity was elicited by the compound **381** (IC_{50} = 1.25 ± 0.35 μM). Compound **381** could be CSF1R/DAPK dual inhibitor as it was bestowed with potent CSF1R and DAPK inhibitory values. Selectivity was reversed on substitution of phenyl ring appended to amine NH of 2-aminopyrimidine with pyridine-5-yl from CSF1R to DAPK. Just slight reduction in the size of atom and increase in electronegativity for C → N atom substitution has completely varied its pharmacological activity.

Molecular docking of compound **383** (Fig. 148) with DAPK has revealed some interesting facts. The dimethoxybenzoyl moiety has shown interactions with Leu111, Lys108 and Ala106. The amide carbonyl has resulted hydrogen bond interaction with Leu111. The morpholine ring was exposed to solvent exposure region whereas *p*-methoxyphenyl has interactions with Asn243 and Glu239. Where as, in the flipped binding mode, dimethoxyphenyl moiety of compound **383** has made interactions with Leu19, Val27, Ala40, Glu94, and Ile160. Alongside these, interaction of Lys42 and Asp161 residues with pyrimidine ring was observed.

8. Terpenoids

Terpenoids are versatile pharmacological agents reported to be found in plants, microorganisms, insects and some marine organisms.

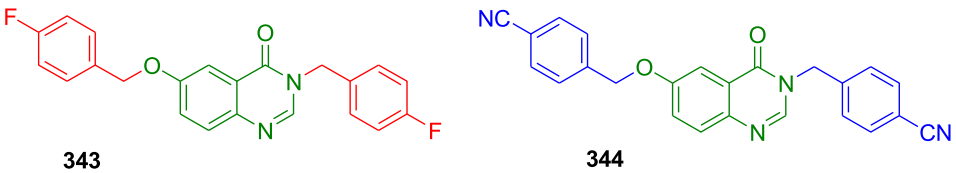

Fig. 127. Structures of MAO-B active quinazolinone derivatives.

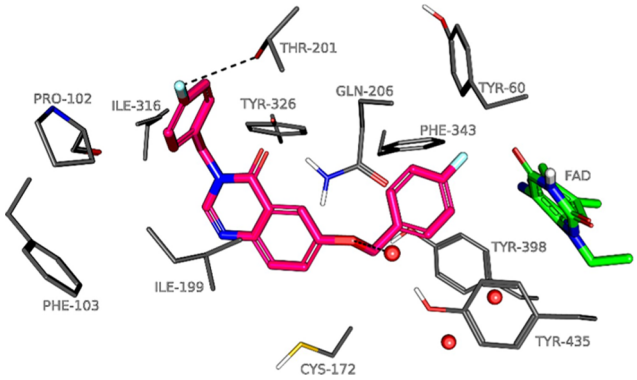

Fig. 128. Illustration of binding interaction of derivative **343** in MAO-B active site [239].

Terpenoids represent diverse set of natural products; and estimated to be more than 80,000 structurally characterized terpenoids [291].

Terpenoids are produced *via* terpene synthases utilizing polyisoprenoid pyrophosphatses as substrates. Thereby formation of various terpene skeletons such as mono-, sesqui-, di-, sester-, tri-, tetra-, and polyterpenes. Structural diversity of terpenoids pave to the wide range of biological applications *viz.*, antimalarial and antitumor properties and other prominent medicial properties.

8.1. *Euphorbia dendroides L. latex*

Plant extracts have been well characterized owing to their antioxidant properties [292]. Alongwith plant extract, latex of the plants has been reported to possess secondary metabolites such as alkaloids,

Table 19
Potent MAO-B inhibitors of chalcone derivatives.

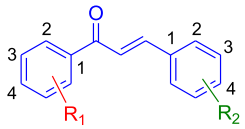

Compd	R_1	R_2	IC_{50} (μM)
			*h*MAO-B
345	3-Br	2,3-OCH_2O	0.081 ± 0.012
346	3-Cl	2,3-OCH_2O	0.058 ± 0.009
347	4-F	4-NO_2	0.069 ± 0.006
348	4-Cl	4-NO_2	0.034 ± 0.006
349	3,4- OCH_2O	4-F	0.043 ± 0.004
350	3,4- OCH_2O	4-Cl	0.050 ± 0.002
351	3,4- OCH_2O	4-NO_2	0.069 ± 0.004
Pargyline			13
(R)-deprenyl			0.079

terpenoid, polyphenolic compounds, resins and enzymatic protiens [293]. The plant of genus *Euphorbia* described to produce an irritant latex rich in phytochemical compounds which have been well characterized [294]. The bioactivities of most of the phytochemicals of the species *Euphorbia* are determined. In this context, investigation of anti-AChE, antioxidant and other pharmacological properties were carried out on the latex of plant, *Euphorbia dendroides* L [295].

In the free radical scavenging activity against $ABTS^{+\cdot}$ and $DPPH^{\cdot}$ is performed for latex of *Euphorbia dendroides* L, a great free radical scavenging activity was observed with $ABTS^{+\cdot}$ which was comparatively stronger than $DPPH^{\cdot}$; the results indicate that $DPPH^{\cdot}$ is likely to be more selective than $ABTS^{+\cdot}$ in reaction with hydrogen donors. While the acetylcholine inhibitory properties evaluated at concentrations 0.81–13 μM/mL using galanthamine as standard AChE inhibitor exhibited significant potencies. The inhibitory evaluation has shown dose-dependent enzyme inhibition in the range 6.91%–94.62% at highest latex concentration with IC_{50} value 4.46 μM. AChE inhibitory value elicited at highest dose is 1.5 fold higher potency comapared to galathamine (IC_{50} = 6.5 μM); it may be attributed to the synergistic effect produced by the major components of *Euphorbia dendroides* latex, terpenoids and phenolic acids.

8.2. Botryane terpenoids

Recent studies have proved that marine-derived endophytic microorganisms are potential sources of bioactive natural products [296]. Efforts have been put to identify novel secondary metabolites produced by endophytic fungi isolated from the red alga *Asparagopsis taxiformis* [297]. The genus *Nemania* was demonstrated to exhibit interesting applications associated with bioactive small molecules. Diterpenoids have been demonstrated to have cholinesterase inhibitory activities [298,299]. Inspired by these, new terpenoids were isolated from *Nemania bipapillata* and their cholinesterase inhibitory properties were investigated [300]. In this study, isolation and structural elucidation of three new botryane sesquiterpenes, two nonsesquiterpenes and other two terpenoids was accomplished (Fig. 149). These isolated terpenoids were checked for their ability to inhibit cholinesterases and cytotoxicity.

Regarding the determination of cholinesterase inhibitory properties using an immobilized capillary enzyme reactor (ICER), compounds **385–389** have exhibited selective AChE inhibitory properties; whereas compound **384** was found to be non-selective cholinesterase inhibitor possessing similar AChE and BuChE inhibitory effects (Table 21). The results observed were found to be only moderate inhibitory potencies compared to standard inhibitor galanthamine. Amongst the isolated terpenoid molecules, compound **387** has elicited strongest inhibitory value. AChE/BuChE dual inhibitor **384** would transform to a selective AChE inhibitor (**385**) with change in the stereochemistry at one of the carbon. Although the isolated terpenoids were moderate cholinesterase inhibitors, these can be considered as lead compounds for further development as selective potent cholinesterase inhibitory agents. Compound **387** bearing α,β-unsaturated ketone moiety exhibited most significant inhibitory percentage; however with similar structure but change in the stereochemistry at three carbon atoms (compound **388**) has resulted in diminished inhibitory percentage indicating that stereochemistry at every atom is most crucial. Alongside, α,β-unsaturated ketone analogs (**387** and **388**) were proven to be more favorable compared to α,β-unsaturated aldehyde scaffolds (**384–386**).

8.3. Trachyloban-19-oic acid analogs

Trachylobane-19-oic acid **390** is one in the list of trachylobane diterpenes found in the plants of various genera such as Croton [301], Xylopia [302], Arctopus [303] and Iostephane [304]. Biotransformation has been an efficient tool utilized for the preparation of trachylobane diterpene derivatives. The AChE inhibitory work done on trachylobane-19-oic acid and its derivatives has triggered further preparation of trachylobane-19-oic acid analogs through biotransformation by *S. Racemosum* [305].

In this study, the biotransformation has resulted into one known compound **391**, 7-hydroxytrachyloban-19-oic acid and two new compounds **392**, trachyloban-17,19-dioic acid and **393**, ent-16β,17-dihydroxykaur-11-en-19-oic acid (Fig. 150).

All these derivatives were subjected to acetylcholinesterase inhibitory activity using galanthamine as standard positive control. The biotransformed molecules have exhibited descent anti-AChE values. Among the evaluated molecules, compound **392** was found to render most remarkable activity (IC_{50} = 0.06 μM); the activity was sixfold greater activity compared to galanthamine (IC_{50} = 0.38 μM). The strongest activity might be attributed to the two –COOH groups.

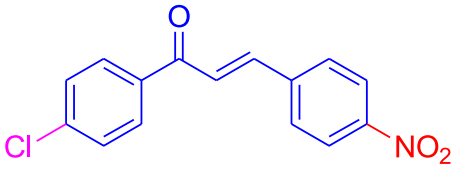

348

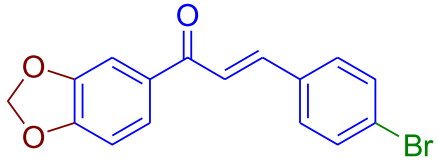

352

Fig. 129. Illustration of structures of reversible MAO-B inhibitors.

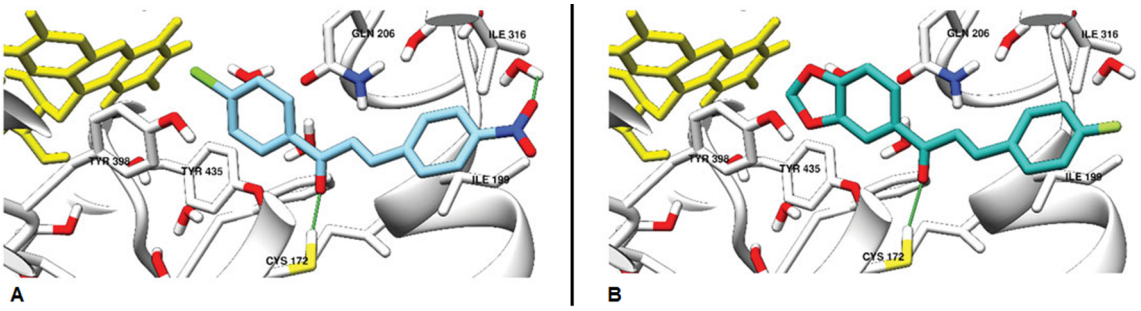

Fig. 130. Representation of molecular docking of compound **348** (A) and **353** (B) in *h*MAO-B active site [241].

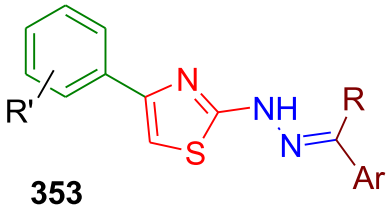

Fig. 131. Demonstration of arylidene-hydrazinyl-thiazole containing thiazoles.

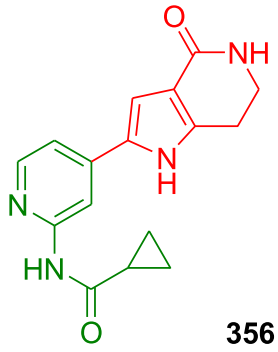

Fig. 134. Structure of GSK-3β inhibitor possessing pyrrolopyridinone moiety.

However, monocarboxylic acid analog **391** with one –OH moiety shown diminished activity (IC_{50} = 0.31 μM) yet potent activity compared to galanthamine. Further reduction in the AChE inhibitory activity (IC_{50} = 0.48 μM) was observed for the compound **393** with two –OH groups. The significant anti-AChE inhibitory activity of compound **392** would lead to redesign and subsequent improvement of anti-AChE properties.

8.4. *Prunus armeniaca L. and P. domestica L. leaf essential oils*

Some of the plant extracts and naturally occuring compounds including alkaloids, polyphenols, and terpenes and so forth have been demonstrated to possess potential neuroprotective properties. Most of these naturally occuring compounds were cholinesterase potential inhibitors. Most of the essential oils and phytochemicals have been described as multi-target inhibitors towards AD [306,307]. Based on previous utility of different essential oils from *Citrus*, *Salivia*, *Cistus* and *Pinus* for AD treatment [308,309], essential oils from the leaves of *Prunus armeniaca and P. domestica* were checked for their antioxidant and cholinesterase inhibitory properties [310].

The essential oils were fractionated based on the major component present in them as **P1**, **P2**, **P3** fractions from *P. armeniaca*; **P4**, **P5** and **P6** fractions from *P. domestica*. In the cholinesterase inhibitory properties, weak inhibitory effects were observed (IC_{50} = 97.60–171.80 μM) compared to physostigmine (IC_{50} = 0.17 ± 0.01 μM). Amongst the

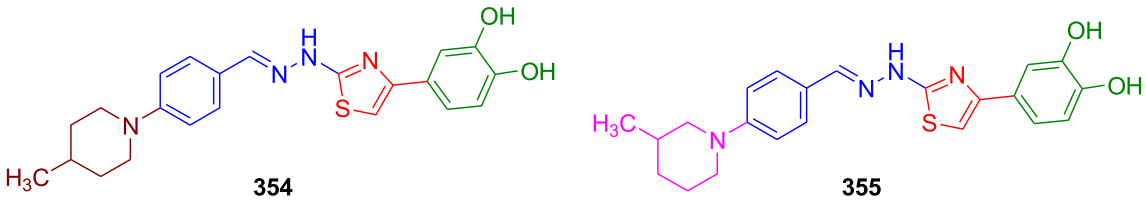

Fig. 132. Structures of significant MAO-A/MAO-B dual inhibitors.

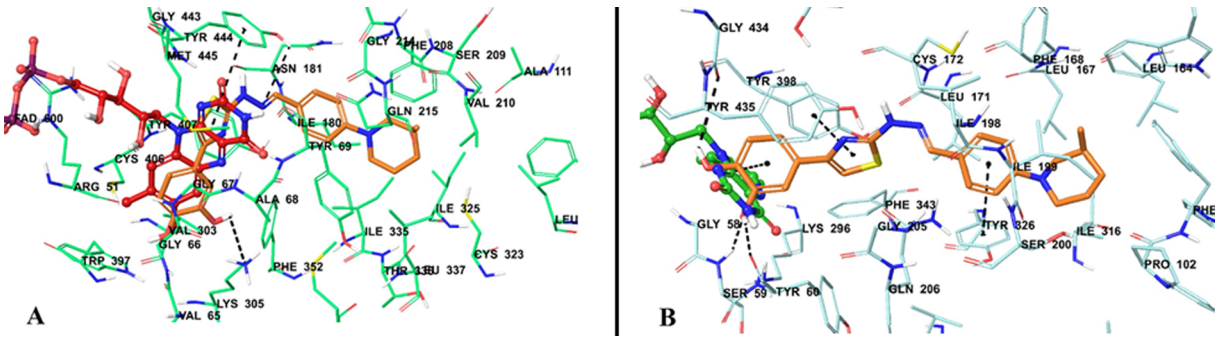

Fig. 133. Demonstration of binding interactions of MAO-A/MAO-B dual inhibitor **355** with MAO-B enzyme (A) and MAO-B enzyme (B) [248].

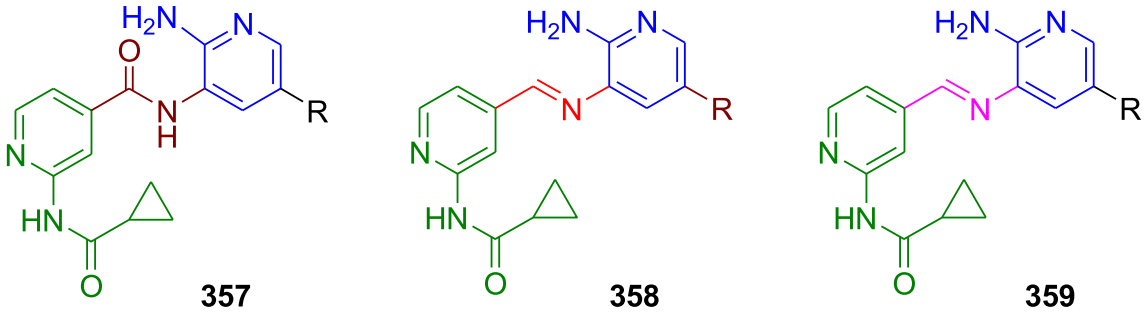

Fig. 135. Design strategy of 2-aminopyridine derivatized *N*-(pyridine-2-yl)cyclopropanecarboxamides.

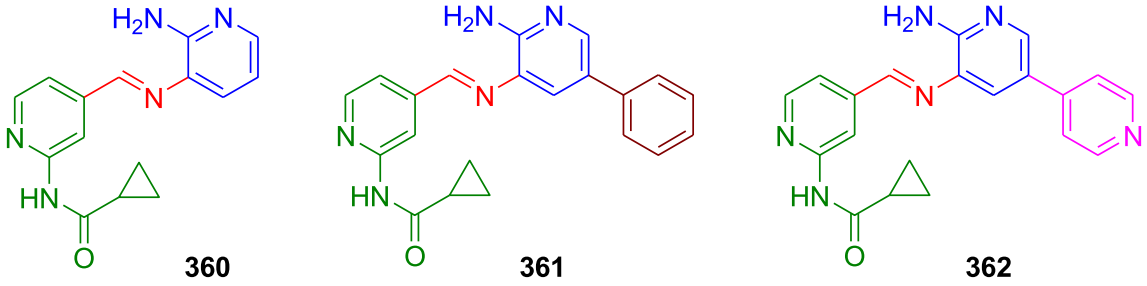

Fig. 136. Demonstration of structures of potent GSK-3β inhibitors.

tested fractions, fraction **P1** has elicited highest AChE inhibitory property (IC_{50} = 97.60 ± 1.94 μM). Where as, the essential fractions **P2**, **P3** and **P4** have exhibited almost similar activities with IC_{50} values 98.20, 98.50 and 98.60 respectively. The essential oil fractions **P1**, **P2**, **P3** and **P4** were reported to constitute mainly phytol, **394** (Fig. 151), a diterpene. Hoping that the phytol was responsible for the potent AChE inhibitory activity, it was purified and tested individually for anti-AChE effects. In this activity, phytol has bestowed with significant AChE (IC_{50} = 2.70 μM) and BuChE (IC_{50} = 5.79 μM) properties.

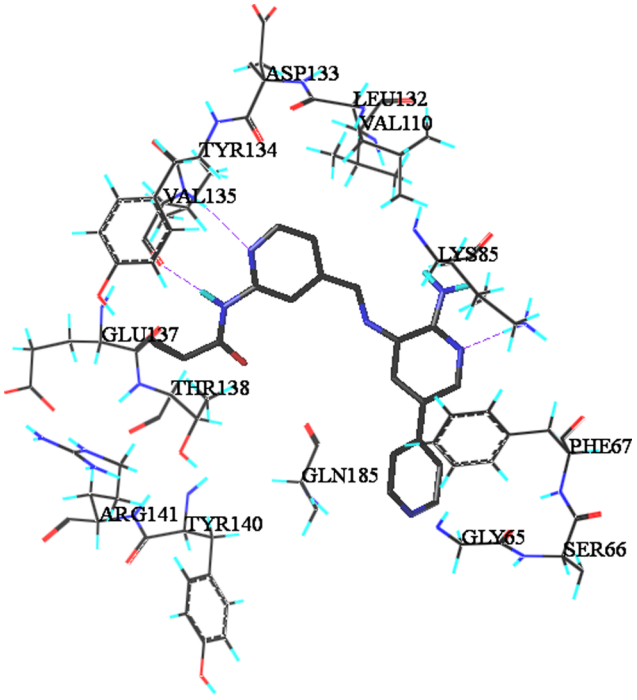

Fig. 137. Demonstration of interaction of compound **362** with GSK-3β active site [260].

In case of BuChE inhibitory properties, poor inhibitory potencies are noticed (IC_{50} = 95.80–226.90 μM) compared to galanthamine (IC_{50} = 2.40 μM) essential oil fractions **P5** and **P6** have been shown to possess descent inhibitory potencies with IC_{50} values 100.20 μM and 95.80 μM.

8.5. Carbazole derivatives

Carbazoles can be listed in the naturally occuring phytochemicals possessing versatile pharmacological properties in addition to AD [311]. Carbazole derivatives have been described to exhibit Aβ inhibitory effects [312]. Further, the substituted cabazole analog carvedilol **395** (Fig. 152) was reported as Aβ fibril inhibitor [313]. Among the series of carbazole derivatives designed through ring opening of the galathamine, derivatve **396** was found to be potent molecule [314].

Carbazole scaffolds have been shown to be representive molecules possessing AD inhibitory properties. To enhance these anti-AD effects, further design of carbazole moiety was undertaken wherein *N*-benzyl-1,2,3-triazole motif was appended to 9*H*-carbazole part in designing and preparing *N*-benzyl-1,2,3-triazole derivatized carbazoles [315]. Amongst the synthesized molecules evaluated towards cholinesterase inhibitory properties, compound **397** (Fig. 153) has exhibited most potent AChE inhibitory activity with IC_{50} value 1.93 μM. However, no single evaluated derivative in this series has exhibited good BuChE inhibitory activity below 100 μM concentration.

8.6. Tetrahydrocarbazole benzyl pyridine derivatives

Based on the selective BuChE inhibitory properties of indole scaffolds [316], design and synthesis of a novel series of 2,3,4,9-tetrahydro-1*H*-carbazole derivatives appended with benzyl pyridine moiety was accomplished [317]. All the designed molecules were investigated for

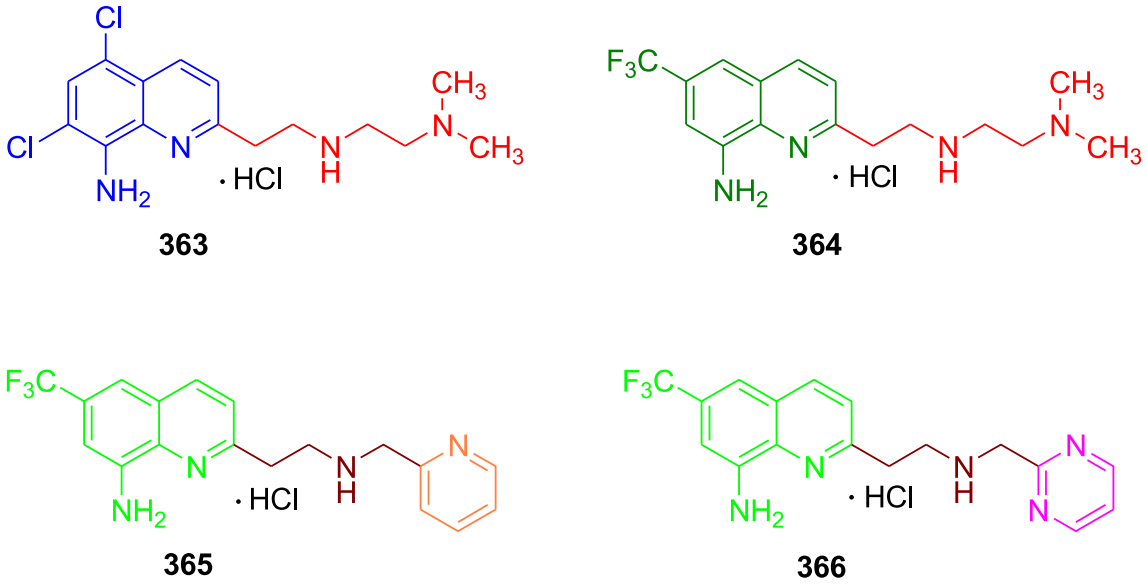

Fig. 138. Structures of significant copper ion chelators.

Table 20
Chelating effects of potent Cu^{2+}-chelators.

Compd	Log K_{app} [*M*-L][a]	
	M = Cu^{2+}	M = Zn^{2+}
363	16.5	4.2
364	15.1	4.1
365	16.0	6.0
366	15.9	5.7

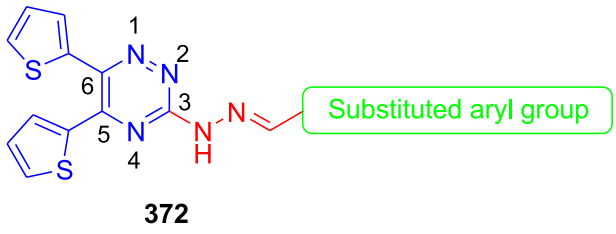

Fig. 141. Illustration of strategic design of thiophenyl-triazine derivatives.

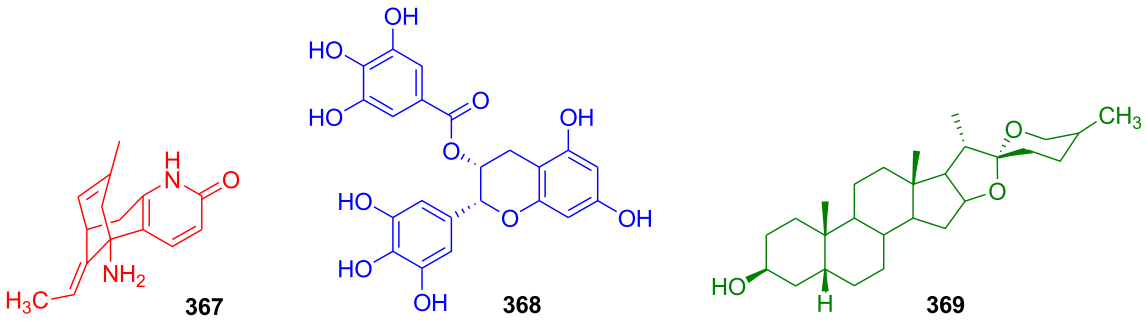

Fig. 139. Structures of heparzine A, epigallocatechin-3-gallate and sarsasapogenin.

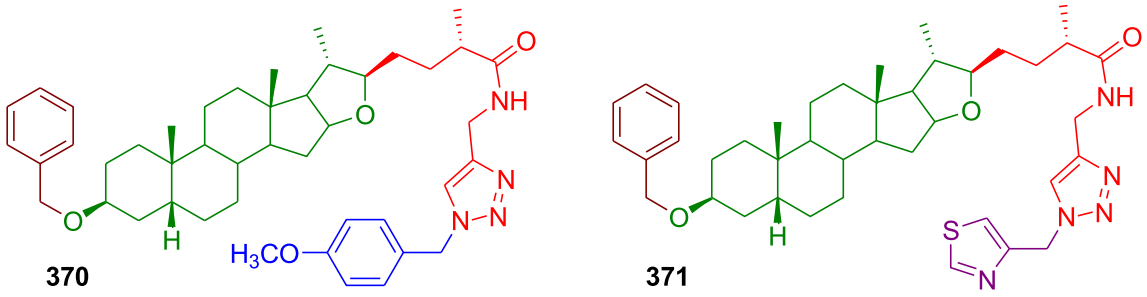

Fig. 140. Structures of most significant Aβ-aggregation inhibitors.

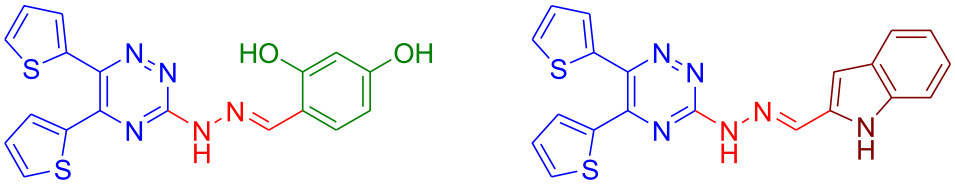

Fig. 142. Structures of significant BACE1 inhibitors.

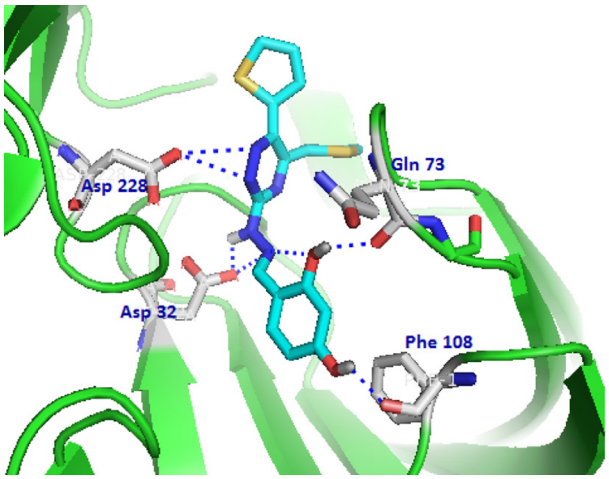

Fig. 143. Diagramatic representation of affinity of compound **373** with BACE1 [279].

their AD inhibitory properties. In the cholinesterase inhibitory activity, weak to moderate AChE inhibitory potentials were observed compared to standard AChE inhibitor donepezil (IC_{50} = 0.023 ± 0.01 μM). The compound **398** (IC_{50} = 4.8 ± 0.10 μM) and **399** (IC_{50} = 5.1 ± 0.20 μM) have exhibited some significant activity. The most remarkable AChE inhibitor **398** (Fig. 154) entails *N*-methylene pyridinium bromide connected to 2,3,4,9-tetrahydro-1*H*-carbazole nitrogen and 3-chlorobenzyl ring was appended to pyridinium nitrogen. Corresponding pyridinium chloride analog with *N*-(3-methyl)benzyl moiety **399** has shown slight diminished activity.

Likewise, pyridinium chloride with *N*-(2-chloro)benzyl moiety further reduced activity (IC_{50} = 6.5 ± 0.10 μM). Also, carbazole derivative possessing pyridinium bromide and *N*-(2-methyl)benzyl moiety rendered good inhibitory activity (IC_{50} = 8.4 ± 0.20 μM). Remaining derivatives have possessed weak AChE activity. All the potent AChE inhibitors possess pyridinium moiety appended to carbazole scaffold *via* pyridinium 4-position.

Where as, a good account of BuChE inhibitory activity was exhibited by the synthesized molecules. Most of them possessed stronger inhibitory activity compared to donepezil (IC_{50} = 0.35 ± 0.02 μM). Out of the potent BuChE inhibitors, compound **400** (Fig. 155) bearing pyridinium chloride and *N*-(4-methyl)benzyl moiety has elicited most remarkable activity (IC_{50} = 0.088 ± 0.02 μM). In this compound, the pyridinium ring is connected to carbazole nitrogen *via* pyridinium 3-position.

The most significant AChE inhibitor **398** was chosen for BACE1 inhibitory using OM99-2 as positive control. Unfortunately only poor BACE1 inhibition (IC_{50} = 30.01 ± 0.1 μM) was observed for the compound **398** compared to OM99-2 (0.003 μM). Further, the compound **398** was subjected to inhibition of AChE-induced and self-

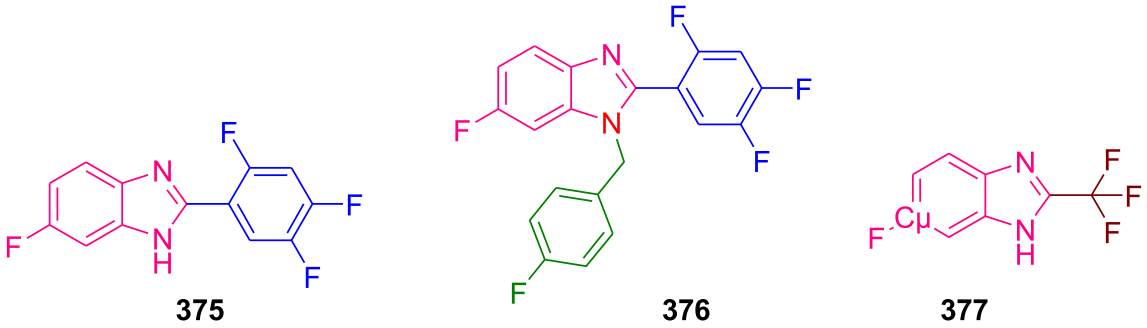

Fig. 144. Structure of fluoro-benzimidazoles with potent BACE1 inhibitory activity.

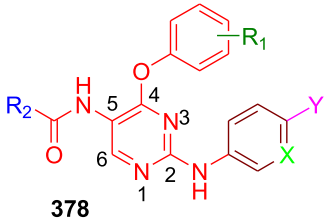

R_1 = 3-OCH_3/4-OCH_3

R_2 = NH_2, 3-CF_3-C_6H_4, 3-OCH_3-C_6H_4, 3,5-diOCH_3-C_6H_3

X = CH/N

Y = F, morpholine, piperidine

Fig. 145. Strategic design of pyridine-pyrimidine-benzamide derivatives.

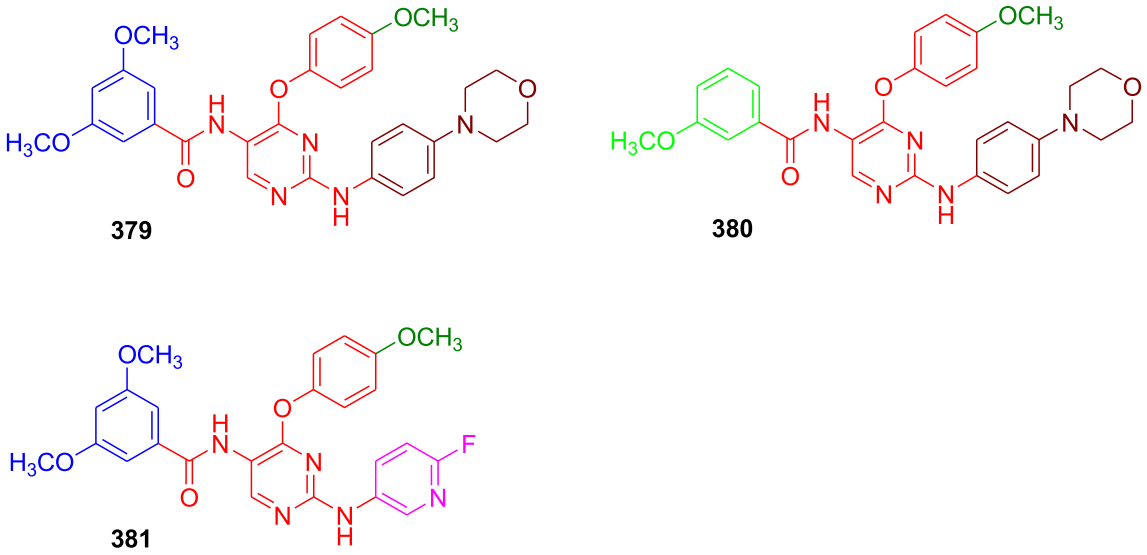

Fig. 146. Demonstration of structures of potent CSF1R inhibitors.

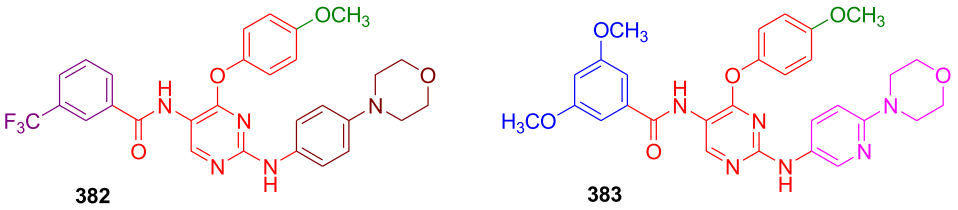

Fig. 147. Structures of potent DAPK inhibitors.

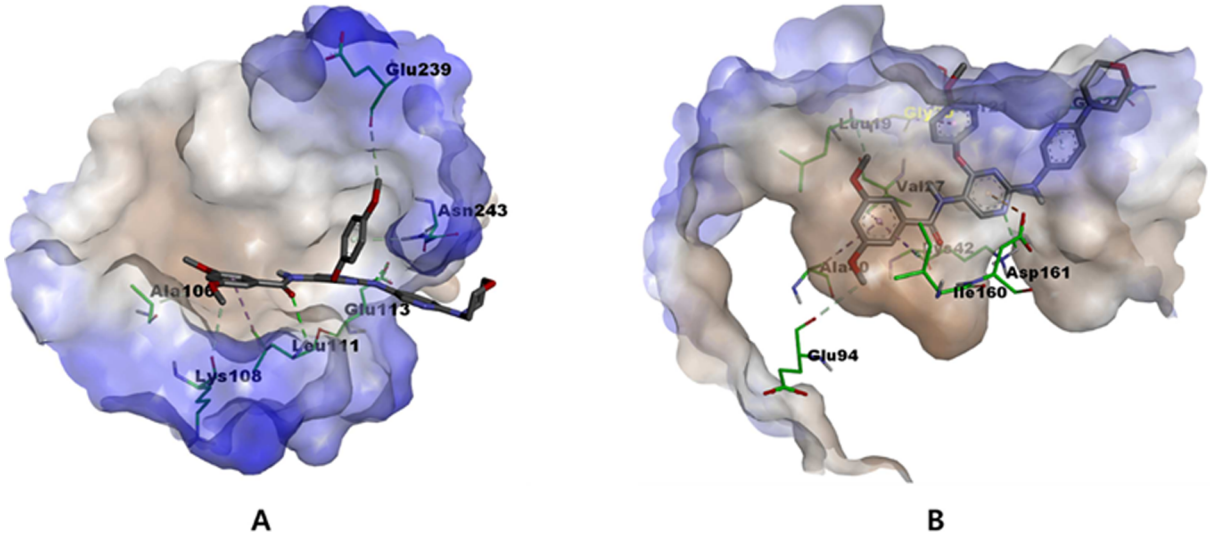

Fig. 148. Illustration of binding interactions of compound **383**; (A) Calculated binding mode of **383** within the substrate-binding site of DAPK1, (B) Calculated binding mode of **383** within the ATP-binding site of DAPK1 [290].

induced Aβ aggregation in presence of reference compound donepezil. The results revealed stronger A$\beta_{1\text{-}42}$ inhibitory effect of compound **398** (55.7 ± 2.9%) compared to donepezil (16.4 ± 1.7%). In continuation, A$\beta_{1\text{-}42}$ inhibitory activity was found to be 51.8 ± 1.5% which was better than the donepezil (25.2 ± 1.1%) and tacrine (7.2 ± 1.2%).

The compound **398** was subjected to molecular docking analysis in AChE active site (Fig. 156). The carbazole moiety has good interaction with Tyr332 through π-π stacking. The negative charge of Trp82 and Glu197 allows the central pyridinium ring to align towards the mentioned aminoacids. The charge transfer binding with Trp82 was thought

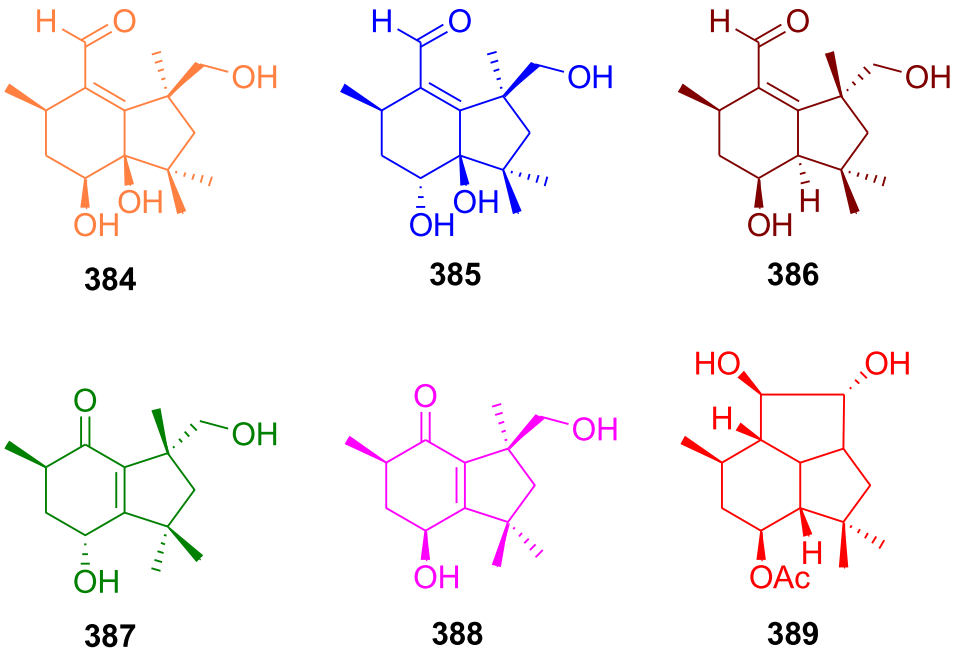

Fig. 149. Structures of terpenoids isolated from *Nemania bipapillata*.

Table 21
Percent inhibition of isolated terpenoids from *Nemania bipapillata*.

Compd	% inhibition	
	*h*AChE (ICER ± SEM)	*h*BuChE (ICER ± SEM)
Galanthamine	90.7 ± 0.0	82.0 ± 0.2
384	19.9 ± 1.7	14.1 ± 1.7
385	18.3 ± 1.8	6.7 ± 0.7
386	21.1 ± 0.1	5.5 ± 1.5
387	27.7 ± 1.3	7.3 ± 1.5
388	22.8 ± 0.8	5.1 ± 0.0
389	19.6 ± 2.7	3.2 ± 1.5

to be favorable for better interaction. Furher, the molecule has established interactions with Ile62, Thr120, Pro84 and Gly121 in hydrophobic pocket.

8.7. Carbazole scaffolds linked to secondary amine

Carbazole analogs (**401**, Fig. 157) were described to inhibit A$\beta_{1\text{-}40}$ [318]. Alongside, pyridinium/quinolinium containing carbazoles have been reported as noteworthy self-induced and AChE-induced Aβ aggregation inhibitors [319]. In addition, β-carbolinium salts have exhibited potential AChE/BuChE inhibitory properties [320]. Inspired by the discovery of potent anti-AD agents, design of a new set of carbazole derivatives incorporated with secondary amine was achieved [321].

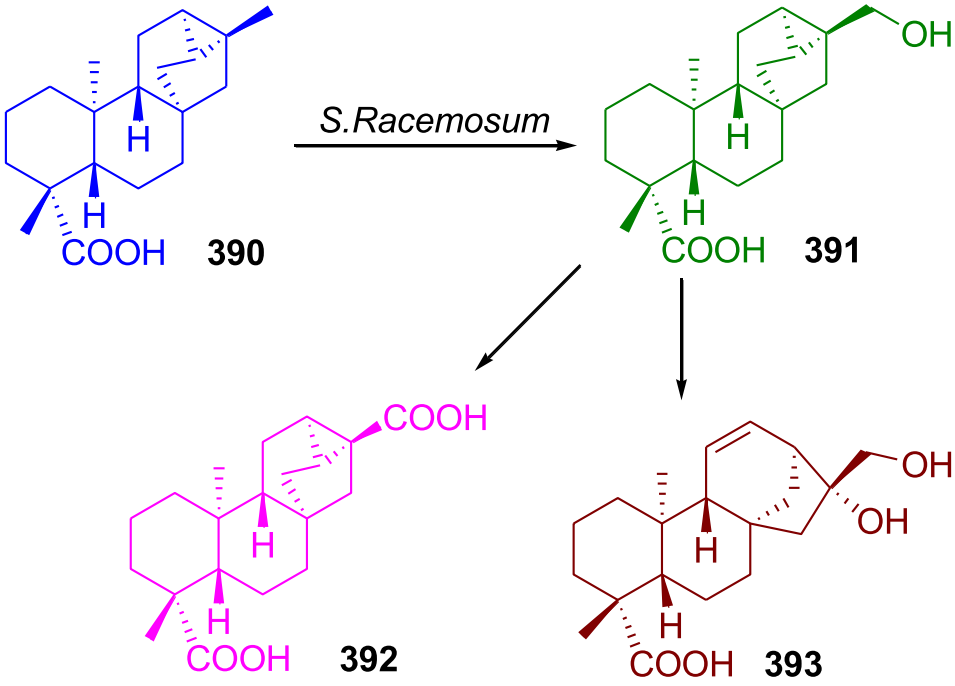

Fig. 150. Formation of biotransformed products of trachyloban-19-oic acid.

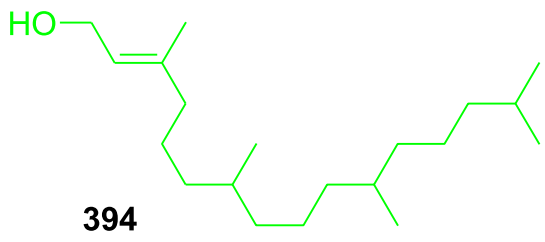

Fig. 151. Structure of a diterpene, phytol.

The prepared molecules were tested for cholinesterase and Aβ-aggregation inhibitory properties. Moderate to descent AChE inhibitory effects were observed among the synthesized compounds wherein derivative **402** (Fig. 158) has bestowed with excellent AChE inhibitory activity (IC_{50} = 0.11 ± 0.18 μM). The second strongest AChE inhibitory property (IC_{50} = 0.44 ± 0.12 μM) was shown by compound **403**. Besides these derivatives, compounds **404** (IC_{50} = 1.4 ± 0.19 μM) and **405** (IC_{50} = 0.17 ± 0.14 μM) have shown good activity. Other carbazole analogs rendered moderate to poor AChE activity.

The remarkable AChE inhibitor **402** comprises carbazole tethered to quinolinium bromide through pentylene chain connected between two nitrogens. However, replacement of quinolone by isoquinoline (compound **403**) led to fourfold reduced activity. Furthermore, compound **404** bearing 3-bromobenzyl ring tethered to carbazole *via* five carbon alkyl chain exhibited descent inhibitory activity; while change in position of –Br atom from benzyl 3-position to benzyl 4-position resulted into slightly diminished AChE activity. Structures of the potent compounds inferred that carabazole derivatives with five carbon spacer were strong AChE inhibitors.

Where as in the BuChE inhibitory property of synthesized molecules, a few compounds have shown best activity. Out of these compounds, the remarkable AChE inhibitors **402–405** have also succeeded in exhibition of good BuChE inhibitory activity. Particularly, compound **402** shown highest inhibitory potential (IC_{50} = 0.02 ± 0.11 μM) followed by compound **403** with fourfold diminished activity (IC_{50} = 0.08 ± 0.15 μM). Also, slightly abated BuChE activities 5.1 ± 1.02 μM and 6.8 ± 1.02 μM were observed for the compounds **404** and **405** respectively. The compound **402** rendered 225 fold greater activity compared to donepezil (IC_{50} = 4.5 ± 0.11 μM). Further, the AChE and BuChE inhibitory values indicated that there is synchronization between the AChE and BuChE of all the carbazole derivatives which infers all the molecules are AChE/BuChE dual inhibitors.

Molecular binding analysis of potent AChE inhibitor **402** in active site of AChE (Fig. 159) revealed good interaction of quinolone motif with Tyr332 through π-stacking interaction. Besides, compound **402** is well fitted into the PAS and anionic site of the AChE indicating higher pharmaceutical activity.

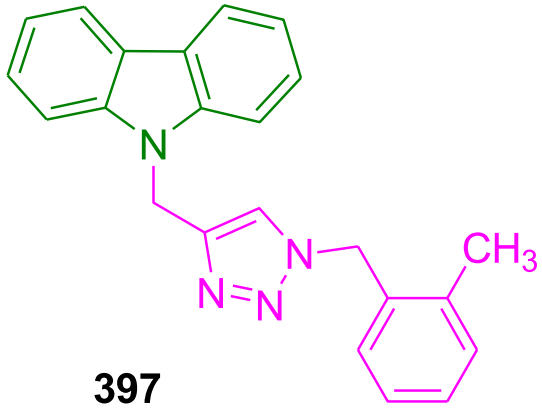

Fig. 153. Structure of carbazole derivative with significant AChE inhibitory activity.

9. Futuristic modeling of Anti-alzheimer's drug based on its recent drug discovery

Based on the very recent advances in Alzheimer drug discovery, some recommendations have been made in order to yield the best results. Taking consideration of most potent molecules (Table 22) having anti-AD properties would pave to futuristic models of the drug those have to be designed and synthesized. Such design is purely a hypothetical, logical and calculated way of approach. The researchers could try these remodels and make a go for synthesis.

The structural similarities of the three compounds **56**, **74** and **266** were observed where some of the pharmacological significant fragments could be appended or substituted to afford a new speculated derivatives presumed to possess better anti-AD properties. From above derivatives, firstly S—C═S fragment in the compound **74** is substituted by amide. Since benzyl group was present in a large number of molecules having AD inhibitory properties, it is subsequently attached at the 4-position of 2-methyl-*N*-piperidine to get a urea derivative **ADM1**. As it was reported that urea/thiourea scaffolds possessed anti-AD properties, potent inhibitory properties of AD would be speculated. Now second model **ADM2** was designed by substitution of 3-chloro-4-methyl-8-oxy coumarin of **74** with 8-hydroxyquinolinium chloride motif and 2-methyl-*N*-piperidine as 2-acetamido-6-methylpiperidine and then appended to S—C═S fragment. The most potent BuChE inhibitory compound **266** was redesigned by modifying the benzyl benzene ring by 3-cyclopropylmethoxy group and difluoromethoxy moiety at 3- and 4-positions respectively to have PDE4D2 inhibitory properties in the derivative **ADM3** (Fig. 160).

The most significant Aβ aggregation inhibitor **11**, prominent BACE1 inhibitor **116** as well as **215**, potent σ_1R inhibitor were utilized to construct new models. The *t*-butyl moiety of potent BACE1 inhibitor **11**

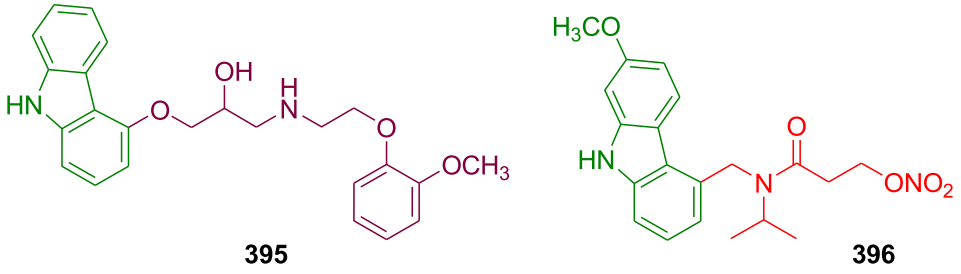

Fig. 152. Structures of carbazole derivatives with potent anti-AD properties.

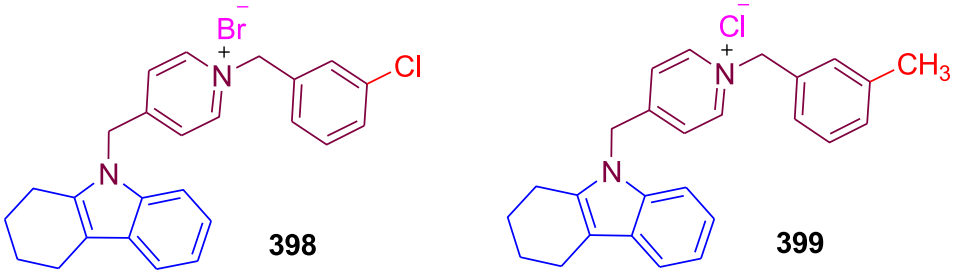

Fig. 154. Illustratation of structures of AChE active carbazole pyridinium derivatives.

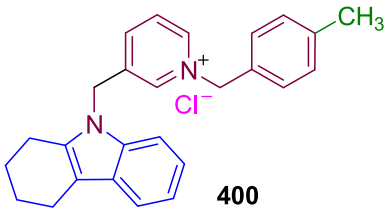

Fig. 155. Carbazole-pyridinium analog with most potent BuChE activity.

is replaced by pharmacological important non-benzenoid compound indole and the free NH at the benzyl end is acetylated to yield **ADM4** which might possess descent anti-AD characteristics. Similarly, the excellent BACE1 inhibitor **116** is modified by substitution of coumarin ring with indole scaffold and 3,4-dimethylbenzyl ring is replaced by diphenylmethine moiety to afford **ADM5** (Fig. 161).

The derivative **216** possessing most remarkable 5-HT4R inhibitory activity, significant neuroinflammation inhibitor **225** and potent MAO-B inhibitor **316** witness the prominent properties pertaining to anti-AD properties. Hence, these molecules could lead to super active molecules by building hybrid compounds *via* fragment replacement process. Here compound **316** is structurally modified upon connecting 3-fluropyridine to the *β*-carbon of α, *β*-unsaturated spacer and then appending 6-hydroxybenzimidazole motif at 2-position of pyridine ring resulting into **ADM6**. It might be credible to bring about the three activities 5-HT4R, NO and MAO-B in structural framework by introduction of *N*-cyclopentylmethylene piperidine tethered with propanoyl chain into

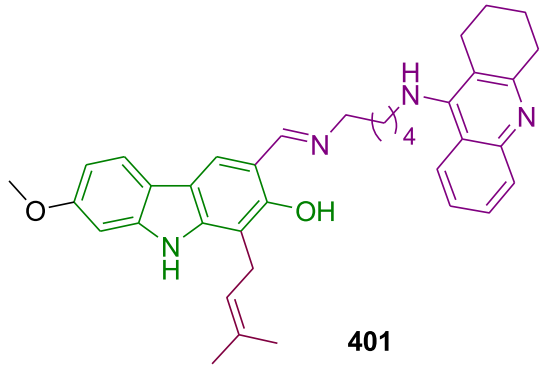

Fig. 157. Structure of potent $A\beta_{1\text{-}40}$ inhibitor.

compound **225** and transformation of 6-hydroxybenzimidazole to 6-hydroxyindole by N3-removal; this would pave to future anti-alzheimer agent **ADM7** (Fig. 162).

The structural changes are made for the DAPK/CSF1R dual inhibitor **381**; wherein *m*-trifluoromethyl phenyl moiety at 6-position of pyrimidine ring is substituted with cyclopropyl ring tethered pyridine through amide linkage of significant GSK-3*β* inhibitor **362** and subsequently transforming amide functionality into imine led to **ADM8**. Likewise the structural vivacity of compound **94** towards H3R inhibition is made use in remodeling. 4-Substituted phenoxy motif of compound **94** is replaced by pyrimdine-2-amine structural unit of derivative

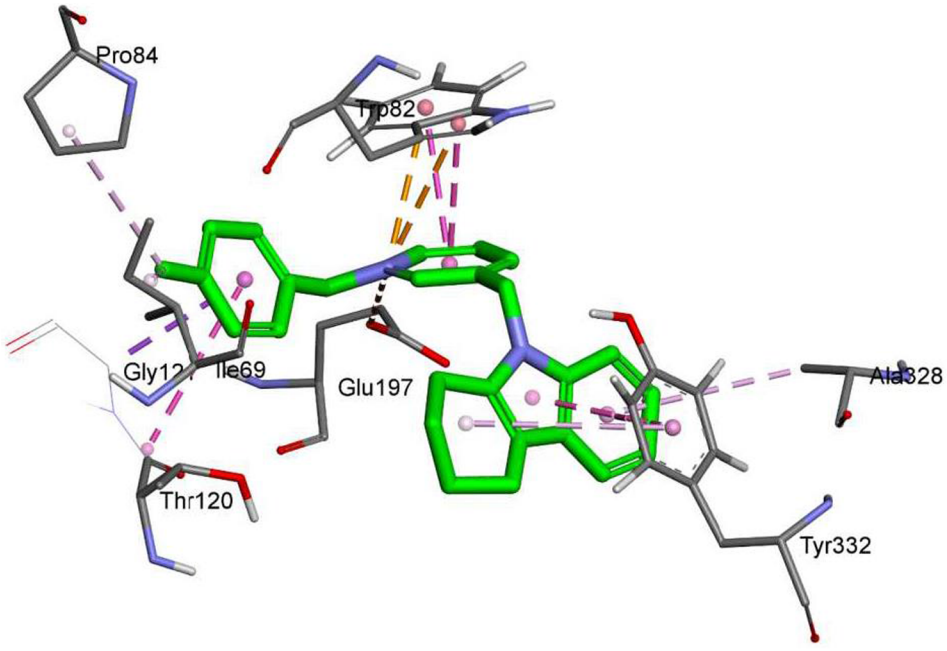

Fig. 156. Molecular docking analysis of compound **398** with AChE active site [317].

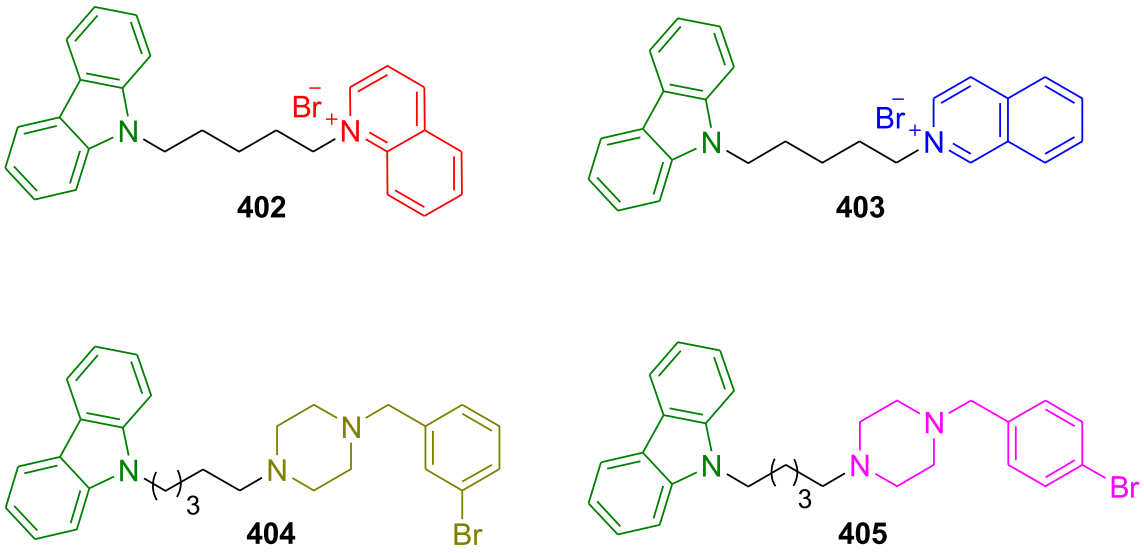

Fig. 158. Illustration of structures of potent AChE inhibitors.

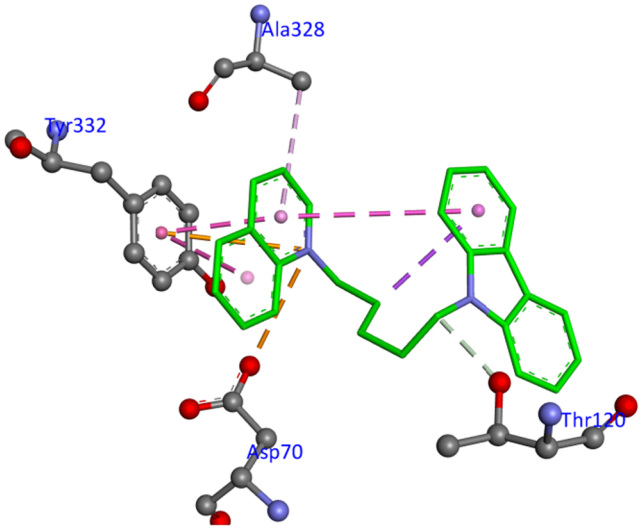

Fig. 159. Demonstration of molecular binding studies of compound **402** with AChE active site [321].

381. *N*-Ethylpiperidine is attached to NH of 2-aminopyridine moiety. Another slight modification include replacement of alkoxyamine chain at 7-position of chromone scaffold by trifluoromethyl unit yielding **ADM9** (Fig. 163).

The CSF1R inhibitory activity could be introduced into the compound **215** in addition to σ_1R inhibitory properties. This is made possible on transformation of pyridine ring into pyrimidine ring retaining indole motif intact in the molecule. Alongside, the benzyl benzene ring is appended at its 4-position by *N*-morpholine structural unit. Such modifications have resulted into the formation of pryridinium scaffold **ADB10**. Furthermore, compound **71** possessing remarkable *h*MAO-A inhibitory activity is made to undergo structural modification; wherein piperidine ring attached to S—C═S fragment is replaced with pyridinium-2-amine motif of **379** and on the other end 4-methoxyphenoxy group is connected to coumarin at 5-position in addition to introduction of imine functional group in the alkyl chain to get **ADM11** (Fig. 164).

A single structural framework is constructed with hypothesized anti-AD properties. In this regard compound **11** is utilized for modeling of descent inhibitor **ADM12**; where in retaining the basic structure of an excellent AChE inhibitor **74**, introducing unsaturation at carbon next to the oxygen of coumarin at 8-position and 1,1-diphenylethylene motif of derivative **11** is attached to *β*-carbon of newly created α, *β*-unsaturated group. Chloro group at 3-position of coumarin moiety is exchanged with highly electronegative fluoro atom speculating higher potencies towards AD. In continuation, potent MAO-B inhibitor **316** was made use in the structural modification of compound **11**. Keeping diaminohydroxybutyl chain and diphenylmethine moieties intact, *m*-*t*-butylphenyl is replaced by 6-*t*-butyl chromene. While on the other end of the molecule, one of the diphenylmethine benzenes is fluorinated at 4-position to afford **ADM13** (Fig. 165).

In this set of models, the derivatives namely; CSF1R/DAPK dual inhibitor **381**, significant BACE inhibitor **116** along with **216** possessing strongest 5-HT4R inhibitory potency are considered for remodeling of the drug. Structural modification is allowed for the compound **116**; wherein central coumarin unit is substituted with indole of compound **216**, secondly cyclopentylmethoxy group is attached at 4-position of the indole scaffold. Finally the third modification entails tethering of 3-trifluoromethyl phenyl part at 3-position of indole *via* amide linkage giving **ADM14**. The BACE1 inhibitor is structurally modified in order to inculcate other inhibition properties of AD. To accomplish this, replacement of coumarin is brought about using pyrimidine-2-amine structural unit. Finally the benzyl benzene linked to piperidine is connected with $-CF_3$ group at 3-position of benzyl benzene leading to **ADM15** (Fig. 166).

Structural engineered molecules could be built form the derivatives possessing inhibitory effects towards AD. Here, a set two Alzheimer models could be designed using remarkable PDE4D2 inhibitor **56**, compound **225** most active towards neuroinflammation inhibition and the structural features of GSK-3*β* **362** are also included. Compound **56** is redesigned using pharmacological significant structural features of derivative **316**; wherein the hydroxy group at 8-position of quinolinium motif is exchanged with fluoro atom followed by inter conversion of amide linkage to imine linkage. Furthermore, benzene attached to imine carbon is transformed into chromene by fusing 3,4-unsaturated pyran ring at 5,6-positions of benzene resulting into **ADM16** with anticipated inhibitory properties of AD. The neuroinflammation inhibitor **225** could be restructured to possess additional anti-AD properties. In this regard benzene fused piperidine is modified as chromene alongside insertion of amide functionality in between pyridine ring and indole motif. Subsequent structural changes include; replacement of 6-hydroxy group by difluoromethoxy group and new addition of cyclopropylmethoxy moiety at indole 7-position. These modifications have resulted into incarnation of anti-AD model **ADM17** (Fig. 167).

Table 22
Most potent anti-AD compounds with their inhibitory values.

Sl. No.	Structure	Inhibitory activity	Inhibitory value (IC_{50}, μM)
1	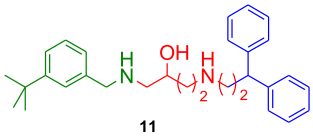 11	Aβ-aggregation	84.9% ± 0.8, IC_{50} = 1.22 μM
2	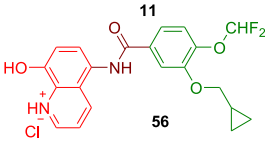 56	PDE4D2	0.399 ± 0.021
3	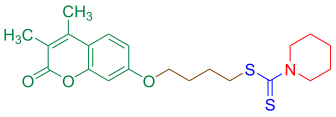 71	*h*MAO-A	0.654 ± 0.021
4	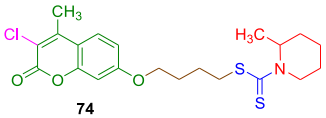 74	*ee*AChE	0.0068 ± 0.0002
5	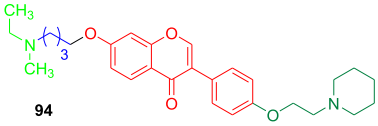 94	H3R	0.27 ± 0.004
6	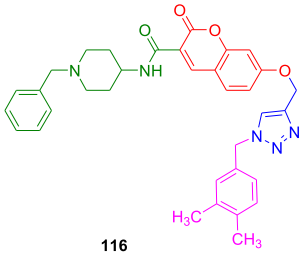 116	BACE1	0.014
7	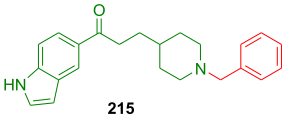 215	σ_1R	K_i = 0.0033 ± 0.7
8	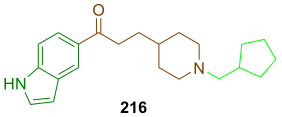 216	5-HT4R	K_i = 0.025 ± 1.6
9	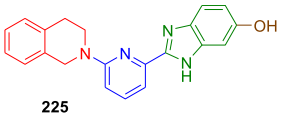 225	NO	3.80 ± 0.42
10	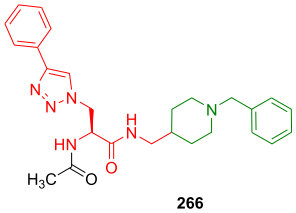 266	BuChE	0.00017 ± 0.000021
11	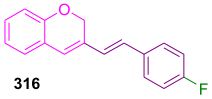 316	MAO-B	0.010
12	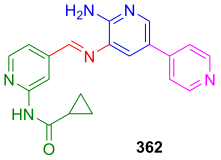 362	GSK-3β	38 ± 2.8

(*continued on next page*)

Table 22 (*continued*)

Sl. No.	Structure	Inhibitory activity	Inhibitory value (IC_{50}, μM)
13	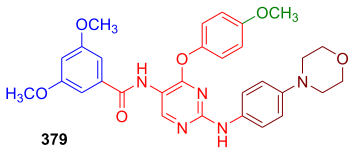 **379**	CSF1R	0.12 ± 0.003
14	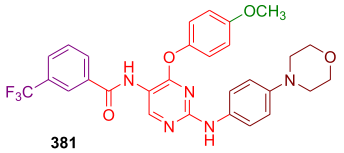 **381**	DAPK	1.25 ± 0.35

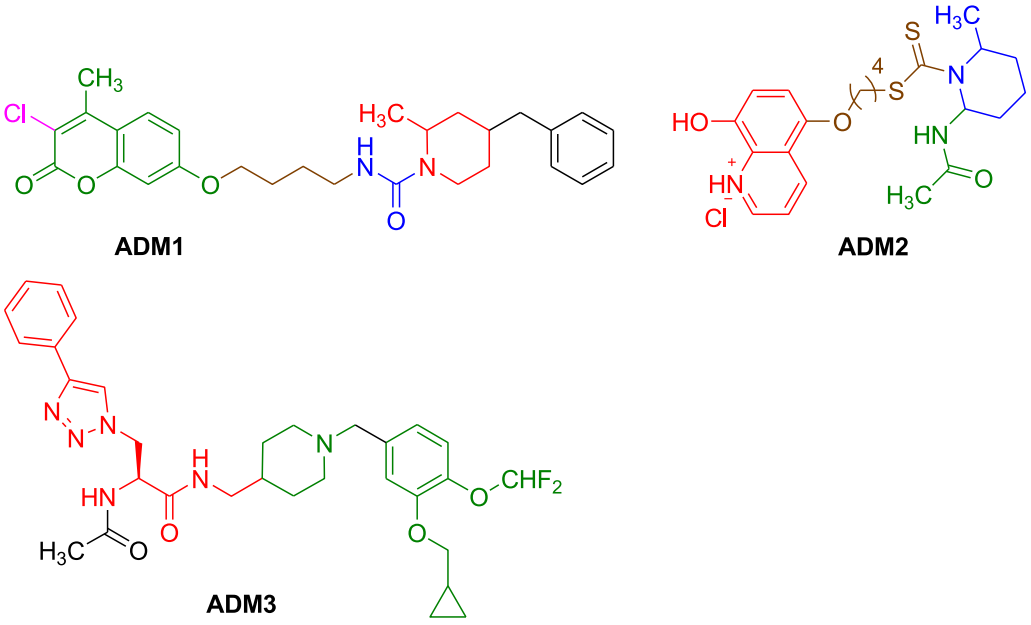

Fig. 160. Illustration of structures of **ADM1**-**ADM3.**

10. Conclusive discussion

The work done regarding the anti-AD drug design in the recent years is sorted out in an apt way. In spite of continuous research is being carried out, only few drug molecules turned out to be potent scaffolds for AD treatment. Most of the research has been done on discovery of anti-AD agents as multifunctional/multi-target drug molecules. In this conjuncture, the design of 1-benzylamino-2-hydroxyalkyl derivatives were possessed moderate inhibitory activities. Amongst them compound **11** has most potent A*β* inhibitory activity of all. There was no much significant inhibition observed in case of 2, 5-dihydroxyterephthalamide derivatives. 3-Phenylcoumarin–lipoic acid conjugates have not managed to be remarkable inhibitors towards AD. Moderate AChE inhibitory effects were observed for the 5, 6-dimethoxybenzo[*d*]isothiazol-3(2*H*)-one-*N*-alkylbenzylamine derivatives. Likewise significant inhibitory activity was seen for the 2,4-dioxochroman benzyl modified pyridinium derivatives. Although phenylpyridazine bearing carboxamide & propanamide derivatives were designed as multifunctional drugs, the synthesized molecules have displayed some AChE inhibitory activity. The impressive PDE4D2 inhibitory property was shown by compound **56** possessing 8-hydroxyquinolinium motif. Significant AChE inhibitory properties have been

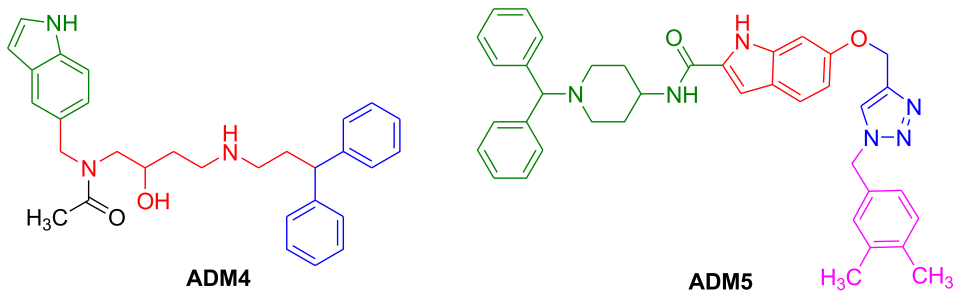

Fig. 161. Demonstration of structures of futuristic anti-AD drugs.

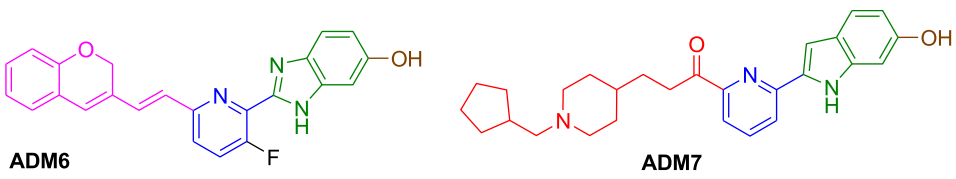

Fig. 162. Structures of future AD significant remodeled drugs.

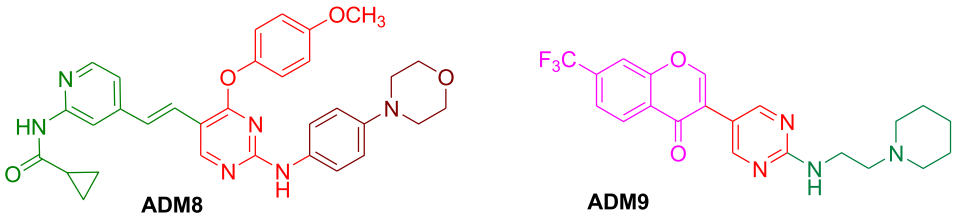

Fig. 163. Structural designed molecules as anti-AD derivatives.

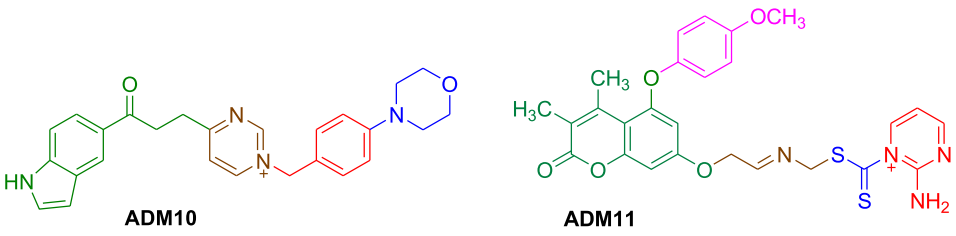

Fig. 164. Structures of speculated potent drug molecules with descent activity.

displayed by the coumarin-dithiocarbamate hybrids. Another series of coumarin-dithiocarbamate derivatives have bestowed with descent MAO inhibitory activity. The compound **74** designed as a part of coumarin-dithiocarbamate derivatives was the best AChE inhibitor. Miconozole analogs have not turned out to be potent AD inhibitors. In the series of isoflavone derivatives designed compound **94** exhibited most potent H3R inhibitory activity. While the piperidinehydrazide-hydrazones got only moderate inhibitory activity. Good LOX-5 inhibitory activity was displayed by flavonoid–*N*,*N*-dibenzyl(*N*-methyl) amine hybrids. The most significant BACE1 inhibitory activity has been exhibited by compound **116**, one of the derivatives in 1,2,3-triazole-chromenone carboxamides. 3-Arylcoumarin scaffolds could not exhibit strong inhibitory activity. Weak anti-AD properties have been displayed by the 3-hydrazinyl 1,2,4-triazine analogs. Various natural products were screened for inhibition of anti-AD properties; no single compound has shown prominent activity. 4′-Hydroxy-flurbiprofen mannich base derivatives have failed to show good potencies. The designed chalcone mannich base derivatives have exhibited good AChE inhibitory effects. Remarkable cholinesterase inhibitory properties were elicited by cyclopentaquinoline hybrids. Most of the hybrids of donepezil, chromone and melatonin resulted descent AChE inhibitory activity. Bis-aryltriazole derivatives were designed and found to be good Aβ aggregation inhibitory properties. BACE1 inhibitory properties have been displayed by the *N*-benzylpiperidine scaffolds. Again the AChE and BuChE inhibitory properties were exhibited by *N*-benzylpyridinium-based analogs up to nanomolar level. Selective MAO-B inhibitory activities have been bestowed for the pyrazolone schiff bases. Descent anti-AD activities were exhibited by indole-piperidine analogs; wherein compound **216** has turned out to be most significant 5-HT4R inhibitor. Tetrahydroisoquinoline-benzimidazole hybrids have been reported as neuroinflammation inhibitors; wherein compound **225** has yielded most potent results. Most of the synthesized 1,2,3-triazole appended tacrine-coumarin derivatives have elicited remarkable cholinesterase inhibitory activity. Further, 2-benzofuran carboxamide-benzylpyridinum salts have exhibited selective BuChE inhibitory properties. A descent BuChE inhibitory properties were observed for aryl-1,2,3-triazolyl benzylpiperidine scaffolds in which compound **266** shown elite BuChE inhibitory activity. 4-Aminobenzoic acid derivatives have designed to show potent anti-AD properties and found to be selective AChE inhibitors. The descent AChE inhibitory properties were observed in case of designed tricyclic fused ring scaffolds. While the significant BuChE inhibitory activity was exhibited by indol-3-acetic acid-tacrine hybrids. Regarding inhibitory activity towards MAO-B, 3-(*E*)-styryl-2*H*-chromene derivatives were reported to be the best inhibitors; wherein compound **316** has elicited the most potent activity. Also, 4(3*H*)-quinazolinone derivatives and chalcone analogs possessed potential MAO-B inhibitors. Furthermore the inhibition towards GSK-3β was displayed by 2,3-diaminopyridine analogs; particularly compound **362** was finest inhibitor. Relatively strong Aβ aggregation inhibitory activity was shown by sarsasapogenin-triazolyl analogs. Pyridine-pyrimidine-

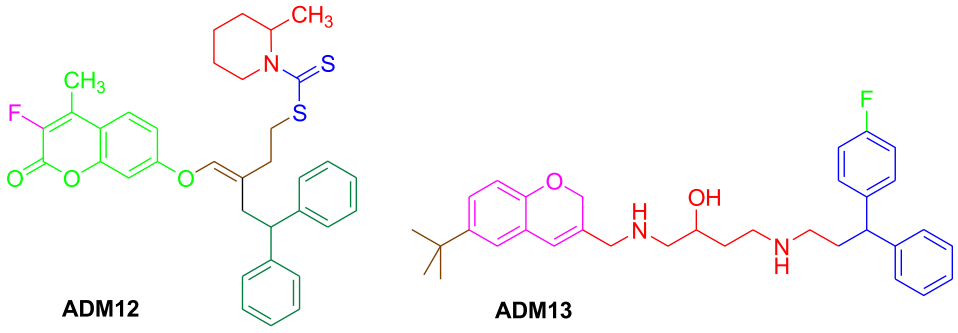

Fig. 165. Demonstration of structures of remodeled drugs as anti-AD inhibitors.

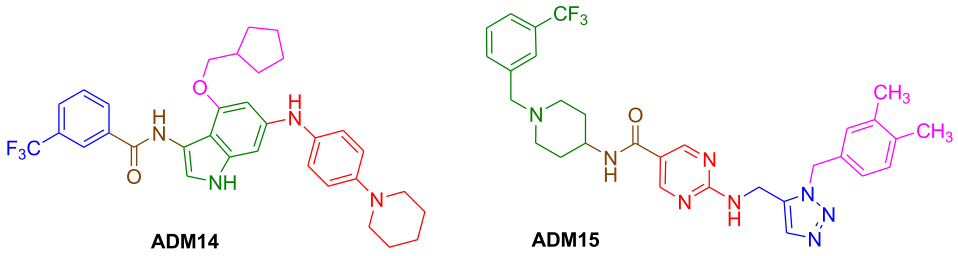

Fig. 166. Illustration of redesigned molecules as anti-AD agents.

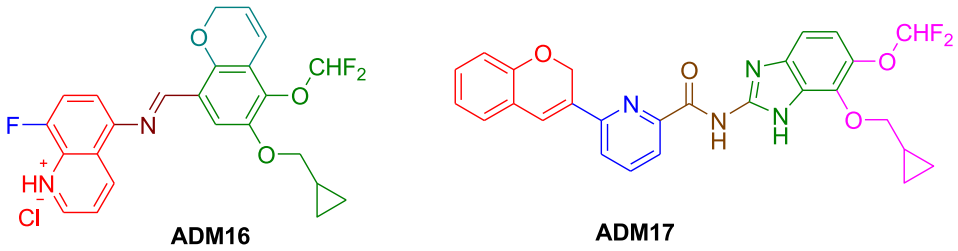

Fig. 167. Depiction of novel designed drug molecules.

benzamide analogs have been reported as tau inhibitors; where in compound **379** was found to be potent CSF1R inhibitor and derivative **381** has remarkable CSF1R/DAPK dual potency. The fraction of the *Euphorbia dendroides* L. plant extract is found to exhibit 0.81 μM. Meanwhile, the terpenoid **384** has exhibited AChE/BuChE dual inhibitory property and diterpene oil fraction having phytol exhibited descent AChE activity. When it comes to carbazole analogs, significant BuChE inhibitory potentials were noticed in addition to good BACE1 activity. Besides this, compound **402** has been reported to render AChE/BuChE inhibitory activity. The structural activity relationship of the most potent inhibitors was discussed qualitatively. The potential inhibitory activities of the compounds were supported by the molecular docking studies.To encourage the research on AD drug discovery, futuristic AD drug models are designed considering the pharmacological significant structural features of the potent inhibitors of AD.

Acknowledgements

I acknowledge my sincere gratitude to SCI-HUB for granting access to large number of full length scientific research papers.

Declaration of Competing Interest

The authors declared that there is no conflict of interest.

References

[1] A. Burns, S. Iliffe, Alzheimer's disease, BMJ 338 (2009) b158.
[2] Clive Ballard, Serge Gauthier, Anne Corbett, Carol Brayne, Dag Aarsland, Emma Jones, Alzheimer's disease, Lancet 377 (9770) (2011) 1019–1031 https://linkinghub.elsevier.com/retrieve/pii/S0140673610613499https://doi.org/10.1016/S0140-6736(10)61349-9.
[3] H.W. Querfurth, F.M. LaFerla, Alzheimer's disease, N. Engl. J. Med. 362 (2010) 329–344.
[4] GBD 2015 Disease Injury Incidence Prevalence Collaborators (October 2016), Global, regional, and national incidence, prevalence, and years lived with disability for 310 diseases and injuries, 1990–2015: a systematic analysis for the Global Burden of Disease Study, Lancet 388 (2015) 1545–1602.
[5] S.C. Waring, R.N. Rosenberg, Genome-wide association studies in Alzheimer disease, Arch. Neurol. 65 (2008) 329–334.
[6] D.J. Selkoe, Translating cell biology into therapeutic advances in Alzheimer's disease, Nature 399 (1999) A23–A31.
[7] J.H. Kim, Genetics of Alzheimer's disease, Dement. Neurocogn. Disord. 17 (2018) 131–136.
[8] P.T. Francis, A.M. Palmer, M. Snape, G.K. Wilcock, The cholinergic hypothesis of Alzheimer's disease: a review of progress, J. Neurol. Neurosurg. Psych. 66 (1999) 137–147.
[9] A. Martorana, Z. Esposito, G. Koch, Beyond the cholinergic hypothesis: do current drugs work in Alzheimer's disease? CNS Neurosci. Ther. 16 (2010) 235–245.
[10] J. Hardy, D. Allsop, Amyloid deposition as the central event in the aetiology of Alzheimer's disease, Trends Pharmacol. Sci. 12 (1991) 383–388.
[11] A. Mudher, S. Lovestone, Alzheimer's disease-do tauists and baptists finally shake hands?“, Trends Neurosci. 25 (2002) 22–26.
[12] N. Guzior, A. Wieckowska, D. Panek, B. Malawska, Recent development of multifunctional agents as potential drug candidates for the treatment of Alzheimer's disease, Curr. Med. Chem. 22 (2015) 373–404.
[13] E. Viayna, R. Sabate, D. Munoz-Torrero, Dual inhibitors of β-amyloid aggregation and acetylcholinesterase as multi-target anti-Alzheimer drug candidates, Curr. Top. Med. Chem. 13 (2013) 1820–1842.
[14] D. Panek, A. Wiecknowska, J. Jonczyk, J. Godyn, M. Bajda, T. Wichur, A. Pasieka, D. Knez, A. Pislar, J. Korabecny, O. Soukup, V. Sepsova, R. Sabate, J. Kos, S. Gobec, B. Malawska, Design, synthesis, and biological evaluation of 1-benzylamino-2-hydroxyalkyl derivatives as new potential disease-modifying multifunctional anti-Alzheimer's agents, ACS Chem. Neurosci. 9 (2018) 1074–1094.
[15] G.P. Lim, F. Yang, T. Chu, et al., Ibuprofen suppresses plaque pathology and inflammation in a mouse model for Alzheimer's disease, J. Neurosci. 20 (2000) 5709–5714.
[16] Y.P. Tang, S.Z. Haslam, S.E. Conrad, C.L. Sisk, Estrogen increasesbrain expression of the mRNA encoding transthyretin, an amyloid beta scavenger protein, J. Alzheimer's Dis. 6 (2004) 413–420.
[17] S. Muraoka, T. Miura, Inactivation of cholinesterase induced by non-steroidal anti-inflammatory drugs with horseradish peroxidase: implication for Alzheimer's disease, Life Sci. 84 (2009) 272–277.
[18] X. Qiang, Z. Sang, W. Yuan, et al., synthesis and evaluation of genistein-*O*-alkylbenzylamines as potential multifunctional agents for the treatment of Alzheimer's disease, Eur. J. Med. Chem. 76 (2014) 314–331.
[19] A. Cavalli, M.L. Bolognesi, S. Capsoni, et al., A small molecule targeting the multifactorial nature of Alzheimer's disease, Angew. Chem. Int. Ed. 46 (2007) 3689–3692.
[20] Q. Song, Y. Li, Z. Cao, H. Liu, C. Tian, Z. Yang, X. Qiang, Z. Tan, Y. Deng, Discovery of novel 2,5-dihydroxyterephthalamide derivatives as multifunctional agents for the treatment of Alzheimer's disease, Bioorg. Med. Chem. 26 (2018) 6115–6127.
[21] M. Rosini, V. Andrisano, M. Bartolini, P. Hrelia, A. Tarozzi, V. Andrisano, et al., Rational approach to discover multipotent anti-Alzheimer drugs, J. Med. Chem. 48 (2005) 360–363.
[22] S.S. Xie, X.B. Wang, J.Y. Li, L. Yang, L.Y. Kong, Design, synthesis and evaluation of novel tacrine-coumarin hybrids as multifunctional cholinesterase inhibitors against Alzheimer's disease, Eur. J. Med. Chem. 64 (2013) 540–553.
[23] S.M. Bagheri, M. Khoobi, H. Nadri, A. Moradi, S. Emami, L. Jalili-Baleh, F. Jafarpour, F.H. Moghadam, A. Foroumadi, A. Shafiee, Synthesis and anticholinesterase activity of 4-hydroxycoumarin derivatives containing substituted benzyl-1,2,3-triazole moiety, Chem. Biol. Drug Des. 86 (2015) 1215–1220.
[24] A. Tarozzi, M. Bartolini, L. Piazzi, L. Valgimigli, R. Amorati, C. Bolondi, et al., From the dual function lead AP2238 to AP2469, a multi-target-directed ligand for the treatment of Alzheimer's disease, Pharma. Res. Per. 2 (2014) e00023.
[25] M. Roussaki, C.A. Kontogiorgis, D. Hadjipavlou-Litina, S. Hamilakis, A. Detsi, A novel synthesis of 3-aryl coumarins and evaluation of their antioxidant and lipoxygenase inhibitory activity, Bioorg. Med. Chem. Lett. 20 (2010) 3889–3892.
[26] L. Jalili-Baleh, H. Nadri, H. Forootanfar, A. Samzadeh-Kermani, T. Tuylu Kucukkilinc, B. Ayazgok, M. Rahimifard, M. Baeeri, M. Doostmohammadi, L. Firoozpour, S.N.A. Bukhari, M. Abdollahi, M.R. Ganjali, S. Emami, M. Khoobi, A. Foroumadi, Novel 3-phenylcoumarin–lipoic acid conjugates as multi-functional agents for potential treatment of Alzheimer's disease, Bioorg. Chem. 79 (2018)

223–234.
[27] M. Tavari, S.F. Malan, J. Joubert, MedChemComm. 7 (2016) 1628.
[28] N. Szalaj, M. Bajda, K. Dudek, B. Brus, S. Gobec, B. Malawska, Arch. Pharm. 348 (2015) 556.
[29] R. Xu, G. Xiao, Y. Li, H. Liu, Q. Song, X. Zhang, Z. Yang, Y. Zheng, Z.I. Tan, Y. Deng, Multifunctional 5,6-dimethoxybenzo[*d*]isothiazol-3(2*H*)-one-Nalkylbenzylamine derivatives with acetylcholinesterase, monoamine oxidases and b-amyloid aggregation inhibitory activities as potential agents against Alzheimer's disease, Bioorg. Med. Chem. 26 (2018) 1885–1895.
[30] R. Bullock, A. Dengiz, Cognitive performance in patients with Alzheimer's disease receiving cholinesterase inhibitors for up to 5 years, Int. J. Clin. Pract. 59 (2005) 817–822.
[31] E. Giacobini, Cholinesterase inhibitors: new roles and therapeutic alternatives, Pharmacol. Res. 50 (2004) 433–440.
[32] M. Mostofi, G.M. Ziarani, M. Mahdavi, A. Moradi, H. Nadri, S. Emami, H. Alinezhad, A. Foroumadi, A. Shafiee, Synthesis and structure-activity relationship study of benzofuran-based chalconoids bearing benzylpyridinium moiety as potent acetylcholinesterase inhibitors, Eur. J. Med. Chem. 103 (2015) 361–369.
[33] M. Alipour, M. Khoobi, A. Foroumadi, H. Nadri, A. Moradi, A. Sakhteman, M. Ghandi, A. Shafiee, Novel coumarin derivatives bearing *N*-benzyl pyridinium moiety: potent and dual binding site acetylcholinesterase inhibitors, Bioorg. Med. Chem. 20 (2012) 7214–7222.
[34] M. Molazadeh, M. Mohammadi-Khanaposhtani, A. Zonouzi, H. Nadri, Z. Najafi, B. Larijani, M. Mahdavi, New benzyl pyridinium derivatives bearing 2,4-dioxo-chroman moiety as potent agents for treatment of Alzheimer's disease: design, synthesis, biological evaluation, and docking study, Bioorg. Chem. (2019), https://doi.org/10.1016/j.bioorg.2019.03.012.
[35] J.M. Contreras, Y.M. Rival, S. Chayer, J.J. Bourguignon, C.G. Wermuth, Aminopyridazines as acetylcholinesterase inhibitors, J. Med. Chem. 42 (4) (1999) 730–741.
[36] C. Yamali, H.O. Gulcan, B. Kahya, S. Cobanoglu, M.K. Sukuroglu, D.S. Dogruer, Synthesis of some 3(2*H*)-pyridazinone and 1(2*H*)-phthalazinone derivatives incorporating aminothiazole moiety and investigation of their antioxidant, acetylcholinesterase, and butyrylcholinesterase inhibitory activities, Med. Chem. Res. 24 (2015) 1210–1217.
[37] B. Kilic, H. Ozan Gulcan, M. Yalcin, F. Aksakal, A. Dimoglo, M. Fethi Sahin, D. Songul Dogruer, Synthesis of some new 1 (2*H*)-phthalazinone derivatives and evaluation of their acetylcholinesterase and butyrylcholinesterase inhibitory activities, Lett. Drug. Des. Discov. 14 (2017) 159–166.
[38] B. Kilic, H.O. Gulcan, F. Aksakal, T. Ercetin, N. Oruklu, E.U. Bagriacik, D.S. Dogruer, Design and synthesis of some new carboxamide and propanamide derivatives bearing phenylpyridazine as a core ring and the investigation of their inhibitory potential on in-vitro acetylcholinesterase and butyrylcholinesterase, Bioorg. Chem. 79 (2018) 235–249.
[39] J.B. Torres, E.M. Andreozzi, J.T. Dunn, M. Siddique, I. Szanda, D.R. Howlett, K. Sunassee, P.J. Blower, PET imaging of copper trafficking in a mouse model of Alzheimer disease, J. Nucl. Med. 57 (2016) 109–114.
[40] Z. Lv, M.M. Condron, D.B. Teplow, Y.L. Lyubchenko, Nanoprobing of the effect of Cu2+ cations on misfolding, interaction and aggregation of amyloid β peptide, J. Neuroimm. Pharm. 8 (2013) 262–273.
[41] S. Parthasarathy, B. Yoo, D. Mcelheny, W. Tay, Y. Ishii, Capturing a reactive state of amyloid aggregates: NMR-based characterization of copper-bound Alzheimer disease amyloid β-fibrils in a redox cycle, J. Biol. Chem. 289 (2014) 9998–10010.
[42] D.F. Tardiff, L.E. Brown, X. Yan, R. Trilles, N.T. Jui, M.I. Barrasa, K.A. Caldwell, G.A. Caldwell, S.E. Schaus, S. Lindquist, Dihydropyrimidine-thiones and clioquinol synergize to target β-amyloid cellular pathologies through a metal-dependent mechanism, ACS Chem. Neurosci. 8 (2017) 2039–2055.
[43] R. Zebda, A.S. Paller, Phosphodiesterase 4 inhibitors, J. Am. Acad. Dermatol. 78 (2018) S43–S52.
[44] B. Gong, O.V. Vitolo, F. Trinchese, S. Liu, M. Shelanski, O. Arancio, Persistent improvement in synaptic and cognitive functions in an Alzheimer mouse model after rolipram treatment, J. Clin. Invest. 114 (2004) 1624–1634.
[45] J. Hu, T. Pan, B. An, Z. Li, X. Li, L. Huang, Synthesis and evaluation of clioquinol-rolipram/roflumilast hybrids as multitarget-directed ligands for the treatment of Alzheimer's disease, Eur. J. Med. Chem. (2019), https://doi.org/10.1016/j.ejmech.2018.12.013.
[46] I. Kostova, S. Bhatia, P. Grigorov, S. Balkansky, V.S. Parmar, A.K. Prasad, L. Saso, Curr. Med. Chem. 18 (2011) 3929–3951.
[47] P. Anand, B. Singh, N. Singh, A review on coumarins as acetylcholinesterase inhibitors for Alzheimer's disease, Bioorg. Med. Chem. 20 (2012) 1175–1180.
[48] Y.C. Duan, Y.C. Ma, E. Zhang, X.J. Shi, M.M. Wang, X.W. Ye, H.M. Liu, Eur. J. Med. Chem. 62 (2013) 11–19.
[49] J.S. Lan, Y. Ding, Y. Liu, P. Kang, J.W. Hou, X.Y. Zhang, S.S. Xie, T. Zhang, Eur. J. Med. Chem. 139 (2017) 48–59.
[50] N. Jiang, Q. Huang, J. Liu, N. Liang, Q. Li, Q. Li, S.S. Xie, Design, synthesis and biological evaluation of new coumarin-dithiocarbamate hybrids as multifunctional agents for the treatment of Alzheimer's disease, Eur. J. Med. Chem. 146 (2018) 287–298.
[51] Q. Sun, D.Y. Peng, S.G. Yang, X.L. Zhu, W.C. Yang, G.F. Yang, Syntheses of coumarin-tacrine hybrids as dual-site acetylcholinesterase inhibitors and their activity against butylcholinesterase, Abeta aggregation, and beta-secretase, Bioorg. Med. Chem. 22 (2014) 4784–4791.
[52] L. Pisani, R. Farina, O. Nicolotti, D. Gadaleta, R. Soto-Otero, M. Catto, M. Di Braccio, E. Mendez-Alvarez, A. Carotti, In silico design of novel 2*H*-chromen-2-one derivatives as potent and selective MAO-B inhibitors, Eur. J. Med. Chem. 89 (2015) 98–105.
[53] I.E. Orhan, H.O. Gulcan, Coumarins: auspicious cholinesterase monoamine oxidase inhibitors, Curr. Top Med. Chem. 15 (2015) 1673–1682.
[54] Q. He, J. Liu, J.-S. Lan, J. Ding, Y. Sun, Y. Fang, N. Jiang, Z. Yang, L. Sun, Y. Jin, S.-S. Xie, Coumarin-dithiocarbamate hybrids as novel multitarget AChE and MAO-B inhibitors against Alzheimer′s Disease: design, synthesis and biological evaluation, Bioorg. Chem. (2018), https://doi.org/10.1016/j.bioorg.2018.09.010.
[55] R.M. Lane, S.G. Potkin, A. Enz, Targeting acetylcholinesterase and butyrylcholinesterase in dementia, Int. J. Neuropsychopharmacol. 9 (2006) 101–124.
[56] S. Diamant, E. Podoly, A. Friedler, H. Ligumsky, O. Livnah, H. Soreq, Butyrylcholinesterase attenuates amyloid fibril formation in vitro, PNAS 103 (2006) 8628–8633.
[57] L.C. Souza, C.R. Jesse, M.S. Antunes, et al., Indoleamine-2,3-dioxygenase mediates neurobehavioral alterations induced by an intracerebroventricular injection of amyloid-beta1-42 peptide in mice, Brain Behav. Immun. 56 (2016) 363–377.
[58] Y. Chen, X. Xu, T. Fu, W. Li, Z. Liu, H. Sun, Discovery of new scaffolds from approved drugs as acetylcholinesterase inhibitors, RSC Adv. 5 (2015) 90288–90294.
[59] U.F. Rohrig, S.R. Majjigapu, M. Chambon, et al., Detailed analysis and follow-up studies of a high-throughput screening for indoleamine 2,3-dioxygenase 1 (IDO1) inhibitors, Eur. J. Med. Chem. 84 (2014) 284–301.
[60] X. Lu, Q. Si-yu He, H. Li, X. Yang, H. Jiang, Y. Lin, W. Chen, F. Qu, Y. Feng, Y. Bian, H. Sun Zhou, Investigation of multi-target-directed ligands (MTDLs) with butyrylcholinesterase (BuChE) and indoleamine 2,3-dioxygenase 1 (IDO1) inhibition: the design, synthesis of miconazole analogues targeting Alzheimer's disease, Bioorg. Med. Chem. 26 (2018) 1665–1674.
[61] A. Contestabile, The history of the cholinergic hypothesis, Behav. Brain Res. 221 (2011) 334–340.
[62] B. Sadek, A. Saad, A. Sadeq, F. Jalal, H. Stark, Histamine H3 receptor as a potential target for cognitive symptoms in neuropsychiatric diseases, Behav. Brain Res. 312 (2016) 415–430.
[63] B. Feng, X. Li, J. Xia, S. Wu, Discovery of novel isoflavone derivatives as AChE/BuChE dual-targeted inhibitors: synthesis, biological evaluation and molecular modelling, J. Enzyme Inhib. Med. Chem. 32 (2017) 968–977.
[64] G. Wen, Q. Liu, H. Hu, D. Wang, S. Wu, Design, synthesis, biological evaluation, and molecular docking of novel flavones as H3R inhibitors, Chem. Biol. Drug Des. 90 (2017) 580–589.
[65] D. Wang, M. Hu, X. Li, D. Zhang, C. Chen, J. Fu, S. Shao, G. Shi, Y. Zhou, S. Wu, T. Zhang, Design, synthesis, and evaluation of isoflavone analogs as multifunctional agents for the treatment of Alzheimer's disease, Eur. J. Med. Chem. (2019), https://doi.org/10.1016/j.ejmech.2019.02.053.
[66] L.M. Refolo, H.M. Fillit, Drug discovery for Alzheimer's disease: the end of the beginning, J. Mol. Neurosci. 24 (2004) 1–8.
[67] A.S. Alpan, S. Parlar, L. Carlino, A.H. Tarikogullari, V. Alptüzün, H.S. Gunes, Synthesis, biological activity and molecular modeling studies on 1*H*-benzimidazole derivatives as acetylcholinesterase inhibitors, Bioorg. Med. Chem. 21 (2013) 4928–4937.
[68] P. Kapkova, N. Stiefl, U. Surig, B. Engels, K. Baumann, U. Holzgrabe, Synthesis, biological activity, and docking studies of new acetylcholinesterase inhibitors of the bispyridinium type, Arch. Pharm. Pharm. Med. Chem 336 (2003) 523–540.
[69] S. Parlar, G. Sayar, A. Hande Tarikogullari, S. Sozer Karadagli, V. Alptuzun, E. Erciyas, U. Holzgrabe, Synthesis, bioactivity and molecular modeling studies on potential anti-Alzheimer piperidinehydrazide-hydrazones, Bioorg. Chem. (2018), https://doi.org/10.1016/j.bioorg.2018.11.051.
[70] J.A. Joseph, D.R. Fisher, V. Cheng, A.M. Rimando, B. Shukitt-Hale, Cellular and behavioral effects of stilbene resveratrol analogues: implications for reducing the deleterious effects of aging, J. Agr. Food Chem. 56 (2008) 10544–10551.
[71] J. Chang, A. Rimando, M. Pallas, A. Camins, D. Porquet, J. Reeves, B. Shukitt-Hale, M.A. Smith, J.A. Joseph, G. Casadesus, Low-dose pterostilbene, but not resveratrol, is a potent neuromodulator in aging and Alzheimer's disease, Neurobiol. Ag. 33 (2012) 2062–2071.
[72] H. Tang, L.Z. Zhao, H.T. Zhao, S.L. Huang, S.M. Zhong, J.K. Qin, Z.F. Chen, Z.S. Huang, H. Liang, Hybrids of oxoisoaporphine-tacrine congeners: novel acetylcholinesterase and acetylcholinesterase-induced b-amyloid aggregation inhibitors, Eur. J. Med. Chem. 46 (2011) 4970–4979.
[73] Y.X. Li, X.M. Qiang, Y. Li, X. Yang, L. Li, G. Xiao, Z. Cao, Pterostilbene-Oacetamidoalkylbenzylamines derivatives as novel dual inhibitors of cholinesterase with anti-b-amyloid aggregation and antioxidant properties for the treatment of Alzheimer's disease, Bioorg. Med. Chem. Lett. 26 (2016) 2035–2039.
[74] Y. Zheng, X. Qiang, R. Xu, Q. Song, C. Tian, H. Liu, W. Li, Z. Tan, Y. Deng, Design, synthesis and evaluation of pterostilbene β-amino alcohol derivatives as multifunctional agents for Alzheimer's disease treatment, Bioorg. Chem. 78 (2018) 298–306.
[75] P.C. May, R.A. Dean, S.L. Lowe, et al., Robust central reduction of amyloid-β in humans with an orally available, non-peptidic b-secretase inhibitor, J. Neurosci. 31 (2011) 16507–16516.
[76] G. Evin, G. Lessene, S. Wilkins, BACE inhibitors as potential drugs for the treatment of Alzheimer's disease: focus on bioactivity, Recent Pat. CNS Drug Discov. 6 (2011) 91–106.
[77] J. Chu, P.F. Giannopoulos, C. Ceballos-Diaz, et al., 5-Lipoxygenase gene transfer worsens memory, amyloid, and tau brain pathologies in a mouse model of Alzheimer disease, Ann. Neurol. 72 (2012) 442–454.
[78] J. Chu, J.G. Li, D. Pratico, Zileuton improves memory deficits, amyloid and tau pathology in a mouse model of Alzheimer's disease with plaques and tangles, PLoS One 8 (2013) e70991.
[79] Y. Shimmyo, T. Kihara, A. Akaike, et al., Flavonols and flavones as BACE-1

inhibitors: structure-activity relationship in cellfree, cell-based and in silico studies reveal novel pharmacophore features, Biochim. Biophys. Acta 1780 (2008) 819–825.
[80] D. Ribeiro, M. Freitas, S.M. Tome, et al., Inhibition of LOX by flavonoids: a structure-activity relationship study, Eur. J. Med. Chem. 72 (2014) 137–145.
[81] S. Carradori, M.C. Gidaro, A. Petzer, et al., Inhibition of human monoamine oxidase: biological and molecular modeling studies on selected natural flavonoids, J. Agric. Food Chem. 64 (2016) 9004–9011.
[82] S. Rizzo, M. Bartolini, L. Ceccarini, et al., Targeting Alzheimer's disease: novel indanone hybrids bearing a pharmacophoric fragment of AP2238, Bioorg. Med. Chem. 18 (2010) 1749–1760.
[83] M. Estrada-Valencia, C. Herrera-Arozamena, C. Perez, D. Vina, J.A. Morales-Garcia, A. Perez-Castillo, E. Ramos, A.O. Romero, E. Laurini, S. Pricl, M.I. Rodriguez-Franco, New flavonoid – N,N-dibenzyl(Nmethyl) amine hybrids: multi-target-directed agents for Alzheimeŕs disease endowed with neurogenic properties, J. Enzyme Inhib. Med. Chem. 34 (2019) 712–727.
[84] S. Marumoto, M. Miyazawa, Structure–activity relationships for naturally occurring coumarins as β-secretase inhibitor, Bioorg. Med. Chem. 20 (2012) 784–788.
[85] S.K. Mamidyala, M.G. Finn, In situ click chemistry: probing the binding landscapes of biological molecules, Chem. Soc. Rev. 39 (2010) 1252–1261.
[86] A. Asadipour, M. Alipour, M. Jafari, M. Khoobi, S. Emami, H. Nadri, A. Sakhteman, A. Moradi, V. Sheibani, F.H. Moghadam, A. Shafiee, A. Foroumadi, Novel coumarin-3-carboxamides bearing N-benzylpiperidine moiety as potent acetylcholinesterase inhibitors, Eur. J. Med. Chem. 70 (2013) 623–670.
[87] W.G. Lewis, L.G. Green, F. Grynszpan, Z. Radic, P.R. Carlier, P. Taylor, M.G. Finn, K.B. Sharpless, Click chemistry in situ: acetylcholinesterase as a reaction vessel for the selective assembly of a femtomolar inhibitor from an array of building blocks, Angew. Chem. Int. Ed. 41 (2002) 1053–1057.
[88] A. Iraji, O. Firuzi, M. Khoshneviszadeh, M. Tavakkoli, M. Mahdavi, H. Nadri, N. Edraki, R. Miri, Multifunctional iminochromene-2*H*-carboxamide derivatives containing different aminomethylene triazole with BACE1 inhibitory, neuroprotective and metal chelating properties targeting Alzheimer's disease, Eur. J. Med. Chem. 141 (2017) 690–702.
[89] A. Rastegari, H. Nadri, M. Mahdavi, A. Moradi, S.S. Mirfazli, N. Edraki, F.H. Moghadam, B. Larijani, T. Akbarzadeh, M.A. Saeedi, Design, synthesis and anti-Alzheimer's activity of novel 1,2,3-triazolechromenone carboxamide derivatives, Bioorg. Chem. 83 (2019) 391–401.
[90] I.E. Orhan, H.O. Gulcan, Coumarins: auspicious cholinesterase and monoamine oxidase inhibitors, Curr. Top. Med. Chem. 15 (2015) 1673–1682.
[91] D. Secci, S. Carradori, A. Bolasco, et al., Synthesis and selective human monoamine oxidase inhibition of 3-carbonyl, 3-acyl, and 3-carboxyhydrazido coumarin derivatives, Eur. J. Med. Chem. 46 (2011) 4846–4852.
[92] Z.M. Wang, X.M. Li, G.M. Xue, et al., Synthesis and evaluation of 6-substituted 3-arylcoumarin derivatives as multifunctional acetylcholinesterase/monoamine oxidase B dual inhibitors for the treatment of Alzheimer's disease, RSC Adv. 5 (2015) 104122–104137.
[93] J. Yang, P. Zhang, Y. Hu, T. Liu, J. Sun, X. Wang, Synthesis and biological evaluation of 3-arylcoumarins as potential anti-Alzheimer's disease agents, J. Enzyme Inhib. Med.l Chem. 34 (2019) 651–656.
[94] J. Yuan, S. Venkatraman, Y. Zheng, B.M. McKeever, L.W. Dillard, S.B. Singh, Structure-based design of beta-site APP cleaving enzyme 1 (BACE1) inhibitors for the treatment of Alzheimer's disease, J. Med. Chem. 56 (2013) 4156–4180.
[95] A. Iraji, O. Firuzi, M. Khoshneviszadeh, H. Nadri, N. Edraki, R. Miri, Synthesis and structure-activity relationship study of multi-target triazine derivatives as innovative candidates for treatment of Alzheimer's disease, Bioorg. Chem. 77 (2018) 223–235.
[96] M. Yazdania, N. Edrakic, R. Badri, M. Khoshneviszadeh, A. Iraji, O. Firuzi, Multi-target inhibitors against Alzheimer disease derived from 3-hydrazinyl 1,2,4-triazine scaffold containing pendant phenoxy methyl-1,2,3-triazole: Design, synthesis and biological evaluation, Bioorg. Chem. 84 (2019) 363–371.
[97] S.S. Bharate, S. Mignani, R.A. Vishwakarma, Why are the majority of active compounds in the CNS domain natural products? A critical analysis, J Med. Chem. 61 (2018) 10345–10374.
[98] S.B. Bharate, S. Manda, P. Joshi, B. Singh, R.A. Vishwakarma, Total synthesis and anti-cholinesterase activity of marine-derived bisindole alkaloid fascaplysin, MedChemComm 3 (2012) 1098–1103.
[99] Y.P. Ng, T.C.T. Or, N.Y. Ip, Plant alkaloids as drug leads for Alzheimer's disease, Neurochem. Int. 89 (2015) 260–270.
[100] W. Fang, D. Sun, S. Yang, N. Guo, β-Secretase (BACE1) inhibitors from natural products, in: P.B. Andrade, P. Valentão, D.M. Pereira (Eds.), Natural Products Targeting Clinically Relevant Enzymes, Wiley-VCH Verlag GmbH & Co. KGaA, Weinheim, Germany, 2017, pp. 93–134.
[101] D. Szwajgier, Anticholinesterase activity of selected phenolic acids and flavonoids – interaction testing in model solutions, Ann. Agric. Environ. Med. 22 (2015) 690–694.
[102] V.K. Nuthakki, A. Sharma, A. Kumar, S.B. Bharate, Identification of embelin, a 3-undecyl-1,4-benzoquinone from Embelia ribes as a multitargeted anti-Alzheimer agent, Drug Dev. Res. (2019) 1–11.
[103] I. Carreras, A.C. McKee, J.K. Choi, et al., R-flurbiprofen improves tau, but not Aβ pathology in a triple transgenic model of Alzheimer's disease, Brain Res. 1541 (2013) 115–127.
[104] Z.C. Cao, J. Yang, R. Xu, et al., Design, synthesis and evaluation of 4′-OH-flurbiprofenchalcone hybrids as potential multifunctional agents for Alzheimer's disease treatment, Bioorg. Med. Chem. 26 (2018) 1102–1115.
[105] D.H. Park, S.K. Venkatesan, V. Kim, Antioxidant properties of Mannich bases, Bioorg. Med. Chem. Lett. 22 (2012) 6362–6367.
[106] G. Roman, Mannich bases in medicinal chemistry and drug design, Eur. J. Med. Chem. 89 (2015) 743–816.
[107] H. Liu, X. Qiang, Q. Song, W. Li, Y. He, C. Ye, Z. Tan, Y. Deng, Discovery of 4′-OH-flurbiprofen Mannich base derivatives as potential Alzheimer′s disease treatment with multiple inhibitory activities, Bioorg. Med. Chem. 27 (2019) 991–1001.
[108] H.L. Zheng, M. Fridkin, M. Youdim, From single target to multi-target/network therapeutics in Alzheimer's therapy, Pharmaceuticals 7 (2014) 113–135.
[109] F. Prati, E. Uliassi, M.L. Bolognesi, Two diseases, one approach: multi-target drug discovery in Alzheimer's and neglected tropical diseases, Med. Chem. Comm. 5 (2014) 853.
[110] S.S. Xie, J.S. Lan, X.B. Wang, N. Jiang, G. Dong, Z.R. Li, K.D. Wang, P.P. Guo, L.Y. Kong, Multifunctional tacrine-trolox hybrids for the treatment of Alzheimer's disease with cholinergic, antioxidant, neuroprotective and hepatoprotective properties, Eur. J. Med. Chem. 93 (2015) 42–50.
[111] J.W. Choi, B.K. Jang, N.C. Cho, et al., Synthesis of a series of unsaturated ketone derivatives as selective and reversible monoamine oxidase inhibitors, Bioorg. Med. Chem. 23 (2015) 6486–6496.
[112] T. Fuchigami, Y. Yamashita, M. Haratake, et al., Synthesis and evaluation of ethyleneoxylated and allyloxylated chalcone derivatives for imaging of amyloid β plaques by SPECT, Bioorg. Med. Chem. 22 (2014) 2622–12268.
[113] X. Zhang, Q. Song, Z. Cao, Y. Li, C. Tian, Z. Yang, H. Zhang, Y. Deng, Design, synthesis and evaluation of chalcone Mannich base derivatives as multifunctional agents for the potential treatment of Alzheimer's disease, Bioorg. Chem. 87 (2019) 395–408.
[114] P. Anand, B. Singh, A review on cholinesterase inhibitors for Alzheimer's disease, Arch. Pharm. Res. 36 (2013) 375–399.
[115] S.-Y. Li, X.-B. Wang, S.-S. Xie, N. Jiang, K.D.G. Wang, H.-Q. Yao, H.-B. Sun, L.-Y. Kong, Multifunctional tacrine–flavonoid hybrids with cholinergic, β-amyloid-reducing, and metal chelating properties for the treatment of Alzheimer's disease, Eur. J. Med. Chem. 69 (2013) 632–646.
[116] M.A. Ceschi, J.S. da Costa, J.P.B. Lopes, V.S. Câmara, L.F. Campo, A.C.D.A. Borges, C.A.S. Gonçalves, D.F. de Souza, E.L. Konrath, A.L.M. Karl, I.A. Guedes, L.E. Dardenne, Novel series of tacrine-tianeptine hybrids: Synthesis, cholinesterase inhibitory activity, S100B secretion and a molecular modeling approach, Eur. J. Med. Chem. 121 (2016) 758–772.
[117] K. Czarnecka, N. Chufarova, K. Halczuk, K. Maciejewska, M. Girek, R. Skibinski, J. Jonczyk, M. Bajda, J. Kabzinski, I. Majsterek, P. Szymanski, Tetrahydroacridine derivatives with dichloronicotinic acid moiety as attractive, multipotent agents for Alzheimer's disease treatment, Eur. J. Med. Chem. 145 (2018) 760–769.
[118] M.A. Rogawski, G.L. Wenk, The neuropharmacological basis for the use of memantine in the treatment of Alzheimer's disease, CNS Drug Reviews 9 (2006) 275–308.
[119] M. Horak, K. Holubova, E. Nepovimova, et al., The pharmacology of tacrine at *N*-methyl-d-aspartate receptors, Prog. Neuropsychopharmacol. Biol. Psych. 75 (2017) 54–62.
[120] S. Qian, L. He, M. Mak, et al., Synthesis, biological activity, and biopharmaceutical characterization of tacrine dimers as acetylcholinesterase inhibitors, Int. J. Pharm. 477 (2014) 442–453.
[121] K. Czarnecka, M. Girek, K. Maciejewska, R. Skibinski, J. Jonczyk, M. Bajda, J. Kabzinski, P. Solowiej, I. Majsterek, P. Szymanski, New cyclopentaquinoline hybrids with multifunctional capacities for the treatment of Alzheimer's disease, J. Enzyme Inhib. Med. Chem. 33 (2018) 158–170.
[122] H.-M. Zhang, Y. Zhang, Melatonin: a well-documented antioxidant with conditional pro-oxidant actions, J. Pineal. Res. 57 (2014) 131–146.
[123] L.C. Manchester, A. Coto-Montes, J.A. Boga, et al., Melatonin: an ancient molecule that makes oxygen metabolically tolerable, J. Pineal. Res. 59 (2015) 403–419.
[124] J.G. Masilamoni, E.P. Jesudason, S. Dhandayuthapani, et al., The neuroprotective role of melatonin against amyloid b peptide injected mice, Free Radic. Res. 42 (2008) 661–673.
[125] L.J. Legoabe, A. Petzer, J.P. Petzer, Selected chromone derivatives as inhibitors of monoamine oxidase, Bioorg. Med. Chem. Lett. 22 (2012) 5480–5484.
[126] I. Pachon-Angona, B. Refouvelet, R. Andrys, H. Martin, V. Luzet, I. Iriepa, I. Moraleda, D. Diez-Iriepa, M. Oset-Gasque, J. Marco-Contelles, K. Musilek, L. Ismaili, Donepezil + chromone + melatonin hybrids as promising agents for Alzheimer's disease therapy, J. Enzyme Inhib. Med. Chem. 34 (2019) 479–489.
[127] L. Ismaili, B. Refouvelet, M. Benchekroun, et al., Multitarget compounds bearing tacrine- and donepezil-like structural and functional motifs for the potential treatment of Alzheimer's disease, Prog. Neurobiol. 151 (2017) 4–34.
[128] R. Leon, A.G. Garcia, J. Marco-Contelles, Recent advances in the multitarget-directed ligands approach for the treatment of Alzheimer's disease, Med. Res. Rev. 33 (2013) 139–189.
[129] S. Emami, S.J. Hosseinimehr, S.M. Taghdisi, S. Akhlaghpoor, Kojic acid and its manganese and zinc complexes as potential radioprotective agents, Bioorg. Med. Chem. Lett. 17 (2007) 45–48.
[130] Y. Dgachi, H. Martin, R. Malek, D. Jun, J. Janockova, V. Sepsova, O. Soukup, I. Iriepa, I. Moraleda, E. Maalej, M.C. Carreiras, B. Refouvelet, F. Chabchoub, J. Marco-Contelles, L. Ismaili, Synthesis and biological assessment of KojoTacrines as new agents for Alzheimer's disease therapy, J. Enzyme Inhib. Med. Chem. 34 (2019) 163–170.
[131] W. Qu, M.P. Kung, C. Hou, S. Oya, H.F. Kung, Quick assembly of 1,4–diphenyltriazoles as probes targeting beta-amyloid aggregates in Alzheimer's disease, J. Med. Chem. 50 (2007) 3380–3387.
[132] S. Das, S.D. Smid, Identification of dibenzylimidazolidine and triazole acetamide derivatives through virtual screening targeting amyloid beta aggregation and neurotoxicity in PC12 cells, Eur. J. Med. Chem. 130 (2017) 354–364.
[133] M.R. Jones, E. Mathieu, C. Dyrager, S. Faissner, Z. Vaillancourt, K.J. Korshavn,

M.H. Lim, A. Ramamoorthy, V.W. Yong, S. Tsutsui, P.K. Stys, T. Storr, Multi–target–directed phenol–triazole ligands as therapeutic agents for Alzheimer's disease, Chem. Sci. 8 (2017) 5636–5643.
[134] J. Jiaranaikulwanitch, P. Govitrapong, V.V. Fokin, O. Vajragupta, From BACE1 inhibitor to multifunctionality of tryptoline and tryptamine triazole derivatives for Alzheimer's disease, Molecules 17 (2012) 8312–8333.
[135] A. Kaura, S.I. Mann, A. Kaur, N. Priyadarshi, B. Goyal, N.K. Singhal, D. Goyal, Multi-target-directed triazole derivatives as promising agents for the treatment of Alzheimer's disease, Bioorg. Chem. 87 (2019) 572–584.
[136] E. Mezeiova, K. Spilovska, E. Nepovimova, L. Gorecki, O. Soukup, R. Dolezal, D. Malinak, J. Janockova, D. Jun, K. Kuca, Profiling donepezil template into multipotent hybrids with antioxidant properties, J. Enzyme Inhib. Med. Chem. 33 (2018) 583–606.
[137] G. Kryger, I. Silman, J.L. Sussman, Structure of acetylcholinesterase complexed with E2020 (Aricept®): implications for the design of new anti-Alzheimer drugs, Structure 7 (1999) 297–307.
[138] P. Costanzo, L. Cariati, D. Desiderio, R. Sgammato, A. Lamberti, R. Arcone, R. Salerno, M. Nardi, M. Masullo, M. Oliverio, Design, synthesis, and evaluation of donepezil-like compounds as AChE and BACE-1 inhibitors, ACS Med. Chem. Lett. 7 (2016) 470–475.
[139] P. Sharma, A. Tripathi, P.N. Tripathi, S.K. Prajapati, A. Seth, M.K. Tripathi, P. Srivastava, V. Tiwari, S. Krishnamurthy, S.K. Shrivastava, Design and development of multitargetdirected *N*-Benzylpiperidine analogs as potential candidates for the treatment of Alzheimer's disease, Eur. J. Med. Chem. 167 (2019) 510–524.
[140] S. Ghanei-Nasab, M. Khoobi, F. Hadizadeh, A. Marjani, A. Moradi, H. Nadri, S. Emami, A. Foroumadi, A. Shafiee, Synthesis and anticholinesterase activity of coumarin-3-carboxamides bearing tryptamine moiety, Eur. J. Med. Chem. 121 (2016) 40–46.
[141] F. Baharloo, M.H. Moslemin, H. Nadri, A. Asadipour, M. Mahdavi, S. Emami, L. Firoozpour, R. Mohebat, A. Shafiee, A. Foroumadi, Benzofuran-derived benzylpyridinium bromides as potent acetylcholinesterase inhibitors, Eur. J. Med. Chem. 93 (2015) 196–201.
[142] H. Akrami, B.F. Mirjalili, M. Khoobi, H. Nadri, A. Moradi, A. Sakhteman, S. Emami, A. Foroumadi, A. Shafiee, Indolinone-based acetylcholinesterase inhibitors: synthesis, biological activity and molecular modeling, Eur. J. Med. Chem. 84 (2014) 375–381.
[143] I. Diner, J. Dooyema, M. Gearing, L.C. Walker, N.T. Seyfried, Generation of clickable Pittsburgh compound B for the detection and capture of β-amyloid in Alzheimer's disease brain, Bioconjug. Chem. 28 (2017) 2627–2637.
[144] L. Huang, T. Su, W. Shan, Z. Luo, Y. Sun, F. He, X. Li, Inhibition of cholinesterase activity and amyloid aggregation by berberine-phenyl-benzoheterocyclic and tacrine-phenyl-benzoheterocyclic hybrids, Bioorg. Med. Chem. 20 (2012) 3038–3048.
[145] N. Salehi, B.B.F. Mirjalili, H. Nadri, Z. Abdolahi, H. Forootanfar, A. Samzadeh-Kermani, T.T. Kucukkilinc, B. Ayazgok, S. Emami, I. Haririan, M. Sharifzadeh, A. Foroumadi, M. Khoobi, Synthesis and biological evaluation of new N-benzylpyridinium-based benzoheterocycles as potential anti-Alzheimer's agents, Bioorg. Chem. 83 (2019) 559–568.
[146] L. Jalili-Baleh, E. Babaei, S. Abdpour, S. Nasir Abbas Bukhari, A. Foroumadi, A. Ramazani, M. Sharifzadeh, M. Abdollahi, M. Khoobi, A review on flavonoidbased scaffolds as multi-target-directed ligands (MTDLs) for Alzheimer's disease, Eur. J. Med. Chem. 152 (2018) 570–589.
[147] A. Kaur, V. Sharma, A. Budhiraja, H. Kaur, V. Gupta, R. Kant, M.P.S. Ishar, Synthesis and evaluation of substituted 4,4a-dihydro-3H,10H-pyrano[4,3-*b*][1]benopyran-10-one as antimicrobial agent, ISRN Med. Chem. (2013) 11 ID 619535.
[148] J. Nagai, H. Shi, Y. Kubota, K. Bandow, N. Okudaira, Y. Uesawa, H. Sakagami, M. Tomomura, A. Tomomura, K. Takao, Y. Sugita, Quantitative structure – cytotoxicity relationship of pyrano[4,3-*b*]chromones, Anticanc. Res. 38 (2018) 4449–4457.
[149] K. Takao, Y. Kubota, H. Kamauchi, Y. Sugita, Synthesis and biological evaluation of pyrano[4,3-*b*][1]benzopyranone derivatives as monoamine oxidase and cholinesterase inhibitors, Bioorg. Chem. 83 (2019) 432–437.
[150] B. Kaya-Cavusoglu, B.N. Saglik, Y. Ozkay, B. Inci, Z.A. Kaplancikli, Bioorg. Chem. 76 (2018) 177–187.
[151] K. Karrouchi, S. Radi, Y. Ramli, J. Taoufik, Y.N. Mabkhot, F.A. Al-Aizari, M. Ansar, Molecules 23 (2018) 134.
[152] A. Rahman, M. Choudhary, Multifunctional Enzyme Inhibition for Neuroprotection-A Focus on MAO, NOS and AChE Inhibitors, Drug Design and Discovery in Alzheimer's Disease, Bentham Science Publishers, 2015, pp. 291–365.
[153] F. Tok, B. Kocyigit-Kaymakcioglu, B.N. Saglik, S. Levent, Y. Ozkay, Z.A. Kaplancikl, Synthesis and biological evaluation of new pyrazolone Schiff bases as monoamine oxidase and cholinesterase inhibitors, Bioorg. Chem. 84 (2019) 41–50.
[154] J. Lalut, D. Karila, P. Dallemagne, C. Rochais, Modulating 5-HT4 and 5-HT6 receptors in Alzheimer's disease treatment, Future Med. Chem. 9 (2017) 781–795.
[155] M. Cochet, R. Donneger, E. Cassier, F. Gaven, S.F. Lichtenthaler, P. Marin, J. Bockaert, A. Dumuis, S. Claeysen, 5-HT4 receptors constitutively promote the non-amyloidogenic pathway of APP cleavage and interact with ADAM10, ACS Chem. Neurosci. 4 (2013) 130–140.
[156] P. Giannoni, F. Gaven, D. de Bundel, K. Baranger, E. Marchetti-Gauthier, F.S. Roman, E. Valjent, P. Marin, J. Bockaert, S. Rivera, S. Claeysen, Early administration of RS 67333, a specific 5-HT4 receptor agonist, prevents amyloidogenesis and behavioral deficits in the 5XFAD mouse model of Alzheimer's disease, Front. Ag. Neurosci. 5 (2013) 96.
[157] T. Maurice, N. Goguadze, Role of s1 receptors in learning and memory and Alzheimer's disease-type dementia, Adv. Exp. Med. Biol. 964 (2017) 213–233.
[158] R.R. Luedtke, E. Perez, S.-H. Yang, R. Liu, S. Vangveravong, Z. Tu, R.H. Mach, J.W. Simpkins, Neuroprotective effects of high affinity sigma 1 receptor selective compounds, Brain Res. 1441 (2012) 17–26.
[159] J. Lalut, G. Santoni, D. Karila, C. Lecoutey, A. Davis, F. Nachon, I. Silman, J. Sussman, M. Weik, T. Maurice, P. Dallemagne, C. Rochais, Novel multitarget-directed ligands targeting acetylcholinesterase and s1 receptors as lead compounds for treatment of Alzheimer's disease: synthesis, evaluation, and structural characterization of their complexes with acetylcholinesterase, Eur. J. Med. Chem. 162 (2019) 234–248.
[160] Q. Songa, Y. Li, Z. Cao, X. Qiang, Z. Tan, Y. Deng, Novel salicylamide derivatives as potent multifunctional agents for the treatment of Alzheimer's disease: design, synthesis and biological evaluation, Bioorg. Chem. 84 (2019) 137–149.
[161] T.H. Al-Tel, M.H. Semreen, R.A. Al-Qawasmeh, M.F. Schmidt, R. El-Awadi, M. Ardah, R. Zaarour, S.N. Rao, O. El-Agnaf, Design, synthesis, and qualitative structure-activity evaluations of novel beta-secretase inhibitors as potential Alzheimer's drug leads, J. Med. Chem. 54 (2011) 8373–8385.
[162] H. Sun, X. He, C. Liu, L. Li, R. Zhou, T. Jin, S. Yue, D. Feng, J. Gong, J. Sun, J. Ji, L. Xiang, Effect of oleracein E, a neuroprotective tetrahydroisoquinoline, on rotenone-induced Parkinson's disease cell and animal models, ACS Chem. Neurosci. 8 (2017) 155–164.
[163] Y. Fang, H. Zhou, Q. Gu, J. Xu, Synthesis and evaluation of tetrahydroisoquinoline-benzimidazole hybrids as multifunctional agents for the treatment of Alzheimer's disease, Eur. J. Med. Chem. 167 (2019) 133–145.
[164] D. Panek, A. Wieckowska, T. Wichur, M. Bajda, J. Godyn, J. Jonczyk, K. Mika, J. Janockova, O. Soukup, D. Knez, J. Korabecny, S. Gobec, B. Malawska, Design, synthesis and biological evaluation of new phthalimide and saccharin derivatives with alicyclic amines targeting cholinesterases, beta-secretase and amyloid beta aggregation, Eur. J. Med. Chem. 125 (2017) 676–695.
[165] L. Cheewakriengkrai, S. Gauthier, A 10-year perspective on donepezil, Exp. Opin. Pharmacother. 14 (2013) 331–338.
[166] B. Bakthavachalam, J.T. Wu, Production of natural butylated hydroxytoluene as anantioxidant by freshwater phytoplankton1, J. Phycol. 44 (2008) 1447–1454.
[167] P. Cai, S. Fang, H. Yang, X. Yang, Q. Liu, L. Kong, X. Wang, Donepezil-butylated hydroxytoluene (BHT) hybrids as Anti-Alzheimer's disease agents with cholinergic, antioxidant, and neuroprotective properties, Eur. J. Med. Chem. 157 (2018) 161–176.
[168] L.G. de Souza, M.N. Renna, J.D. Figueroa-Villar, Coumarins as cholinesterase inhibitors: a review, Chem. Biol. Interact. 254 (2016) 11–23.
[169] Z. Najafi, M. Mahdavi, M. Saeedi, R. Sabourian, M. Khanavi, M. Safavi, M. Barazandeh Tehrani, A. Shafiee, A. Foroumadi, T. Akbarzadeh, Akbarzadeh, 1,2,3-Triazoleisoxazole based acetylcholinesterase inhibitors: synthesis, biological evaluation and docking study, Lett. Drug Des. Discov. 14 (2017) 58–65.
[170] Z. Najafia, M. Mahdavi, M. Saeedid, E. Karimpour-Razkenarie, N. Edraki, M. Sharifzadeh, M. Khanavi, T. Akbarzadeh, Novel tacrine-coumarin hybrids linked to 1,2,3-triazole as anti-Alzheimer's compounds: in vitro and in vivo biological evaluation and docking study, Bioorg. Chem. 83 (2019) 303–316.
[171] L. Piazzi, A. Rampa, A. Bisi, S. Gobbi, F. Belluti, A. Cavalli, M. Bartolini, V. Andrisano, P. Valenti, M. Recanatini, 3-(4-{[benzyl (methyl) amino] methyl} phenyl)-6, 7-dimethoxy-2h-2-chromenone(ap2238) inhibits both acetylcholinesterase and acetylcholinesterase-induced β-amyloid aggregation: a dual function lead for Alzheimer's disease therapy, J. Med. Chem. 46 (2003) 2279–2282.
[172] A. Hiremathad, K. Chand, L. Tolayan, R.S. Rajeshwari, A.R. Keri, S.M. Esteves, S. Cardoso, M.A. Chaves, Santos, Hydroxypyridinone-benzofuran hybrids with potential protective roles for Alzheimer's disease therapy, J. Inorg. Biochem. 179 (2018) 82–96.
[173] B. Pouramiri, S. Moghimi, M. Mahdavi, H. Nadri, A. Moradi, E. Tavakolinejad-Kermani, L. Firoozpour, A. Asadipour, A. Foroumadi, Synthesis and anticholinesterase activity of new substituted benzo[d]oxazole-based derivatives, Chem. Biol. Drug. Des. 89 (2017) 783–789.
[174] F. Abedinifar, S. Morteza, F. Farnia, M. Mahdavi, H. Nadri, A. Moradi, J.B. Ghasemi, T.T. Kucukkilmc, L. Firoozpour, A. Foroumadi, Synthesis and cholinesterase inhibitory activity of new 2-benzofuran carboxamide-benzylpyridinum salts, Bioorg. Chem. 80 (2018) 180–188.
[175] S. Jalhan, S. Singh, R. Saini, N.S. Sethi, U.K. Jain, Various biological activities of coumarin and oxadiazole derivatives, Asian J. Pharm. Clin. Res. 10 (2017) 38–43.
[176] M. Saeedi, M. Safavi, E. Karimpour-Razkenari, M. Mahdavi, N. Edraki, F.H. Moghadam, M. Khanavi, T. Akbarzadeh, Synthesis of novel chromenones linked to 1, 2, 3-triazole ring system: investigation of biological activities against Alzheimer's disease, Bioorg. Chem. 70 (2017) 86–93.
[177] F. Vafadarnejad, M. Saeedi, M. Mahdavi, A. Rafinejad, E. Karimpour-Razkenari, B. Sameem, M. Khanavi, T. Akbarzadeh, Novel indole-isoxazole hybrids: synthesis and in vitro anti-cholinesterase activity, Lett. Drug Des. Dis. 14 (2017) 712–717.
[178] F. Vafadarnejad, M. Mahdavi, E. Karimpour-Razkenari, N. Edraki, B. Sameem, M. Khanavi, M. Saeedi, T. Akbarzadeh, Design and synthesis of novel coumarin-pyridinium hybrids: in vitro cholinesterase inhibitory activity, Bioorg. Chem. 77 (2018) 311–319.
[179] P.D. Andrade, S.P. Mantoani, G.P.S. Nunes, C.R. Magadan, C. Perez, D.J. Xavier, E.T.S. Hojo, N.E. Campillo, A. Martínez, I. Carvalho, Highly potent and selective aryl-1,2,3-triazolyl benzylpiperidine inhibitors toward butyrylcholinesterase in alzheimer's disease, Bioorg. Med. Chem. 27 (2018) 931–943.
[180] Y.K. Yoon, M.A. Ali, A.C. Wei, et al., Synthesis, characterization, and molecular docking analysis of novel benzimidazole derivatives as cholinesterase inhibitors, Bioorg. Chem. 49 (2013) 33–39.
[181] K. Shalini, P.K. Sharma, N. Kumar, Imidazole and its biological activities: a review,

Der. Chem. Sin. 1 (2010) 36–47.
[182] F. Rahim, M.T. Javed, H. Ullah, et al., Synthesis, molecular docking, acetylcholinesterase and butyrylcholinesterase inhibitory potential of thiazole analogs as new inhibitors for Alzheimer disease, Bioorg Chem. 62 (2015) 106–116.
[183] A.S. Gurjar, M.N. Darekar, K.Y. Yeong, L. Ooi, In silico studies, synthesis and pharmacological evaluation to explore multi-targeted approach for imidazole analogues as potential cholinesterase inhibitors with neuroprotective role for Alzheimer's disease, Bioorg. Med. Chem. 26 (2018) 1511–1522.
[184] S.K. Sinha, S.K. Shrivastava, Synthesis, evaluation and molecular dynamics study of some new 4-aminopyridine semicarbazones as an antiamnesic and cognition enhancing agents, Bioorg. Med. Chem. 21 (2013) 5451–5460.
[185] S.K. Sinha, S.K. Shrivastava, Design, synthesis and evaluation of some new 4-aminopyridine derivatives in learning and memory, Bioorg. Med. Chem. Lett. 23 (2013) 2984–2989.
[186] J. Trujillo-Ferrara, L.M. Cano, M. Espinoza-Fonseca, Synthesis, anticholinesterase activity and structure–activity relationships of *m*-Aminobenzoic acid derivatives, Bioorg. Med. Chem. Lett. 13 (2003) 1825–1827.
[187] J. Correa-Basurto, I.V. Alcántara, L.M. Espinoza-Fonseca, J.G. Trujillo-Ferrara, *p*-Aminobenzoic acid derivatives as acetylcholinesterase inhibitors, Eur. J. Med. Chem. 40 (2005) 732–735.
[188] S.K. Shrivastava, S.K. Sinha, P. Srivastava, P.N. Tripathi, P. Sharma, M.K. Tripathi, A. Tripathi, P.K. Choubey, D.K. Waiker, L.M. Aggarwal, M. Dixit, S.C. Kheruka, S. Gambhir, S. Shankar, R.K. Srivastava, Design and development of novel *p*-aminobenzoic acid derivatives as potential cholinesterase inhibitors for the treatment of Alzheimer's disease, Bioorg. Chem. 82 (2019) 211–223.
[189] O. Temiz-Arpaci, M. Arisoy, D. Sac, F. Doganc, M. Tasci, S. Senol Fatma, E. Orhan Ilkay, Biological evaluation and docking studies of some benzoxazole derivatives as inhibitors of acetylcholinesterase and butyrylcholinesterase, Zeitschrift fur Naturforschung C (2016) 409.
[190] K. Hirbod, L. Jalili-baleh, H. Nadri, S.E.S. Ebrahimi, A. Moradi, B. Pakseresht, A. Foroumadi, A. Shafiee, M. Khoobi, Coumarin derivatives bearing benzoheterocycle moiety: synthesis, cholinesterase inhibitory, and docking simulation study, Iran. J. Basic Med. Sci. 20 (2017) 631–638.
[191] M.H. Baig, K. Ahmad, G. Rabbani, M. Danishuddin, I. Choi, Computer aided drug design and its application to the development of potential drugs for neurodegenerative disorders, Curr. Neuropharmacol. 16 (2018) 740–748.
[192] P. Srivastava, P.N. Tripathi, P. Sharma, S.N. Rai, S.P. Singh, R.K. Srivastava, S. Shankar, S.K. Shrivastava, Design and development of some phenyl benzoxazole derivatives as a potent acetylcholinesterase inhibitor with antioxidant property to enhance learning and memory, Eur. J. Med. Chem. 163 (2019) 116–135.
[193] B.Z. Kurt, I. Gazioglu, F. Sonmez, M. Kucukislamoglu, Synthesis, antioxidant and anticholinesterase activities of novel coumarylthiazole derivatives, Bioorg. Chem. 59 (2015) 80–90.
[194] V. Pejchal, S.S. Pankova, M. Pejchalova, K. Kralovec, R. Havelek, et al., Synthesis, structural characterization, docking, lipophilicity and cytotoxicity of 1-[(1*R*)-1-(6-fluoro-1,3-benzothiazol-2-yl)ethyl]-3- alkyl carbamates, novel acetylcholinesterase and butyrylcholinesterase pseudo-irreversible inhibitors, Bioorg. Med. Chem. 24 (2016) 1560–1572.
[195] A. Mumtaz, M. Shoaib, S. Zaib, M.S. Shah, H.A. Bhatti, A. Saeed, I. Hussain, J. Iqbal, Synthesis, molecular modelling and biological evaluation of tetra-substituted thiazoles towards cholinesterase enzymes and cytotoxicity studies, Bioorg. Chem. 78 (2018) 141–148.
[196] B. Tasso, M. Catto, O. Nicolotti, F. Novelli, M. Tonelli, I. Giangreco, L. Pisani, A. Sparatore, V. Boido, A. Carotti, Quinolizidinyl derivatives of bi-and tricyclic systems as potent inhibitors of acetyl-and butyrylcholinesterase with potential in Alzheimer's disease, Eur. J. Med. Chem 46 (2011) 2170–2184.
[197] G. Tin, T. Mohamed, N. Gondora, M.A. Beazelya, P.P. Rao, Tricyclic phenothiazine and phenoselenazine derivatives as potential multi-targeting agents to treat Alzheimer's disease, Med. Chem. Commun 6 (2015) 1930–1941.
[198] S. Tahir Tanoli, M. Ramzan, A. Hassan, A. Sadiq, M. Saeed Jan, F.A. Khan, F. Ullah, H. Ahmad, M. Bibi, T. Mahmood, U. Rashid, Design, synthesis and bioevaluation of tricyclic fused ring system as dual binding site acetylcholinesterase inhibitors, Bioorg. Chem. 83 (2019) 336–347.
[199] M. Ozil, H.T. Balaydın, M. Senturk, Synthesis of 5-methyl-2,4-dihydro-3*H*-1,2,4-triazole-3-one's aryl Schiff base derivatives and investigation of carbonic anhydrase and cholinesterase (AChE, BuChE) inhibitory properties, Bioorg. Chem. 86 (2019) 705.
[200] H. Cavdar, M. Senturk, M. Guney, et al., Inhibition of acetylcholinesterase and butyrylcholinesterase with uracil derivatives: kinetic and computational studies, J. Enzyme Inhib. Med. Chem. 34 (2019) 429–437.
[201] Y. Hu, J. Yang, Y. Zhang, K. Liu, T. Liu, J. Sun, X. Wang, Synthesis and biological evaluation of 3–(4-aminophenyl)-coumarin derivatives as potential anti-Alzheimer's disease agents, J. Enzyme Inhib. Med. Chem. 34 (2019) 1083–1092.
[202] H. Irannejad, H. Nadri, N. Naderi, S.N. Rezaeian, N. Zafari, A. Foroumadi, M. Amini, M. Khoobi, Anticonvulsant activity of 1, 2, 4-triazine derivatives with pyridyl sidevchain: synthesis, biological, and computational study, Med. Chem. Res. 24 (2015) 2505–2513.
[203] Z. Jin, L. Yang, H. Xu, E. Huang, D.C. Wan, S. Li, H. Lin, C. Hu, Synthesis and biological activity of 3, 6-diaryl-7*H*-thiazolo [3, 2-*b*][1, 2, 4] triazin-7-one derivatives as novel acetylcholinesterase inhibitors, Sci. China Chem. 53 (2010) 2297–2303.
[204] A. Sinha, R.S. Tamboli, B. Seth, A.M. Kanhed, S.K. Tiwari, S. Agarwal, S. Nair, R. Giridhar, R.K. Chaturvedi, M.R. Yadav, Neuroprotective role of novel triazine derivatives by activating Wnt/β catenin signaling pathway in rodent models of Alzheimer's disease, Mol. Neurobiol. 52 (2015) 638–652.
[205] H. Irannejad, M. Amini, F. Khodagholi, N. Ansari, S.K. Tusi, M. Sharifzadeh, A. Shafiee, Synthesis and in vitro evaluation of novel 1, 2, 4-triazine derivatives as neuroprotective agents, Bioorg. Med. Chem. 18 (2010) 4224–4230.
[206] A. Wieckowska, T. Wichur, J. Godyn, A. Bucki, M. Marcinkowska, A. Siwek, K. Wieckowski, P. Zareba, D. Knez, M. Gluch-Lutwin, Novel multitarget-directed ligands aiming at symptoms and causes of alzheimer's disease, ACS Chem. Neurosci. 9 (2018) 1195–1214.
[207] P.N. Tripathia, P. Srivastava, P. Sharmaa, M.K. Tripathia, A. Setha, A. Tripathia, S.N. Raib, S.P. Singh, S.K. Shrivastava, Biphenyl-3-oxo-1,2,4-triazine linked piperazine derivatives as potential cholinesterase inhibitors with anti-oxidant property to improve the learning and memory, Bioorg. Chem. 85 (2019) 82–96.
[208] C.S. Jiang, Y. Fu, L. Zhang, J.X. Gong, Z.Z. Wang, W. Xiao, H.Y. Zhang, Y.W. Guo, Bioorg. Med. Chem. Lett. 25 (2015) 216–220.
[209] J.C. Li, J. Zhang, M.C. Rodrigues, D.J. Ding, L.P. Longo, R.B. Azevedo, L.A. Muehlmann, C.S. Jiang, Bioorg. Med. Chem. Lett. 26 (2016) 3881–3885.
[210] Z. Cheng, K. Zhu, J. Zhang, J. Song, L.A. Muehlmann, C. Jiang, C. Liu, H. Zhang, Molecular-docking-guided design and synthesis of new IAA-tacrine hybrids as multifunctional AChE/BChE inhibitors, Bioorg. Chem. 83 (2019) 277–288.
[211] A. Palasz, D. Ciez, In search of uracil derivatives as bioactive agents. Uracils and fused uracils: synthesis, biological activity and applications, Eur. J. Med. Chem. 97 (2015) 582–611.
[212] S. Durdagi, M. Senturk, M. Guney, et al., Design of novel uracil derivatives as inhibitors of carbonic anhydrase I & II, acetylcholinesterase, butyrylcholinesterase, and glutathione reductase using in silico, synthesis and in vitro studies, FEBS J. 283 (2016) 106.
[213] H. Cavdar, M. Senturk, M. Guney, S. Durdagi, G. Kayik, C.T. Supuran, D. Ekinci, Inhibition of acetylcholinesterase and butyrylcholinesterase with uracil derivatives: kinetic and computational studies, J. Enzyme Inhib. Med. Chem. 34 (2019) 429–437.
[214] C.C. Wang, E. Billett, A. Borchert, H. Kuhn, C. Ufer, Cell Mol. Life Sci. 70 (2013) 599.
[215] F. Caraci, A. Copani, F. Nicoletti, F. Drago, Eur. J. Pharmacol. 626 (2010) 64.
[216] P.O. Patil, S.B. Bari, S.D. Firke, P.K. Deshmukh, S.T. Donda, D.A. Patil, Bioorg. Med. Chem. 21 (2013) 2434.
[217] Z.Y. Cai, Mol. Med. Rep. 9 (2014) 1533.
[218] A. Fonseca, J. Reis, T. Silva, M.J. Matos, D. Bagetta, F. Ortuso, S. Alcaro, E. Uriarte, F. Borges, Coumarin versus chromone monoamine oxidase B inhibitors: quo vadis? J. Med. Chem. 60 (2017) 7206–7212.
[219] A. Gaspar, T. Silva, M. Yáñez, D. Vina, F. Orallo, F. Ortuso, E. Uriarte, S. Alcaro, F. Borges, Chromone, a privileged scaffold for the development of monoamine oxidase inhibitors, J. Med. Chem. 54 (2011) 5165–5173.
[220] E.M. Van der Walt, E.M. Milczek, S.F. Malan, D.E. Edmondson, N. Castagnoli Jr, J.J. Bergh, J.P. Petzer, Inhibition of monoamine oxidase by (*E*)-styrylisatin analogues, Bioorg. Med. Chem. Lett. 19 (2009) 2509–2513.
[221] N. Vlok, S.F. Malan, N. Castagnoli Jr, J.J. Bergh, J.P. Petzer, Inhibition of monoamine oxidase B by analogues of the adenosine A2A receptor antagonist (E)-8-(3-chlorostyryl)caffeine (CSC), Bioorg. Med. Chem. 14 (2006) 3512–3521.
[222] K. Takao, H. Yahagi, Y. Uesawa, Y. Sugita, 3-(*E*)-Styryl-2*H*-chromene derivatives as potent and selective monoamine oxidase B inhibitors, Bioorg. Chem. 77 (2018) 436–442.
[223] J.P. Crandall, N. Barzilai, Exploring the promise of resveratrol: where do we go from here, Diabetes 62 (2013) 1022.
[224] S.S. Kulkarni, C. Cantó, The molecular targets of resveratrol, Biochim. Et Biophys. Acta 2015 (1852) 1114–1123.
[225] Y. Wang, Y. Zhu, L. Gao, H. Yin, Z. Xie, D. Wang, Z. Zhu, X. Han, Formononetin attenuates IL-1b-induced apoptosis and NF-kB activation in INS-1 cells, Molecules 17 (2012) 10052–10064.
[226] T. Yang, L. Fang, C. Nopoolazabal, J. Condori, L. Nopoolazabal, C. Balmaceda, F. Medinabolivar, Enhanced production of resveratrol, piceatannol, arachidin-1 and arachidin-3 in hairy root cultures of peanut *co*-treated with methyl jasmonate and cyclodextrin, J. Agric. Food Chem. 63 (2015) 3942–3950.
[227] S. Nicotra, M.R. Cramarossa, A. Mucci, U.M. Pagnoni, S. Riva, L. Forti, Biotransformation of resveratrol: synthesis of trans-dehydrodimers catalyzed by laccases from Myceliophtora thermophyla and from Trametes pubescens, Tetrahedron 60 (2004) 595–600.
[228] Y.-W. Tang, C.-J. Shi, H.-L. Yang, P. Cai, Q.-H. Liu, X.-L. Yang, L.-Y. Kong, X.-B. Wang, Synthesis and evaluation of isoprenylation-resveratrol dimer derivatives against Alzheimer's disease, Eur. J. Med. Chem. 163 (2019) 307–319.
[229] L. Francesco, C. Carmelida, P. Leonardo, et al., Solid-phase synthesis and insights into structure activity relationships of safinamide analogues as potent and selective inhibitors of type B monoamine oxidase, J. Med. Chem. 50 (2007) 4909–4916.
[230] B. Moussa, A. Youdim, Rasagiline [N-propargyl-1R (+)-Amin-oindan], a selective and potent inhibitor of mitochondrial monoamine oxidase, Brit. J. Pharmacol. 132 (2001) 500–506.
[231] S. Zhoua, G. Chena, G. Huang, Design, synthesis and biological evaluation of lazabemide derivatives as inhibitors of monoamine oxidase, Bioorg. Med. Chem. 26 (2018) 4863–4870.
[232] S. Bahadur, M. Saxena, Syntheses and biological activities of some new 4(3*H*)-quinazolinones, Arch. Pharm. (Weinheim) 316 (1983) 964–968.
[233] N. Gokhan-Kelekci, S. Koyunoglu, S. Yabanoglu, K. Yelekci, O. Ozgen, G. Ucar, K. Erol, E. Kendi, A. Yesilada, New pyrazoline bearing 4(3*H*)-quinazolinone inhibitors of monoamine oxidase: synthesis, biological evaluation, and structural determinants of MAO-A and MAO-B selectivity, Bioorg. Med. Chem. 17 (2009) 675–689.
[234] M. Shrimali, R. Kalsi, K.S. Dixit, J.P. Barthwal, Substituted quinazolones as potent anticonvulsants and enzyme inhibitors, Arzneimittelforschung 41 (1991) 514–519.

[235] A. Lata, R.K. Satsangi, V.K. Srivastava, K. Kishor, Monoamine oxidase inhibitory and CNS activities of some quinazolinones, Arzneimittelforschung 32 (1982) 24–27.
[236] R.S. Misra, A. Chaudhari, A.K. Chaturvedi, S.S. Parmar, B.V. Rama Sastry, Styrlquinazolones as monoamine oxidase inhibitors, Pharmacol. Res. Commun. 9 (5) (1977) 437–446.
[237] V. Rastogi, J. Barthwal, S.S. Parmar, Synthesis of substituted 2-methyl-3 (4′-hydrazinocarbonyl-methylene-oxy-phenyl)-4-quinazolones as monoamine oxidase inhibitors, J. Prakt. Chem. 314 (1972) 187–192.
[238] M.K. Srivastav, M. Shamshuddin, S. Shantakumar, Design, synthesis and characterization of novel 6, 7-dimethoxy-*N* 2-(substituted benzyl)-*N* 2-propylquinazoline-2, 4-diamine derivatives as anxiolytic and antidepressant agents, Am. J. Chem. 3 (2013) 14–22.
[239] M.A. Qhobosheane, L.J. Legoabe, A. Petzer, J.P. Petzer, The monoamine oxidase inhibition properties of C6-mono- and N3/C6-disubstituted derivatives of 4(3*H*)-quinazolinone, Bioorg. Chem. 85 (2019) 60–65.
[240] A. Hammuda, R. Shalaby, S. Rovida, et al., Design and synthesis of novel chalcones as potent selective monoamine oxidase-B inhibitors, Eur. J. Med. Chem. 114 (2016) 162–169.
[241] R. Shalaby, J.P. Petzer, A. Petzer, U.M. Ashraf, E. Atari, F. Alasmari, S. Kumarasamy, Y. Sari, A. Khalil, SAR and molecular mechanism studies of monoamine oxidase inhibition by selected chalcone analogs, J Enzyme Inhib. Med. Chem. 34 (2019) 863–876.
[242] D. Secci, A. Bolasco, S. Carradori, M. D'Ascenzio, R. Nescatelli, M. Yanez, Eur. J. Med. Chem. 58 (2012) 405–417.
[243] S. Gritsch, S. Guccione, R. Hoffmann, A. Cambria, G. Raciti, T. Langer, J. Enzyme Inhib. 16 (2001) 199–215.
[244] M. D'Ascenzio, S. Carradori, D. Secci, L. Mannina, A.P. Sobolev, C. De Monte, R. Cirilli, M. Yanez, S. Alcaro, F. Ortuso, Bioorg. Med. Chem. 22 (2014) 2887–2895.
[245] M. D'Ascenzio, P. Chimenti, M.C. Gidaro, C. De Monte, D. De Vita, A. Granese, L. Scipione, R. Di Santo, G. Costa, S. Alcaro, M. Yáñez, S. Carradori, J. Enzyme Inhib. Med. Chem. 30 (2015) 908–919.
[246] F. Chimenti, D. Secci, A. Bolasco, P. Chimenti, A. Granese, S. Carradori, M. Yanez, F. Orallo, M.L. Sanna, B. Gallinella, R. Cirilli, J. Med. Chem. 53 (2010) 6516–6520.
[247] N.O. Can, D. Osmaniye, S. Levent, B.N. Saglik, B. Korkut, O. Atli, Y. Ozkay, Z.A. Kaplancikli, Eur. J. Med. Chem. 144 (2018) 68–81.
[248] B.N. Saglik, B.K. Cavusoglu, D. Osmaniye, S. Levent, U.A. Cevik, S. Ilgin, Y. Ozkay, Z.A. Kaplancikl, Y. Ozturk, In vitro and in silico evaluation of new thiazole compounds as monoamine oxidase inhibitors, Bioorg. Chem. 85 (2019) 97–108.
[249] D.J. Selkoe, J. Hardy, The amyloid hypothesis of Alzheimer's disease at 25 years, EMBO Mol. Med. 8 (2016) 595–608.
[250] J. Hardy, D.J. Selkoe, The amyloid hypothesis of Alzheimer's disease: progress and problems on the road to therapeutics, Science (Washington, DC, U. S.) 297 (2002) 353–356.
[251] S.H. Barage, K.D. Sonawane, Amyloid cascade hypothesis: pathogenesis and therapeutic strategies in Alzheimer's disease, Neuropeptides 52 (2015) 1–18.
[252] T. Mohamed, A. Shakeri, P.P.N. Rao, Amyloid cascade in Alzheimer's disease: recent advances in medicinal chemistry, Eur. J. Med. Chem. 113 (2016) 258–272.
[253] M.L. Bolognesi, V. Andrisano, M. Bartolini, R. Banzi, C.J. Melchiorre, Med. Chem. 48 (2005) 24.
[254] M. Maqbool, M. Mobashir, N. Hoda, Pivotal role of glycogen synthase kinase-3: a therapeutic target for Alzheimer's disease, Eur. J. Med. Chem. 107 (2016) 63–81.
[255] O.O. Leary, Y. Nolan, Glycogen synthase kinase-3 as a therapeutic target for cognitive dysfunction in neuropsychiatric disorders, CNS Drugs 29 (2015) 1–15.
[256] D.M. Holtzman, M.C. Carrillo, J.A. Hendrix, L.J. Bain, A.M. Catafau, L.M. Gault, M. Goedert, E. Mandelkow, E.-M. Mandelkow, D.S. Miller, S. Ostrowitzki, M. Polydoro, S. Smith, M. Wittmann, M. Hutton, Tau: from research to clinical development, Alzheimers Dement 12 (2016) 1033–1039.
[257] Z.Y. Cai, Y. Zhao, B. Zhao, Roles of glycogen synthase kinase 3 in Alzheimer's disease, Curr. Alzheimer Res. 9 (2012) 864–879.
[258] M. Llorens-Martín, J. Jurado, F. Hernández, J. Ávila, GSK-3*β*, a pivotal kinase in Alzheimer disease, Front. Mol. Neurosci. 7 (2014) 46.
[259] P. Sivaprakasam, X. Han, R.L. Civiello, S. Jacutin-Porte, K. Kish, M. Pokross, H.A. Lewis, N. Ahmed, N. Szapiel, J.A. Newitt, E.T. Baldwin, H. Xiao, C.M. Krause, H. Park, M. Nophsker, J.S. Lippy, C.R. Burton, D.R. Langley, J.E. Macor, G.M. Dubowchik, Discovery of new acylaminopyridines as GSK-3 inhibitors by a structure guided in-depth exploration of chemical space around a pyrrolopyridinone core, Bioorg. Med. Chem. Lett. 25 (2015) 1856–1863.
[260] X.-L. Shi, J.-D. Wu, P. Liu, Z.-P. Liu, Synthesis and evaluation of novel GSK-3*β* inhibitors as multifunctional agents against Alzheimer's disease, Eur. J. Med. Chem. 167 (2019) 211–225.
[261] K.J. Barnham, A.I. Bush, Chem. Soc. Rev. 43 (2014) 6727–6749.
[262] A. Robert, Y. Liu, M. Nguyen, B. Meunier, Acc. Chem. Res. 48 (2015) 1332–1339.
[263] M. Nguyen, C. Bijani, N. Martins, B. Meunier, A. Robert, Chem. Eur. J. 21 (2015) 17085–17090.
[264] M. Nguyen, L. Vendier, J.-L. Stigliani, B. Meunier, A. Robert, Eur. J. Inorg. Chem. 3 (2017) 600–608.
[265] A. Robert, W. Zhang, D. Huang, M. Huang, J. Huang, D. Wang, M. Nguyen, L. Vendier, S. Mazeres, B. Meunier, Y. Liu, L. Xingguo, Preparation of new tetradentate copper chelators as potential anti-Alzheimer agents, ChemMedChem 13 (2018) 684–704.
[266] R. Wang, H. Yan, X.C. Tang, Progress in studies of huperzine A, a natural cholinesterase inhibitor from Chinese herbal medicine, Acta Pharmacol. Sin. 27 (2006) 1–26.
[267] F. Yang, G.P. Lim, A.N. Begum, O.J. Ubeda, M.R. Simmons, S.S. Ambegaokar, P.P. Chen, R. Kayed, C.G. Glabe, S.A. Frautschy, G.M. Cole, Curcumin inhibits formation of amyloid beta oligomers and fibrils, binds plaques, and reduces amyloid in vivo, J. Biol. Chem. 280 (2005) 5892–5901.
[268] Y. Feng, X.P. Wang, S.G. Yang, Y.J. Wang, X. Zhang, X.T. Du, X.X. Sun, M. Zhao, L. Huang, R.T. Liu, Resveratrol inhibits beta-amyloid oligomeric cytotoxicity but does not prevent oligomer formation, Neurotoxicology 30 (2009) 986–995.
[269] A. Mahler, S. Mandel, M. Lorenz, U. Ruegg, E.E. Wanker, M. Boschmann, F. Paul, Epigallocatechin-3-gallate: a useful, effective and safe clinical approach for targeted prevention and individualised treatment of neurological diseases? EPMA J. 4 (2013) 5.
[270] Q. Chen, Z.Q. Xia, Y.E. Hu, Effects of sarsasapogenin on deposition of *β*-amyloid peptide and cholinergic function in rats with *β*-amyloid injection into right nucleus basalis magnocellularis, Zhong Guo Yao Li Xue Tong Bao 1 (2002) 390–393.
[271] H. Pan, P. Van Khang, D. Dong, R. Wang, L. Ma, Synthesis and SAR study of novel sarsasapogenin derivatives as potent neuroprotective agents and NO production inhibitors, Bioorg. Med. Chem. Lett. 27 (2017) 662–665.
[272] Z.D. Wang, G.D. Yao, W. Wang, W.B. Wang, S.J. Wang, S.J. Song, Synthesis and evaluation of -amino acid methyl ester substituted sarsasapogenin derivatives as neuroprotective agents for Alzheimer's disease, Steroids 125 (2017) 93–106.
[273] M.R. Jones, C. Dyrager, M. Hoarau, K.J. Korshavn, M.H. Lim, A. Ramamoorthy, T. Storr, Multifunctional quinoline-triazole derivatives as potential modulators of amyloid-beta peptide aggregation, J. Inorg. Biochem. 158 (2016) 131–138.
[274] W. Wang, W. Wang, G. Yao, Q. Ren, D. Wang, Z. Wang, P. Liu, P. Gao, Y. Zhang, S. Wang, S. Song, Novel sarsasapogenin-triazolyl hybrids as potential anti-Alzheimer's agents: design, synthesis and biological evaluation, Eur. J. Med. Chem. 151 (2018) 351–362.
[275] J.R.M. Coimbra, D.F.F. Marques, S.J. Baptista, C.M.F. Pereira, P.I. Moreira, T.C.P. Dinis, A.E. Santos, J.A.R. Salvador, Highlights in BACE1 inhibitors for Alzheimer's disease treatment, Front. Chem. 6 (2018) 178.
[276] B. De Strooper, R. Vassar, T. Golde, The secretases: enzymes with therapeutic potential in Alzheimer disease, Nat. Rev. Neurol. 6 (2010) 99–107.
[277] A. Iraji, O. Firuzi, M. Khoshneviszadeh, H. Nadri, N. Edraki, R. Miri, Synthesis and structure-activity relationship study of multi-target triazine derivatives as innovative candidates for treatment of Alzheimer's disease, Bioorg. Chem. 77 (2018) 223–235.
[278] A.K. Ghosh, H.L. Osswald, BACE1 (beta-secretase) inhibitors for the treatment of Alzheimer's disease, Chem. Soc. Rev. 43 (2014) 6765–6813.
[279] Z. Haghighijoo, O. Firuzi, B. Hemmateenejad, S. Emami, N. Edraki, R. Miri, Synthesis and biological evaluation of quinazolinone-based hydrazones with potential use in Alzheimer's disease, Bioorg. Chem. 74 (2017) 126–133.
[280] S. Ali, M.H.H.B. Asad, S. Maity, W. Zada, A.A. Rizvanov, J. Iqbal, B. Babak, I. Hussain, Fluoro-benzimidazole derivatives to cure Alzheimer′s disease: in-silico studies, synthesis, structure-activity relationship and in vivo evaluation for *β*-secretase enzyme inhibition, Bioorg. Chem. 88 (2019) 102936.
[281] M. Margittai, R. Langen, Side chain-dependent stacking modulates tau filament structure, J. Biol. Chem. 281 (2006) 37820–37827.
[282] V.M. Bergen, et al., Assembly of τ protein into Alzheimer paired helical filaments depends on a local sequence motif (306VQIVYK311) forming *β* structure, Proc. Natl. Acad. Sci. USA 97 (2000) 5129–5134.
[283] M. Goedert, D.S. Eisenberg, R.A. Crowther, Propagation of tau aggregates and neurodegeneration, Annu. Rev. Neurosci. 40 (2017) 189–210.
[284] A.K. Farag, E.J. Roh, Death-associated protein kinase (DAPK) family modulators: current and future therapeutic outcomes, Med. Res. Rev. 39 (2018) 349–385.
[285] L.K. Chico, L.J. Van Eldik, D.M. Watterson, Targeting protein kinases in central nervous system disorders, Nat. Rev. Drug Discov. 8 (2009) 892–909.
[286] H. Tsui, Q. Zeng, K. Chen, X. Zhang, Inhibiting kinases in the CNS, in: S. Chackalamannil, D. Rotella, S.E. Ward (Eds.), Comprehensive Medicinal Chemistry III, Elsevier, Oxford, 2017, pp. 408–446.
[287] A. Martinez-Muriana, R. Mancuso, I. Francos-Quijorna, A. Olmos-Alonso, R. Osta, V.H. Perry, X. Navarro, D. Gomez-Nicola, R. Lopez-Vales, CSF1R blockade slows the progression of amyotrophic lateral sclerosis by reducing microgliosis and invasion of macrophages into peripheral nerves, Sci. Rep. 6 (2016) 25663.
[288] A. Olmos-Alonso, S.T.T. Schetters, S. Sri, K. Askew, R. Mancuso, M. Vargas-Caballero, C. Holscher, V.H. Perry, D. Gomez-Nicola, Pharmacological targeting of CSF1R inhibits microglial proliferation and prevents the progression of Alzheimer's-like pathology, Brain J. Neurol. 139 (2016) 891–907.
[289] H. Asai, S. Ikezu, S. Tsunoda, M. Medalla, J. Luebke, T. Haydar, B. Wolozin, O. Butovsky, S. Kügler, T. Ikezu, Depletion of microglia and inhibition of exosome synthesis halt tau propagation, Nat. Neurosci. 18 (2015) 1584–1593.
[290] A.K. Farag, A.H.E. Hassan, H. Jeong, Y. Kwon, J.G. Choi, M.S. Oh, K.D. Park, Y.K. Kim, E.J. Roh, First-in-class DAPK1/CSF1R dual inhibitors: discovery of 3,5-dimethoxy-*N*-(4-(4-methoxyphenoxy)-2-((6-morpholinopyridin-3-yl)amino)pyrimidin-5-yl)benzamide as a potentialanti-tauopathies agent, Eur. J. Med. Chem. 169 (2019) 161–175.
[291] T.A. Pemberton, M. Chen, G.G. Harris, W.K. Chou, L. Duan, M. Koksal, et al., Exploring the influence of domain architecture on the catalytic function of diterpene synthases, Biochemistry 56 (2017) 2010–2023.
[292] L. Iauk, R. Acquaviva, S. Mastrojeni, A. Amodeo, M. Pugliese, M. Ragusa, M.R. Loizzo, F. Menichini, R. Tundis, Antibacterial antioxidant and hypoglycaemic effects of Thymus capitatus (L.) Hoffmanns. et Link leaves' fractions, J. Enzyme Inhib. Med. Chem. 30 (2015) 360–365.
[293] J.M. Hagel, E.C. Yeung, P.J. Peter, Facchini Got milk? The secret life of laticifers, Trends Plant Sci. 13 (2008) 631–639.
[294] Q.W. Shi, X.H. Su, H. Kiyota, Chemical and pharmacological research of the plants in genus Euphorbia, Chem. Rev. 108 (2008) 4295–4327.
[295] A. Smeriglio, S. Ragusa, M.T. Monforte, V. D'angelo, C. Circosta, Phytochemical

analysis and evaluation of antioxidant and anti-acetylcholinesterase activities of Euphorbia dendroides L. (Euphorbiaceae) latex, Plant Biosyst. Int. J. Deal. Asp. Plant Biol. 153 (2019) 498–505.
[296] A.J. Flewelling, J. Currie, C.A. Gray, J.A. Johnson, Endophytes from marine macroalgae: promising sources of novel natural products, Curr. Sci. 109 (2015) 88–111.
[297] R.P. Medina, et al., Aromatic compounds produced by endophytic fungi isolated from red alga Asparagopsis taxiformis - Falkenbergia stage, Nat. Prod. Res. 33 (2019) 443–446.
[298] Y. Sangnoi, et al., Acetylcholinesterase-inhibiting activity of pyrrole derivatives from a novel marine gliding bacterium, Rapidithrix thailandica, Mar. Drugs 6 (2008) 578–586.
[299] A.P. Murray, M.B. Faraoni, M.J. Castro, N.P. Alza, V. Cavallaro, Natural AChE inhibitors from plants and their contribution to Alzheimer's disease therapy, Curr. Neuropharmacol. 11 (2013) 388–413.
[300] R.P. Medina, A.R. Araujo, J.M. Batista Jr, C.L. Cardoso, C. Seidl, A.F.L. Vilela, H.V. Domingos, L.V. Costa-Lotufo, R.J. Andersen, D.H.S. Silva, Botryane terpenoids produced by Nemania bipapillata, an endophytic fungus isolated from red alga Asparagopsis taxiformis -Falkenbergia stage, Sci. Rep. 9 (2019) 12318.
[301] P.K.S. Uchoa, J.N. da Silva Jr., E.R. Silveira, M.A.S. Lima, Quim. Nova 36 (2013) 778–782.
[302] J.F. Tavares, K.F. Queiroga, M.V.B. Silva, M.F.F.M. Diniz, J.M.B. Filho, E.V.L. da-Cunha, C.A. de Simone, J.X. de Araujo Júnior, P.S. Melo, M. Haun, M.S. da Silva, J. Nat. Prod. 69 (2006) 960–962.
[303] D.K. Olivier, B.-E. Van Wyk, S. Afr, J. Bot. 85 (2013) 94–98.
[304] D.M. Hernandez, G. Diaz-Ruiz, B.E. Rivero-Cruz, R.A. Bye, M.I. Aguilar, J.F. Rivero-Cruz, Fitoterapia 83 (2012) 527–531.
[305] G.F. Dos Santos, G. da Silva Lima, G. Pereira de Oliveira, J.D. de Souza Filho, L. da Silva Amaral, E. Rodrigues-Filho, J.A. Takahashi, New AChE inhibitors from microbial transformation of trachyloban-19-oic acid by Syncephalastrum racemosum, Bioorg. Chem. 79 (2018) 60–63.
[306] M. Ayaz, A. Sadiq, M. Junaid, F. Ullah, F. Subhan, J. Ahmed, Neuroprotective and anti-aging potentials of essential oils from aromatic and medicinal plants, Front. Ag. Neurosci. 9 (2017) 168.
[307] C. Dobetsberger, G. Buchbauer, Actions of essential oils on the central nervous system: an updated review, Flavour Fragr. J. 26 (2011) 300–316.
[308] M.R. Loizzo, M.B. Jemia, F. Senatore, M. Bruno, F. Menichini, R. Tundis, Chemistry and functional properties in prevention of neurodegenerative disorders of five Cistus species essential oils, Food Chem. Toxicol. 59 (2013) 586–594.
[309] R. Tundis, M.R. Loizzo, M. Bonesi, F. Menichini, V. Mastellone, C. Colica, F. Menichini, Comparative study on the antioxidant capacity and cholinesterase inhibitory activity of Citrus aurantifolia Swingle, C. aurantium L. and C. bergamia Risso & Poit peel essential oils, J. Food Sci. 71 (2012) H40–H46.
[310] M. Bonesi, M.C. Tenuta, M.R. Loizzo, V. Sicari, R. Tundis, Potential Application of *Prunus armeniaca* L. and *P. domestica* L. leaf essential oils as antioxidant and of cholinesterases inhibitors, Antioxidants 8 (2019) 2.
[311] S. Thiratmatrakul, C. Yenjai, P. Waiwut, O. Vajragupta, P. Reubroycharoen, M. Tohda, C. Boonyarat, Eur. J. Med. Chem. 75 (2014) 21–30.
[312] W. Yang, Y. Wong, O.T.W. Ng, L.P. Bai, D.W.J. Kwong, Y. Ke, Z.H. Jiang, H.W. Li, K.K.L. Yung, M.S. Wong, Angew. Chem. Int. Ed. 51 (2012) 1804–1810.
[313] D.R. Howlett, A.R. George, D.E. Owen, R.V. Ward, R.E. Markwell, Biochem. J. 343 (1999) 419–423.
[314] L. Fang, X. Fang, S. Gou, A. Lupp, I. Lenhardt, Y. Sun, Z. Huang, Y. Chen, Y. Zhang, C. Fleck, Eur. J. Med. Chem. 76 (2014) 376–386.
[315] H. Akrami, B.F. Mirjalili, M. Khoobi, A. Moradi, H. Nadri, S. Emami, A. Foroumadi, M. Vosooghi, A. Shafiee, 9*H*-carbazole derivatives containing the *N*-Benzyl-1,2,3-triazole moiety as new acetylcholinesterase inhibitors, Arch. Pharm. Chem. Life Sci. 348 (2015) 366–374.
[316] M. de Candia, G. Zaetta, N. Denora, D. Tricarico, M. Majellaro, S. Cellamare, C.D. Altomare, New azepino [4, 3-*b*] indole derivatives as nanomolar selective inhibitors of human butyrylcholinesterase showing protective effects against NMDA-induced neurotoxicity, Eur. J. Med. Chem. 125 (2017) 288–298.
[317] R. Ghobadian, M. Mahdavi, H. Nadri, A. Moradi, N. Edraki, T. Akbarzadeh, M. Sharifzadeh, S.N.A. Bukhari, M. Amini, Novel tetrahydrocarbazole benzyl pyridine hybrids as potent and selective butryl cholinesterase inhibitors with neuroprotective and β-secretase inhibition activities, Eur. J. Med. Chem. 15 (2018) 49–60.
[318] S. Thiratmatrakul, C. Yenjai, P. Waiwut, O. Vajragupta, P. Reubroycharoen, M. Tohda, C. Boonyarat, Synthesis, biological evaluation and molecular modeling study of novel for the treatment of Alzheimer's disease, Eur. J. Med. Chem. 75 (2014) 21–30.
[319] W. Yang, Y. Wong, O.T. Ng, L. Bai, D.W. Kwong, Y. Ke, Z. Jiang, H. Li, K.K. Yung, M.S. Wong, Inhibition of betaamyloid peptide aggregation by multifunctional carbazole based fluorophores, Angew. Chem. Int. Ed. Engl. 51 (2012) 1804–1810.
[320] Y. Rook, K.U. Schmidtke, F. Gaube, D. Schepmann, B. Wunsch, J. Heilmann, J. Lehmann, T. Winckler, Bivalent β-carbolines as potential multitarget anti-alzheimer agents, J. Med. Chem. 53 (2010) 3611–3617.
[321] N. Choubdar, M. Golshani, L. Jalili-Baleh, H. Nadri, T.T. Kucukkilinc, B. Ayazgok, A. Moradi, F.H. Moghadam, Z. Abdolahi, A. Ameri, F. Salehian, New classes of carbazoles as potential multi-functional anti-Alzheimer's agents, Bioorg. Chem. 29 (2019) 29 103164.